
Unified Understanding of Relativity and Quantum Mechanics through the Repulsion Graviton Space Model

Misaki Kasai, Independent Researcher

November 26, 2024

E-mail: regravist.paper@gmail.com

Abstract

In this study, we propose the "Repulsion Graviton Space Model (Re:GraviS Model)" as a unified explanation for gravity, dark matter, and dark energy. This model asserts that **gravity is not an attractive force but an entropic-driven spatial repulsion countering the repulsive force of gravitons against space**. To support this claim, we derive the Galactic Rotation Curve MiSAKi Model by incorporating graviton effects into the circular orbital velocity equation derived from the Schwarzschild solution, which is the spherically symmetric solution of Einstein's field equation, and validate it against the observed galactic rotation curves in the SPARC dataset (175 galaxies). Our analysis successfully reproduces galactic rotation curves, affirming the hypothesis regarding the nature of gravity. Furthermore, we observe a strong correlation between graviton concentration and galactic rotation velocities, suggesting that gravitons act as dark matter on small scales, while their repulsive force drives cosmic expansion as dark energy. Additionally, this model implies that black hole formation begins when spatial repulsion surpasses graviton repulsion, providing a unified explanation for quantum effects at spacetime singularities, the information paradox, and time dilation and acceleration. By considering the equilibrium between graviton and spatial repulsion and the role of gravitons as interdimensional information carriers, a quantum spatial region emerges at singularities, producing quantum effects through interdimensional graviton movement and resolving the information paradox. In moderately strong gravitational fields, graviton repulsion extends space, increasing the Planck length and stretching time. In extremely strong fields, spontaneous spatial collapse exceeds graviton repulsion, compressing the Planck length and shortening time. This model suggests a foundational shift in understanding gravity, opening pathways to a quantum gravity theory that unifies relativity and quantum mechanics. Extending the model to spacetime as the "Repulsion Graviton Space-Time Model (Re:GraviST Model)" is essential for completing quantum gravity theory.

Keywords: Gravity, Quantum Gravity Theory, Graviton, Dark Matter, Dark Energy, Black Hole, Galactic Rotation Curve

1. Introduction

The discrepancy between observed and theoretical rotational velocities at the outer edges of galaxies has long been a major challenge in physics. This study proposes a novel hypothesis: gravitons exert a repulsive force against space, and gravity can be explained as "the entropic-driven reaction of space countering this repulsion." Using the circular orbital velocity equation derived from the spherically symmetric

solution to Einstein's field equations (the Schwarzschild solution) and incorporating the effects of gravitons, we analyze galactic rotation curves through a fitting model, the Galactic Rotation Curve MiSAKi Model. Based on the results, this study explores the potential for addressing the longstanding challenge of unifying general relativity and quantum mechanics while providing new insights into the nature of the cosmos.

2. Model Overview and Theoretical Background

The “Galactic Rotation Curve Graviton-Modified Inverse Square Decay Model (Galactic Rotation Curve MiSAKi Model)” employed in this study was derived by incorporating the effect of gravitons into the circular orbital velocity equation obtained from the Schwarzschild solution, a spherically symmetric solution to Einstein’s field equations. This model is based on the hypothesis that gravitons exert “spherically symmetric repulsive forces” against space, gradually decaying without interacting with matter, with their strength depending on the concentration of gravitons. Furthermore, the model assumes that gravitons act as dark matter on smaller scales, while on larger cosmic scales, they expand space and function as dark energy. By aligning the graviton concentration with the role of dark matter, this model resolves the longstanding mystery of “galactic rotation curves,” a significant challenge in physics.

Galactic Rotation Curve Graviton-Modified Inverse Square Decay Model (Galactic Rotation Curve MiSAKi Model)

$$v_{\text{total}}(r) = \sqrt{\alpha \left(1 - \frac{1}{1 + (\frac{r}{R})^2}\right)}$$

- $v_{\text{total}}(r)$: The total rotational velocity of the galaxy at a distance r from the center.
- α : A variable parameter representing the concentration of gravitons.
- R : A variable parameter representing the range of influence of gravitons.
- r : The radius (distance from the center).

Derivation Process

1. Einstein’s Equation

Einstein’s equation is the fundamental equation in the theory of relativity, describing the relationship between matter distribution and the curvature of space-time.

$$R_{\mu\nu} - \frac{1}{2}g_{\mu\nu}R = \frac{8\pi G}{c^4}T_{\mu\nu} \quad (1)$$

2. Adoption of the Schwarzschild Solution

Assuming that “gravitons exert a spherically symmetric repulsion on space,” we adopt the Schwarzschild solution, which is a spherically symmetric solution to Einstein’s equation.

$$ds^2 = -\left(1 - \frac{2GM}{r}\right)c^2dt^2 + \left(1 - \frac{2GM}{r}\right)^{-1}dr^2 + r^2d\theta^2 + r^2\sin^2\theta d\phi^2 \quad (2)$$

3. Derivation of Circular Orbital Velocity Equation

From the Schwarzschild solution, the velocity equation for circular orbits is derived as follows :

$$v_{\text{orbit}} = \sqrt{\frac{GM}{r}} \quad (3)$$

4. Substitution Based on the New Hypothesis

In the above equation, $\frac{GM}{r}$ represents the gravitational attraction exerted by the central body on an object at distance r . Here, we introduce the hypothesis that “Gravitons exert a repulsive force on a spherically symmetric space that decays gradually without interacting with matter, and the strength of this force depends on the concentration of gravitons.” To reflect this, we designed a modified inverse-square decay function, using the scale parameter R to represent the range of the graviton’s influence, so that the graviton’s repulsive force acts strongly at short distances and gradually maintains its influence at long distances. We replace $\frac{GM}{r}$ with the following function, expressed as the product of the graviton concentration α and the modified inverse-square decay function $1 - \frac{1}{1 + (\frac{r}{R})^2}$:

$$\frac{GM}{r} \rightarrow \alpha \left(1 - \frac{1}{1 + (\frac{r}{R})^2}\right) \quad (4)$$

This equation represents the spherically symmetric repulsion of gravitons on space, decaying according to the inverse-square law as distance r increases. This allows us to incorporate the hypothesis into the formula while retaining the structural meaning of the original circular orbital velocity equation.

5. Final Derived Equation

As a result of applying the above substitution, the final circular orbital velocity equation that reproduces the galactic rotation curve is derived as follows :

$$v_{\text{total}}(r) = \sqrt{\alpha \left(1 - \frac{1}{1 + (\frac{r}{R})^2}\right)} \quad (5)$$

- $v_{\text{total}}(r)$ is the total rotational velocity of the galaxy at distance r from the center
- α is the variable parameter representing the concentration of gravitons
- R is the variable parameter representing the range of influence of gravitons
- r is the radius (distance from the center)

To account for the influence of anti-gravitons, we do not ignore the imaginary component that appears when α is negative, and instead handle it appropriately using numpy functions.

3. Methodology

Using a high-precision fitting verification script developed with AI tools (ChatGPT4.0), we analyzed the alignment between the Galactic Rotation Curve MiSAKi Model and the SPARC dataset of observed galactic rotation curves (175 galaxies). This analysis, performed using nonlinear least squares fitting, involved visualizing results through plots, evaluating adjusted determination coefficients, and examining residuals. To account for the influence of anti-gravitons, imaginary components arising when α takes negative values were appropriately handled using numpy functions, enabling a comprehensive evaluation of the combined effects of gravitons and anti-gravitons. Furthermore, after completing all fittings, we conducted a comprehensive correlation analysis of key parameters, including the graviton concentration (parameter α), the graviton effect range (scale parameter R), and other physical parameters such as observed velocity components, disk components, and bulge components. To mitigate the risk of overfitting, parameter ranges during fitting were constrained to appropriate limits ($-150,000 < \alpha < 150,000$ and $0.1 < R < 200$).

4. Results and Discussion

The analysis confirmed a high degree of fit between the Galactic Rotation Curve MiSAKi Model and most galaxies, with a mean adjusted determination coefficient (adjusted R^2) of 0.802, a median of 0.964, and a standard deviation of 0.332. Across the 175 analyzed cases, the high median adjusted R^2 value of 0.964 and the small standard deviation of 0.332 demonstrate the model's accuracy. Fig. 1 shows the distributions of the determination coefficient (R^2) and the adjusted determination coefficient (adjusted R^2). The left panel illustrates the distribution of R^2 , while the right panel shows the distribution of adjusted R^2 , where negative values were adjusted to 0. It was confirmed that the adjusted R^2 values predominantly remain high across the analyzed galaxies. These findings visually support the robustness and accuracy of the model.

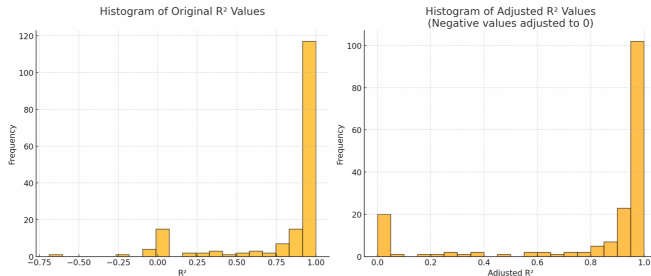


Fig. 1
Distribution of determination coefficient (R^2) and adjusted determination coefficient (Adjusted R^2).

Furthermore, the mean of the residuals across all observations was 0.110, and the standard deviation was 5.58. Fig. 2 shows the distribution of the average residuals for each galaxy, demonstrating that the average residuals are concentrated around 0, which suggests that the model reproduces the observational data without bias. The width of the distribution reflects observational errors, indicating no evidence of overfitting.

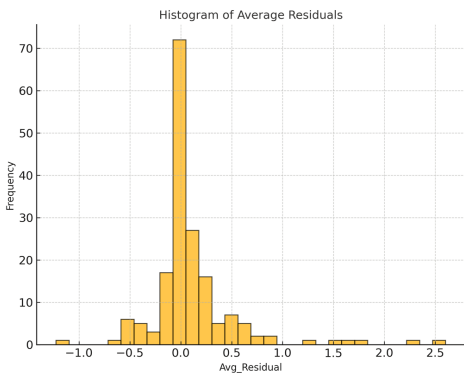


Fig. 2
Histogram of the average residuals for each galaxy.

Fig. 3 presents an autocorrelation plot of the residuals to evaluate their randomness, showing that most of the autocorrelation values fall within the confidence intervals. This result indicates that the residuals are statistically randomly distributed.

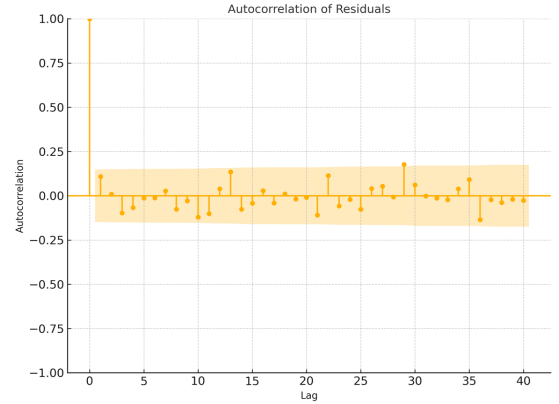


Fig. 3
Autocorrelation plot of residuals. The shaded area indicates the confidence interval.

The lack of bias shown in Fig. 2 and the randomness demonstrated in Fig. 3 together visually support the conclusion that the model appropriately reproduces the observational data while avoiding overfitting.

Additionally, out of the 175 fitting plots obtained, six representative ones with a large number of observational points relative to the radius are shown in Figs. 4–9.

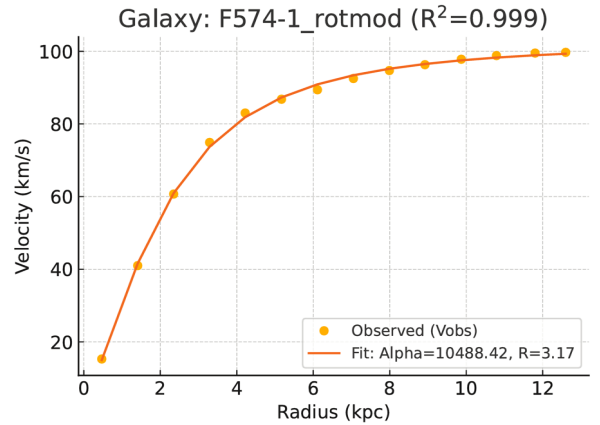


Fig. 4
Rotation curve of galaxy F574-1, showing observed data (dots) and the fitted curve (line) based on the Galactic Rotation Curve MiSAKi Model.
The fit parameters are $\alpha = 10488.42$ and $R = 3.17$. The coefficient of determination ($R^2 = 0.999$) indicates an excellent fit between the observed and fitted data.

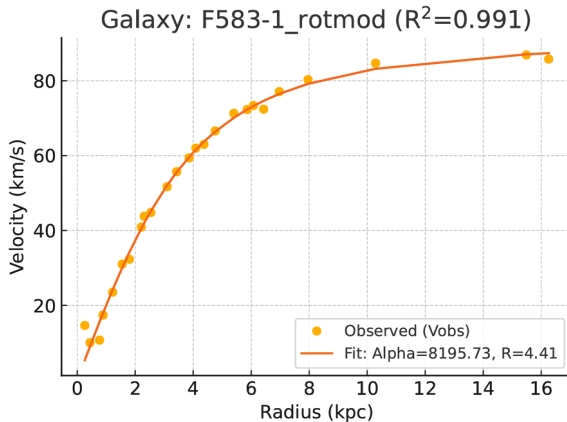


Fig. 5
Rotation curve of galaxy F583-1.
The coefficient of determination is $R^2 = 0.991$.

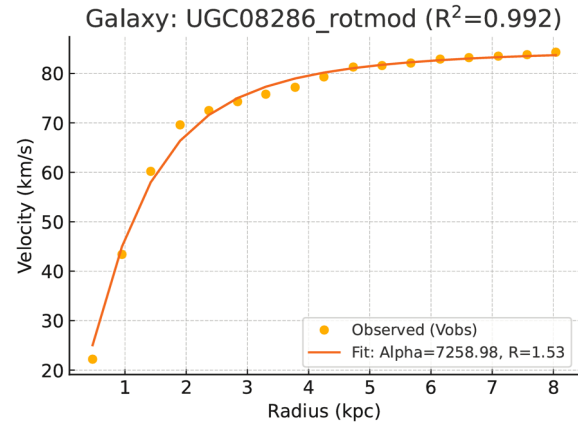


Fig. 8
Rotation curve of galaxy UGC08286.
The coefficient of determination is $R^2 = 0.992$.

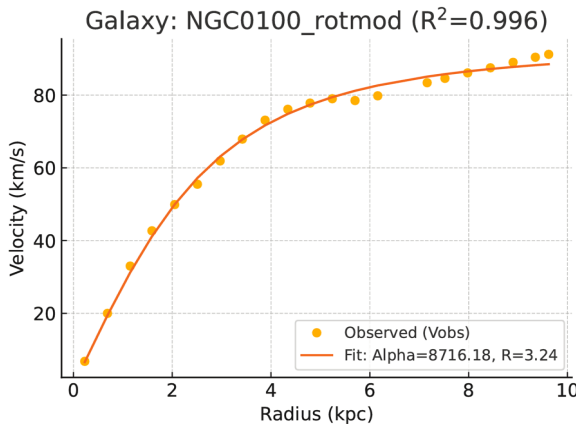


Fig. 6
Rotation curve of galaxy NGC0100.
The coefficient of determination is $R^2 = 0.996$.

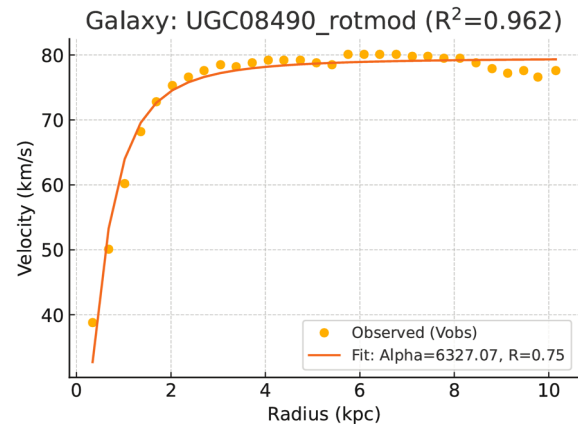


Fig. 9
Rotation curve of galaxy UGC08490.
The coefficient of determination is $R^2 = 0.962$.

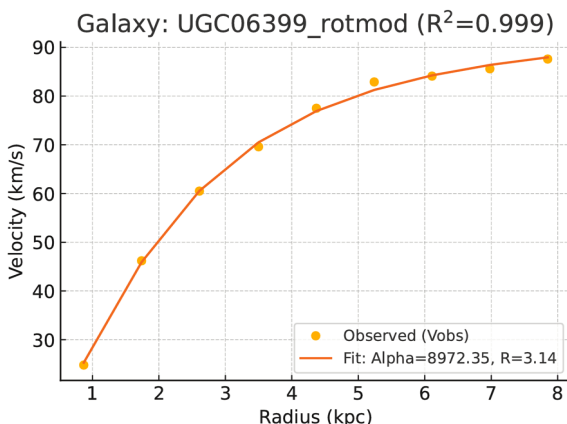


Fig. 7
Rotation curve of galaxy UGC06399.
The coefficient of determination is $R^2 = 0.999$.

The fitting plot figures demonstrate visually high-precision agreement with the observational data, particularly reproducing the rotational curves in the outer regions of the galaxies. These results, shown in Figs. 1–9, visually confirm the model's reproducibility, reliability, and broad applicability to galactic rotation curves.

Pearson correlation analysis further revealed a very strong positive correlation between the graviton concentration parameter (α) and both the observed velocity and the disk velocity components (average observed velocity, Avg Vobs(r): 0.956; average disk velocity, Avg Vdisk(r): 0.863). This suggests that graviton concentration significantly influences galactic rotational velocities and aligns faithfully with the role of dark matter inferred from Einstein's equations. On the other hand, R did not show any significant correlation with α or any other physical parameters. To further illustrate

the strength and direction of these correlations, Fig. 10 presents a grayscale heatmap of the Pearson correlation matrix.

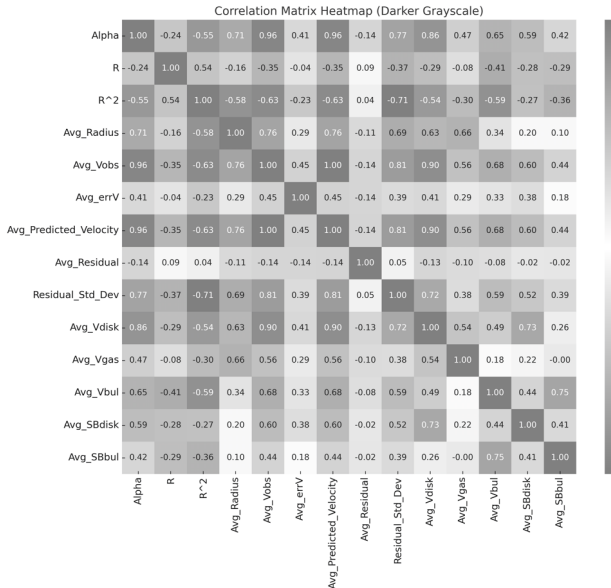


Fig. 10

Pearson correlation grayscale heatmap of the average parameters. Darker shades represent stronger correlations regardless of sign, while the numbers indicate the correlation coefficients with their respective signs.

Additionally, the distributions of α and the scale parameter R were found to be concentrated within specific ranges. For this analysis, 15 galaxies with negative determination coefficients were excluded, leaving 160 galaxies. These distributions are visually illustrated in the histograms shown in Fig. 11.

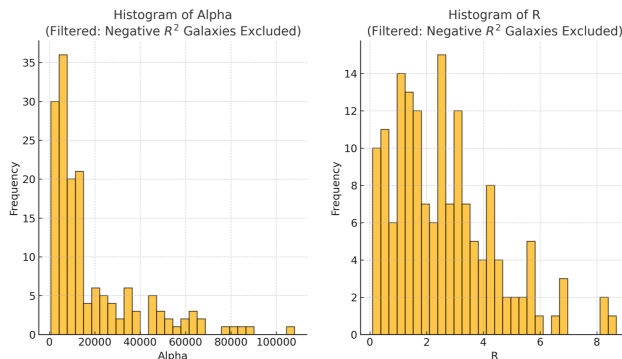


Fig. 11

Histograms of the distributions of α , representing graviton concentration (left panel), and the scale parameter R (right panel) from a total of 175 galaxies, excluding 15 galaxies with negative determination coefficients, leaving 160 galaxies.

The clustering of α suggests a certain threshold or standard for graviton concentration on galactic scales. Furthermore, the scale parameter R , which represents the range of graviton effects, showed no dependency on α or other physical parameters and consistently converged within a specific range. This indicates that graviton effects operate at a fixed scale independent of their concentration or the material density of individual galaxies. These findings clarify that gravitons exhibit no material interactions but instead gradually decay while exerting spherically symmetric repulsive forces against space, contributing to the maintenance of rotational velocities at the outer edges of galaxies through interactions with space. Furthermore, the absence of material interactions implies that gravitons do not interfere with the Higgs field or interact with Higgs particles responsible for imparting mass. This supports the unique characteristics required by conventional quantum mechanics, where gravitons are massless, closed strings capable of interdimensional movement. In this analysis, α did not take zero or negative values, and thus no direct effects of anti-gravitons were observed. However, this result does not directly negate the existence of anti-gravitons because α represents graviton concentration rather than the absolute number of gravitons. Based on these results, this study concludes that the mysterious force maintaining outer galactic rotational velocities is “the graviton’s repulsive force against space.” The model’s fit with observational data and its non-interactive properties suggest that gravity, considered the weakest of the four fundamental forces, originates from “the entropic-driven reaction of space countering the graviton’s repulsive force,” establishing a causal relationship between graviton effects and spatial curvature. Moreover, the findings strongly suggest that the nature of dark matter is “the gravitons themselves,” while the nature of dark energy is “the graviton’s repulsive force against space.” This implies that the mysterious energy accelerating the universe’s expansion at superluminal speeds is highly likely to be “the graviton’s repulsive force against space.” The mechanism by which massless gravitons concentrate may involve their indirect gravitational effects, namely, entropy-driven spatial repulsion confining gravitons within space and causing them to converge at a single point. This process represents a form of self-causality, potentially consistent within black hole event horizons and spacetime singularities, where traditional physical laws are believed to break down. This study suggests that black holes begin to form when spatial repulsion momentarily surpasses the graviton’s repulsive force against space. Spacetime singularities may not form as mere zero-dimensional points but rather as complex spatial regions that compress inward while exhibiting quantum-like spatial spread. When spatial repulsion strength approaches that of graviton repulsion, the resulting spacetime singularity can be interpreted as a spacetime region where graviton repulsion and spatial repulsion are in perfect equilibrium. This framework

allows for quantum effects within spacetime singularities, avoiding the infinities that have long posed challenges in traditional quantum mechanics. However, assuming perfect equilibrium between graviton repulsion and spatial repulsion might prevent quantum spread within the singularity. To reconcile this within quantum mechanics, it may be necessary to consider that gravitons transition from “open string” to “closed string” states under extreme conditions in spacetime singularities, allowing them to transform into energy and escape to other dimensions. In this interpretation, gravitons function as particles transmitting and preserving information across dimensions, ensuring that information is not lost beyond event horizons. This complements and potentially extends recent soft hair theory, providing a new perspective on resolving the black hole information paradox. Spacetime singularities may thus act as interdimensional gateways for gravitons, reconciling the information paradox while permitting quantum spread within singularities. Furthermore, this mechanism for black hole formation not only explains the phenomenon of time dilation in moderately strong gravitational fields but also predicts changes in time within black holes themselves. In moderately strong gravitational fields, including those near black holes, graviton repulsion expands space, lengthening the Planck scale and increasing the minimum unit of quantum motion. This slows physical processes on the quantum level, effectively lengthening time. This matches relativity’s prediction that objects near event horizons experience “time dilation” and appear to freeze from an external observer’s perspective. Reversing this phenomenon to view it from an opposite perspective, the spacetime region near the event horizon where the object is located is characterized by extremely strong graviton repulsion, which significantly expands space. This causes physical motion at the quantum level to slow down, elongating the object’s time. As a result, it can be explained that the observer’s time appears relatively shorter in comparison. This consistency with relativity and actual phenomena further supports the theoretical model. However, within black holes, this relationship may invert. As spatial compression continues spontaneously, the Planck scale shortens, reducing the minimum unit of quantum motion. Consequently, physical processes accelerate on the quantum level, shortening time in the black hole’s spacetime. From the perspective of an observer within the black hole, external objects may appear frozen, providing new insights into time changes in black holes. These findings suggest that observers’ perception of constant time may be a cognitive illusion arising from synchronization with quantum movement speed and Planck scale within their respective spacetime regions. Such spacetime phenomena might require an extended graviton spacetime repulsive model, termed the Repulsion Graviton Space-Time Model (Re:GravIST Model), as an evolution of the Repulsion Graviton Space Model (Re:GraviS Model).

5. Conclusion

In this study, the “Galactic Rotation Curve Graviton-Modified Inverse Square Decay Model (Galactic Rotation Curve MiSAKi Model)” was applied to analyze its alignment with the SPARC dataset of observed galactic rotation curves (175 galaxies). The results confirmed that the model demonstrates a high degree of consistency with observed galactic data, supporting the hypothesis that gravitons exert spherically symmetric repulsive forces against space. Furthermore, it was observed that the role of the parameter α , which represents graviton concentration, aligns with the role of dark matter within galaxies, while the scale parameter R converges within a specific range. These findings led to the following key conclusions and possibilities:

1. Gravitons exert spherically symmetric repulsive forces against space.
2. **The essence of gravity lies in the entropy-driven repulsion of space in response to the repulsive force of gravitons on space.** Furthermore, the reason why gravity is considered the weakest of the four fundamental forces is that it operates through an indirect mechanism mediated by space.
3. Dark matter is composed of gravitons, while dark energy is the repulsive force of gravitons against space.
4. The causal relationship between gravitons and space explains the mechanism of black hole formation and the quantum spread within spacetime singularities, enabling an understanding of singularities within the framework of quantum mechanics and offering a new perspective for resolving the information paradox.
5. The time dilation dependent on the strength of the gravitational field can be explained within the framework of quantum mechanics, and it is also suggested that time may be shortened inside the event horizon.
6. The application of the Repulsion Graviton Space Model (Re:GraviS Model) and its theoretical extension to the Repulsion Graviton Space-Time Model (Re:GravIST Model) suggests the possibility of unifying general relativity and quantum mechanics, which has long been considered challenging.

These insights obtained through this study provide a new understanding of the unresolved fundamental problems in physics, including gravity, dark matter, and dark energy. Moreover, the following issues are highlighted as future research directions based on the results of this analysis:

1. Additional Validation of the Theoretical Model

There is a need to further evaluate the validity of the theoretical model by verifying its consistency with observational data beyond galactic rotation curves, such as gravitational waves and cosmic microwave background radiation.

2. Further Research on Black Hole Formation Mechanisms

It is necessary to apply the relationship between gravitons and space to the process of black hole formation and to verify it in detail through observational data and simulations.

3. Further Research on Black Hole Spacetime Singularities

Detailed simulations are required to investigate the behavior of gravitons and space within spacetime singularities.

4. Interpretation of Proper Time

It is necessary to consider and examine the physical basis of the hypothesis that the “illusion of constant time” arises from the natural synchronization of awareness and bodily reaction speeds with the Planck scale and quantum scale movement speeds of each spacetime region.

Through these future validations, the Repulsion Graviton Space-Time Model (Re:GraviST Model) is strongly expected to be established as an essential foundation for the completion of a “quantum gravity theory.”

Acknowledgements

This study utilized the galactic rotation curve dataset (175 galaxies) provided by the SPARC (Spitzer Photometry and Accurate Rotation Curves) project. We express our gratitude to the researchers who made this dataset publicly available. Additionally, OpenAI’s ChatGPT4o was used for script development. All outputs generated by ChatGPT4o were thoroughly reviewed and refined by the authors, who take full responsibility for the final content.

Funding Statement

This study received no specific grant from any funding agency in the public, commercial, or not-for-profit sectors and was fully supported by the authors’ personal funds.

Ethical Statement

This research did not involve experiments on humans, animals, or biological samples, and thus did not require ethical committee approval.

Conflict of Interest Statement

The authors declare no conflicts of interest related to this manuscript.

Data Availability Statement

The data supporting this study are primarily sourced from the SPARC dataset, publicly available at <http://astroweb.cwru.edu/SPARC>.

Additional data generated during this study, including fitting scripts and raw data, are available at Zenodo: Kasai, M. (2024). ReGraviST_Fitting_Script_and_RawData (Data set). Zenodo. <https://doi.org/10.5281/zenodo.14211634>

References

- [1] Einstein A 1916 *Die Grundlage der allgemeinen Relativitätstheorie Ann. Phys.* 354 769–822
<https://doi.org/10.1002/andp.19163540702>
- [2] Antoci, S., & Liebscher, D.-E. (1999) On the Gravitational Field of a Point-Mass According to Einstein’s Theory.
Available at: <https://arxiv.org/abs/physics/9905030>
- [3] Carroll, S. M. (1997) *Lecture Notes on General Relativity*.
Available at: <https://arxiv.org/abs/gr-qc/9712019>
- [4] Hawking, S. W., Perry, M. J., & Strominger, A. (2016) Soft hair on black holes. *Phys. Rev. Lett.*, 116, 231301.
<https://doi.org/10.1103/PhysRevLett.116.231301>

Supplementary Materials

Fitting Results Table with Average Parameters

Galaxy	Alpha	R	R^2	Avg_Radius	Avg_Vobs	Avg_errV	Avg_Predicted_Velocity	Avg_Residual	Residual_Std_Dev	Avg_Vdisk	Avg_Vgas	Avg_Vbul	Avg_SBdisk	Avg_SBbul
CamB_rotmod	2210.458	3.783776	0.999017	0.9233333	10.87667	1.5	10.89804618	-0.02137951	0.182383624	12.74	6.48	0	11.882222	0
D512-2_rotmod	1553.504	1.289073	0.963444	2.3975	32.375	3.8975	32.39893999	-0.02393999	1.242459275	19.1725	6.465	0	7.09	0
D564-8_rotmod	793.3307	1.594271	0.999021	1.7883333	19.05667	1.75	19.06036862	-0.00370195	0.195194545	8.113333	6.015	0	1.8533333	0
D631-7_rotmod	4317.117	3.489839	0.992485	3.818125	43.03813	2.44063	42.94638123	0.091743766	1.357026671	15.2225	17.9475	0	4.180625	0
DD0064_rotmod	3495.151	1.784168	0.958088	1.3992857	52.355	5.07786	32.31496019	0.220039809	3.015548075	15.10429	10.35786	0	11.647143	0
DD0154_rotmod	2603.474	2.076227	0.987103	3.2083333	38.18333	0.625	38.10278114	0.080552191	1.285813309	9.485	14.01667	0	1.9258333	0
DD0161_rotmod	4824.581	4.250588	0.970902	6.3877419	49.25484	2.34677	48.64029733	0.614541376	2.956133919	18.86387	25.20968	0	6.0625806	0
DD0168_rotmod	3956.083	2.087818	0.96688	2.266	41.46	1.94	41.33529533	0.12470467	2.659847363	15.367	20.458	0	6.114	0
DD0170_rotmod	4172.97	3.801255	0.994259	7.09875	52.25	1.3875	52.28312327	-0.03312327	0.884738741	18.02875	21.895	0	2.07875	0
ESO079-G014_rotmod	37823.77	6.815856	0.969044	7.174	119.3867	5.71867	117.0561581	2.330508567	8.700951744	95.588	17.35333	0	123.336	0
ESO116-G012_rotmod	13398.42	2.623518	0.982282	4.7273333	86.74667	3.13467	86.0702916	0.6763735064	3.828555368	53.40267	19.22733	0	55.321333	0
ESO444-G084_rotmod	4185.995	1.142483	0.985373	2.04	48.28571	3.21571	47.95358152	0.332132765	1.948366069	11.72571	14.79286	0	6.6314286	0
ESO563-G021_rotmod	108091.8	6.550686	0.97625	18.994667	263.31	9.09133	264.5345945	-1.22459445	13.70154806	219.415	25.07133	0	273.68267	0
F561-1_rotmod	2911.844	3.081949	0.988565	5.6416667	43.25	5.83333	43.31263877	-0.06263877	1.113024005	41.21	17.94333	0	16.671667	0
F563-1_rotmod	12008.86	3.440473	0.930814	9.3047059	88.95294	13.5282	89.29376684	-0.34082567	6.782570104	26.28412	20.65647	0	6.3341176	0
F563-V1_rotmod	98.7857	2.691161	0.918356	4.5883333	24.61667	5	24.71183441	-0.09516774	1.937115293	20.40333	13.87667	0	6.2766667	0
F563-V2_rotmod	15106.96	2.445338	0.98923	4.898	86.15	18.232	86.65328704	-0.50328704	4.001410182	32.626	19.396	0	27.042	0
F565-V2_rotmod	9336.22	5.249745	0.997321	5.03	60.47143	7.42857	60.57082044	-0.09939186	1.150216408	17.98571	17.52286	0	3.7528571	0
F567-2_rotmod	2922.527	2.977671	0.92821	5.752	44.32	7.2	44.4017821	-0.08107821	2.66691396	31.162	3.898	0	8.59	0
F568-1_rotmod	20454.02	3.8823	0.996541	5.8183333	100.8833	12.4817	100.9657193	-0.08238592	2.293635569	40.60333	15.7875	0	25.3025	0
F568-3_rotmod	13725.24	5.244496	0.978399	6.6611111	74.81667	8.80389	75.16468207	-0.3480154	4.70537816	41.65667	14.545	0	24.663333	0
F568-V1_rotmod	14069.72	2.675238	0.993927	6.3493333	94.81333	16.28	94.85009207	-0.03675874	2.276224101	39.19667	13.11	0	20.502667	0
F571-8_rotmod	21587.31	4.436582	0.97466	5.4923077	94.16154	5.12308	92.65832977	1.503208687	6.328024763	82.89846	7.603846	0	243.75385	0
F571-V1_rotmod	8273.395	4.850916	0.995559	7.7728571	69.74286	7.28571	69.83922082	-0.09636367	1.272182958	30.40143	22.65429	0	6.0214286	0
F574-1_rotmod	10488.42	3.172759	0.990804	5.7452857	80.74286	4.6	80.73848762	0.004369519	0.765557587	44.21143	13.08	0	23.728571	0
F574-2_rotmod	2604.549	8.688131	0.999024	6.492	28.32	8.8	28.28938982	0.030610179	0.338280309	30.722	10.208	0	8.534	0
F579-V1_rotmod	12527.88	1.36528	0.984067	6.4607143	100.5571	11.8214	100.4391305	0.118012378	2.611163899	60.175	13.11429	0	44.320714	0
F583-1_rotmod	8195.726	4.417122	0.991076	4.7336	53.264	7.5164	53.05504819	0.208591814	2.3465658335	20.4036	7.4496	0	9.2412	0
F583-4_rotmod	4504.928	2.086378	0.970161	4.0416667	51.23333	4.95	50.87365003	0.359683302	3.150214291	32.4725	8.598333	0	20.280833	0
IC2574_rotmod	705929	8.26478	0.978935	5.5444118	43.476473	3.24118	43.20165368	0.274816912	2.40580597	22.48412	13.90735	0	4.9655882	0
IC4202_rotmod	63898.41	3.887482	0.973076	12.807188	219.7188	7.3675	220.3584077	-0.63965771	8.491881353	165.6581	26.15563	120.974	129.87438	148.32906
KK98-251_rotmod	2235.74	2.559089	0.983523	1.48	21.58333	2	21.71947833	-0.136145	1.327731553	9.040667	11.75267	0	4.2046667	0
NGC0024_rotmod	12486.23	1.092277	0.986871	2.5489655	84.65862	7.61621	84.83781329	-0.1791926	2.924749271	53.56448	12.13172	0	128.74586	0
NGC0055_rotmod	8708.065	4.450001	0.989265	3.7635173	72.25238	3.8619	72.17349173	0.078889218	1.898410675	40.49286	33.53048	0	12.447143	0
NGC0100_rotmod	8716.182	2.3373	0.995933	4.937619	67.34333	5.56429	67.26778897	0.075544366	1.539482328	44.00908	10.88571	0	30.564286	0
NGC0247_rotmod	11458.16	4.262198	0.912591	7.8053846	85.17308	5.00385	84.65748739	0.515589537	5.918498704	48.61308	22.60692	0	17.456923	0
NGC0289_rotmod	29950.37	0.1	-0.00017	31.7475	173.0357	11.59	173.0356539	6.04E-05	9.678908912	125.7196	43.53571	0	109.10857	0
NGC0300_rotmod	9145.655	2.677627	0.971142	6.3532	80.664	6.464	80.59065500	0.073344942	2.834361255	43.3308	16.5384	0	15.6932	0
NGC0801_rotmod	50891.09	1.431467	0.750103	22.513846	207.4615	5.28462	207.757885	-0.29635002	17.21844651	218.8808	33.62	0	729.83154	0
NGC0891_rotmod	48199.2	0.1	-0.01811	9.2483333	219.4444	4.495	219.4407147	0.003729782	9.611221657	237.9839	18.04889	110.909	389.13333	76.371667
NGC1003_rotmod	11592.77	3.355035	0.896385	15.749444	99.03056	2.89722	98.88782303	0.142732521	4.852848065	49.30167	26.66472	0	12.88	0
NGC1090_rotmod	28542.46	2.740539	0.973714	15.19833	149.9958	4.55167	150.0713438	-0.07551051	6.338544737	134.8088	25.90583	0	158.92208	0
NGC1705_rotmod	5165.02	2.235732	0.910233	3.1107143	69.65	5.74929	69.64054364	0.009456361	1.85703555	29.65357	14.15071	0	45.336429	0
NGC2366_rotmod	3111.185	2.001128	0.976383	3.0903846	40.49269	2.60731	40.58045171	-0.0877594	2.267027205	17.45077	18.53692	0	8.3938462	0
NGC2403_rotmod	16460.46	1.568216	0.904845	7.0090411	107.9973	2.42082	107.0925478	0.904712428	8.110655109	77.97288	23.5326	0	152.34479	0
NGC2683_rotmod	31559.56	0.1	-0.00097	18.099091	177.6364	9	177.6350801	0.001283512	22.74983922	152.5309	19.71273	43.0318	89.216364	0
NGC2841_rotmod	90866.08	0.1	-0.00079	23.2606	301.42	7.6702	301.4196319	0.00368131	16.93037079	181.0286	40.3046	123.045	138.8096	0.4342
NGC2903_rotmod	39358.78	1.092896	0.81549	10.362353	182.7059	4.02941	183.2272783	-0.52139594	16.22911966	19.7688	22.91765	0	695.72265	0
NGC2915_rotmod	7363.062	1.638209	0.942734	5.1866667	74.11671	8.06433	74.31295234	-0.19628567	4.31359393	27.0067	14.873	0	16.459333	0
NGC2955_rotmod	68126.79	0.989951	0.735151	12.25125	252.125	8.71375	252.0550779	0.069922117	12.74500814	209.4958	37.90083	175.13	356.58375	382.07083
NGC2976_rotmod	16002.31	2.150245	0.987956	10.366667	51.15926	3.50519	51.13397104	0.025288218	7.678591559	51.22667	13.64741	0	228.18741	0
NGC2998_rotmod	43794.64	1.283679	0.876404	16.072308	187.0769	8.76923	185.3566107	1.720312337	14.14852461	154.9508	31.72385	0	455.52308	0
NGC3109_rotmod	6082.007	3.828293	0.996996	3.3532	45.764	2.752	45.7524449	0.038755511	1.033297759	12.3892	13.8656	0	2.972	0
NGC3198_rotmod	23627.13	3.297732	0.978206	13.886279	125.6721	5.04302	125.2808867	0.391206316	5.267032896	100.34385	20.4886	0	128.29349	0
NGC3521_rotmod	46626.26	0.593666	0.909982	4.7143902	207.439	13.4924	207.4391319	-0.0010749	4.798148027	250.331	8.892439	0	908.00561	0
NGC3726_rotmod	27970.53	4.2866	0.863241	15.790833	151.8333	6.87083	151.8898124	-0.05557905	7.43280018	145.6333	30.91333	0	73.666667	0
NGC3741_rotmod	2587.856	2.096111	0.891398	3.0685714	36.18095	2.3019	35.46473281	0.716219569	3.736444762	7.678571	10.40857	0	2.3961905	0
NGC3769_rotmod	14604.													

NGC5005_rotmod	66550.7	0.396295	0.646557	5.325	252.2778	21.2372	252.2436068	0.034171016	9.613871304	244.4211	63.50667	152.914	964.70556	662.97222
NGC5033_rotmod	44854.74	0.157265	0.006304	21.162727	211.5455	4.59091	211.5454934	-3.88E-05	11.83376409	144.7077	37.18864	96.6423	184.18909	164.36864
NGC5055_rotmod	36801.8	0.812704	0.569942	20.879643	187.25	3.35607	187.2654057	-0.01540569	11.37905678	202.3775	29.10857	0	404.14036	0
NGC5371_rotmod	49312.71	0.409792	0.023339	21.353158	221.3684	4.10526	221.3682174	0.000203614	12.34431079	245.6853	30.58053	0	244.00316	0
NGC5585_rotmod	8523.813	2.422593	0.938292	4.1520833	62.1875	2.22333	60.51120343	1.676296566	6.354160661	44.59792	14.97375	0	94.121667	0
NGC5907_rotmod	49144.03	0.439037	0.000648	27.68	221.5789	3.57895	221.5789538	-6.42E-06	8.130395513	177.4289	43.78684	0	53.81	0
NGC5985_rotmod	89402.86	3.144581	0.83058	16.082121	285.4545	6.09424	285.4755696	-0.02105119	8.129909517	193.3982	16.07	58.907	113.49121	0.0321212
NGC6015_rotmod	24750.44	1.638374	0.953891	12.398636	143.2182	3.93182	143.1003943	0.117788464	5.829020407	103.5695	24.72023	0	132.17591	0
NGC6195_rotmod	62180.94	1.201659	0.791319	14.176087	243.0807	7.27435	243.1126874	-0.02573089	7.485853706	189.2204	35.10913	191.784	198.60652	253.64565
NGC6503_rotmod	13645.12	0.84132	0.906513	12.140968	114.2903	2.35484	114.2973247	-0.00700209	2.372564515	76.97871	22.65806	0	56.950323	0
NGC6674_rotmod	64087.82	1.544108	0.219532	37.467333	249.9333	8.26667	249.9513681	-0.01803481	19.12476652	161.1887	32.718	57.9667	75.556667	0.7893333
NGC6789_rotmod	9240.938	0.89293	0.99016	0.405	37.725	5.315	37.20470316	0.02029684	1.911097052	16.67	8.365	0	58.86	0
NGC6946_rotmod	26813.53	0.105252	0.028455	10.275517	163.2931	6.24138	163.2895955	0.003507938	14.51220063	154.9064	28.97241	54.5884	195.24379	95.575517
NGC7331_rotmod	58544.44	0.22051	0.000527	18.055556	241.8611	5.13889	241.8611185	-7.39E-06	8.213335815	262.9008	35.78	63.9536	242.20389	0
NGC7793_rotmod	11052.01	0.997863	0.926744	2.3147826	74.45652	6.93478	73.76944044	0.687081296	8.300140639	69.88326	13.97087	0	312.33783	0
NGC7814_rotmod	50524.26	0.1	-0.07687	10.065	224.6111	5.61056	224.5788244	0.032286698	14.46316444	96.745	10.335	171.889	75.380556	426.38167
PGC51017_rotmod	373.2065	0.1	-0.68741	1.98	19.16667	2.25667	19.15192607	0.014740592	1.183812004	16.62167	11.39	0	10.648333	0
UGC00128_rotmod	16983.29	5.407011	0.979559	27.512727	118.4273	2.63545	118.2541209	0.173151792	3.29976233	44.28045	30.51318	0	7.2718182	0
UGC00191_rotmod	7043.906	1.738069	0.985976	3.3666667	58.97778	2.29667	59.0005182	-0.02277405	2.39196571	33.56667	13.52778	0	39.887778	0
UGC00634_rotmod	13308.88	5.833366	0.988819	11.26	95.7375	2.2725	95.76649098	-0.02899098	1.899036808	36.33	32.16	0	3.185	0
UGC00731_rotmod	5622.306	2.70381	0.956549	5.91	61.78333	2.79667	61.5215353	0.261798006	2.937612256	13.185	21.3475	0	1.8066667	0
UGC00891_rotmod	5316.684	4.053389	0.999266	4.446	49.19	1.284	49.23384433	-0.04384433	0.426795431	18.356	18.79	0	3.304	0
UGC01230_rotmod	12159.58	3.272532	0.949442	13.692727	91.88182	11.3727	92.34764459	-0.46582641	6.416861201	42.39364	25.99818	0	18.681818	0
UGC01281_rotmod	4898.681	3.034268	0.992345	2.072	34.4312	4.8948	34.67666751	-0.24546751	1.55196941	15.7776	7.4136	0	10.0676	0
UGC02023_rotmod	10889.6	5.680342	0.994175	2.27	37.48	8.69	37.27486756	0.205132443	1.275854085	31.256	11.8	0	26.198	0
UGC02259_rotmod	7791.942	1.325097	0.967377	4.58125	79.8375	2.2125	79.79604431	0.041455686	2.021332351	36.25875	18.05875	0	14.94375	0
UGC02455_rotmod	7109.194	4.364588	0.18991	2.26375	37.375	3.64	36.44104651	0.933953485	4.12161104	6.91375	16.8775	0	114.21875	0
UGC02487_rotmod	126069.8	0.1	-0.00038	41.086471	355.0588	6.98235	355.0585963	0.00022722	21.37709592	216.0247	25.61706	124.368	68.601176	3.4958824
UGC02885_rotmod	81725.35	0.1	-0.00296	38.269474	285.8421	10	285.8411656	0.000939694	13.6961017	191.4679	48.85632	98.2158	117.53474	70.172105
UGC02916_rotmod	44044.58	0.212884	0.195427	10.053023	208.7209	8.18349	208.7205683	0.000361915	8.904045367	87.89907	24.96023	195.499	78.455814	631.33465
UGC02953_rotmod	75905.15	0.1	0.068451	14.996174	273.8609	6.85061	273.8018777	0.058991827	27.41397961	213.2462	7.528348	145.675	792.74113	1119.2974
UGC03205_rotmod	50802.77	0.961297	0.815244	11.525833	215.125	7.54521	214.6081275	0.516872516	12.43021628	160.4963	14.60208	97.2083	201.93833	258.59104
UGC03546_rotmod	45058.11	0.1	-0.05397	8.833	212	15.5267	211.9545741	0.045425904	19.5533731	159.68	10.79433	180.201	575.02567	197.024
UGC03580_rotmod	11789.17	1.222001	0.385252	6.1942553	91.70213	5.18596	89.10018109	2.601946565	16.45152982	68.36723	15.52489	64.9047	158.65617	272.64128
UGC04278_rotmod	14195.61	5.802917	0.950907	3.4596	56.8812	6.0452	55.59175419	1.28945806	5.365199748	30.1088	4.5512	0	19.5736	0
UGC04293_rotmod	1290.291	1.08231	0.873779	2.8859091	30.085	3.56	30.3260099	-0.24100699	3.123987377	28.02136	15.42636	0	18.000909	0
UGC04325_rotmod	9373.457	1.383062	0.988561	3.1425	81.05	3.0525	81.1458168	-0.0958168	1.909143838	41.7125	19.0075	0	31.77875	0
UGC04483_rotmod	682.1311	0.476727	0.988696	0.64625	18.27625	1.7975	18.23246828	0.043781715	0.734787243	8.1325	8.60875	0	8.98875	0
UGC04499_rotmod	6050.694	2.582614	0.998358	4.5466667	60.88889	2.94889	60.87185895	0.01702994	0.654645067	34.90111	20.69444	0	13.78	0
UGC05005_rotmod	10910.72	8.122084	0.990123	11.698182	69.67273	12.8736	69.09304962	0.579677654	2.836509251	34.67	22.47	0	11.720909	0
UGC05253_rotmod	59036.34	0.1	-0.20021	9.714657	241.7808	5.95123	241.6640864	0.116735475	10.40095833	124.2797	14.97274	211.814	301.27301	1622.1173
UGC05414_rotmod	4833.036	2.34765	0.996623	2.395	45.18333	2.45167	45.09678411	0.086459226	0.881425505	30.34167	15.74833	0	23.925	0
UGC05716_rotmod	5375.157	2.198769	0.896157	6.713333	64.44167	1.25667	64.21418434	0.227482324	3.699928813	20.7325	20.42667	0	4.0533333	0
UGC05721_rotmod	6573.201	0.625637	0.936771	2.7113043	70.33478	5.34478	70.08312133	0.251661274	4.294350159	31.53826	17.10043	0	62.155217	0
UGC05750_rotmod	7651.331	6.920318	0.990678	6.7936364	48.7	8.53636	49.06496231	-0.36496231	2.466403973	27.30545	14.86636	0	11.105455	0
UGC05764_rotmod	3109.953	0.93284	0.940818	1.993	45.77	1.302	45.7573719	0.012628099	2.724183686	10.619	14.619	0	3.903	0
UGC05829_rotmod	5796.613	4.170415	0.966362	3.7709091	46.36364	5.052	45.87916713	0.484469229	3.033903656	18.38364	15.44455	0	5.7263636	0
UGC05918_rotmod	2072.076	1.500951	0.991455	2.5075	35.2875	3.93	35.22863116	0.058868845	0.852359304	14.42625	9.15875	0	5.08125	0
UGC05986_rotmod	14596.78	2.475162	0.96372	5.021333	96.74	3.26733	96.89393138	-0.15393138	5.12771871	58.738	16.47933	0	41.6	0
UGC05999_rotmod	12035.61	6.94808	0.988484	10.179	83.24	5	83.37907295	-0.13907295	2.351995091	37.54	30.084	0	5.446	0
UGC06399_rotmod	8972.354	3.139692	0.998646	4.3633333	68.75556	4.96667	68.78173343	-0.026177887	0.78672607	38.74333	15.74222	0	19.098889	0
UGC06446_rotmod	6840.387	1.573945	0.947493	5.2876471	72.96471	5	72.83605965	0.128646234	3.211918564	27.66706	21.01882	0	9.9470588	0
UGC06614_rotmod	34714.41	0.1	-9.85E-05	23.960769	186.3077	14.1	186.3073677	5.46E-05	14.76207619	93.23692	94.91538	131.89	28.785385	28.653077
UGC06628_rotmod	1884.872	1.343061	0.991219	4.3957143	39.1	8.27	39.11099001	-0.01099001	0.524415253	41.86286	15.11143	0	22.937143	0
UGC06667_rotmod	8766.028	3.167697	0.995845	4.3633333	67.86667	3.41111	67.7802251	0.08644416	1.337943238	17.28111	15.44889	0	5.5666667	0
UGC06788_rotmod	46397.07	0.188965	0.453396	9.712444	212.3778	7.27356	212.308921	0.068856808	12.08181792	126.8058	15.74111	114.816	175.62244	746.68511
UGC06787_rotmod	58577.09	0.134515	0.379965	10.022676	239.6479	6.79	239.7012568	-0.0533695	14.77332431	106.2089	11.46789	188.655	170.42704	1992.6196

UGC09037_rotmod	25128.78	5.549982	0.959671	15.198182	137.9273	7.23091		137.9297642	-0.00249146	5.038571585	133.8018	48.23864	0	56.964545	0
UGC09133_rotmod	69930.48	0.1	-0.02382	30.110588	264.1765	5.94382		264.1470325	0.0294381	24.08950572	169.375	30.46574	168.779	265.53074	679.11794
UGC09992_rotmod	1154.643	0.546297	0.955462	2.336	32.02	5.66		32.0182487	0.001751295	0.516376247	22.262	13.268	0	11.006	0
UGC10310_rotmod	5887.552	2.192953	0.995664	4.42	62.74286	5.06		62.79480316	-0.05194602	0.952092865	35.38429	18.43	0	15.16	0
UGC11455_rotmod	82092.02	5.728508	0.968982	15.364722	228.2444	7.75556		228.2703069	-0.02586246	12.2402897	249.5939	21.97472	0	396.47528	0
UGC11557_rotmod	9052.717	4.490537	0.981498	4.565	57.31667	7.875		57.78940712	-0.47274045	3.695726741	74.6275	11.3125	0	98.580833	0
UGC11820_rotmod	5766.035	1.552831	0.944763	5.576	51.205	2.938		51.02797629	0.17702371	6.205665124	19.477	16.072	0	29.292	0
UGC11914_rotmod	84855.38	0.440993	0.940862	3.726	279.5231	9.74015		279.5048667	0.0182102	6.114444792	204.6392	9.179692	202.966	859.68077	1058.4545
UGC12506_rotmod	57513.04	2.564688	0.855751	25.406452	228.871	14.4484		228.3227272	0.548240567	11.41613348	140.4713	51.12161	0	60.566774	0
UGC12632_rotmod	5547.564	2.755229	0.985445	5.6866667	60.18667	3.56067		59.98395775	0.202708921	1.810224101	26.414	17.538	0	7.504	0
UGC12732_rotmod	8128.786	3.323883	0.911591	8.1625	75.75	3.62688		75.35639905	0.393600949	5.024140739	29.31188	20.67063	0	6.880625	0
UGCA281_rotmod	1046.985	0.461573	0.996247	0.5785714	22.11429	1.78		22.05844032	0.055845393	0.511977967	14.29571	7.062857	0	36.737143	0
UGCA442_rotmod	3846.251	2.285353	0.989286	3.375	44.7875	2.00375		44.58189554	0.205604459	1.631804162	11.2475	17.46875	0	2.7425	0
UGCA444_rotmod	1557.182	1.21903	0.977357	1.3663889	26.23556	3.90861		26.0496576	0.185897955	1.332897136	4.521667	12.04167	0	0.9616667	0

Summary Statistics

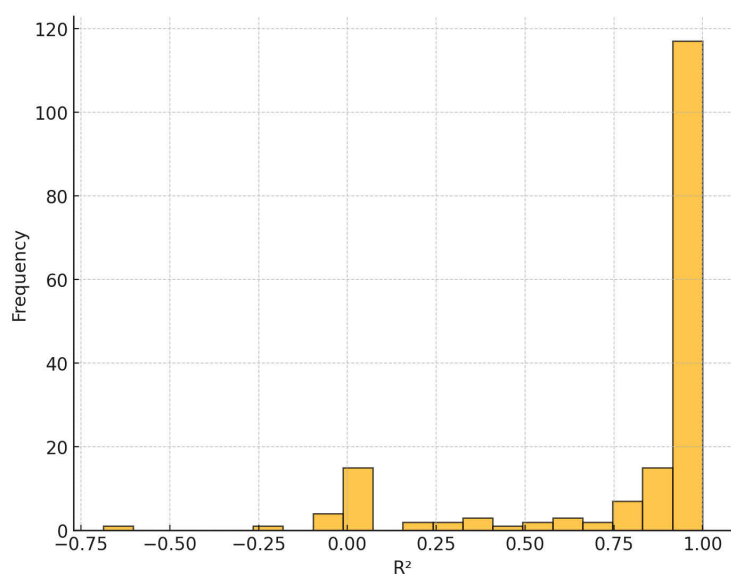
	count	mean	std	min	25%	50%	75%	max	25th Percentile	75th Percentile
Alpha	175	21502.130	23706.282	373.206	5650.550	11458.156	31696.972	126069.768	5650.550	31696.972
R	175	2.379	1.862	0.100	0.969	2.096	3.311	8.688	0.969	3.311
R^2	175	0.796	0.351	-0.687	0.859	0.964	0.988	0.999	0.859	0.988
Avg_Radius	175	8.371	7.599	0.405	3.281	5.672	10.498	41.086	3.281	10.498
Avg_Vobs	175	108.751	76.537	10.689	50.471	80.664	167.094	355.059	50.471	167.094
Avg_errV	175	5.770	3.397	0.625	3.284	5.186	7.280	21.237	3.284	7.280
Avg_Predicted_Velocity	175	108.641	76.599	10.532	50.329	80.591	167.333	355.059	50.329	167.333
Avg_Residual	175	0.110	0.434	-1.225	-0.033	0.008	0.175	2.602	-0.033	0.175
Residual_Std_Dev	175	5.577	5.419	0.182	1.838	3.300	8.130	27.414	1.838	8.130
Avg_Vdisk	175	79.166	70.220	4.522	26.415	44.211	134.305	262.901	26.415	134.305
Avg_Vgas	175	19.716	9.891	3.898	13.398	17.538	24.840	63.507	13.398	24.840
Avg_Vbul	175	22.289	52.434	0.000	0.000	0.000	0.000	211.814	0.000	0.000
Avg_SBdisk	175	104.221	171.701	0.962	10.927	29.292	128.520	964.706	10.927	128.520
Avg_SBbul	175	68.717	255.214	0.000	0.000	0.000	0.000	1992.620	0.000	0.000

R² Summary Statistics

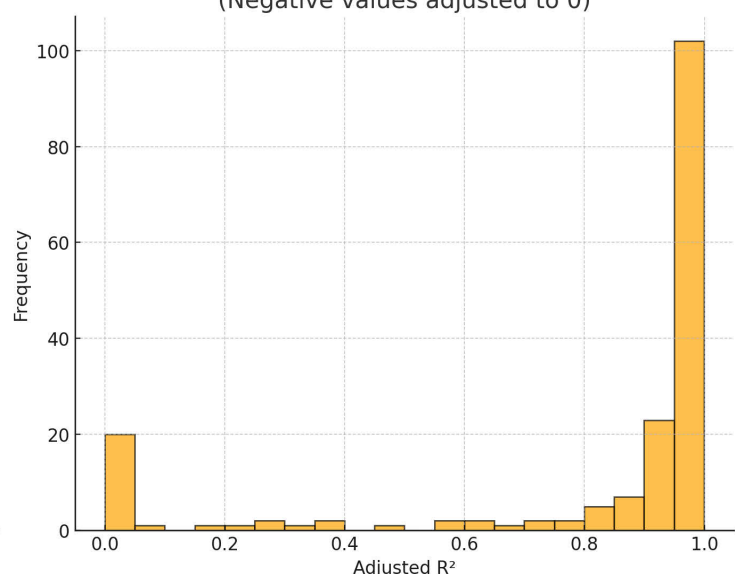
Metric	Original R ²	Adjusted R ²
Mean	0.796	0.802
Median	0.964	0.964
Standard Deviation	0.351	0.332
Min	-0.687	0.000
Max	0.999	0.999

(Negative R² values have been adjusted to 0.)

Histogram of Original R² Values

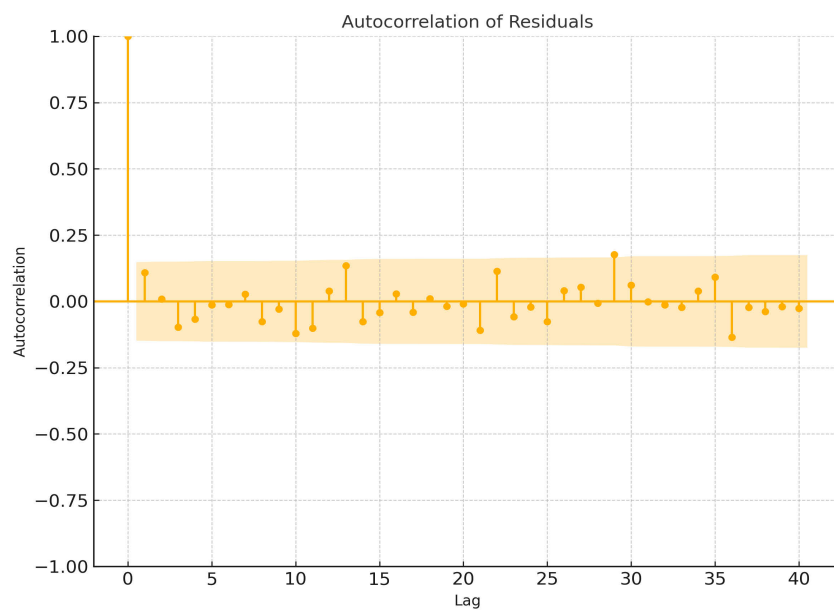
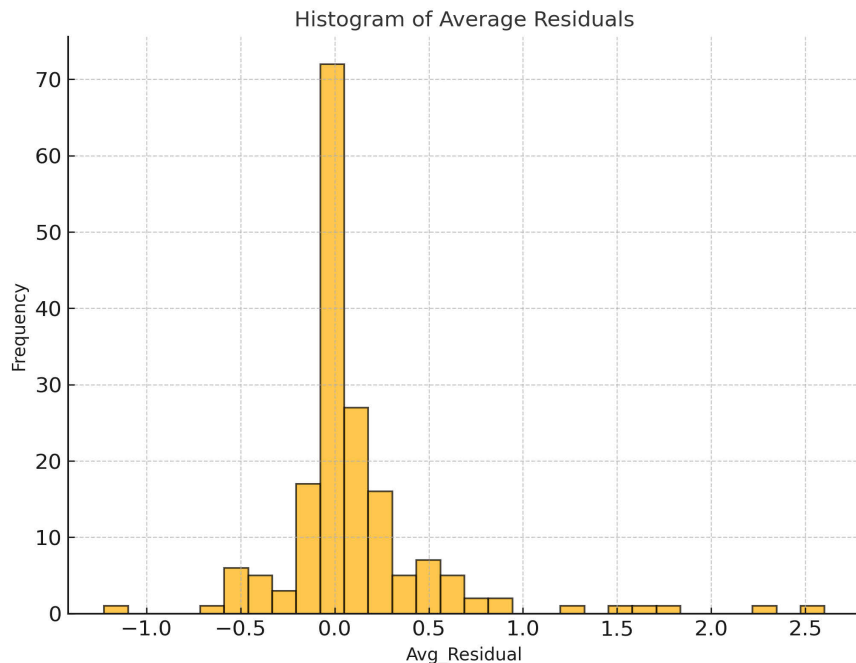


Histogram of Adjusted R² Values
(Negative values adjusted to 0)



Summary of Residuals for All Observations

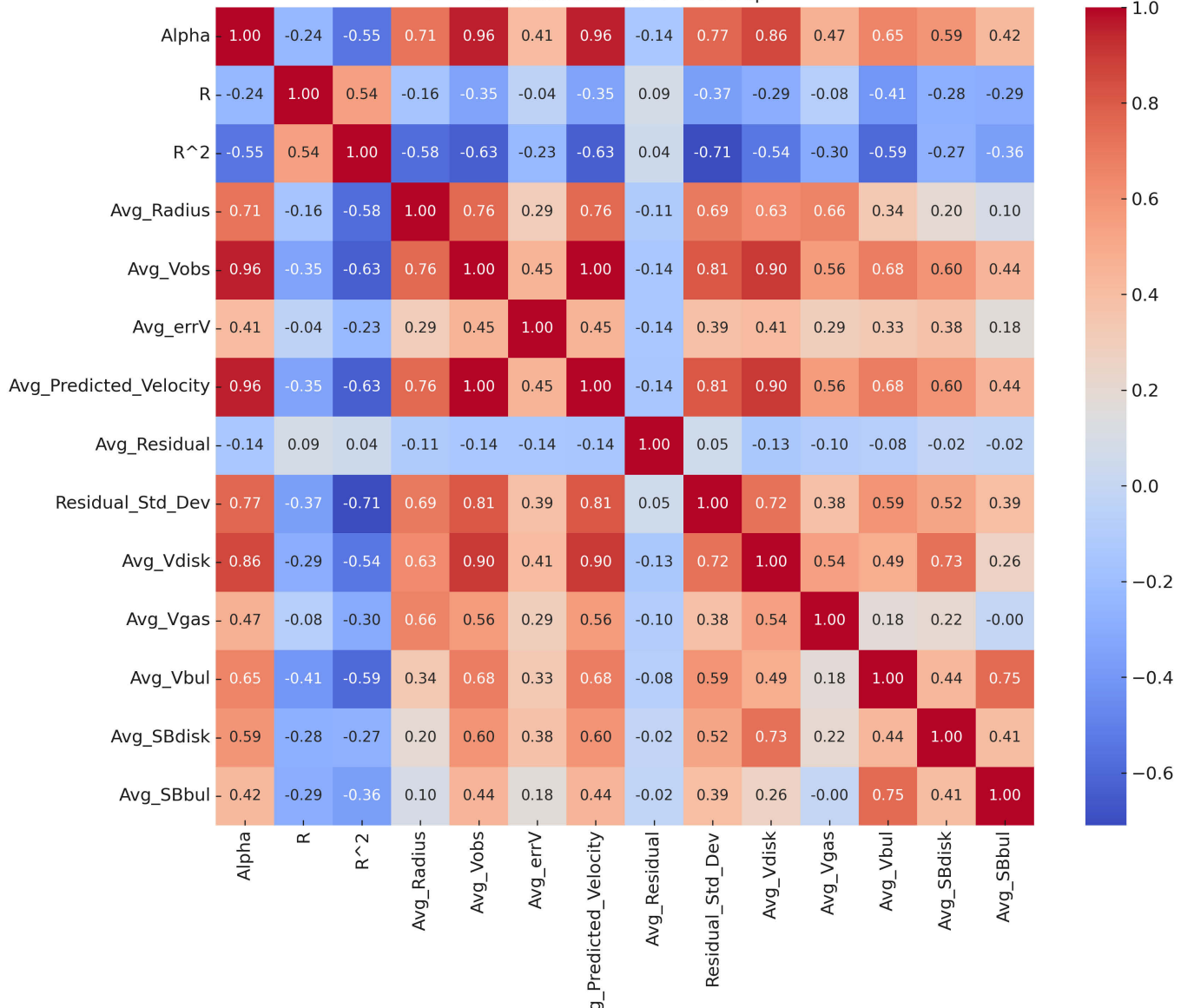
Metric	Value
Overall Average Residual	0.110
Overall Standard Deviation of Residuals	5.58



Pearson Correlation Matrix

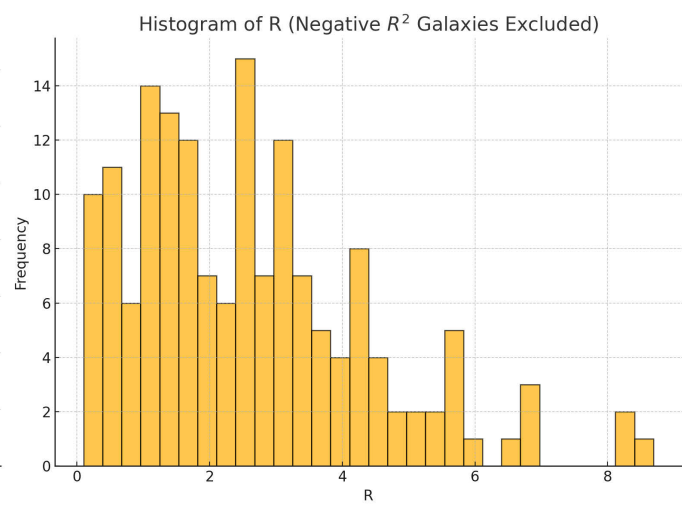
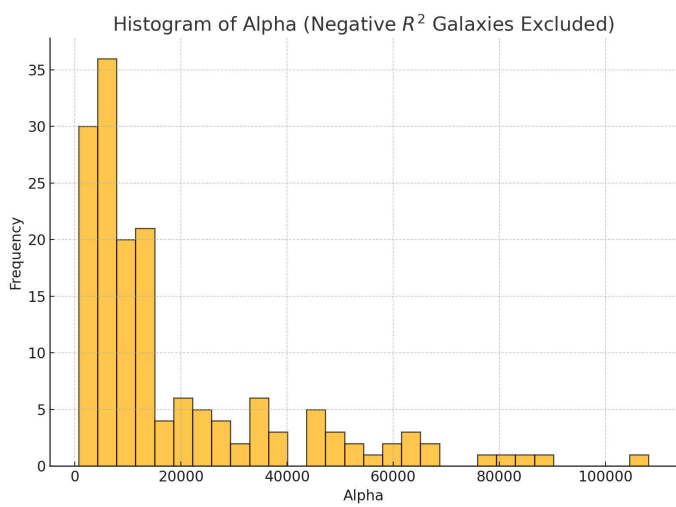
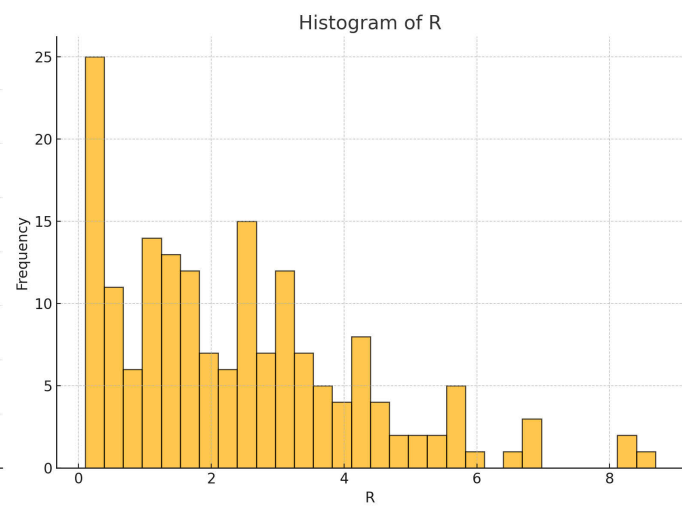
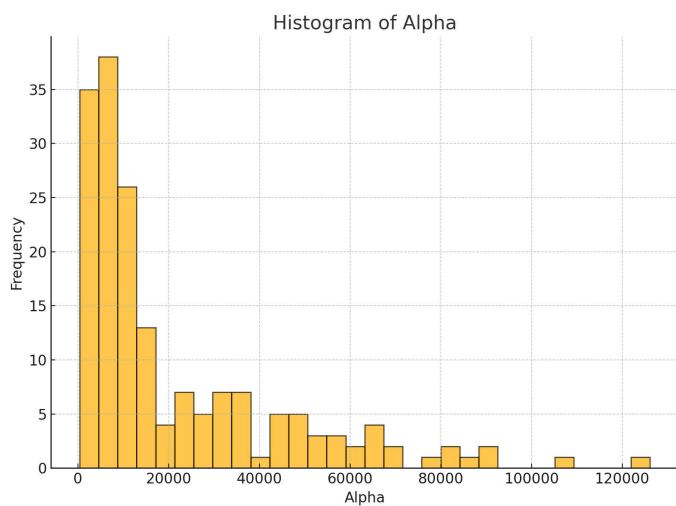
	Alpha	R	R^2	Avg_Radius	Avg_Vobs	Avg_errV	Avg_Predicted_Velocity	Avg_Residual	Residual_Std_Dev	Avg_Vdisk	Avg_Vgas	Avg_Vbul	Avg_SBdisk	Avg_SBbul
Alpha	1	-0.240	-0.548	0.714	0.956	0.411	0.956	-0.137	0.766	0.863	0.469	0.653	0.588	0.419
R	-0.240	1	0.544	-0.157	-0.349	-0.037	-0.349	0.088	-0.366	-0.289	-0.081	-0.408	-0.280	-0.289
R^2	-0.548	0.544	1	-0.579	-0.632	-0.228	-0.632	0.039	-0.709	-0.540	-0.303	-0.591	-0.275	-0.365
Avg_Radius	0.714	-0.157	-0.579	1	0.759	0.293	0.759	-0.109	0.694	0.629	0.665	0.338	0.195	0.095
Avg_Vobs	0.956	-0.349	-0.632	0.759	1	0.450	1.000	-0.138	0.811	0.903	0.564	0.683	0.598	0.443
Avg_errV	0.411	-0.037	-0.228	0.293	0.450	1	0.450	-0.139	0.387	0.412	0.286	0.327	0.377	0.178
Avg_Predicted_Velocity	0.956	-0.349	-0.632	0.759	1.000	0.450	1	-0.144	0.810	0.903	0.564	0.683	0.598	0.443
Avg_Residual	-0.137	0.088	0.039	-0.109	-0.138	-0.139	-0.144	1	0.054	-0.131	-0.099	-0.080	-0.015	-0.024
Residual_Std_Dev	0.766	-0.366	-0.709	0.694	0.811	0.387	0.810	0.054	1	0.722	0.380	0.595	0.522	0.393
Avg_Vdisk	0.863	-0.289	-0.540	0.629	0.903	0.412	0.903	-0.131	0.722	1	0.545	0.485	0.727	0.263
Avg_Vgas	0.469	-0.081	-0.303	0.665	0.564	0.286	0.564	-0.099	0.380	0.545	1	0.181	0.218	-0.002
Avg_Vbul	0.653	-0.408	-0.591	0.338	0.683	0.327	0.683	-0.080	0.595	0.485	0.181	1	0.438	0.749
Avg_SBdisk	0.588	-0.280	-0.275	0.195	0.598	0.377	0.598	-0.015	0.522	0.727	0.218	0.438	1	0.405
Avg_SBbul	0.419	-0.289	-0.365	0.095	0.443	0.178	0.443	-0.024	0.393	0.263	-0.002	0.749	0.405	1

Correlation Matrix Heatmap

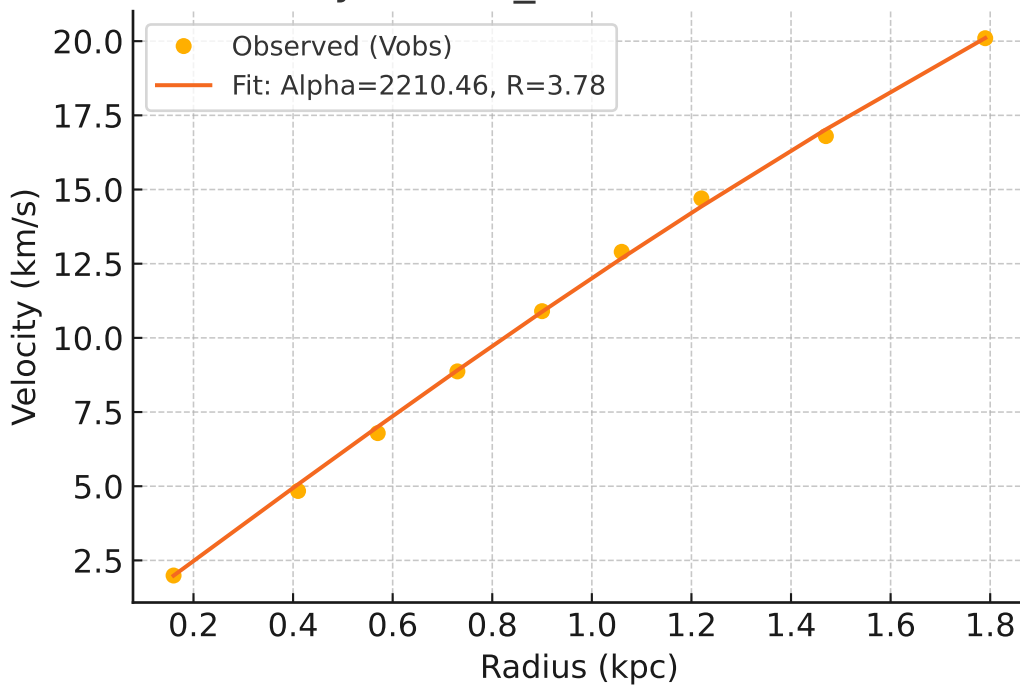


Summary Statistics of Alpha and R (Original and Filtered Dataset)
(Filtered dataset excludes galaxies with negative R^2)

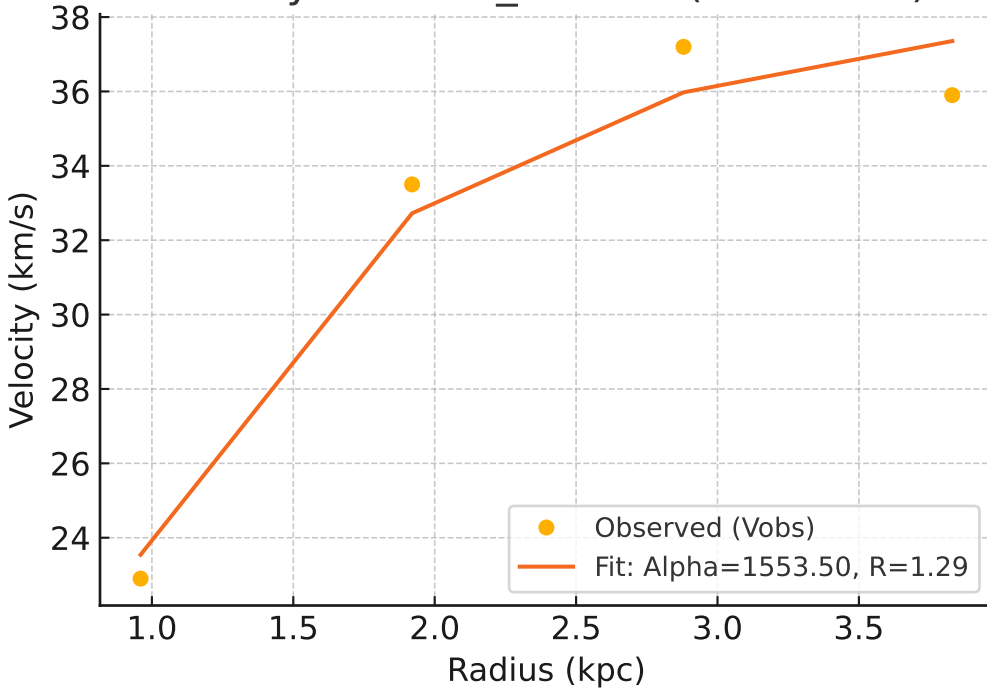
	Count	Mean	Median	Standard Deviation	Min	Max
Alpha	175	21502	11458	23706	373	126070
R	175	2.38	2.10	1.86	0.100	8.69
Alpha (Filtered Dataset)	160	18570	9663	20741	682	108092
R (Filtered Dataset)	160	2.59	2.42	1.80	0.100	8.69



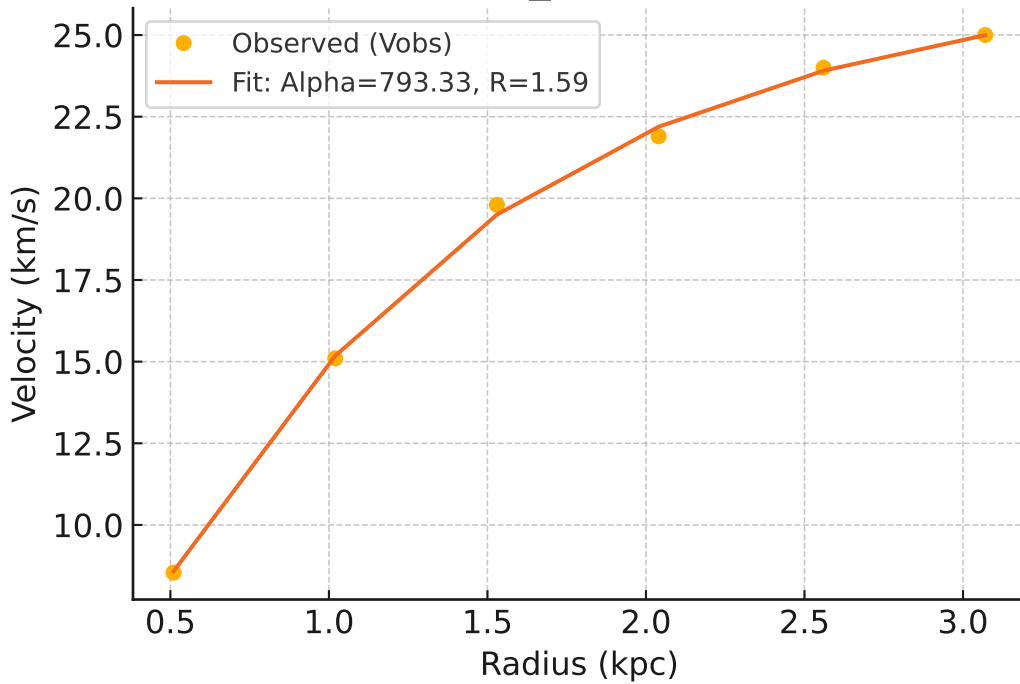
Galaxy: CamB_rotmod ($R^2=0.999$)



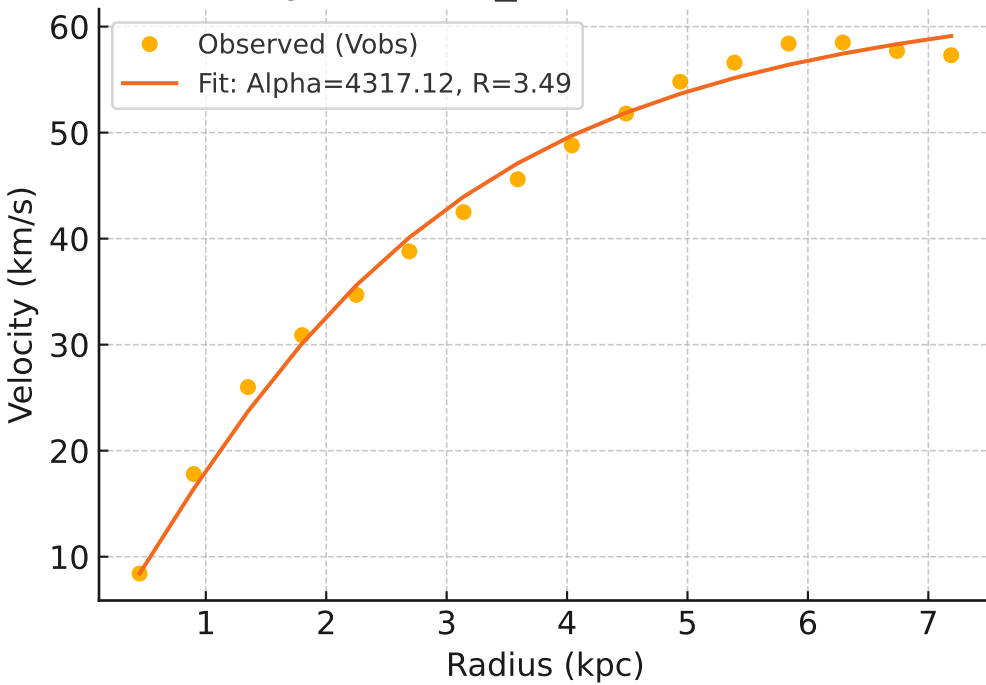
Galaxy: D512-2_rotmod ($R^2=0.963$)



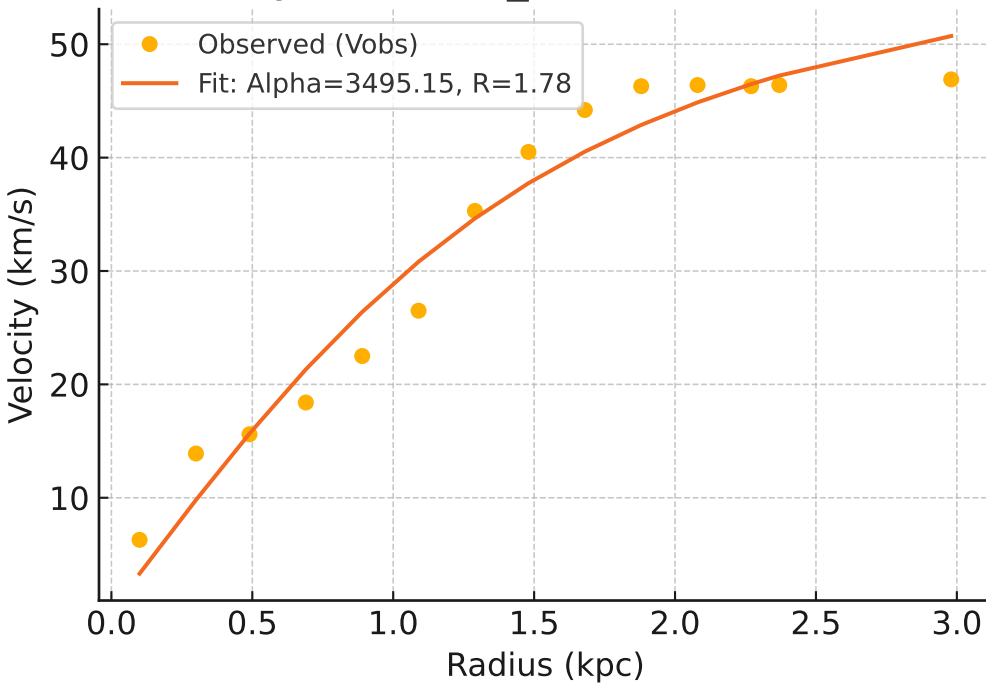
Galaxy: D564-8_rotmod ($R^2=0.999$)



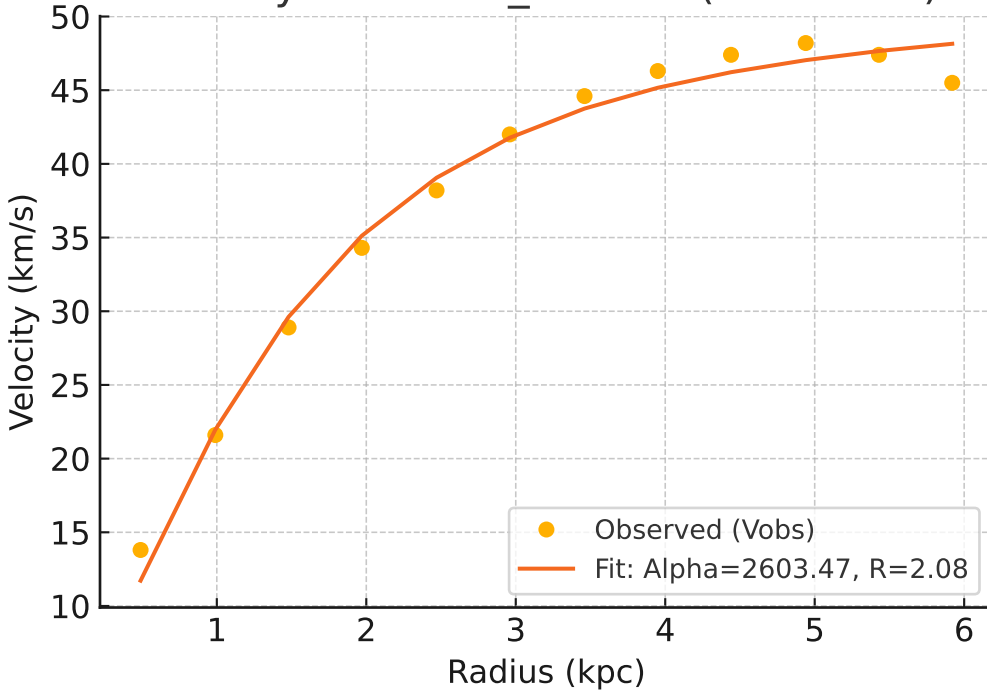
Galaxy: D631-7_rotmod ($R^2=0.992$)



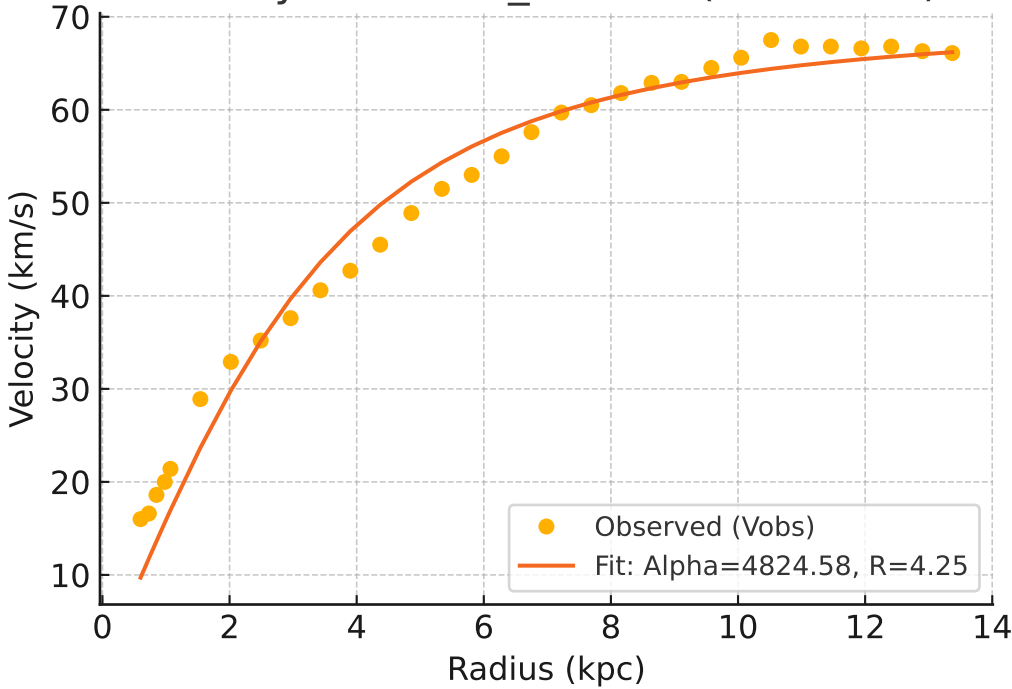
Galaxy: DDO064_rotmod ($R^2=0.958$)



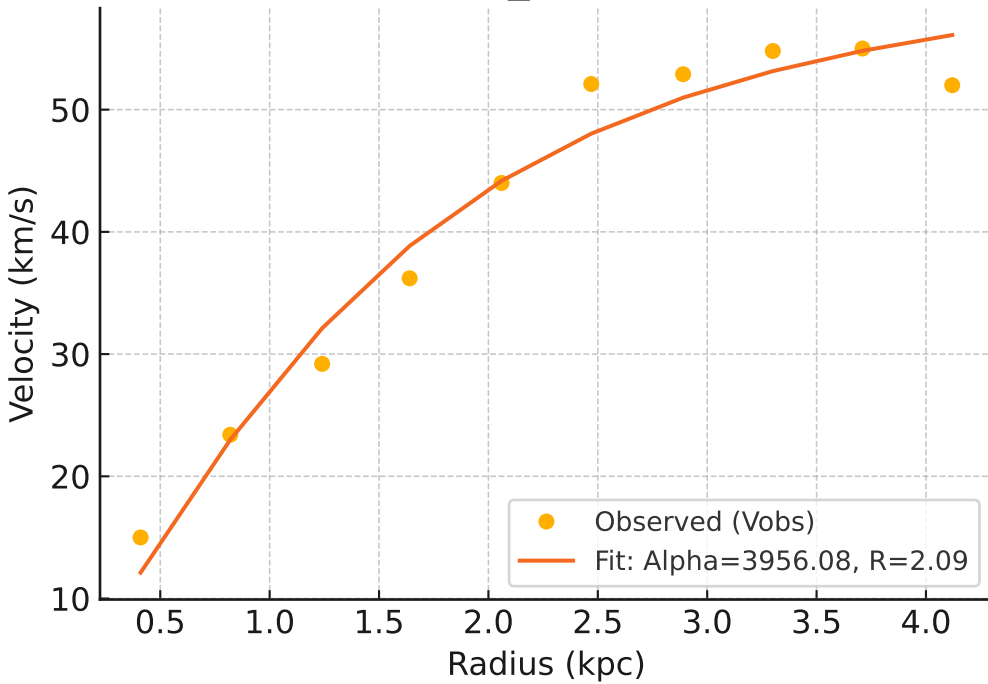
Galaxy: DDO154_rotmod ($R^2=0.987$)



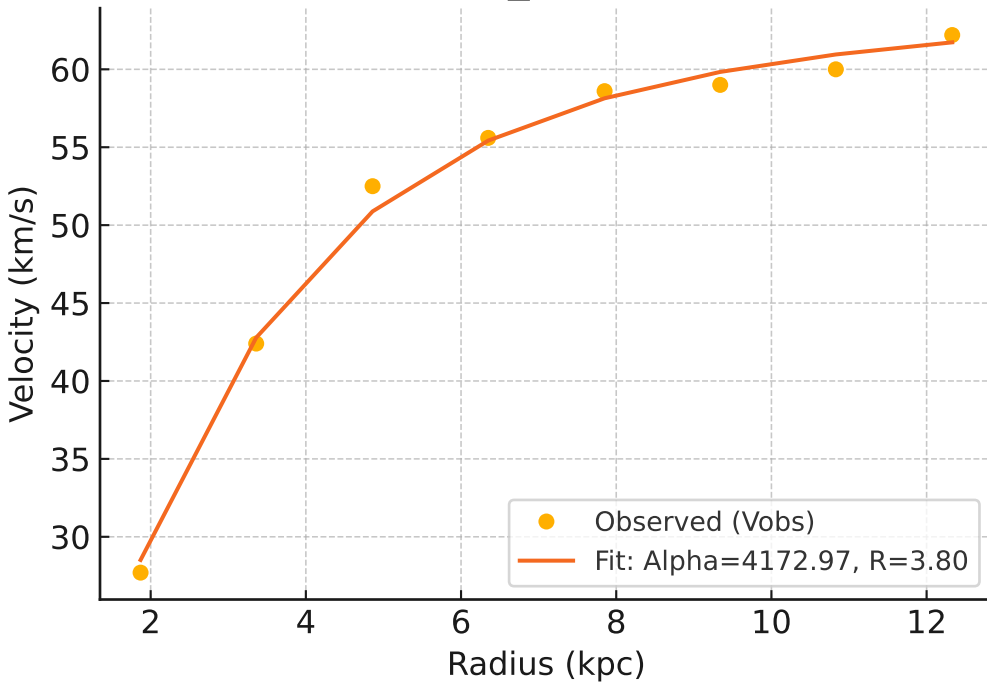
Galaxy: DDO161_rotmod ($R^2=0.971$)



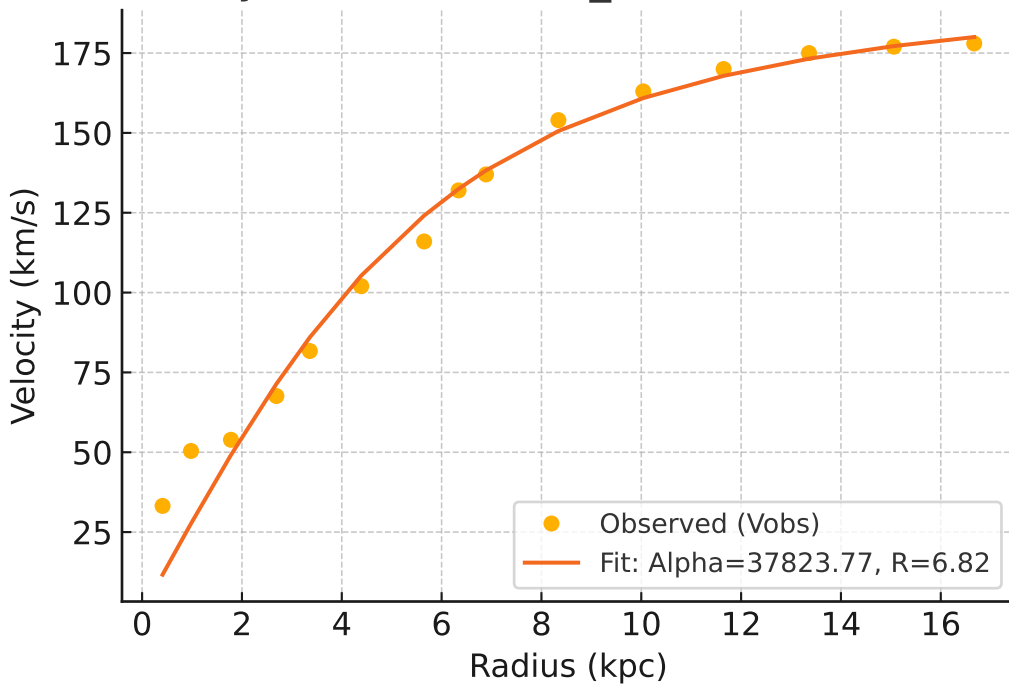
Galaxy: DDO168_rotmod ($R^2=0.967$)



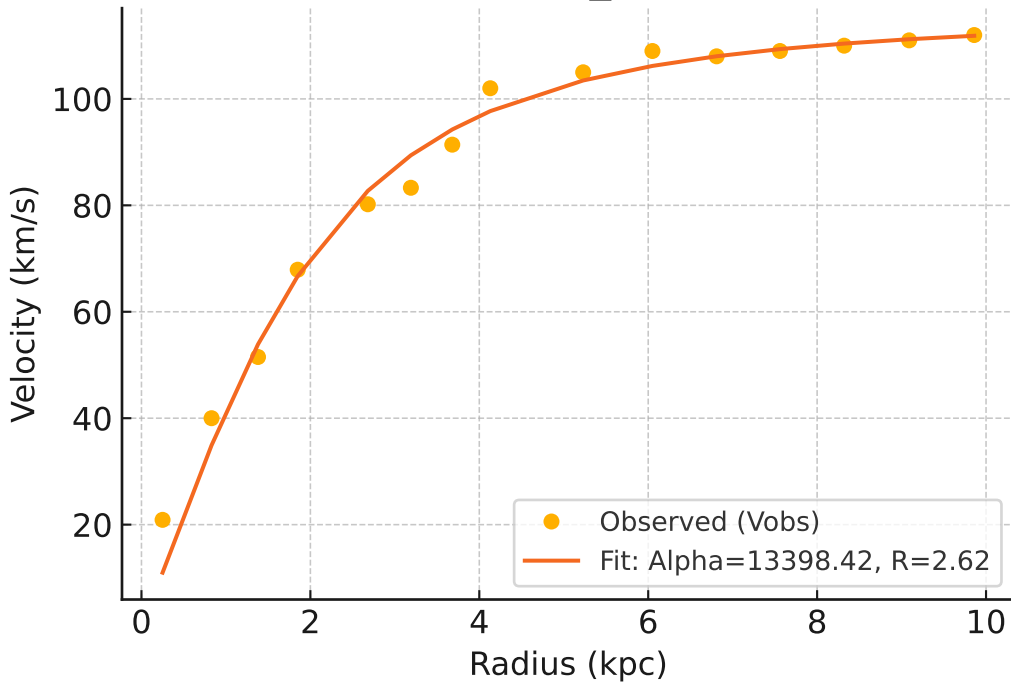
Galaxy: DDO170_rotmod ($R^2=0.994$)



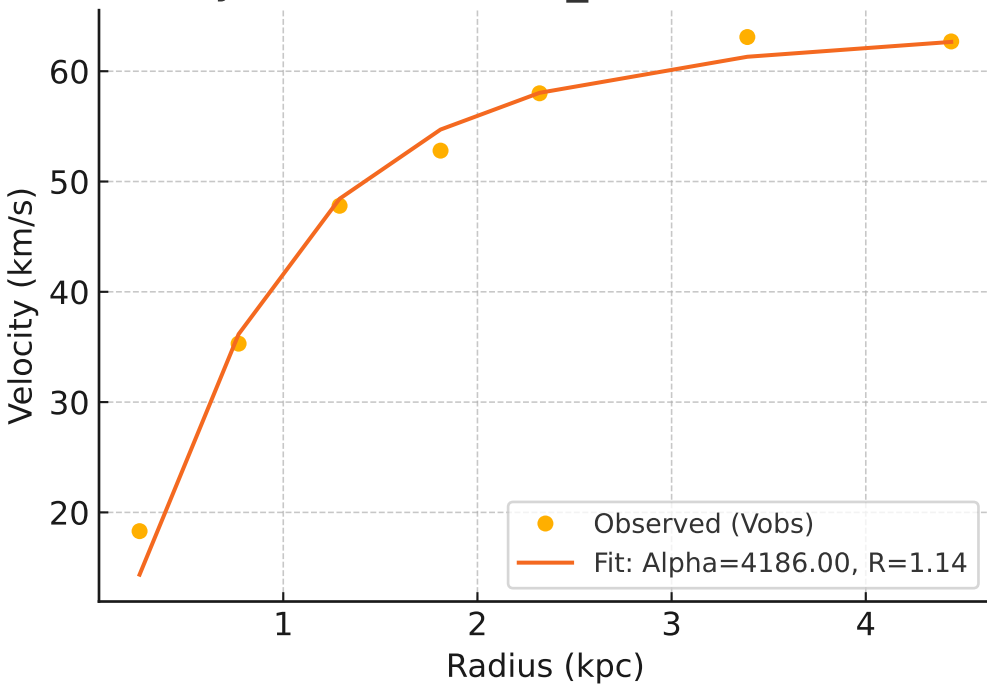
Galaxy: ESO079-G014_rotmod ($R^2=0.969$)



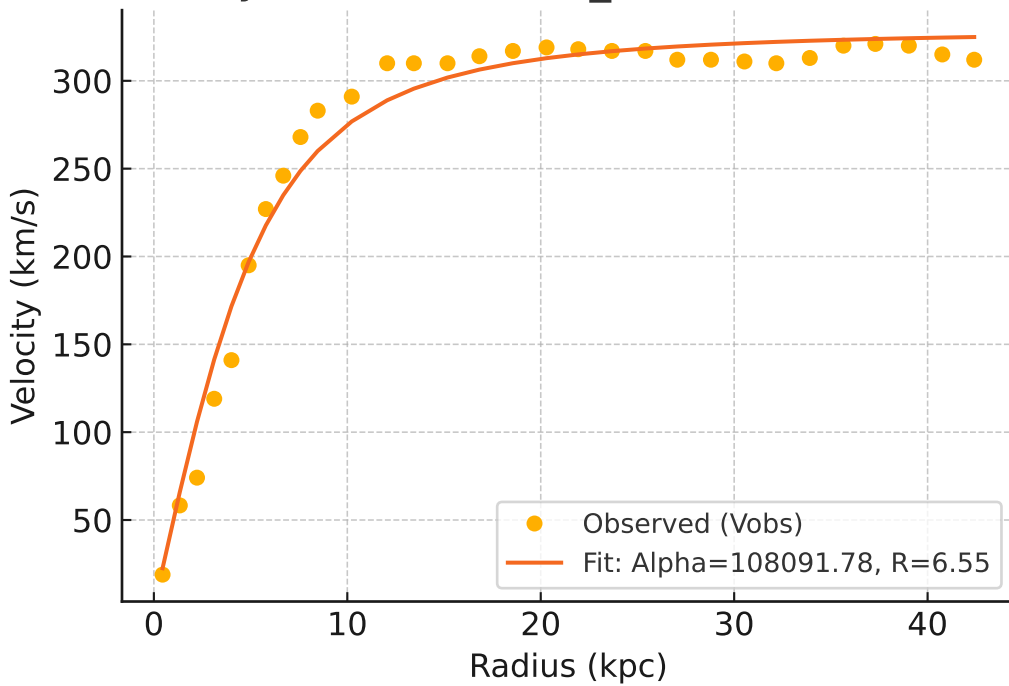
Galaxy: ESO116-G012_rotmod ($R^2=0.982$)



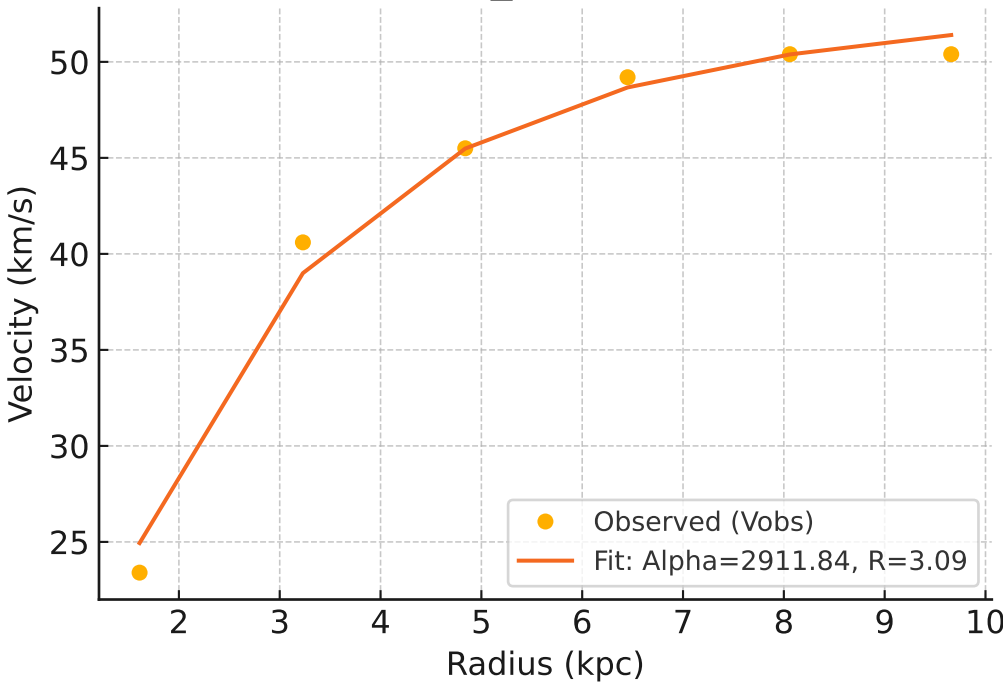
Galaxy: ESO444-G084_rotmod ($R^2=0.985$)



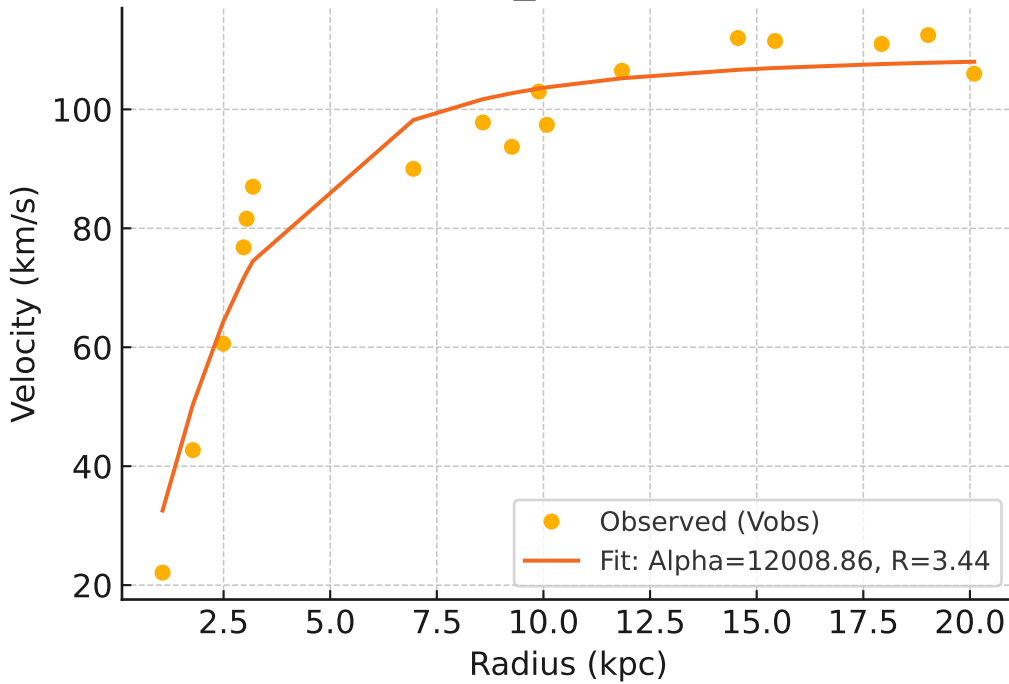
Galaxy: ESO563-G021_rotmod ($R^2=0.976$)



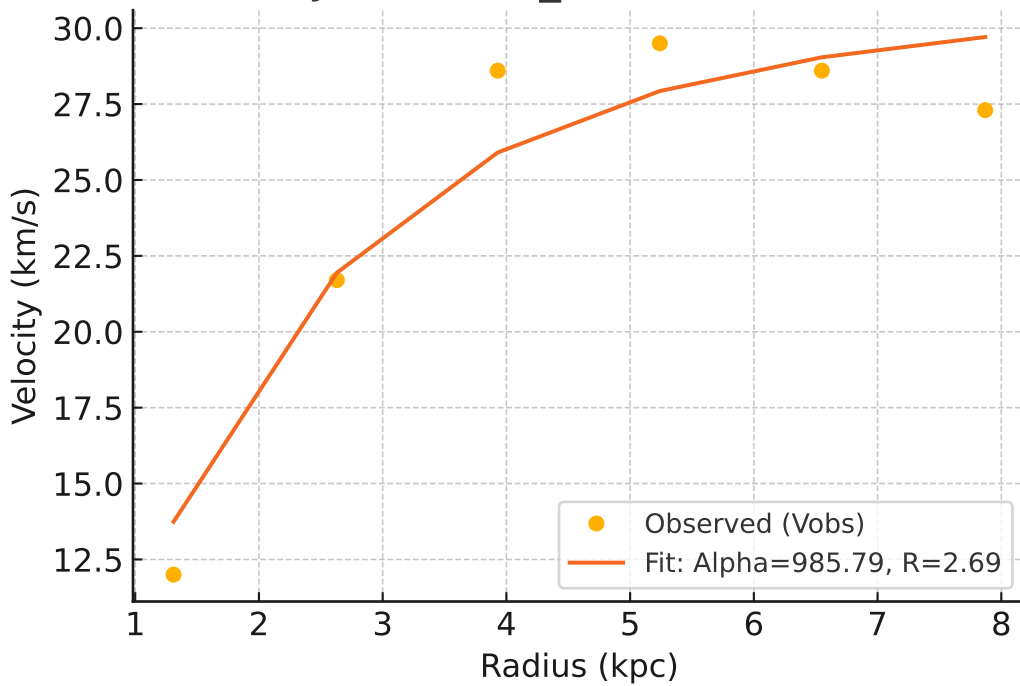
Galaxy: F561-1_rotmod ($R^2=0.989$)



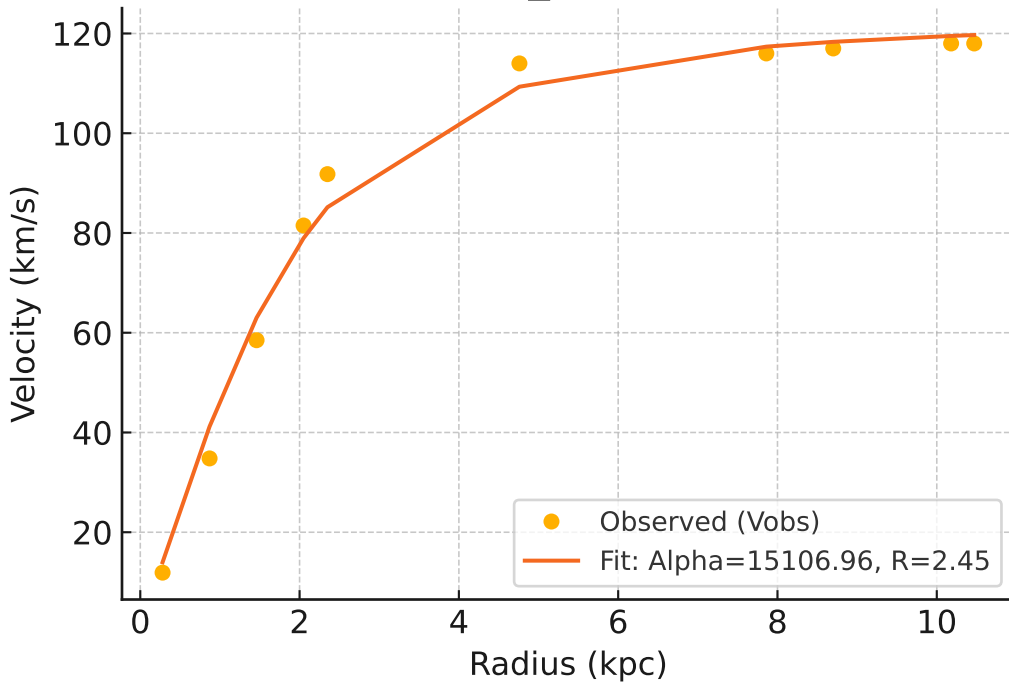
Galaxy: F563-1_rotmod ($R^2=0.931$)



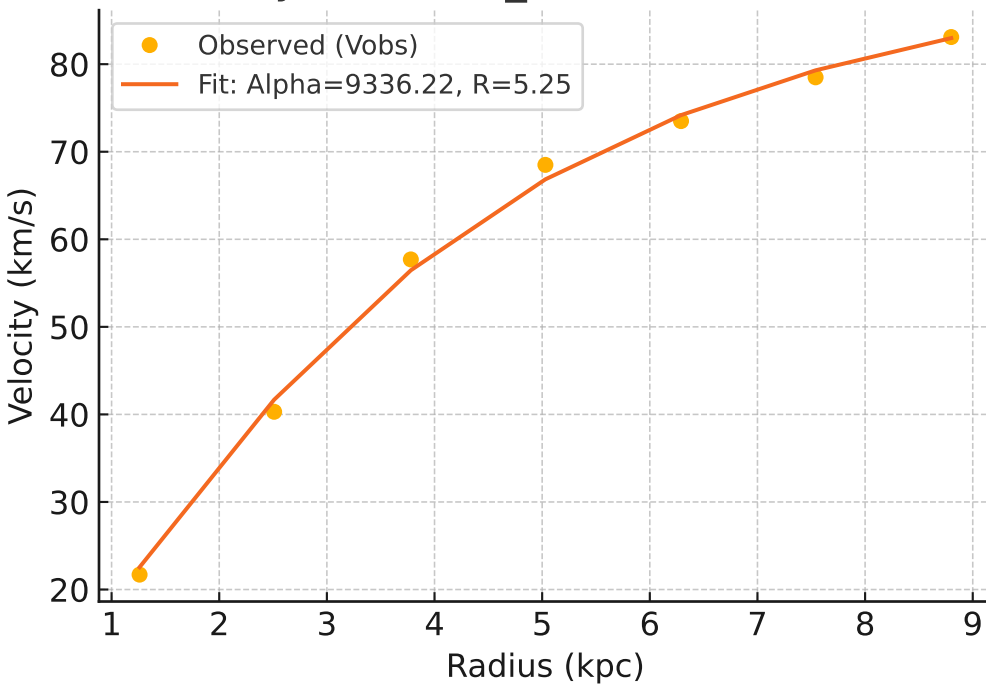
Galaxy: F563-V1_rotmod ($R^2=0.918$)



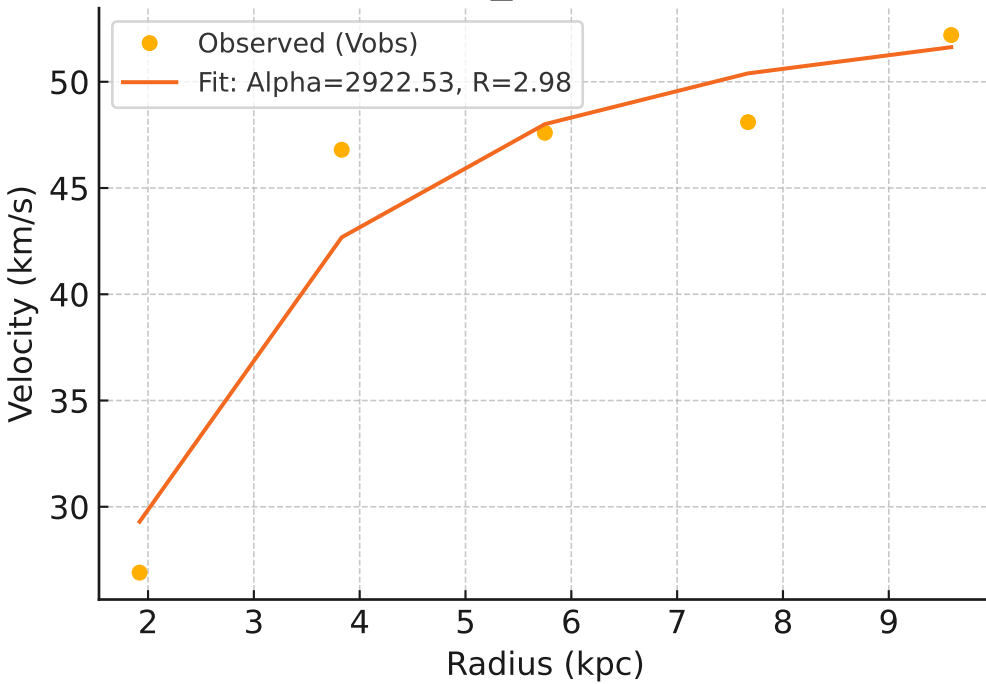
Galaxy: F563-V2_rotmod ($R^2=0.989$)



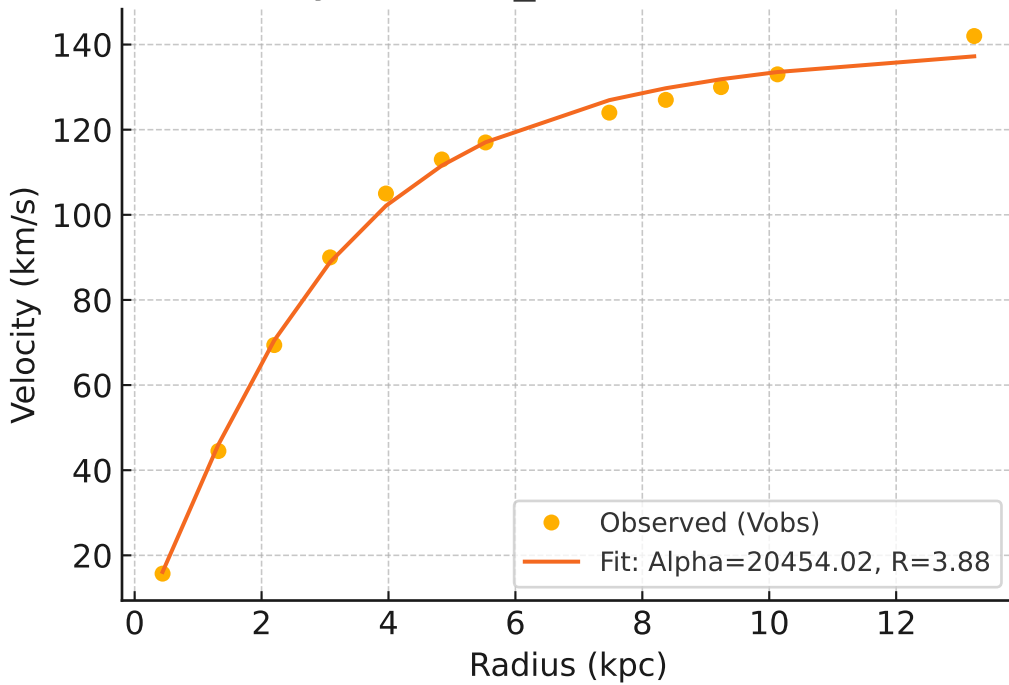
Galaxy: F565-V2_rotmod ($R^2=0.997$)



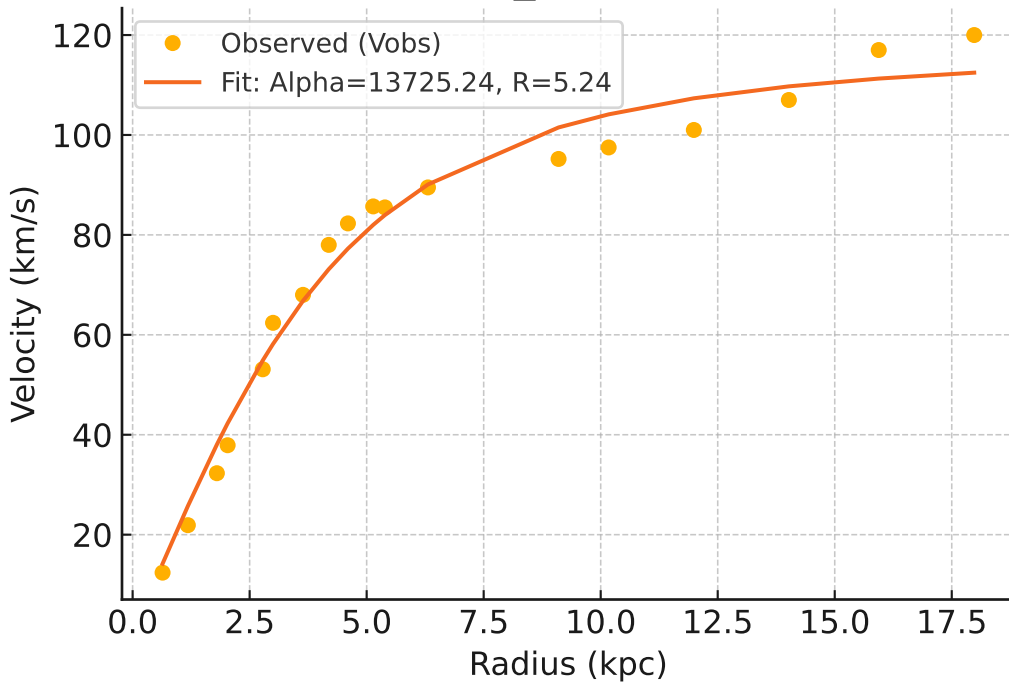
Galaxy: F567-2_rotmod ($R^2=0.928$)



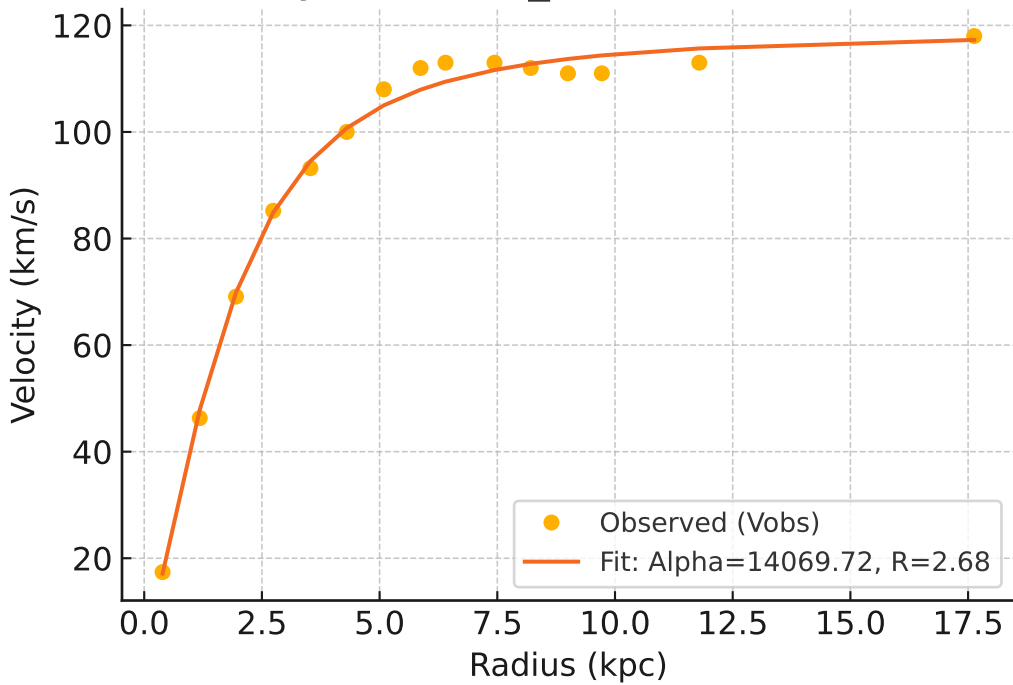
Galaxy: F568-1_rotmod ($R^2=0.997$)



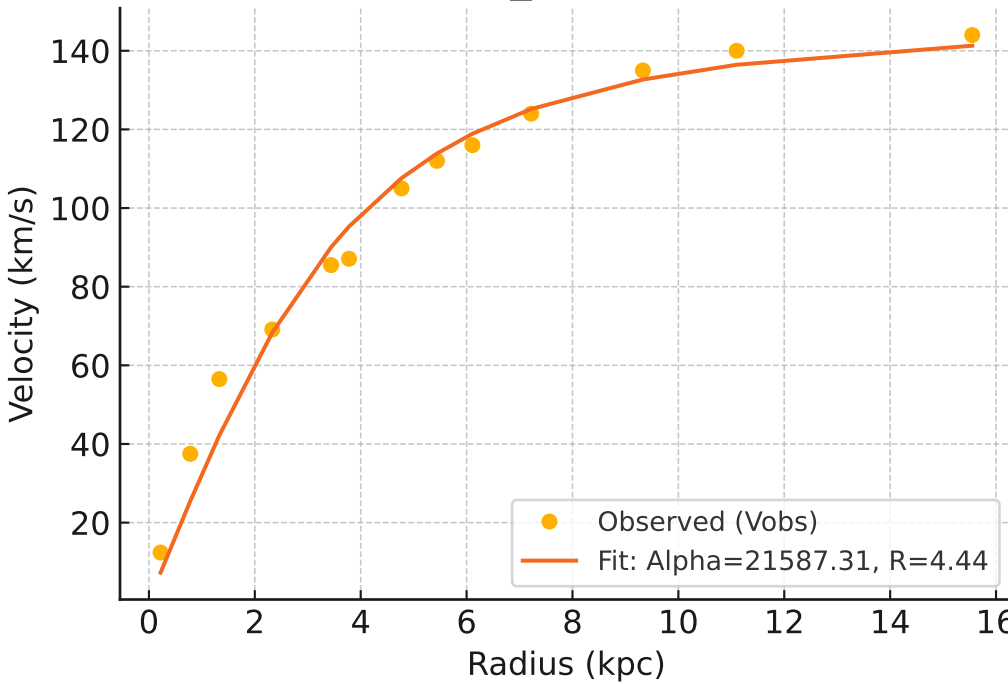
Galaxy: F568-3_rotmod ($R^2=0.978$)



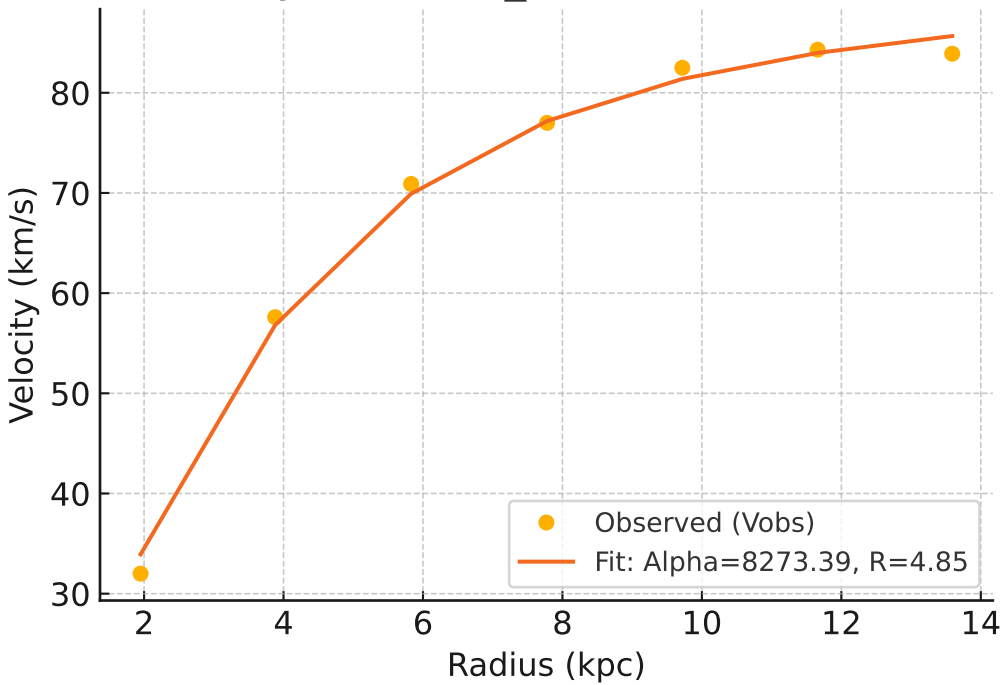
Galaxy: F568-V1_rotmod ($R^2=0.994$)



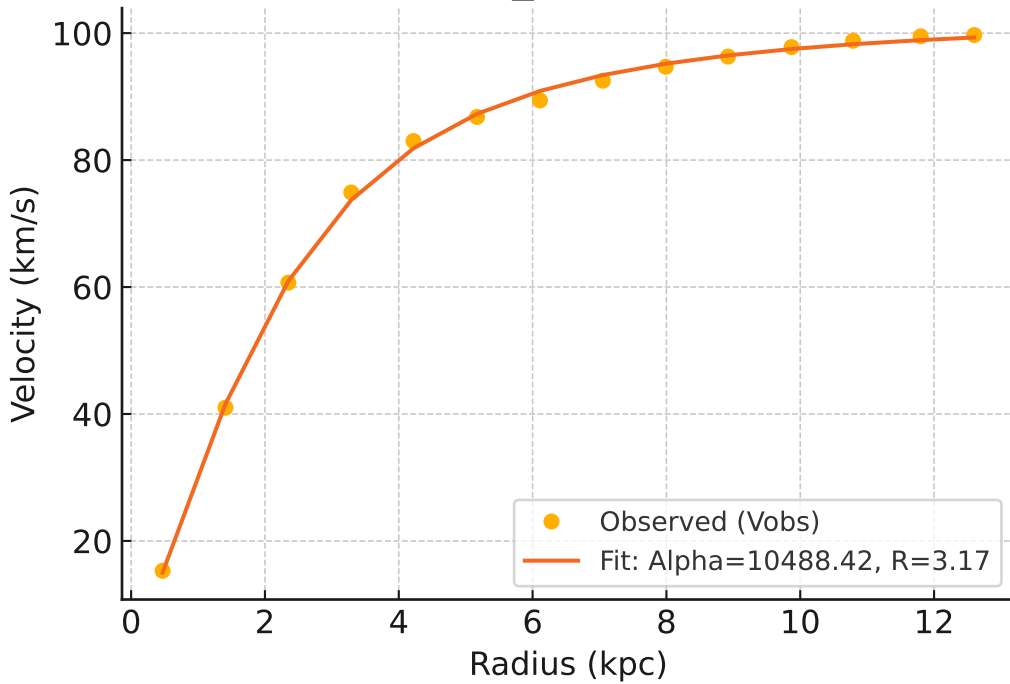
Galaxy: F571-8_rotmod ($R^2=0.975$)



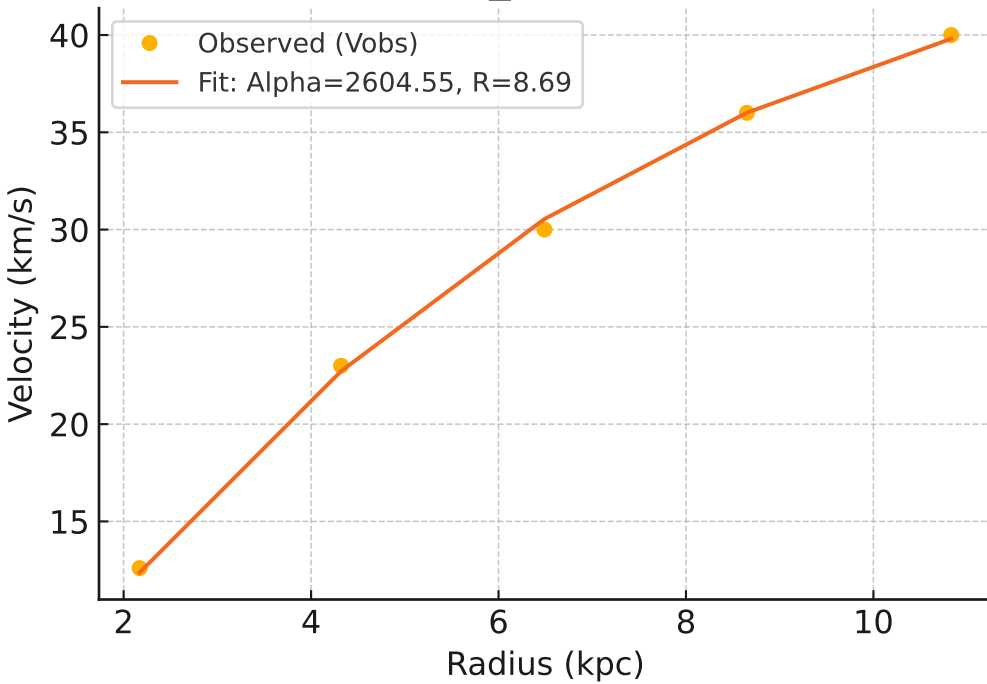
Galaxy: F571-V1_rotmod ($R^2=0.996$)



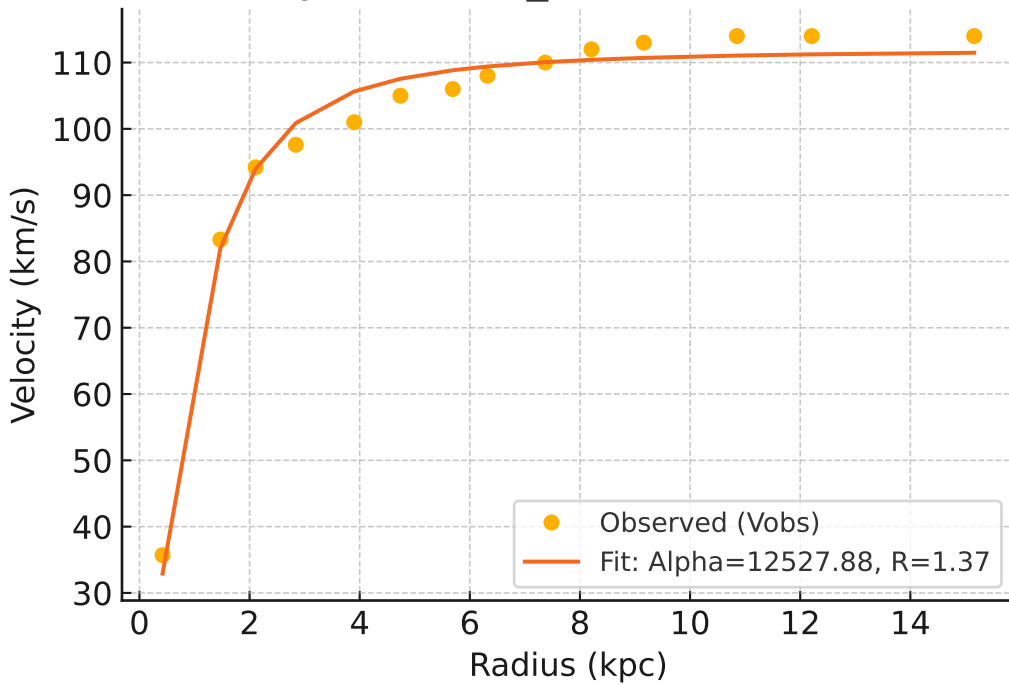
Galaxy: F574-1_rotmod ($R^2=0.999$)



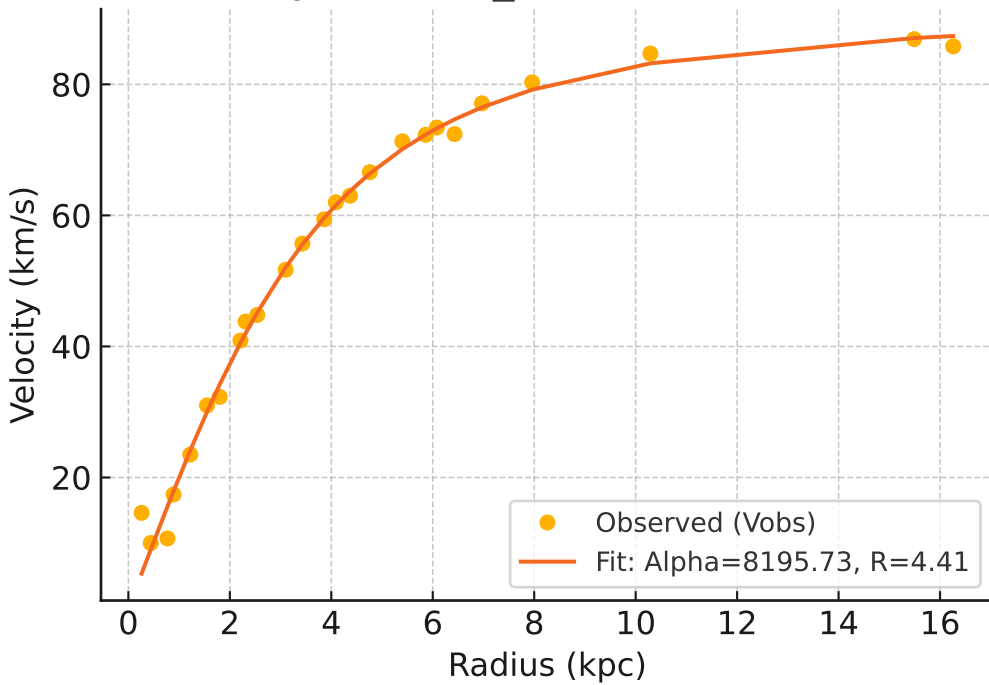
Galaxy: F574-2_rotmod ($R^2=0.999$)



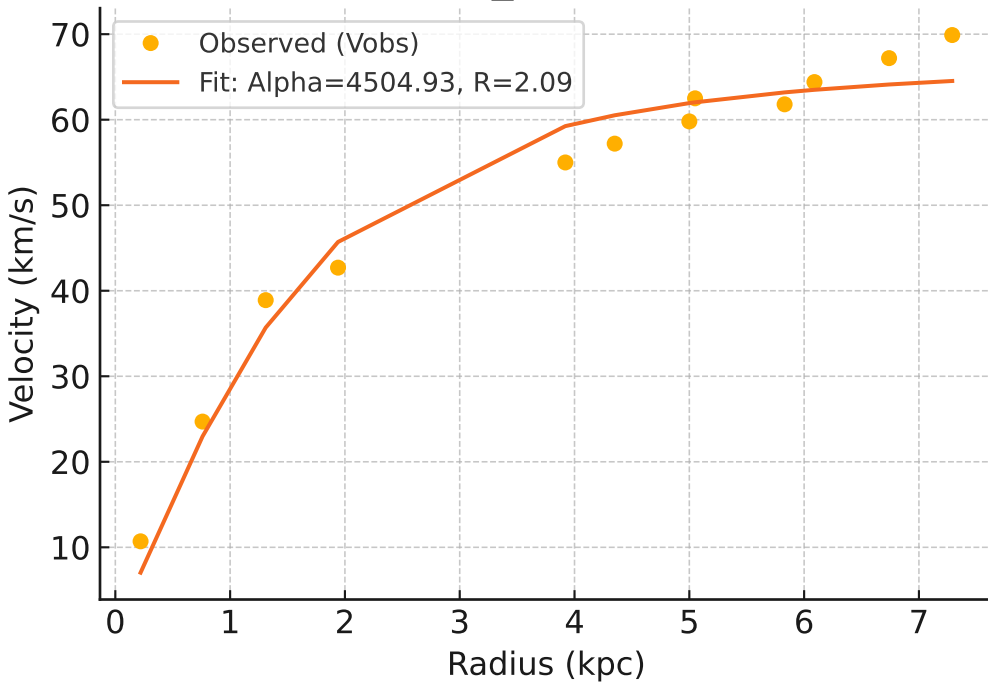
Galaxy: F579-V1_rotmod ($R^2=0.984$)



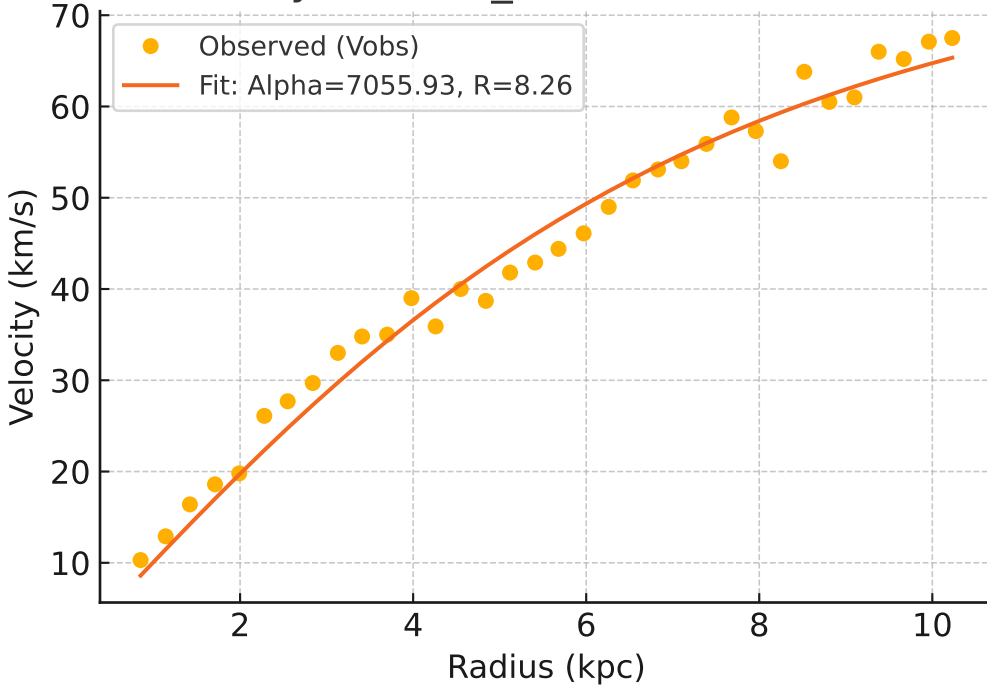
Galaxy: F583-1_rotmod ($R^2=0.991$)



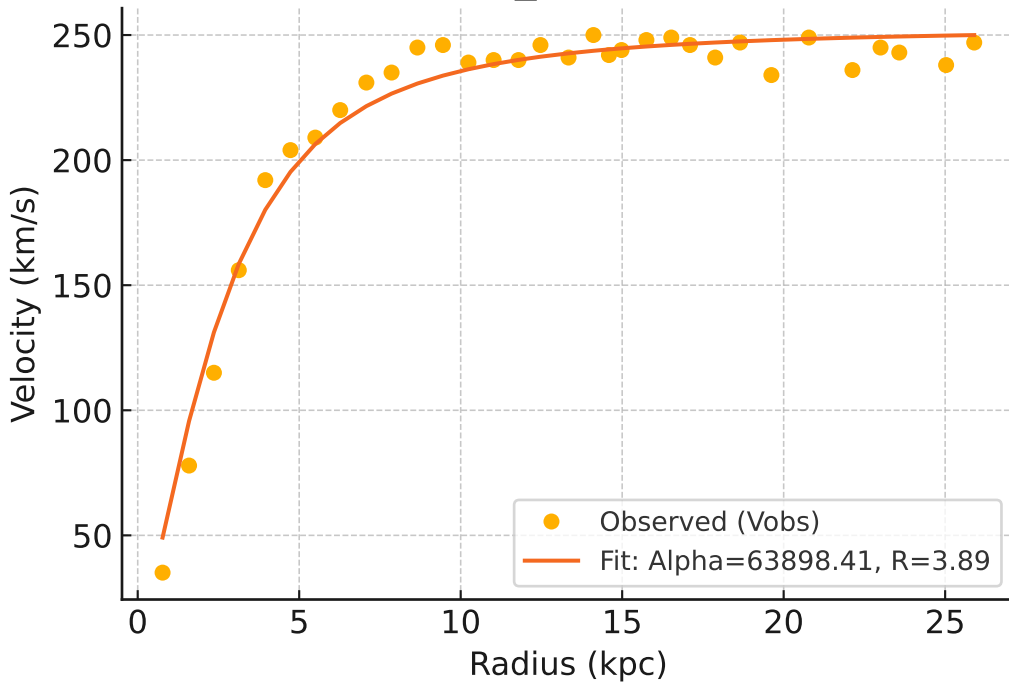
Galaxy: F583-4_rotmod ($R^2=0.970$)



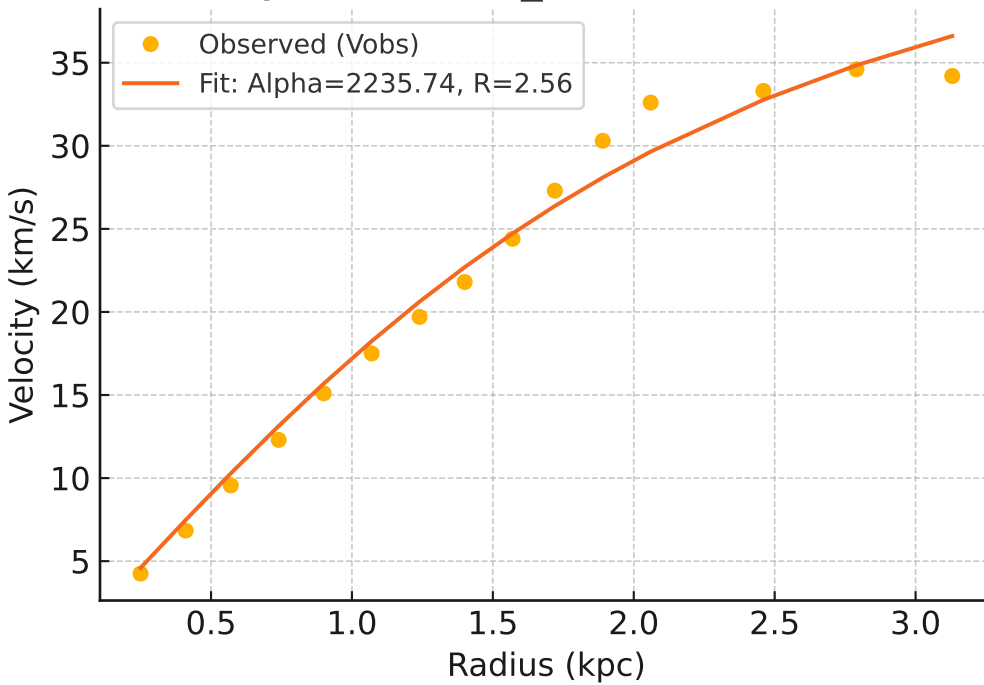
Galaxy: IC2574_rotmod ($R^2=0.979$)



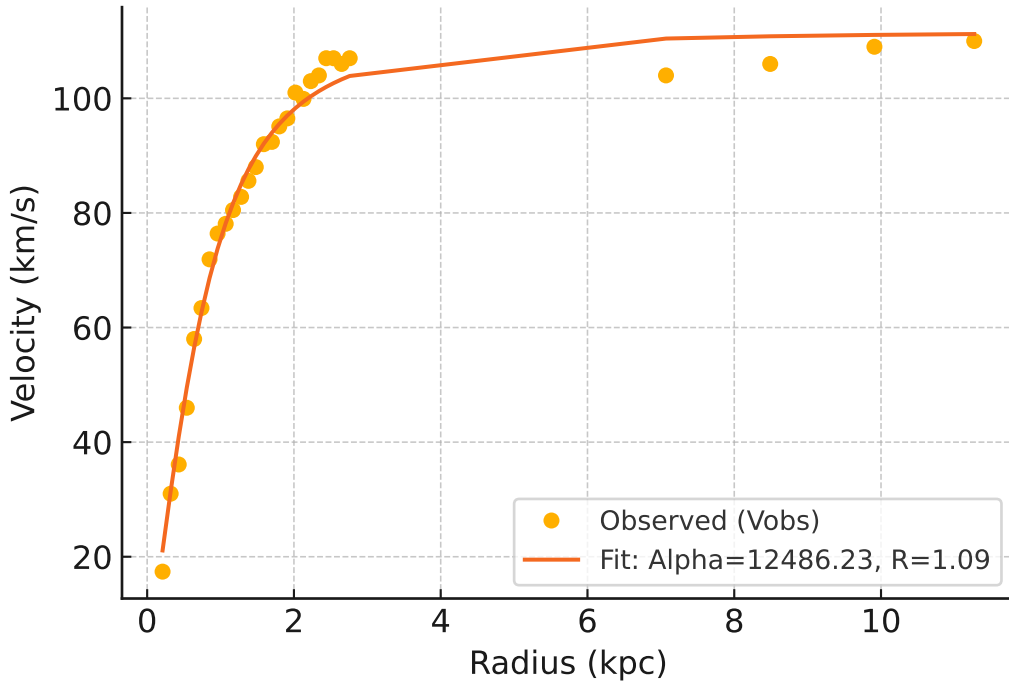
Galaxy: IC4202_rotmod ($R^2=0.973$)



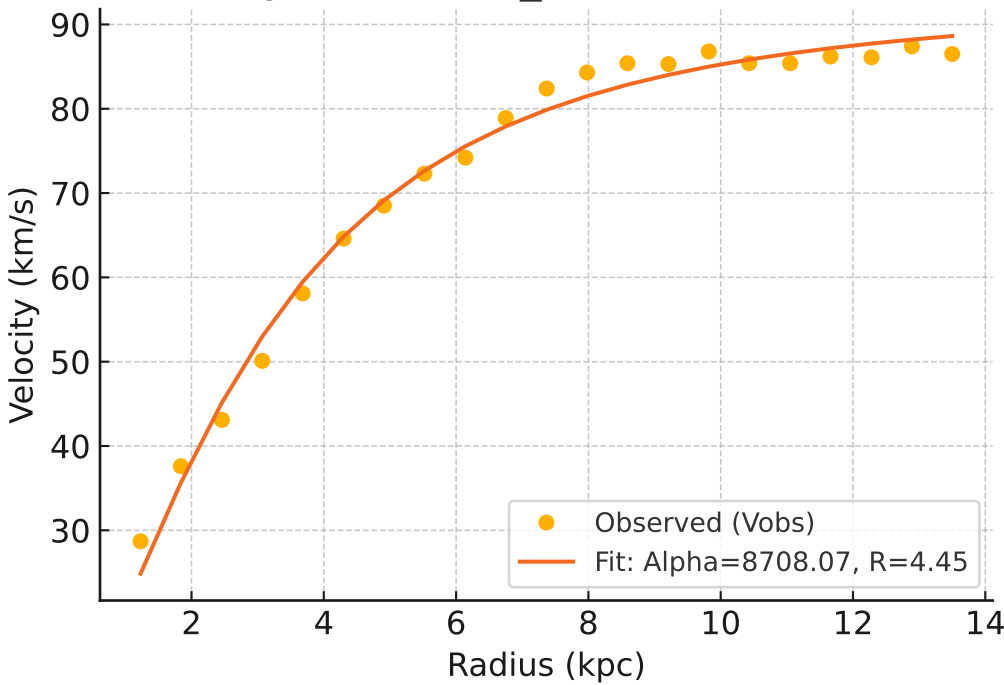
Galaxy: KK98-251_rotmod ($R^2=0.984$)



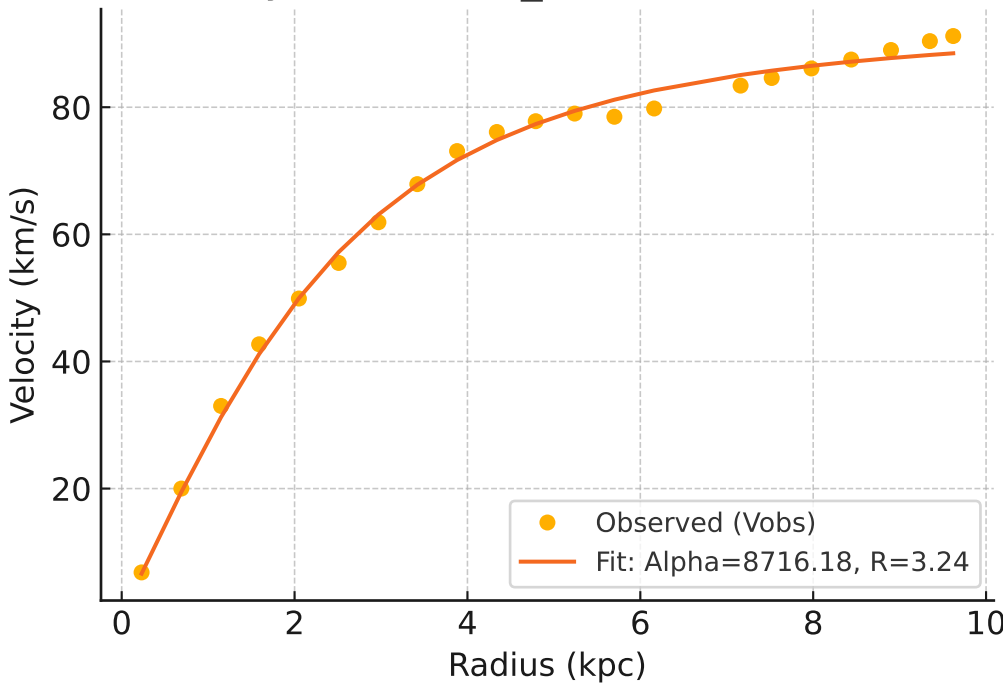
Galaxy: NGC0024_rotmod ($R^2=0.987$)



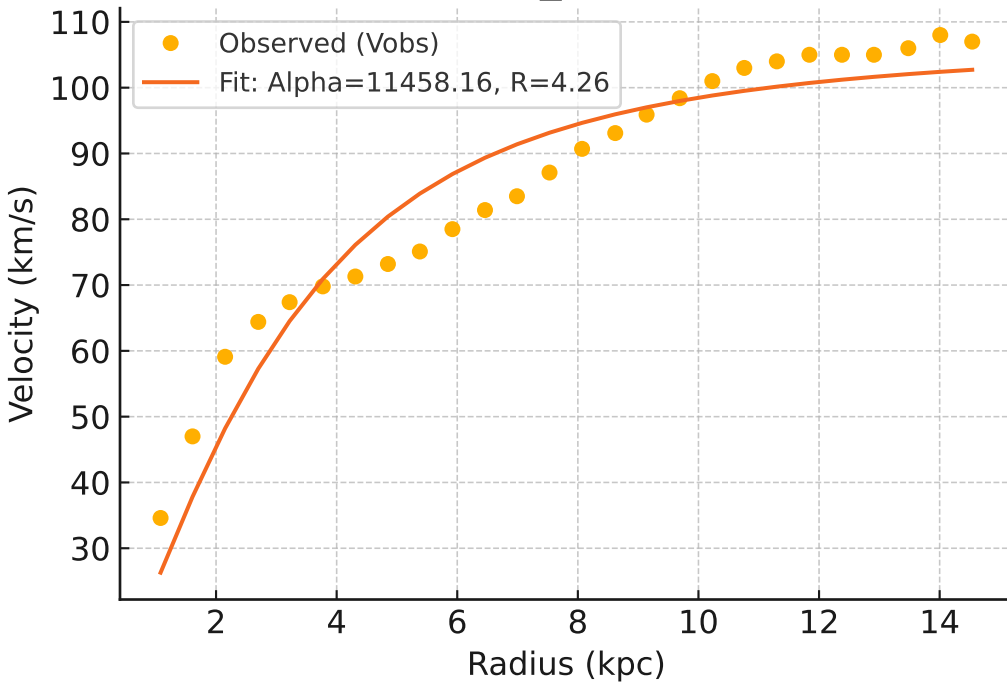
Galaxy: NGC0055_rotmod ($R^2=0.989$)



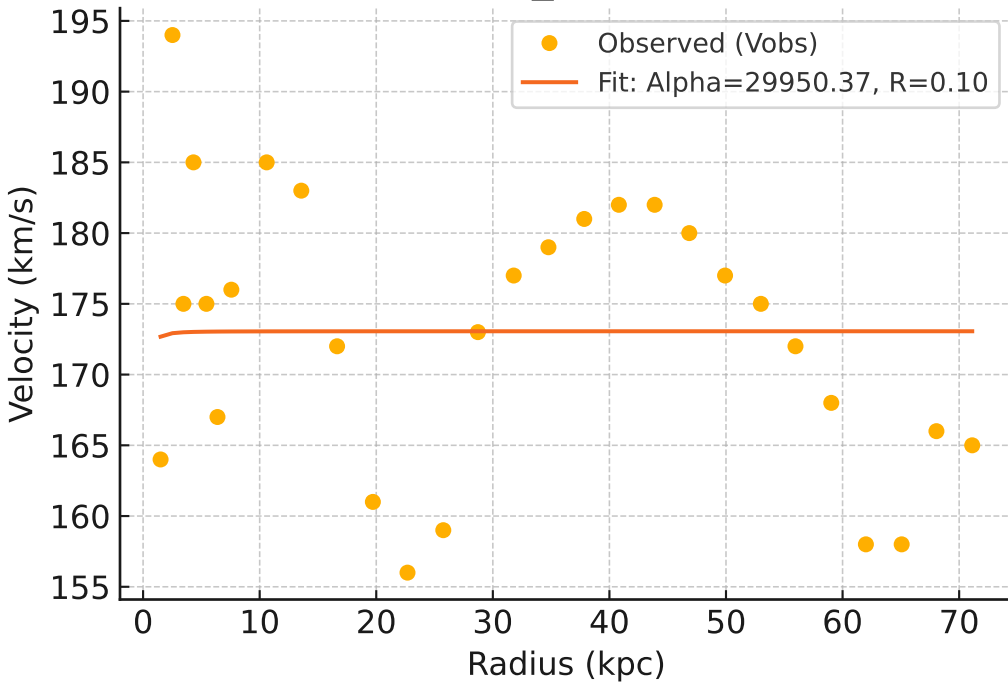
Galaxy: NGC0100_rotmod ($R^2=0.996$)



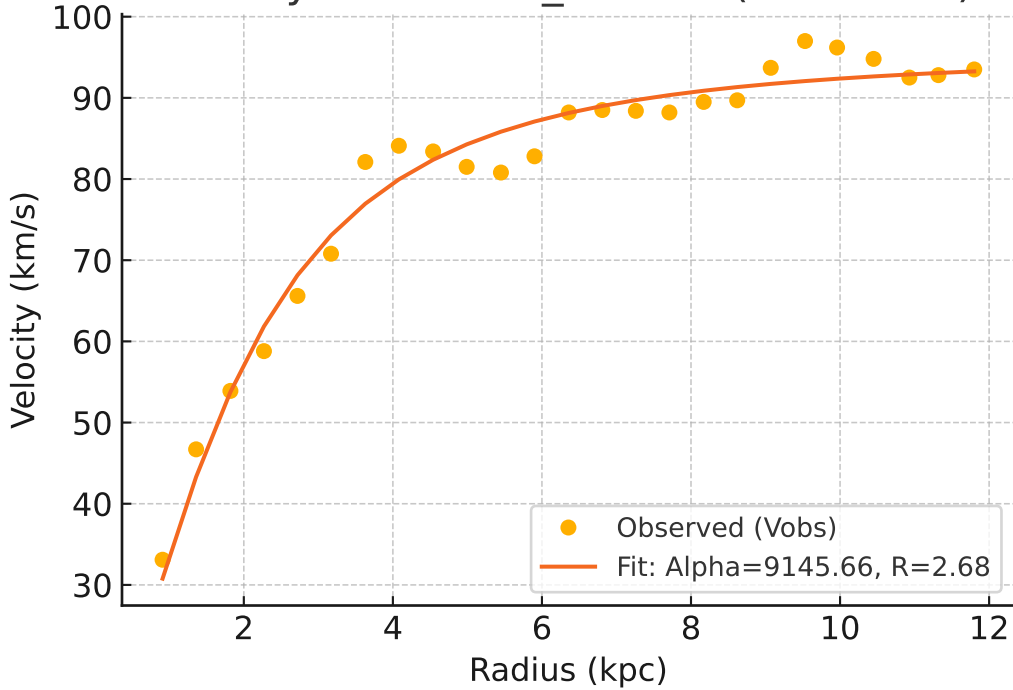
Galaxy: NGC0247_rotmod ($R^2=0.913$)



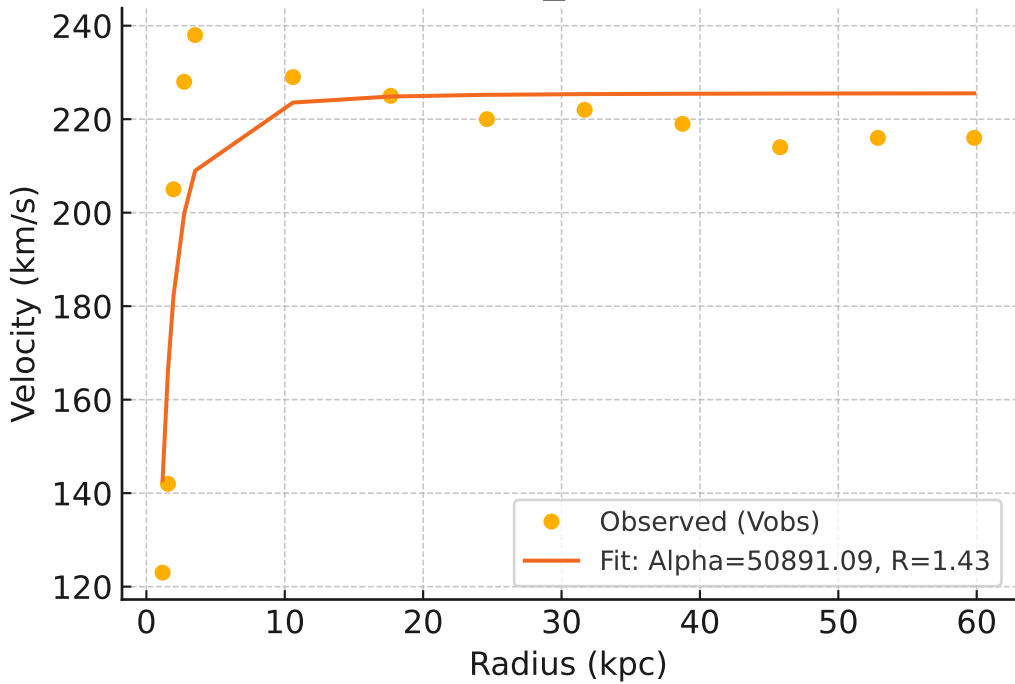
Galaxy: NGC0289_rotmod ($R^2=-0.000$)



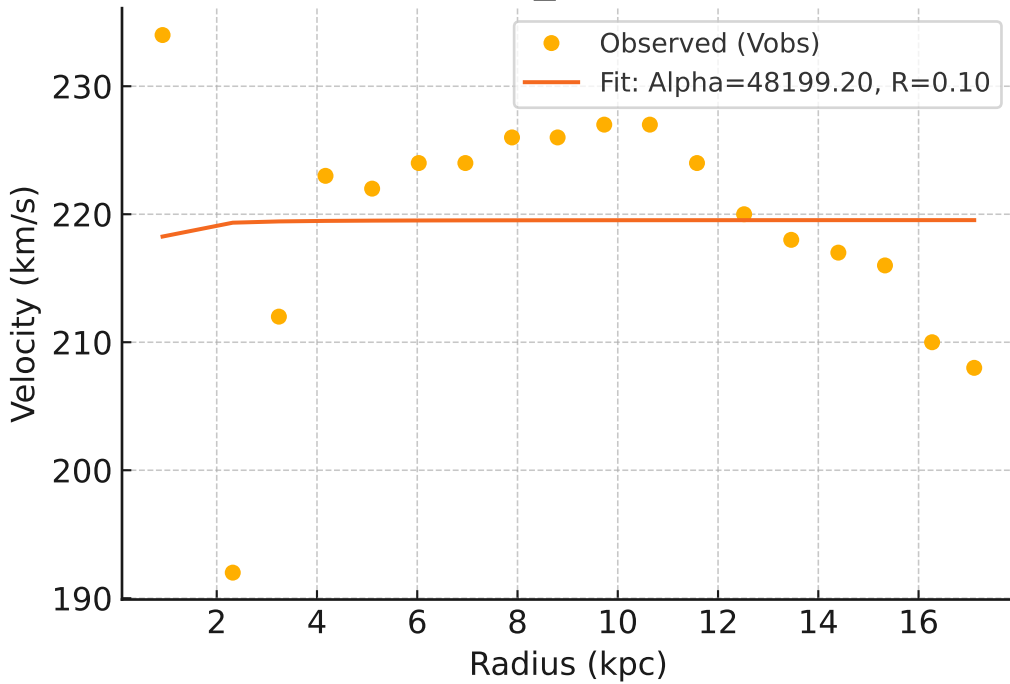
Galaxy: NGC0300_rotmod ($R^2=0.971$)



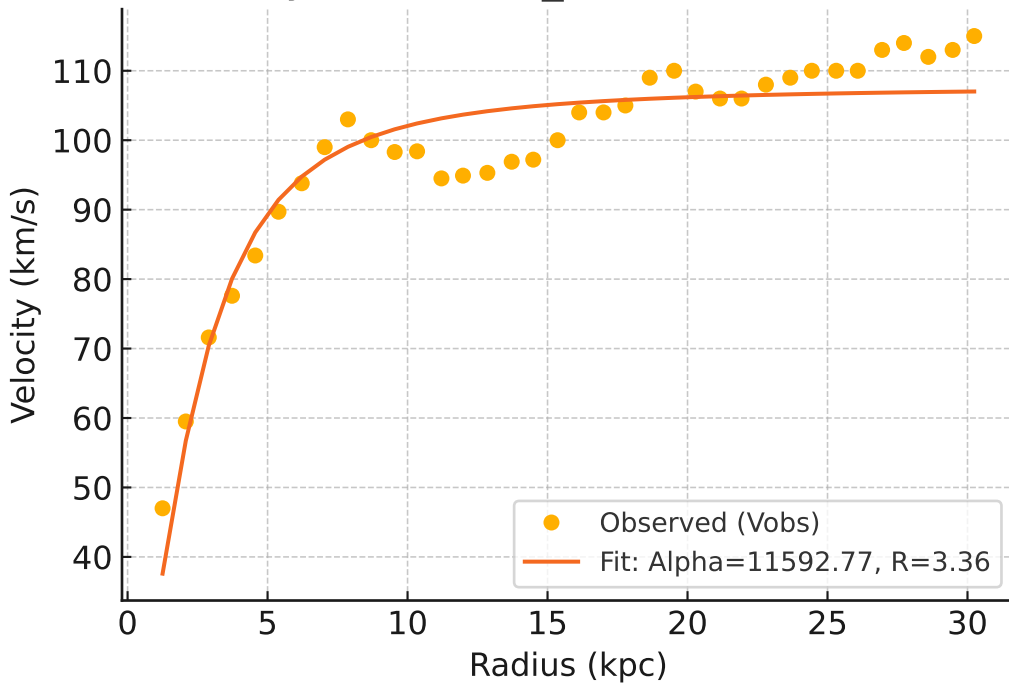
Galaxy: NGC0801_rotmod ($R^2=0.750$)



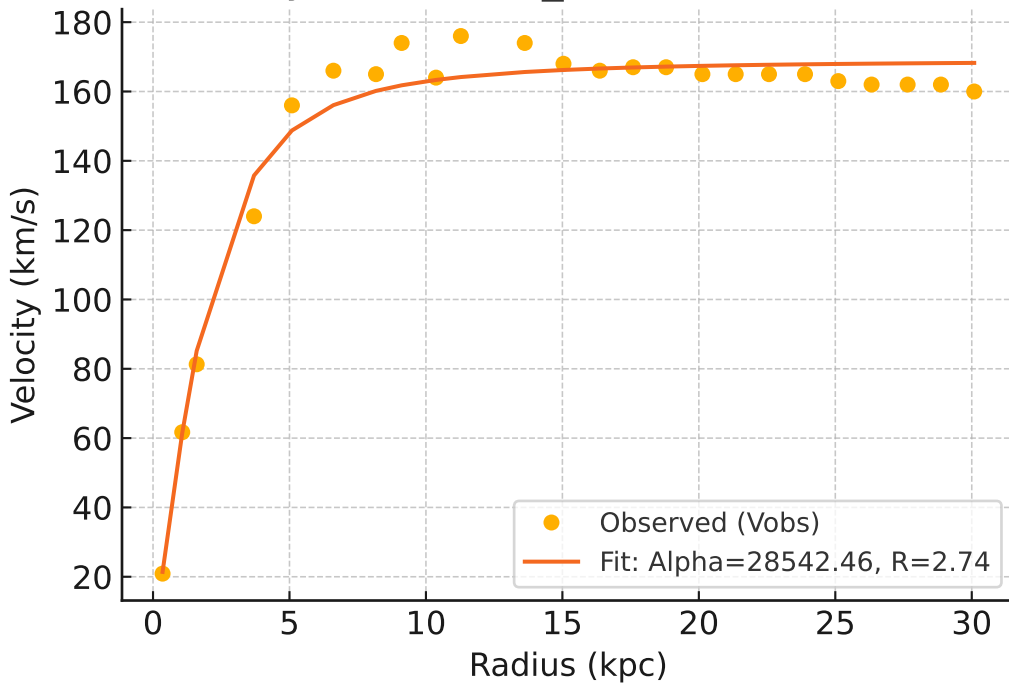
Galaxy: NGC0891_rotmod ($R^2=-0.018$)



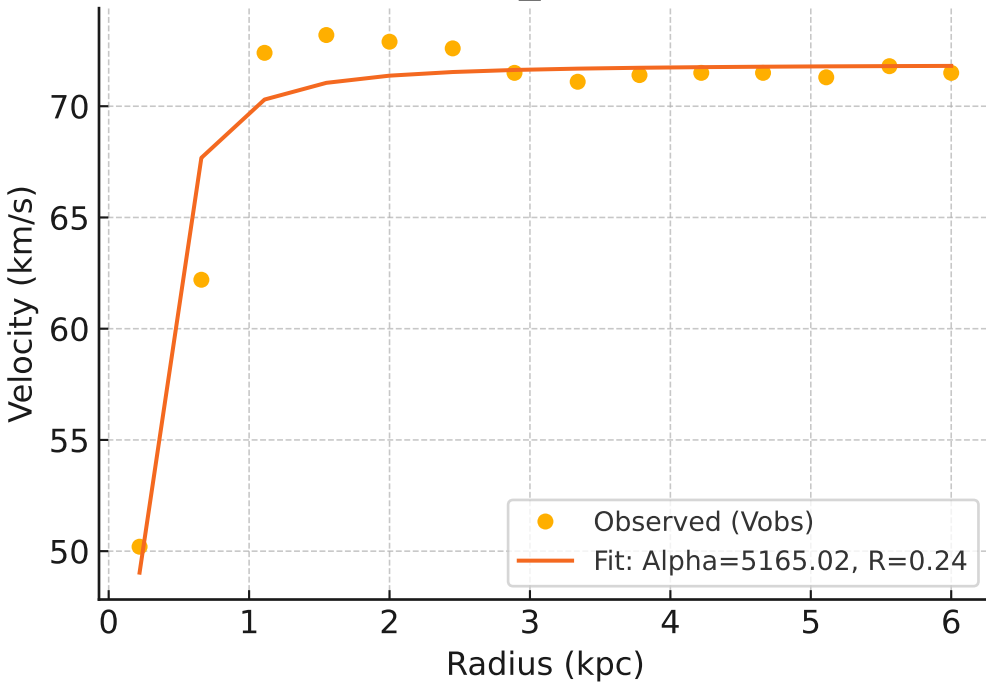
Galaxy: NGC1003_rotmod ($R^2=0.896$)



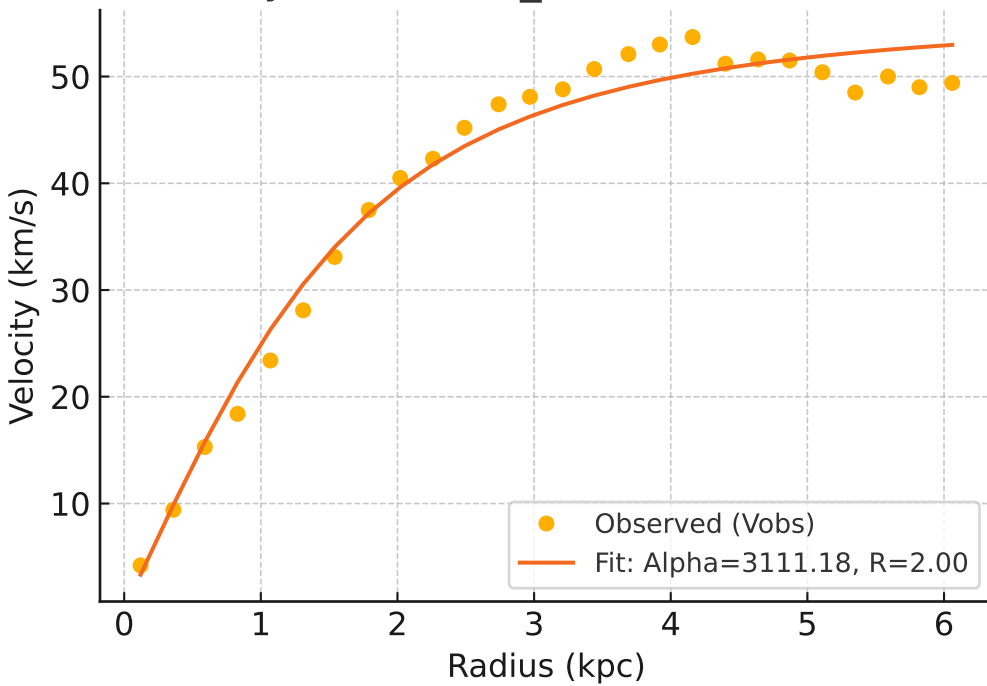
Galaxy: NGC1090_rotmod ($R^2=0.974$)



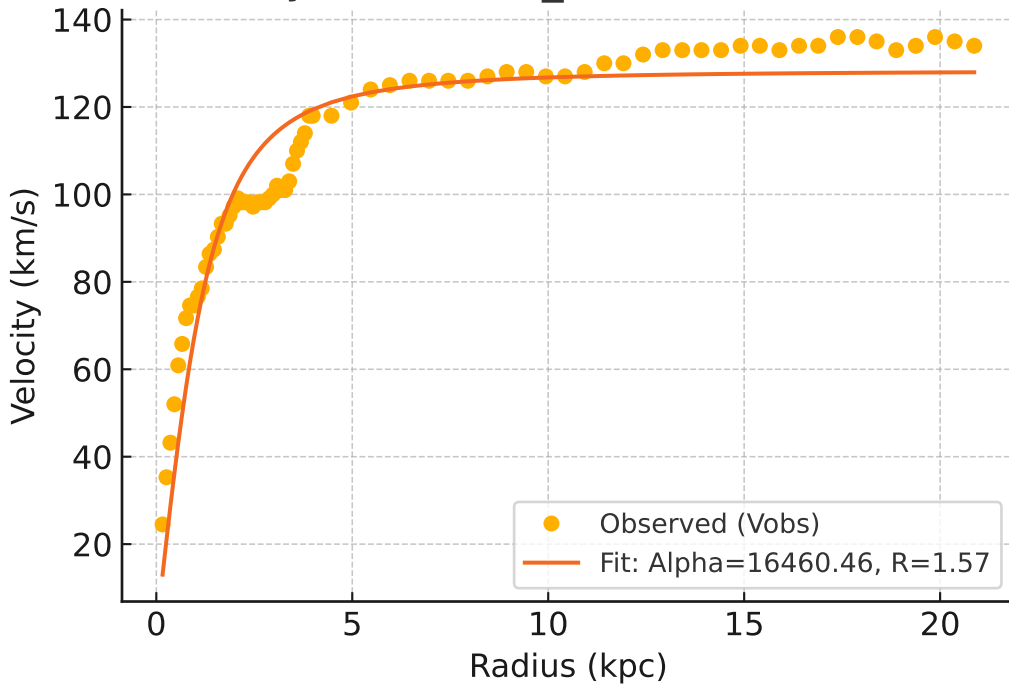
Galaxy: NGC1705_rotmod ($R^2=0.910$)



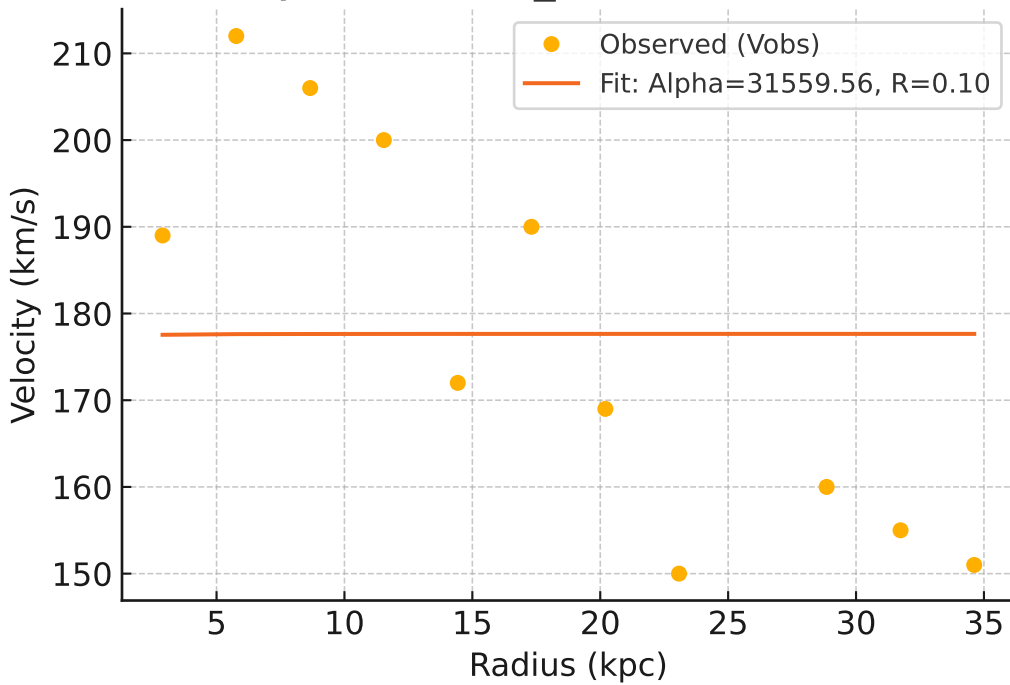
Galaxy: NGC2366_rotmod ($R^2=0.976$)



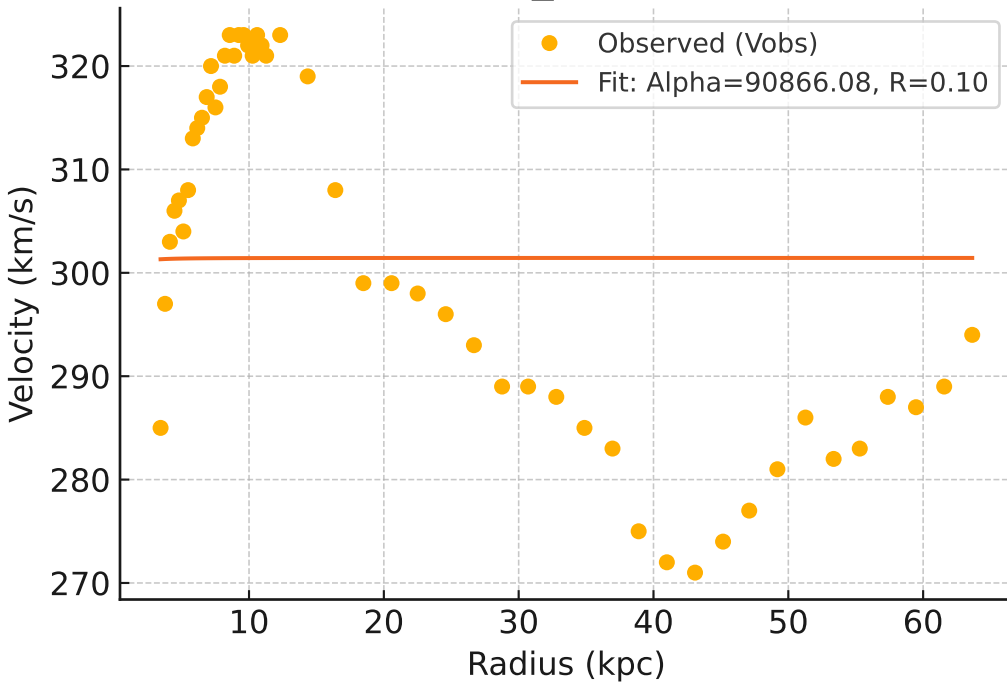
Galaxy: NGC2403_rotmod ($R^2=0.905$)



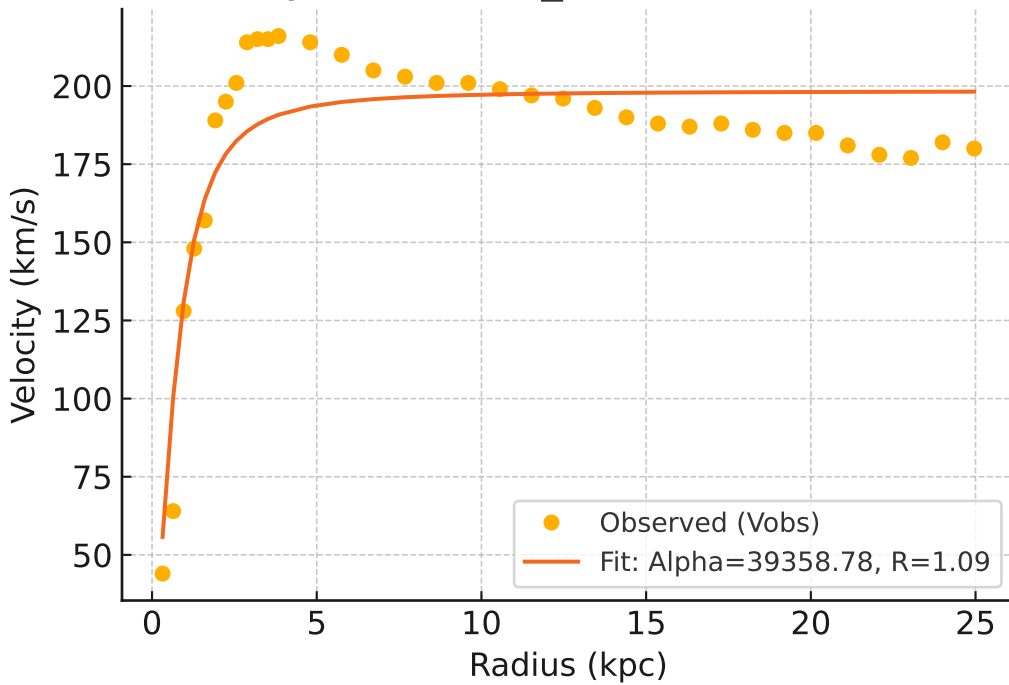
Galaxy: NGC2683_rotmod ($R^2=-0.001$)



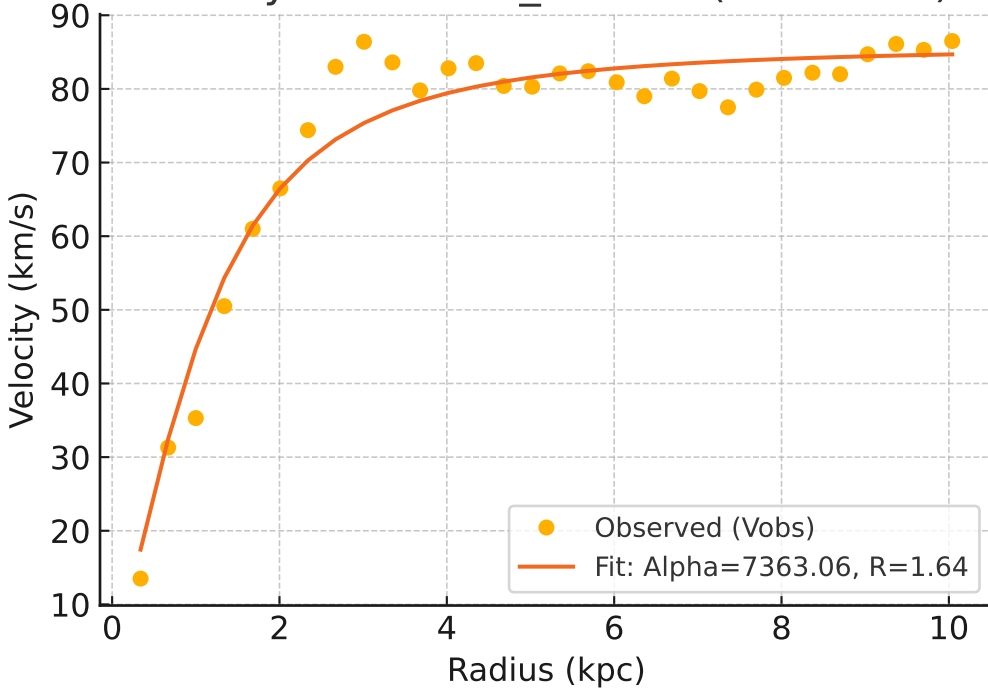
Galaxy: NGC2841_rotmod ($R^2=-0.001$)



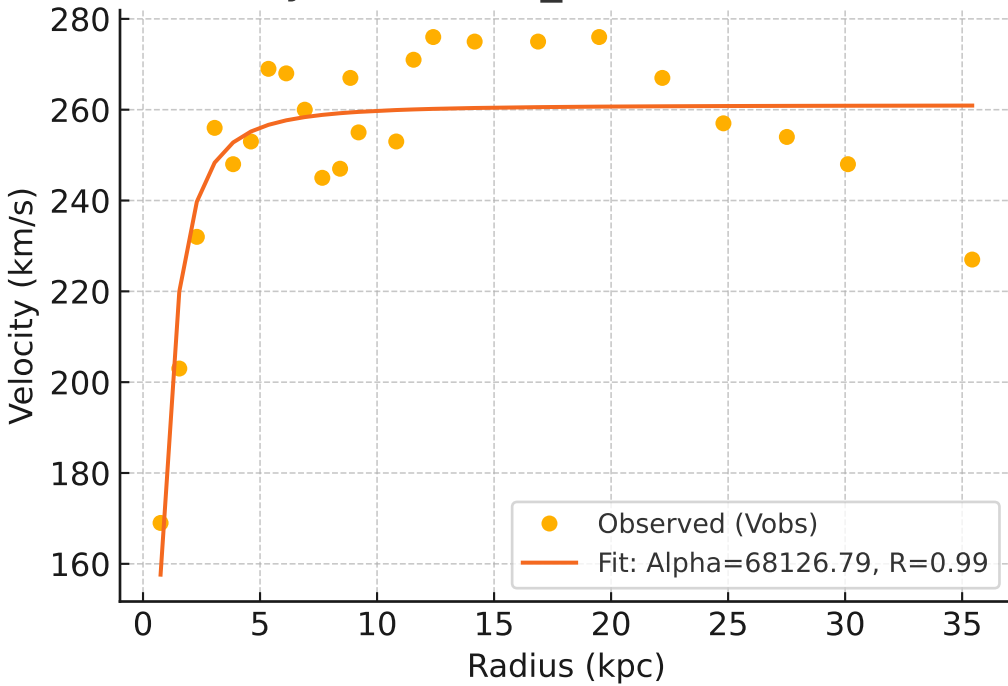
Galaxy: NGC2903_rotmod ($R^2=0.815$)



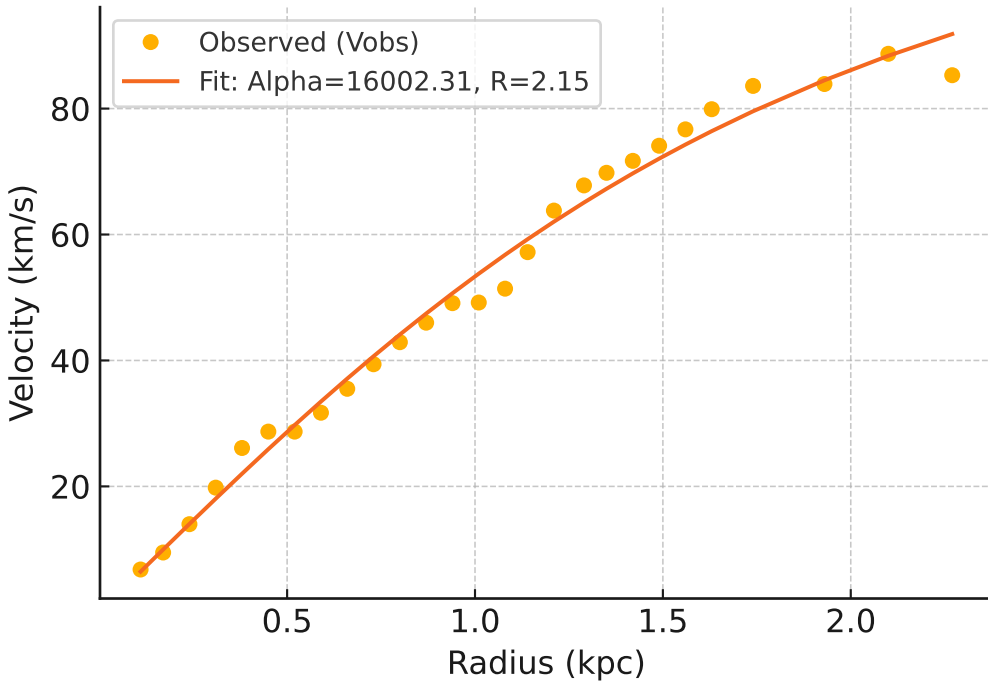
Galaxy: NGC2915_rotmod ($R^2=0.943$)



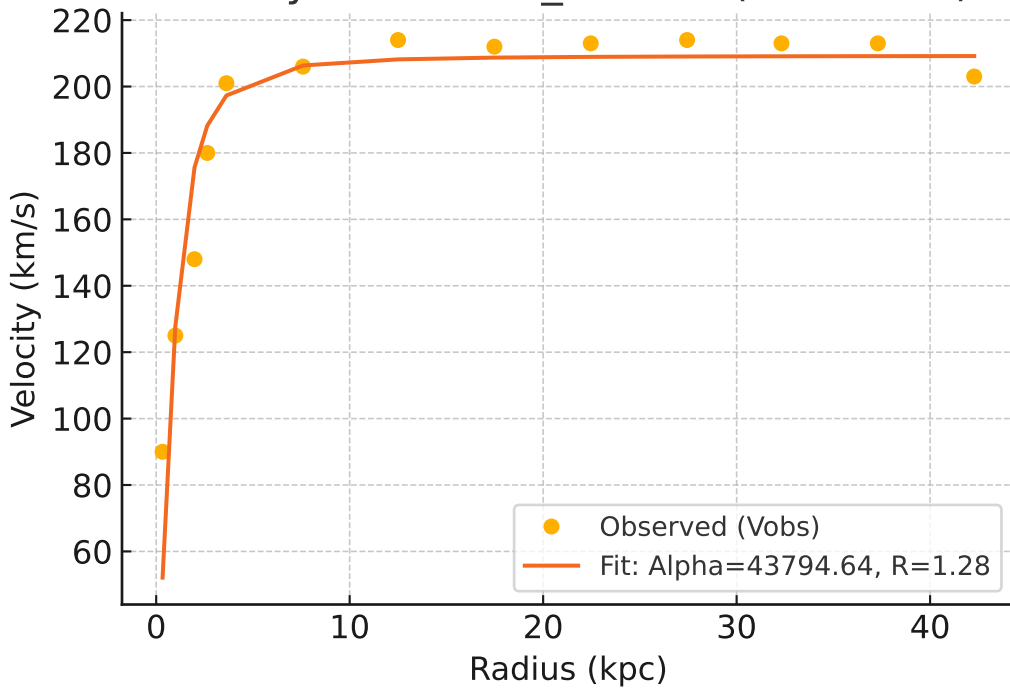
Galaxy: NGC2955_rotmod ($R^2=0.735$)



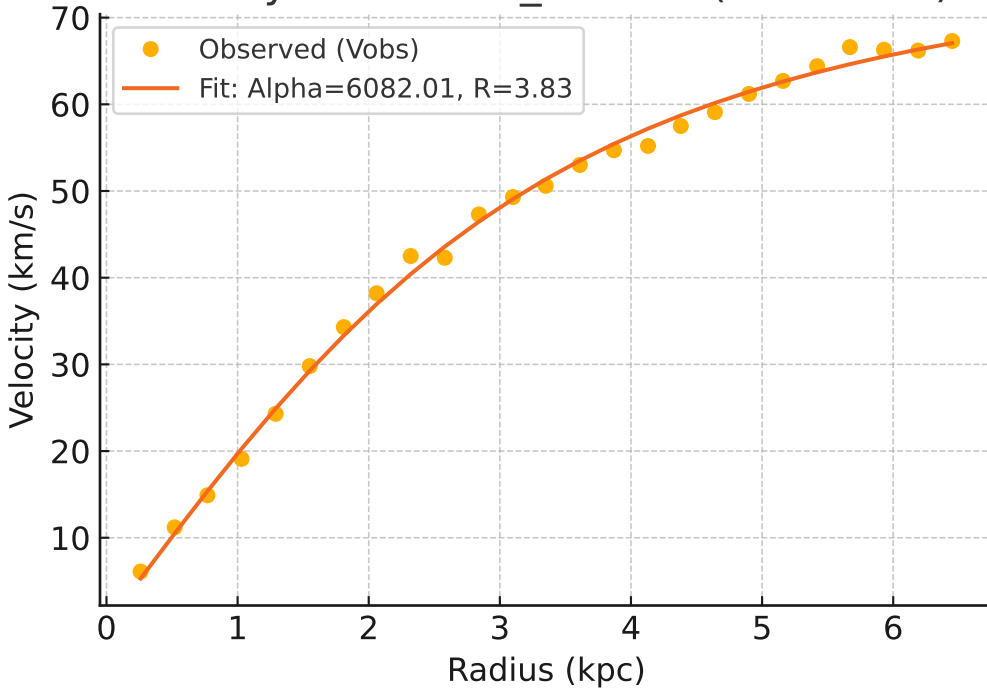
Galaxy: NGC2976_rotmod ($R^2=0.988$)



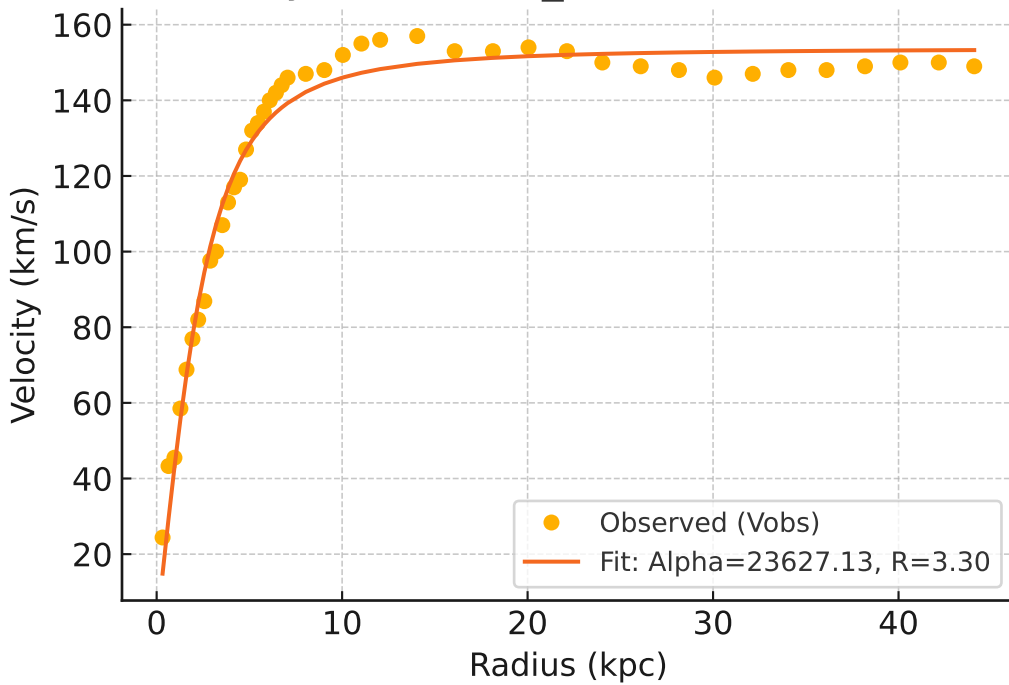
Galaxy: NGC2998_rotmod ($R^2=0.876$)



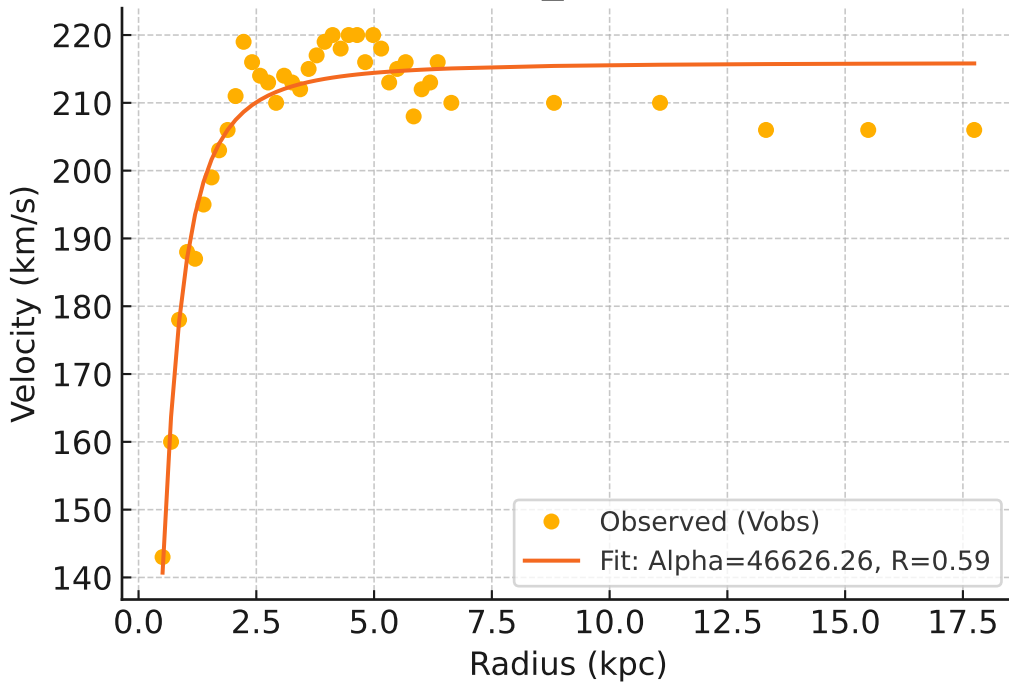
Galaxy: NGC3109_rotmod ($R^2=0.997$)



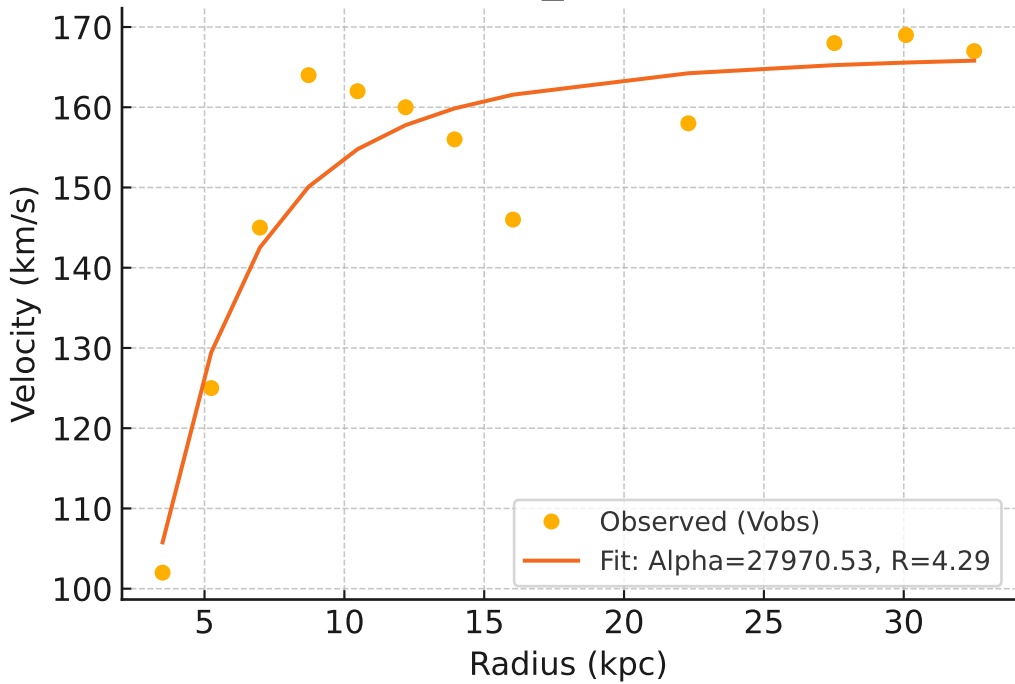
Galaxy: NGC3198_rotmod ($R^2=0.978$)



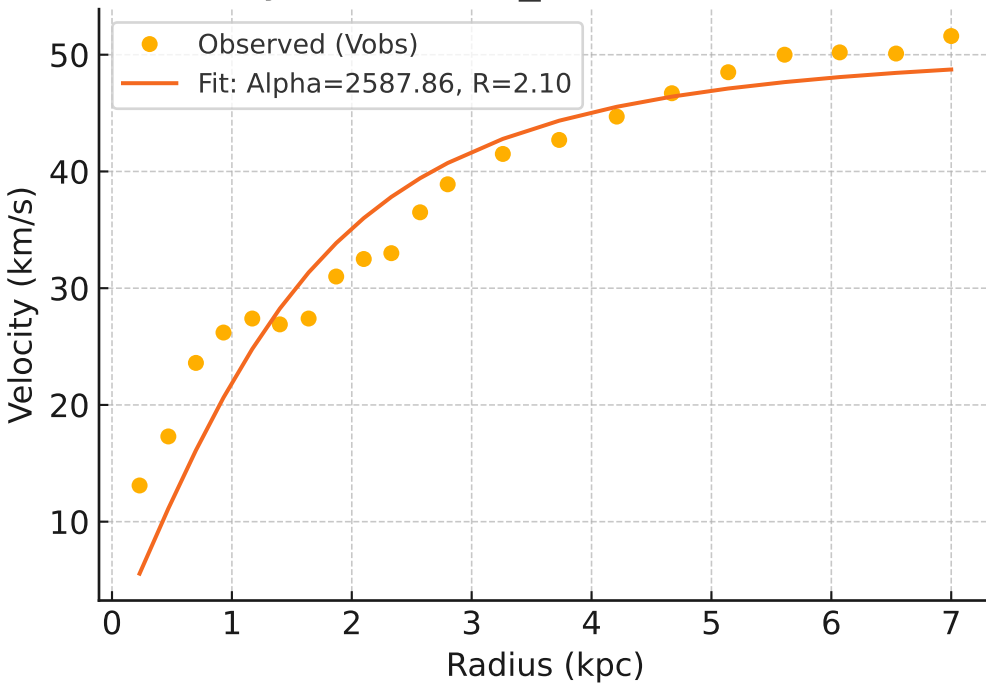
Galaxy: NGC3521_rotmod ($R^2=0.910$)



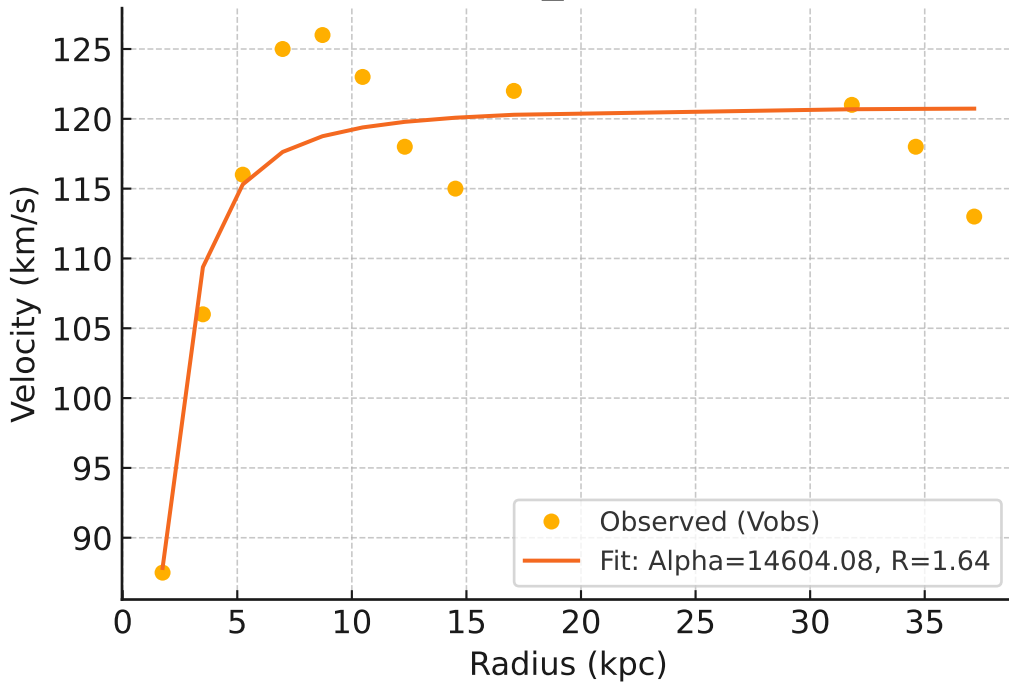
Galaxy: NGC3726_rotmod ($R^2=0.863$)



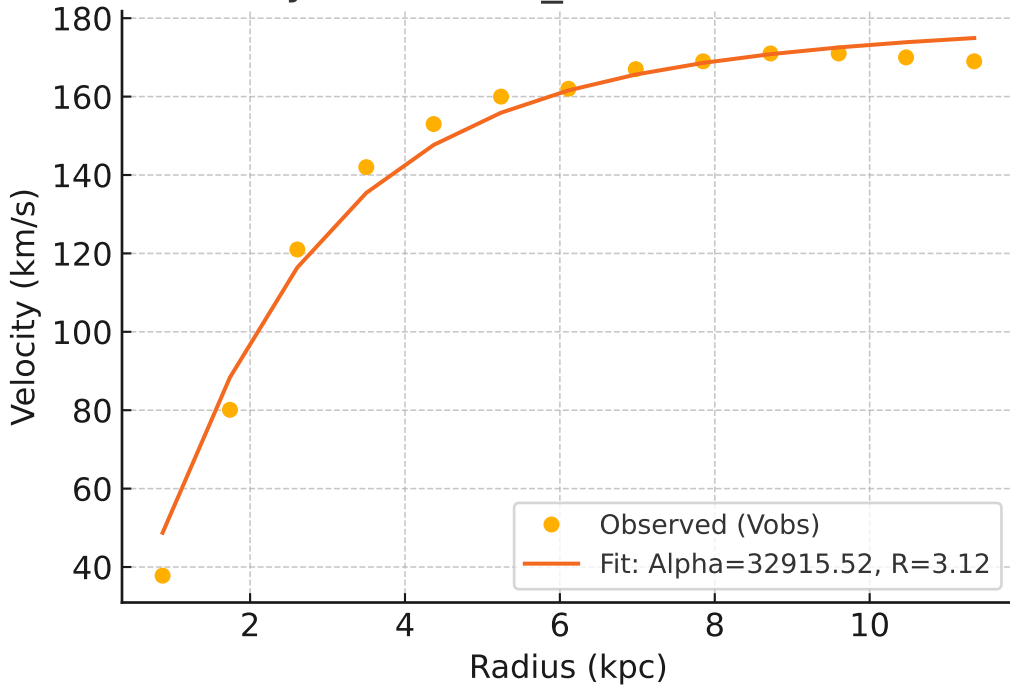
Galaxy: NGC3741_rotmod ($R^2=0.891$)



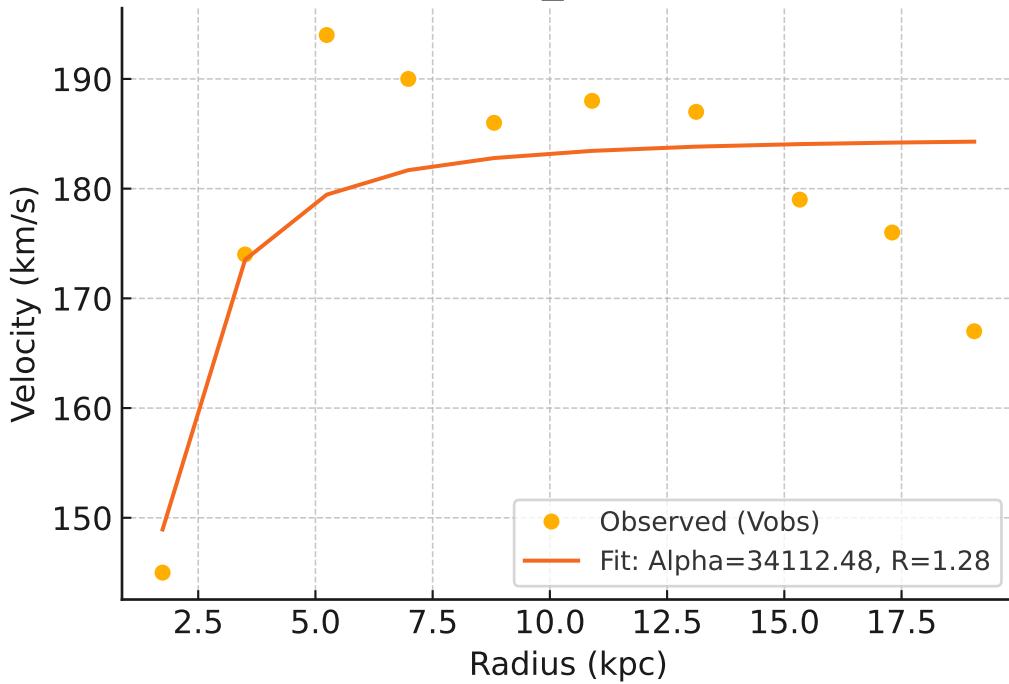
Galaxy: NGC3769_rotmod ($R^2=0.811$)



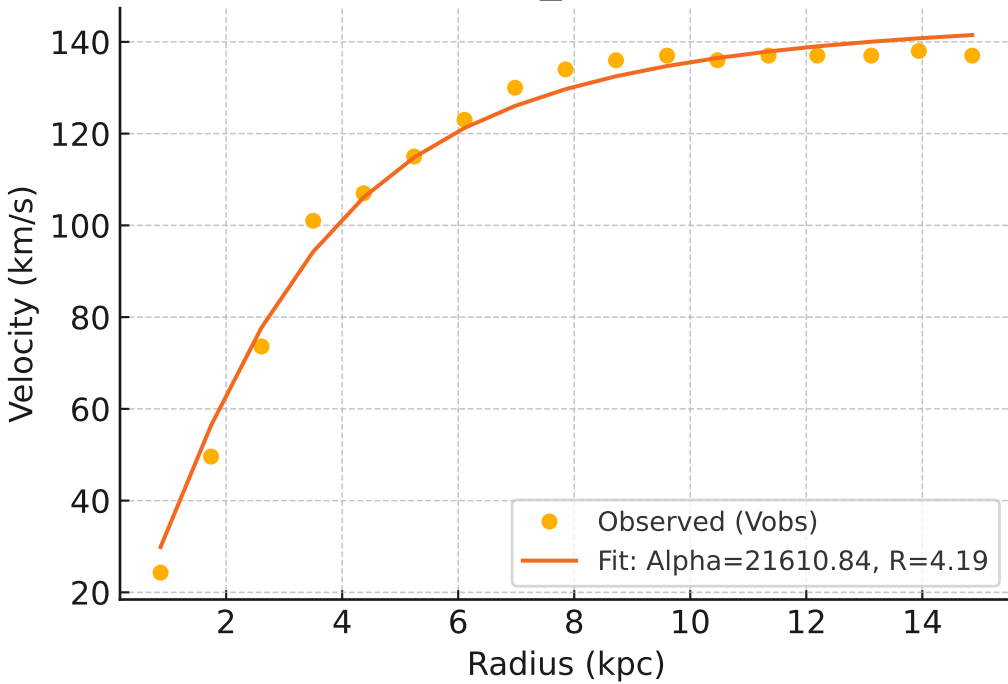
Galaxy: NGC3877_rotmod ($R^2=0.983$)



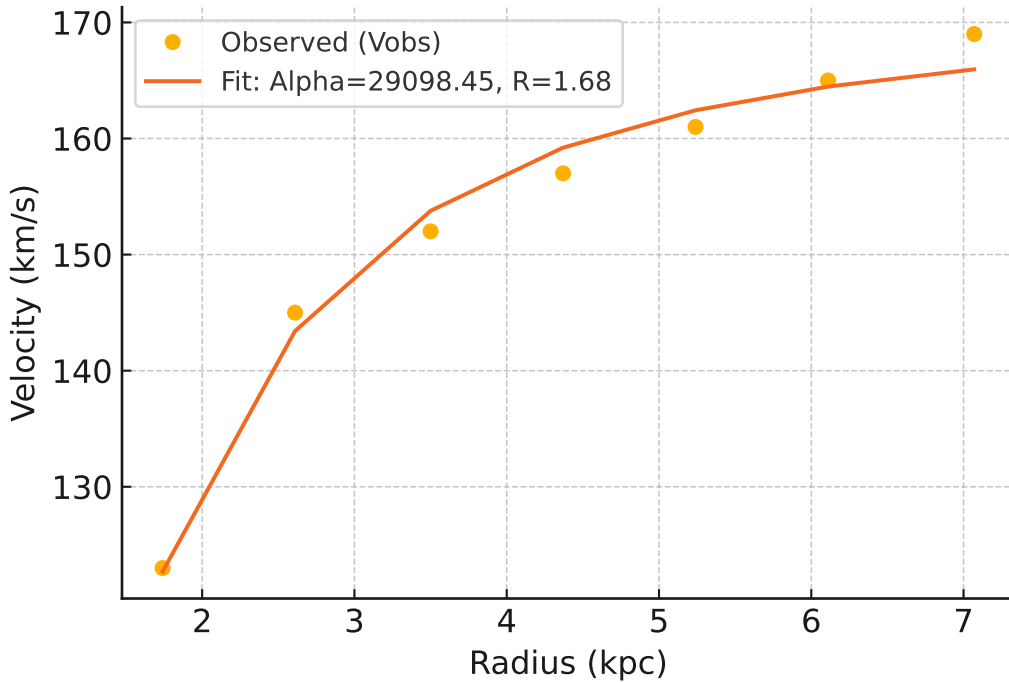
Galaxy: NGC3893_rotmod ($R^2=0.611$)



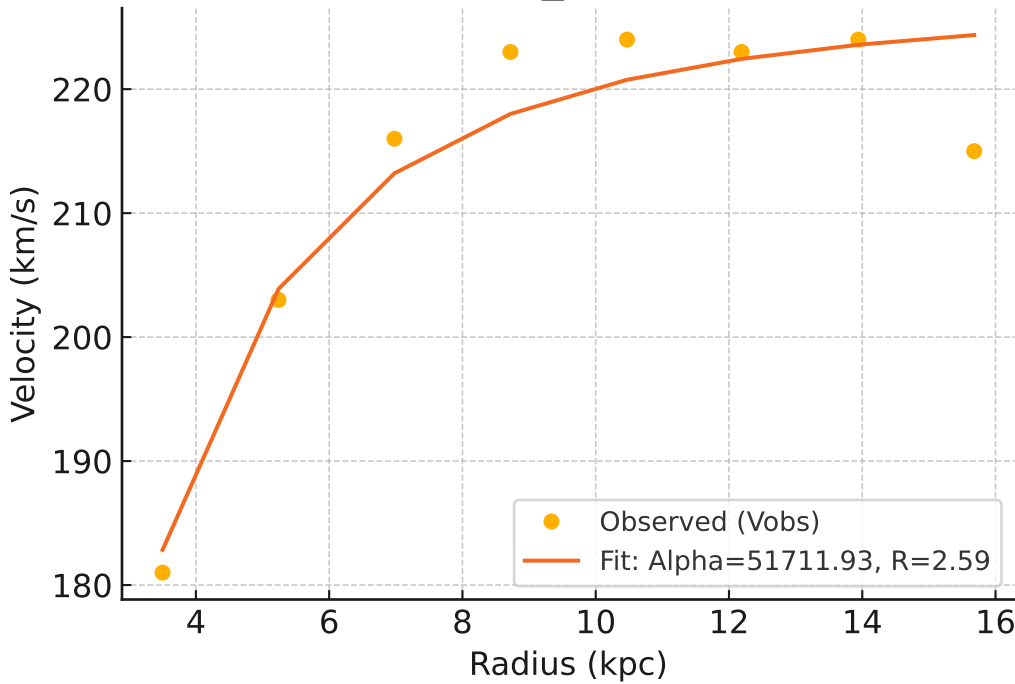
Galaxy: NGC3917_rotmod ($R^2=0.987$)



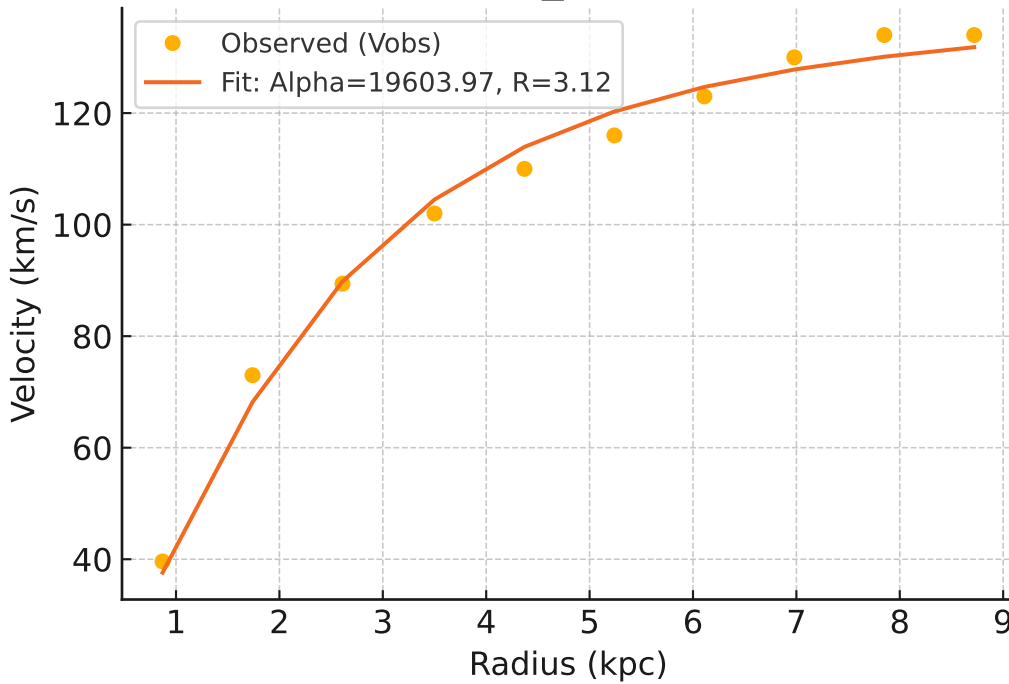
Galaxy: NGC3949_rotmod ($R^2=0.985$)



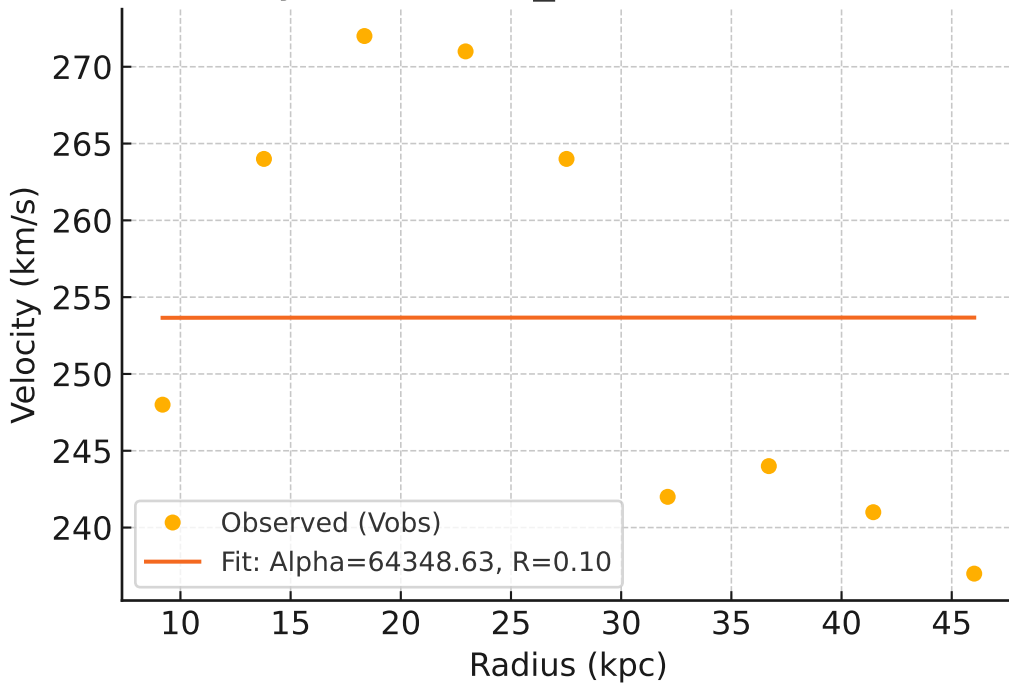
Galaxy: NGC3953_rotmod ($R^2=0.914$)



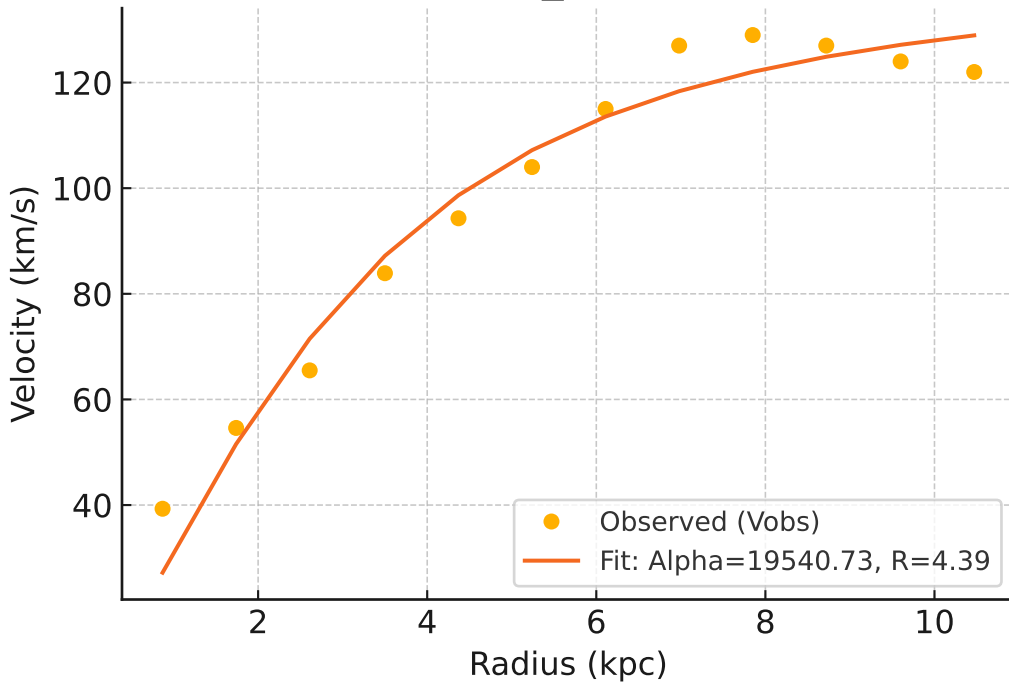
Galaxy: NGC3972_rotmod ($R^2=0.989$)



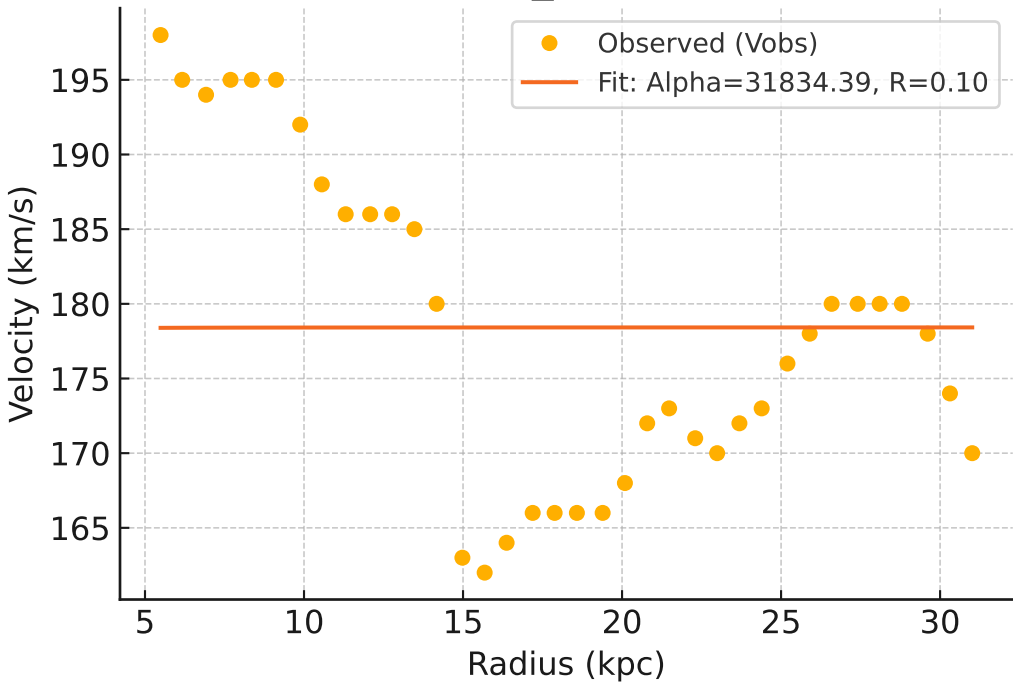
Galaxy: NGC3992_rotmod ($R^2=-0.000$)



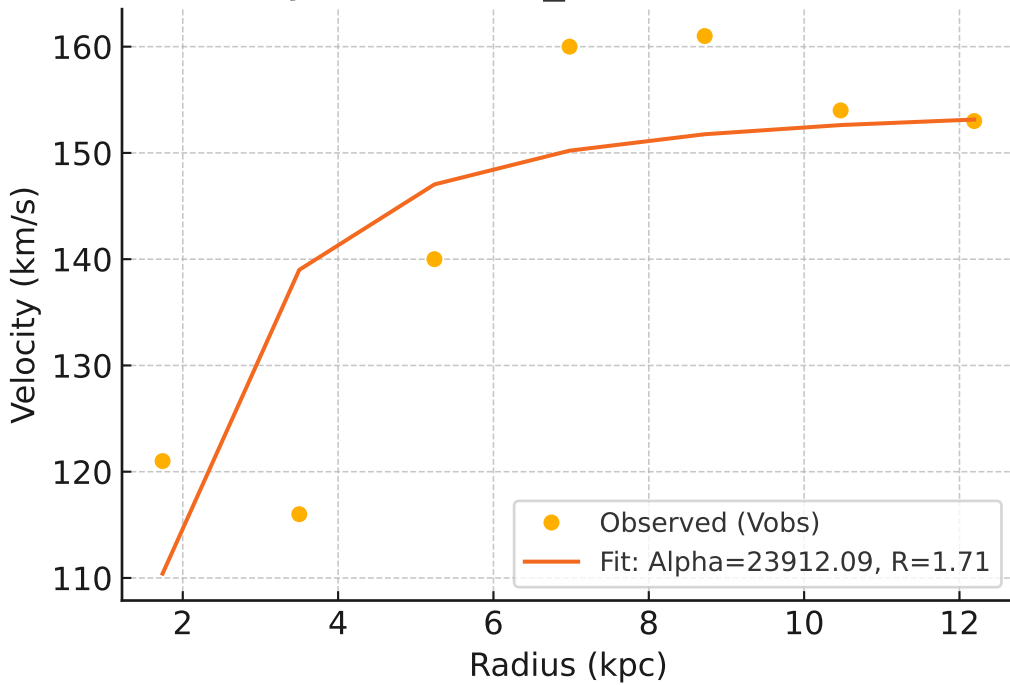
Galaxy: NGC4010_rotmod ($R^2=0.961$)



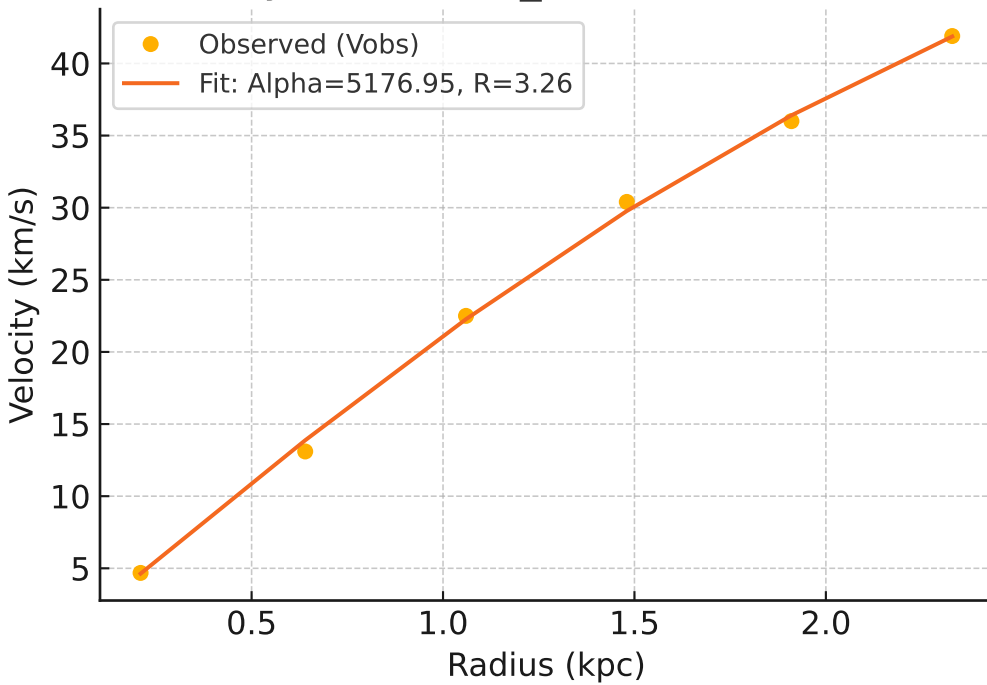
Galaxy: NGC4013_rotmod ($R^2=-0.001$)



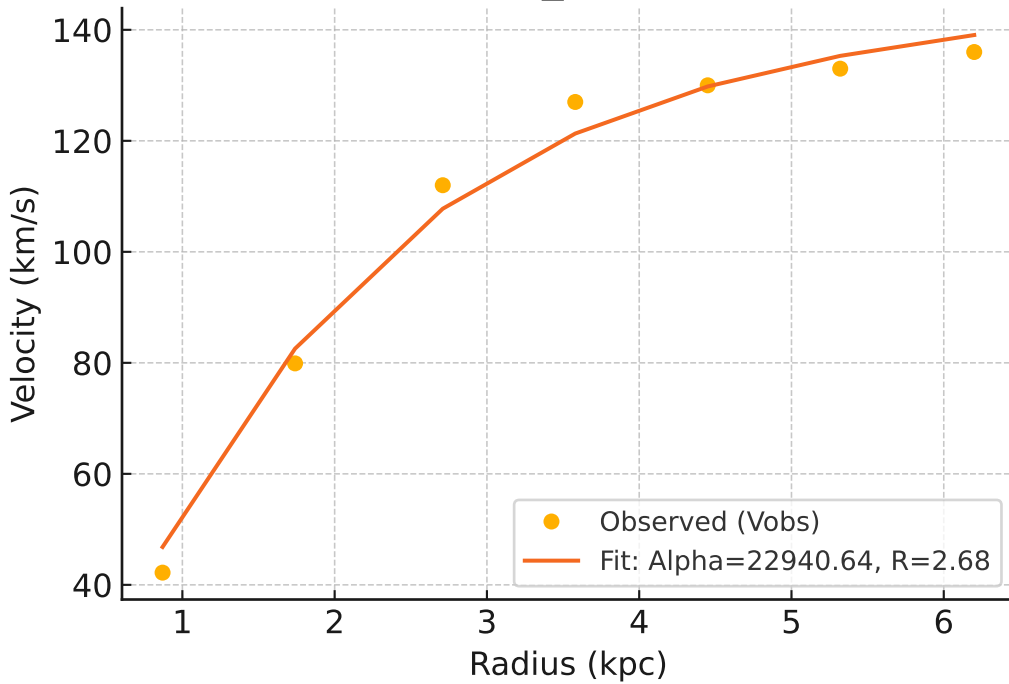
Galaxy: NGC4051_rotmod ($R^2=0.575$)



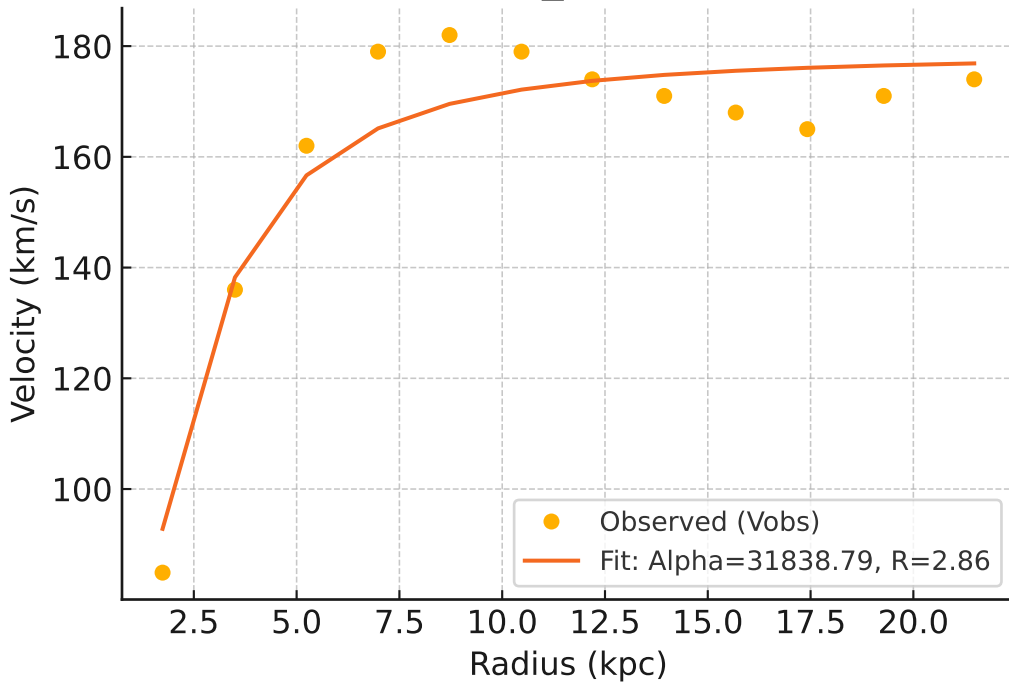
Galaxy: NGC4068_rotmod ($R^2=0.999$)



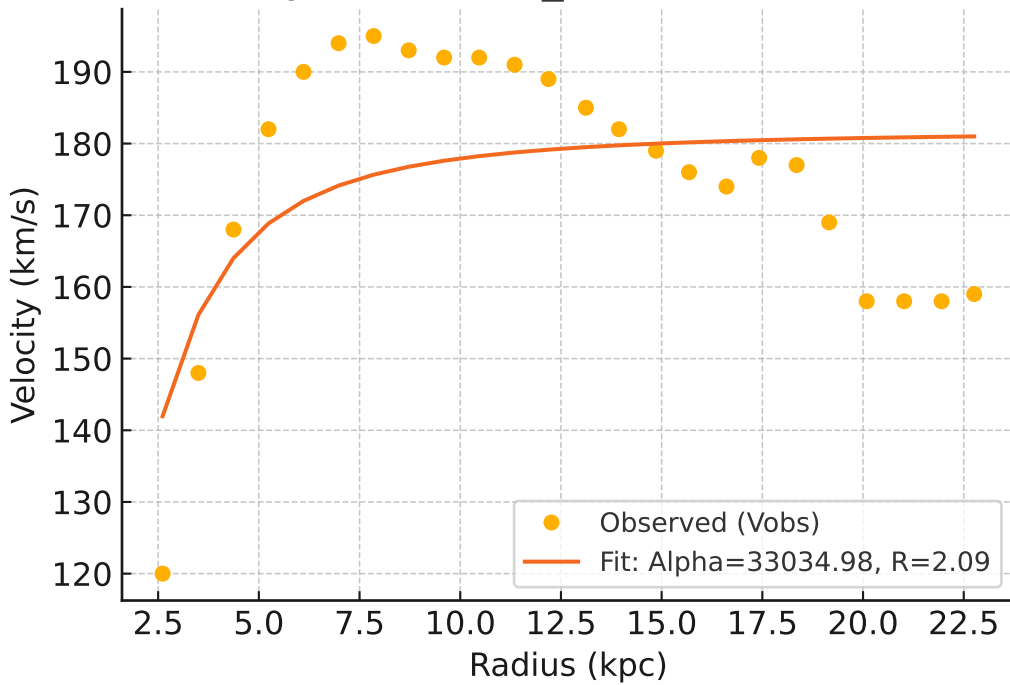
Galaxy: NGC4085_rotmod ($R^2=0.987$)



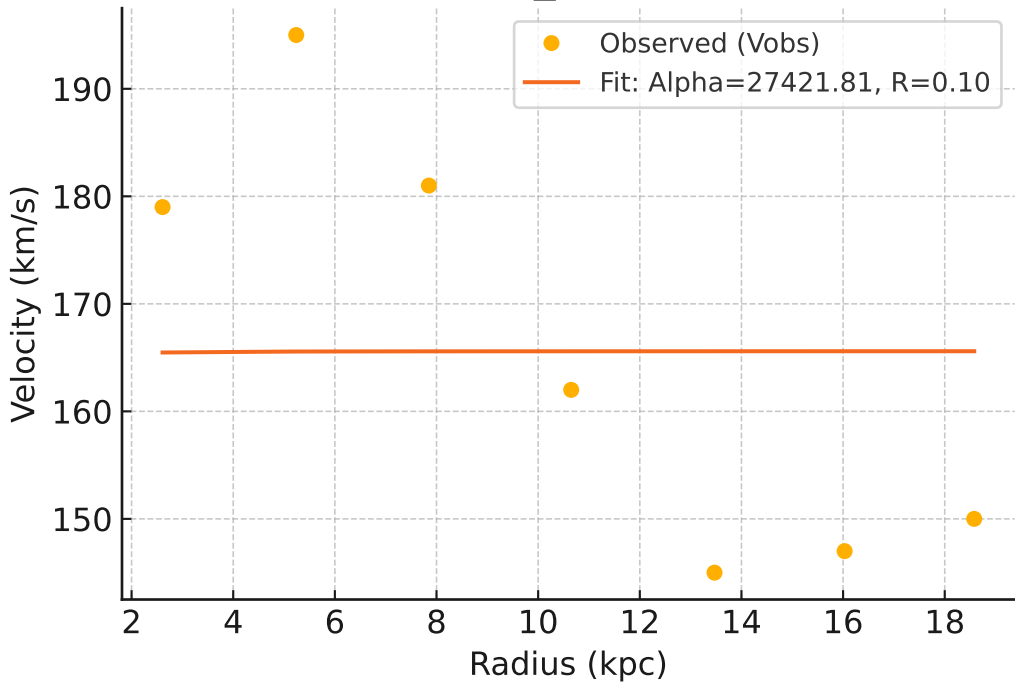
Galaxy: NGC4088_rotmod ($R^2=0.911$)



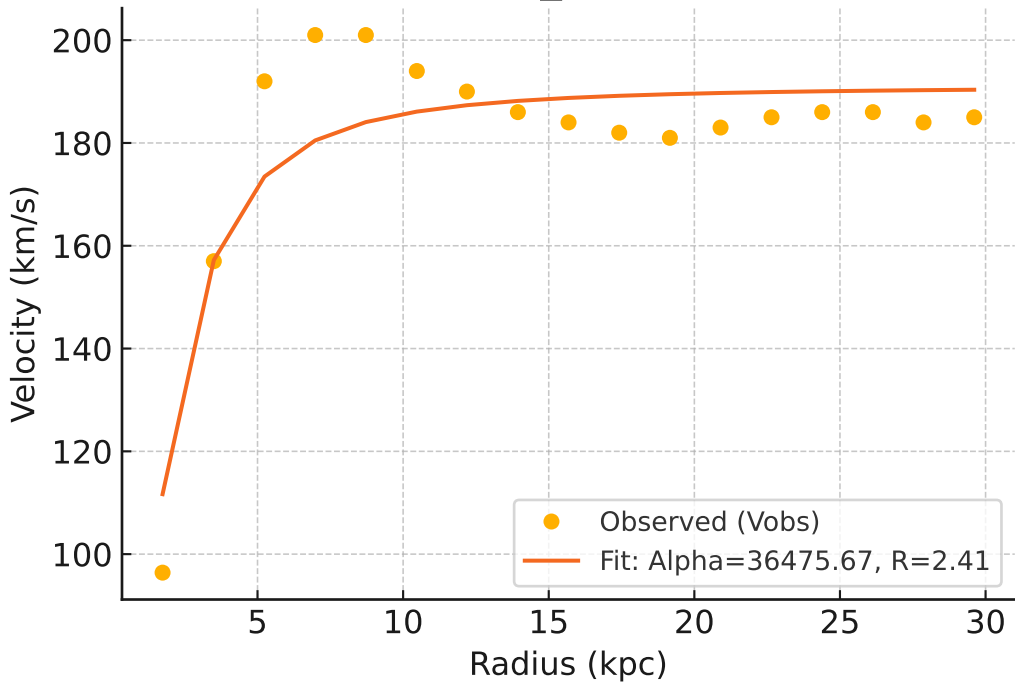
Galaxy: NGC4100_rotmod ($R^2=0.331$)



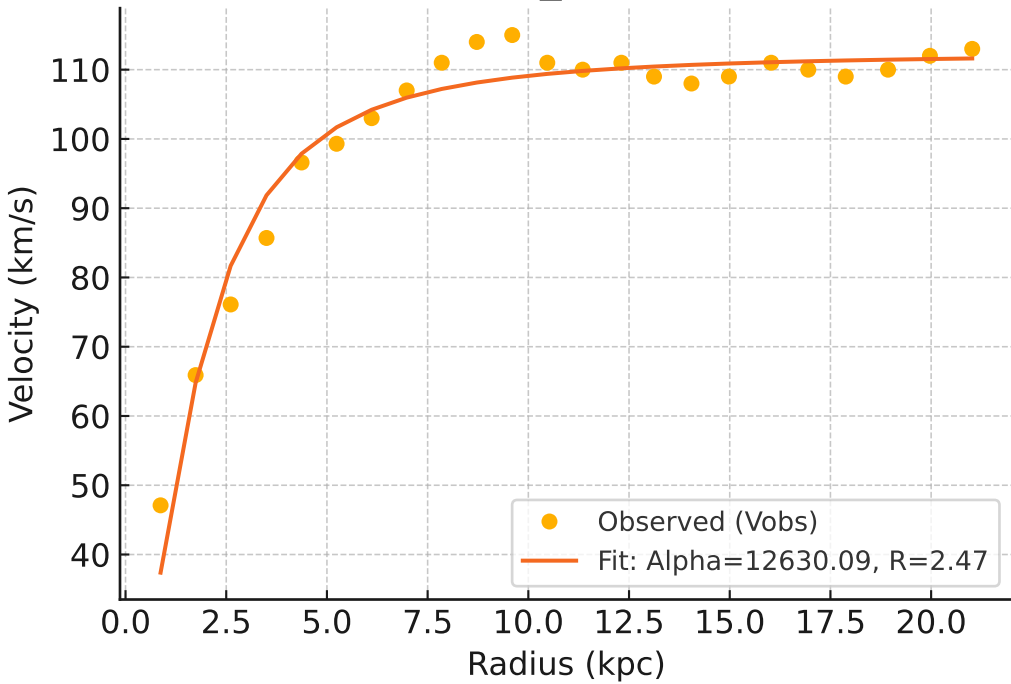
Galaxy: NGC4138_rotmod ($R^2=-0.002$)



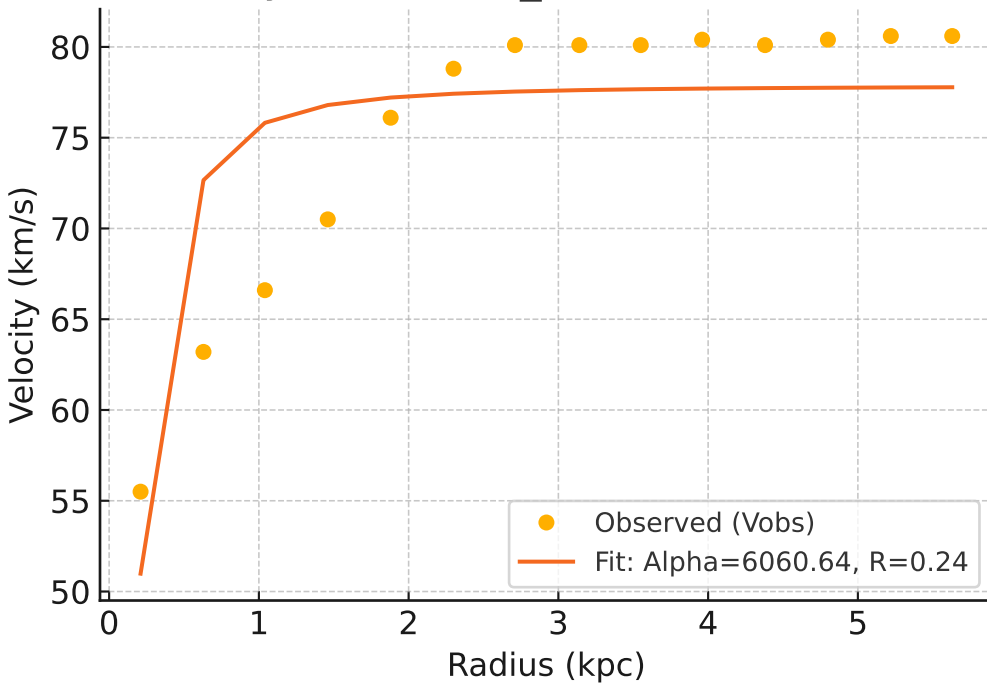
Galaxy: NGC4157_rotmod ($R^2=0.814$)



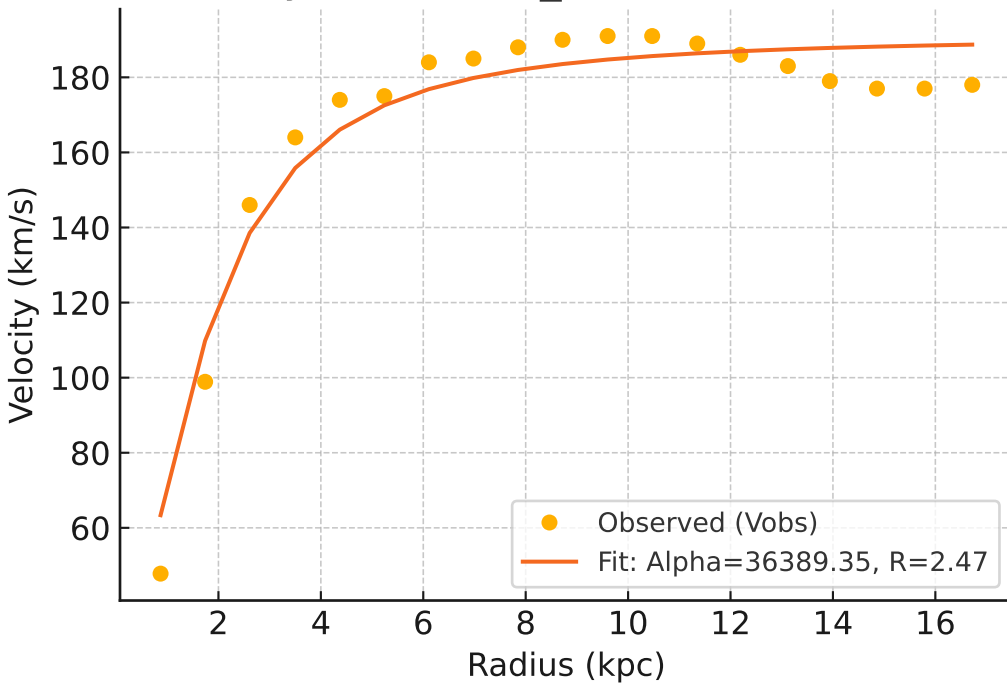
Galaxy: NGC4183_rotmod ($R^2=0.956$)



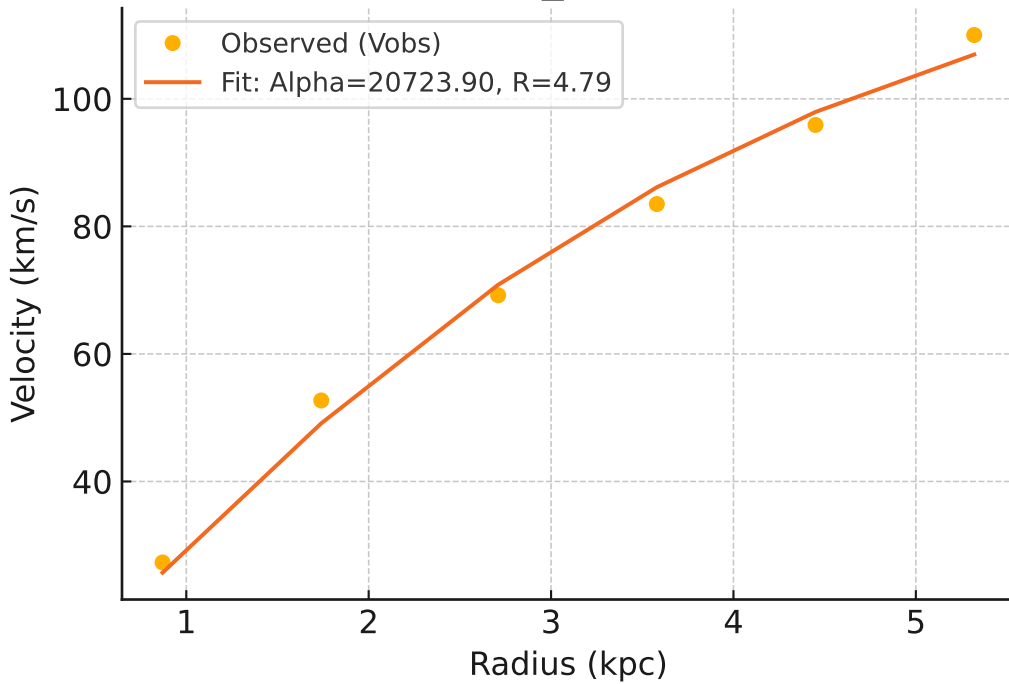
Galaxy: NGC4214_rotmod ($R^2=0.656$)



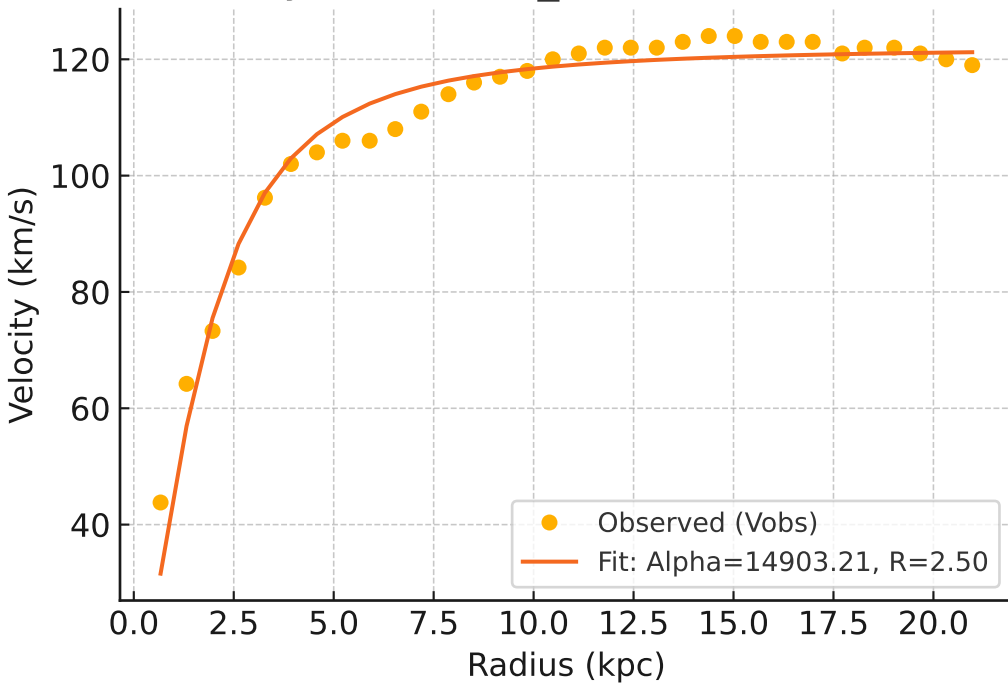
Galaxy: NGC4217_rotmod ($R^2=0.947$)



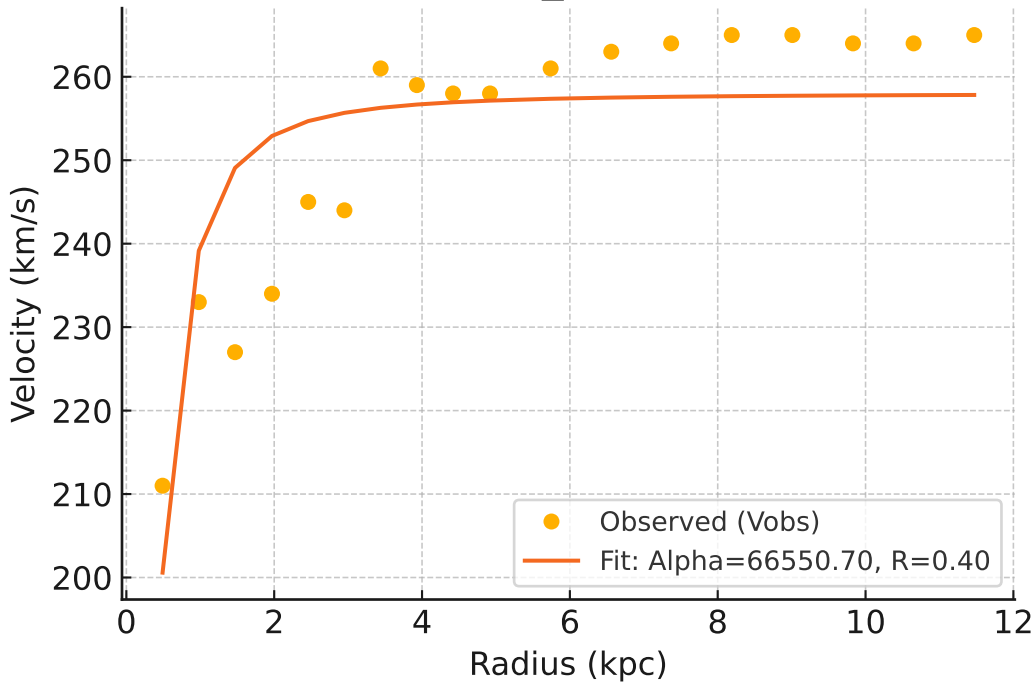
Galaxy: NGC4389_rotmod ($R^2=0.991$)



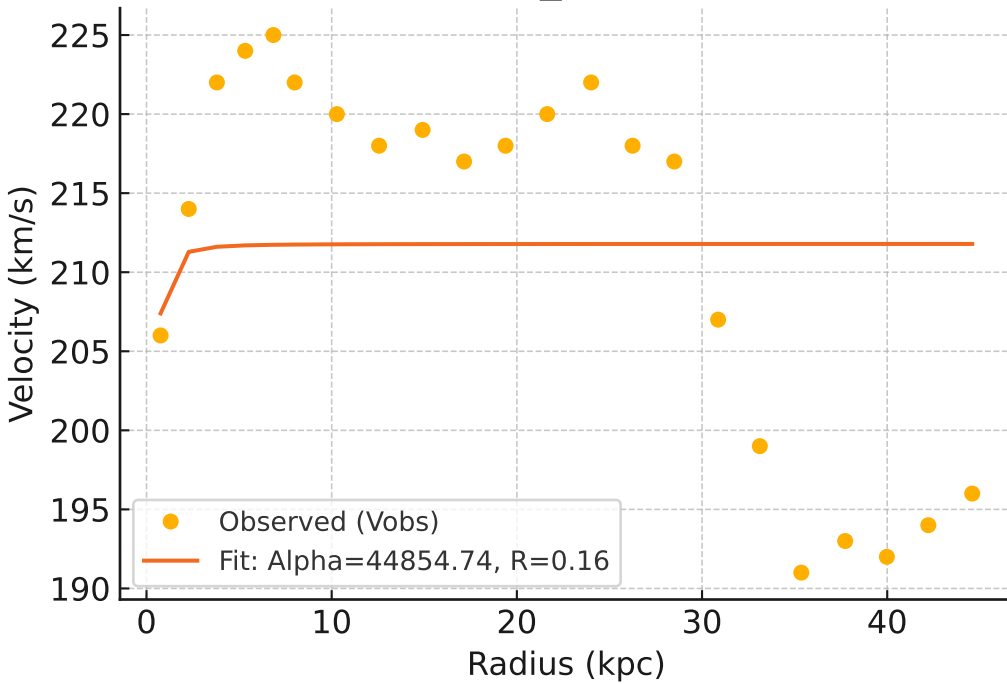
Galaxy: NGC4559_rotmod ($R^2=0.962$)



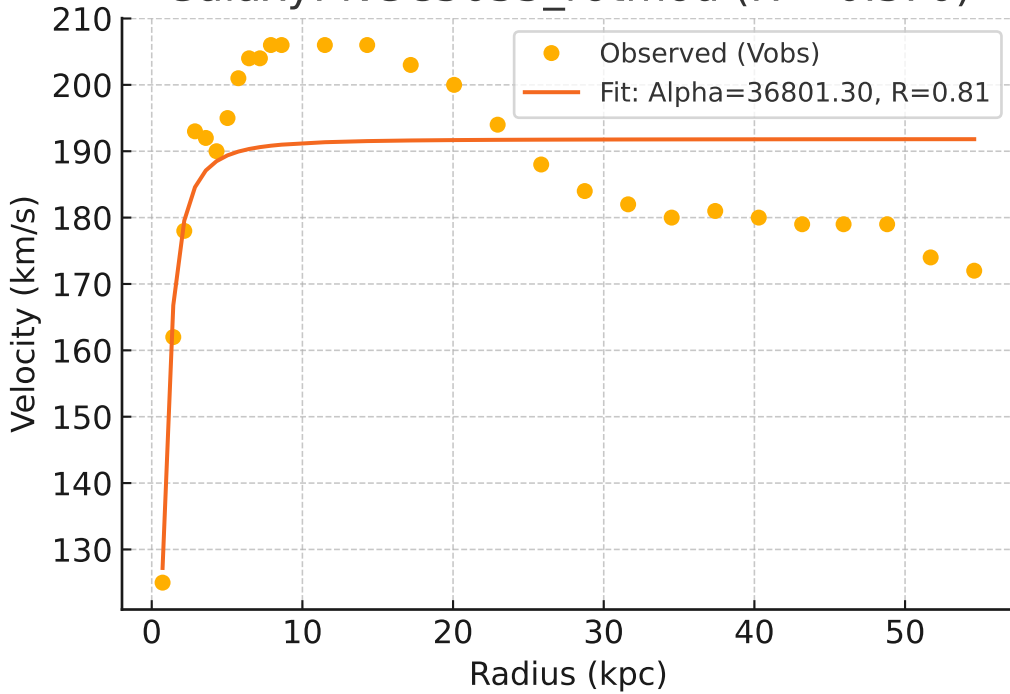
Galaxy: NGC5005_rotmod ($R^2=0.647$)



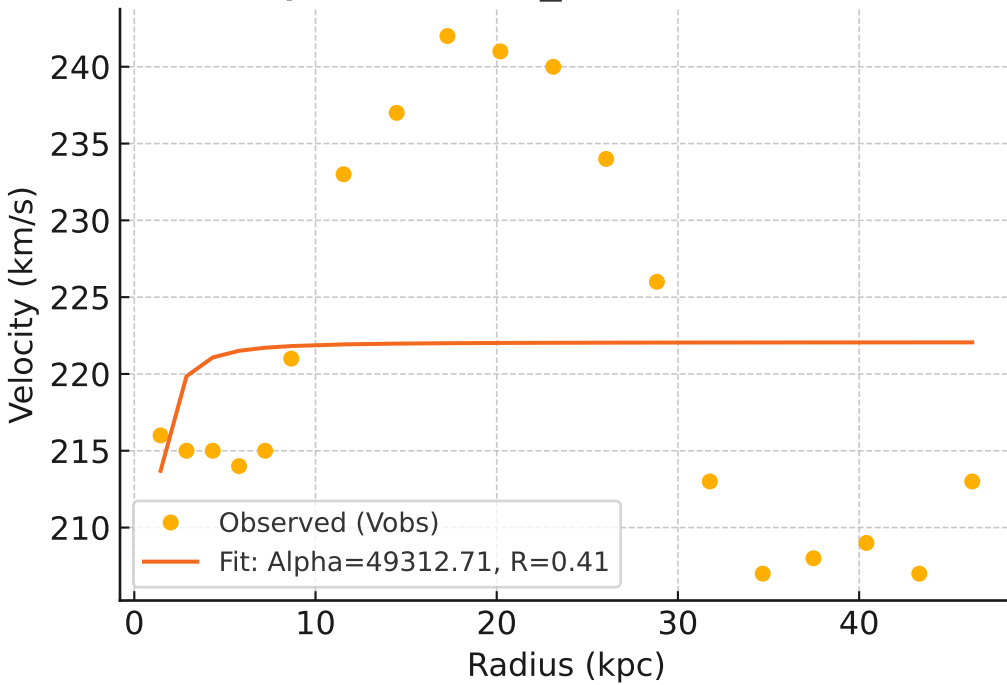
Galaxy: NGC5033_rotmod ($R^2=0.006$)



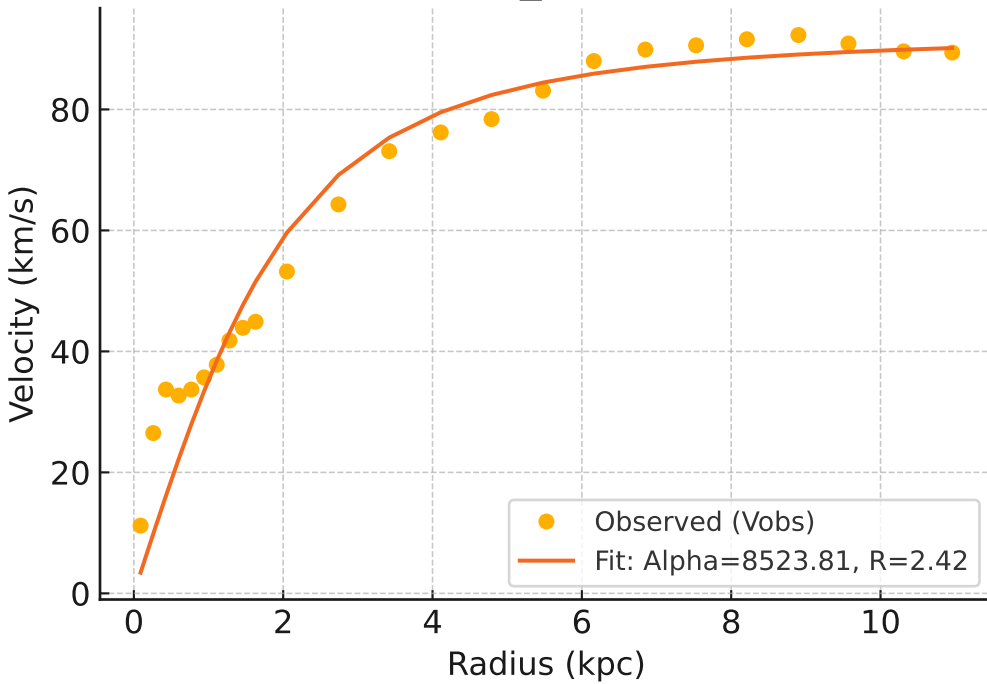
Galaxy: NGC5055_rotmod ($R^2=0.570$)



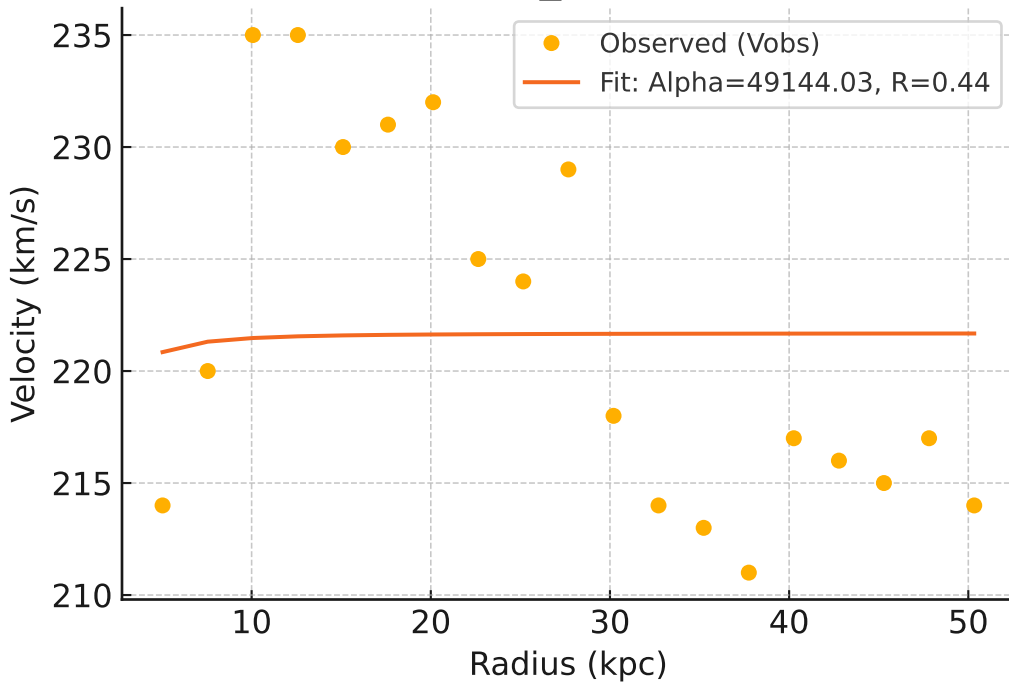
Galaxy: NGC5371_rotmod ($R^2=0.023$)



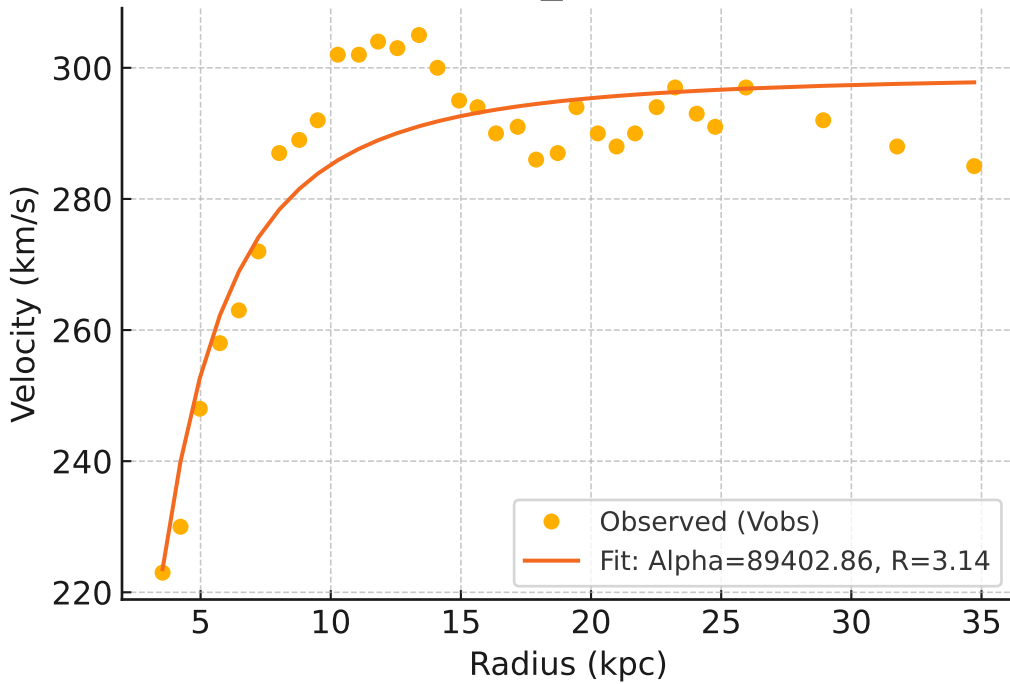
Galaxy: NGC5585_rotmod ($R^2=0.938$)



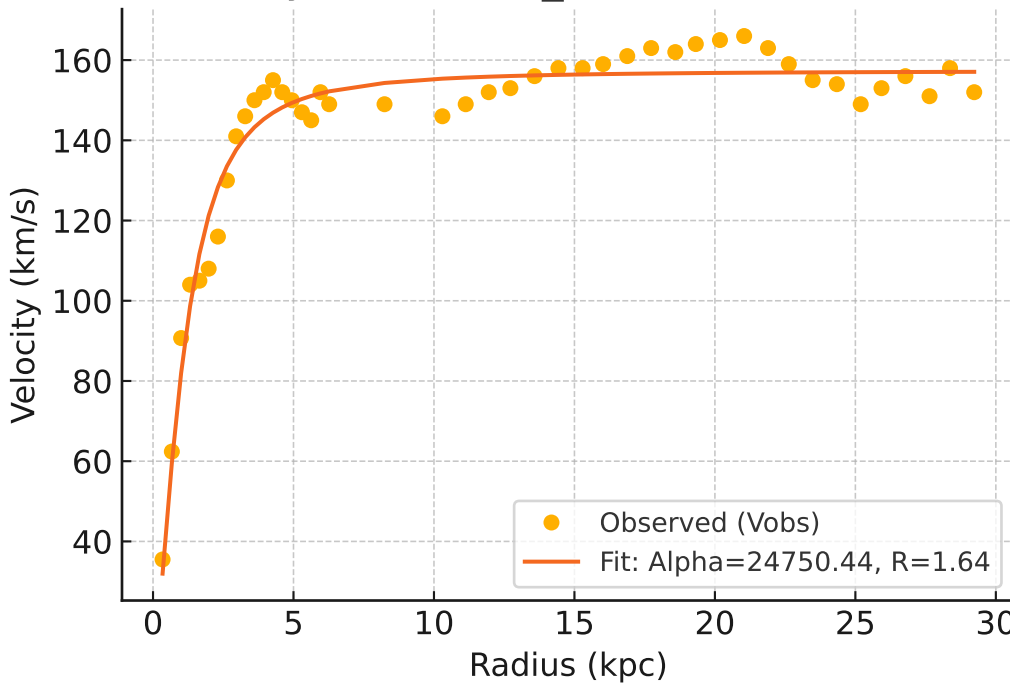
Galaxy: NGC5907_rotmod ($R^2=0.001$)



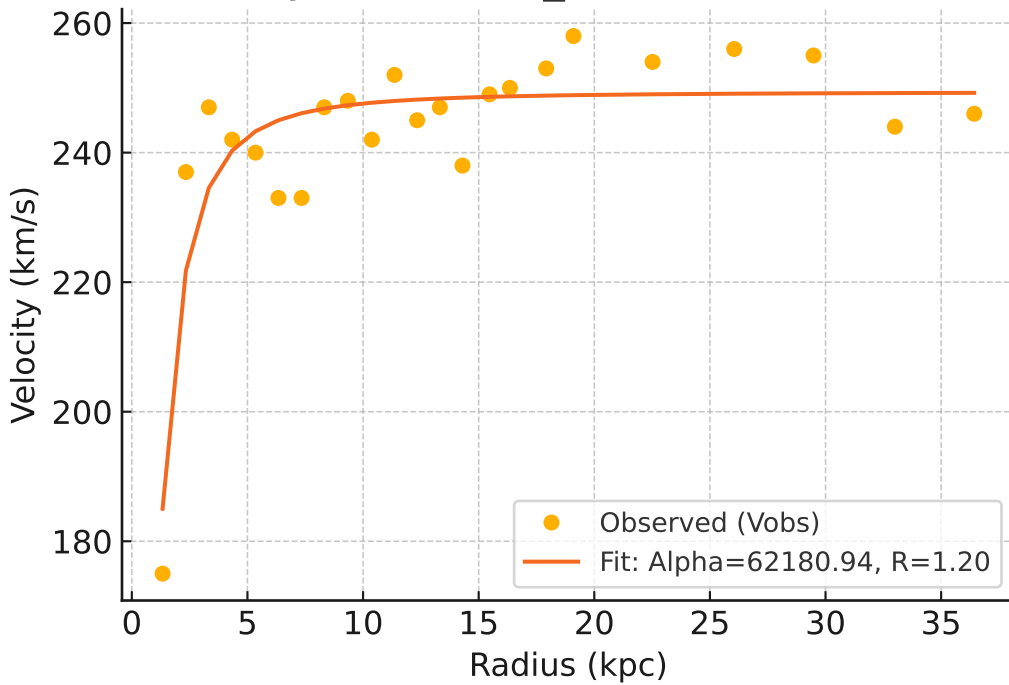
Galaxy: NGC5985_rotmod ($R^2=0.831$)



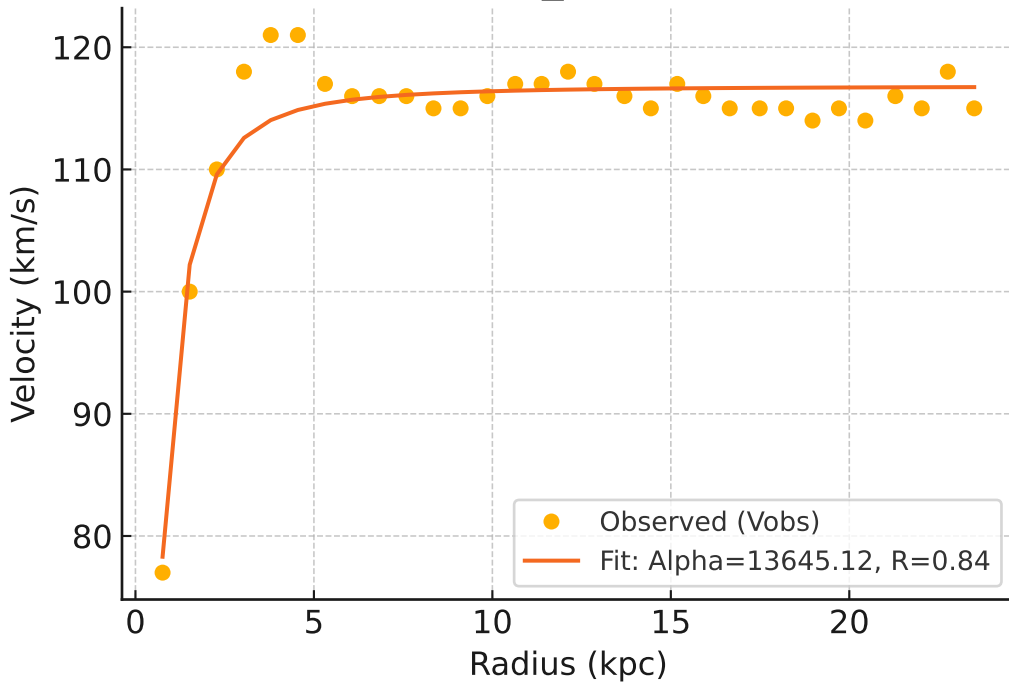
Galaxy: NGC6015_rotmod ($R^2=0.954$)



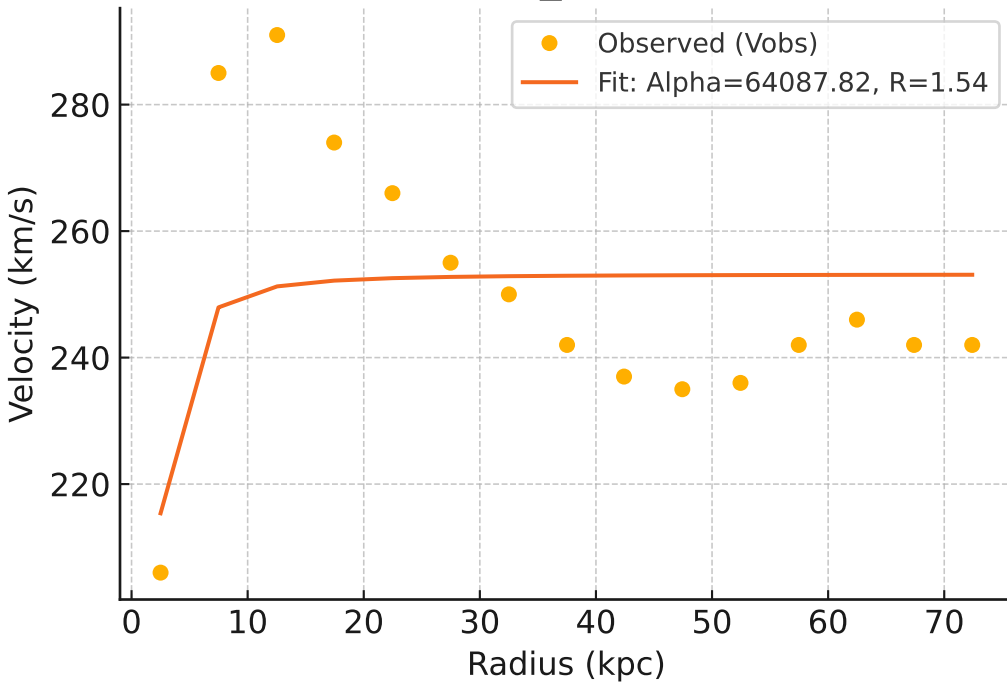
Galaxy: NGC6195_rotmod ($R^2=0.791$)



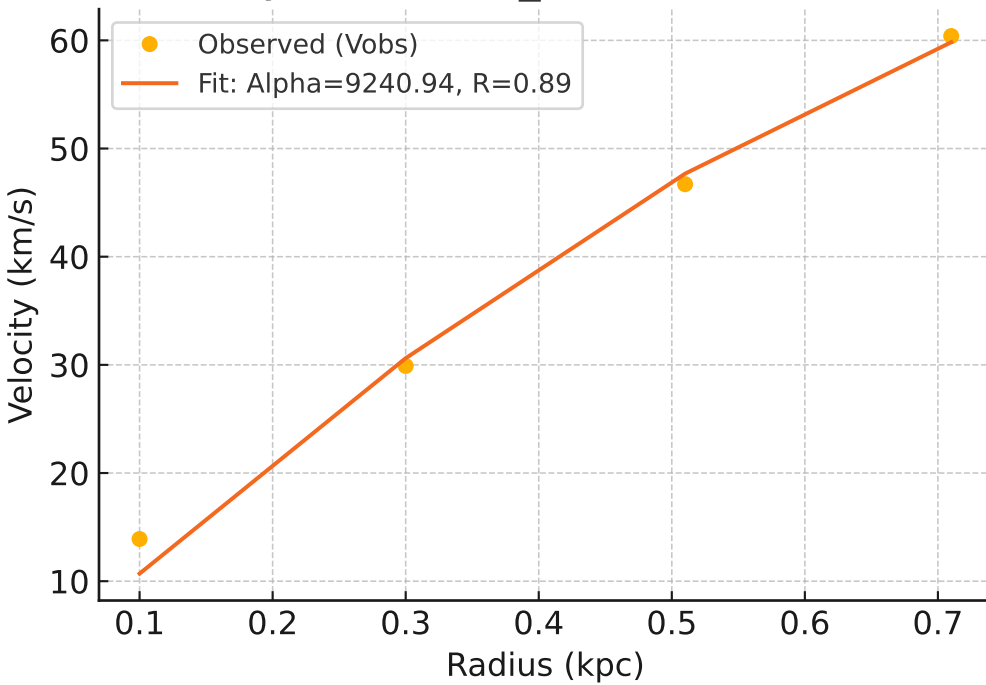
Galaxy: NGC6503_rotmod ($R^2=0.907$)



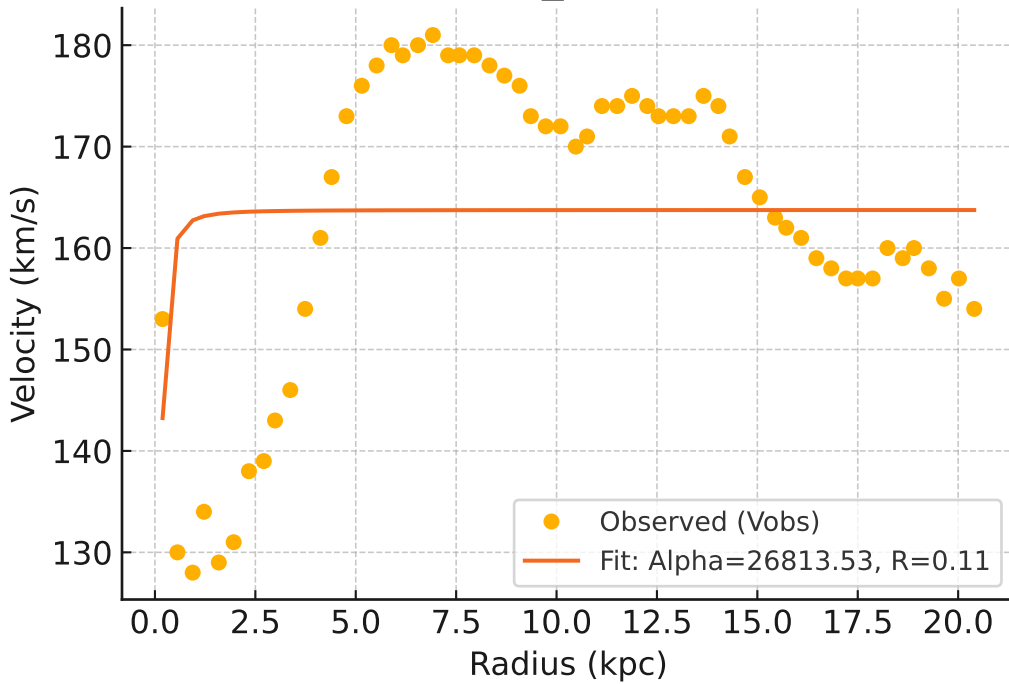
Galaxy: NGC6674_rotmod ($R^2=0.220$)



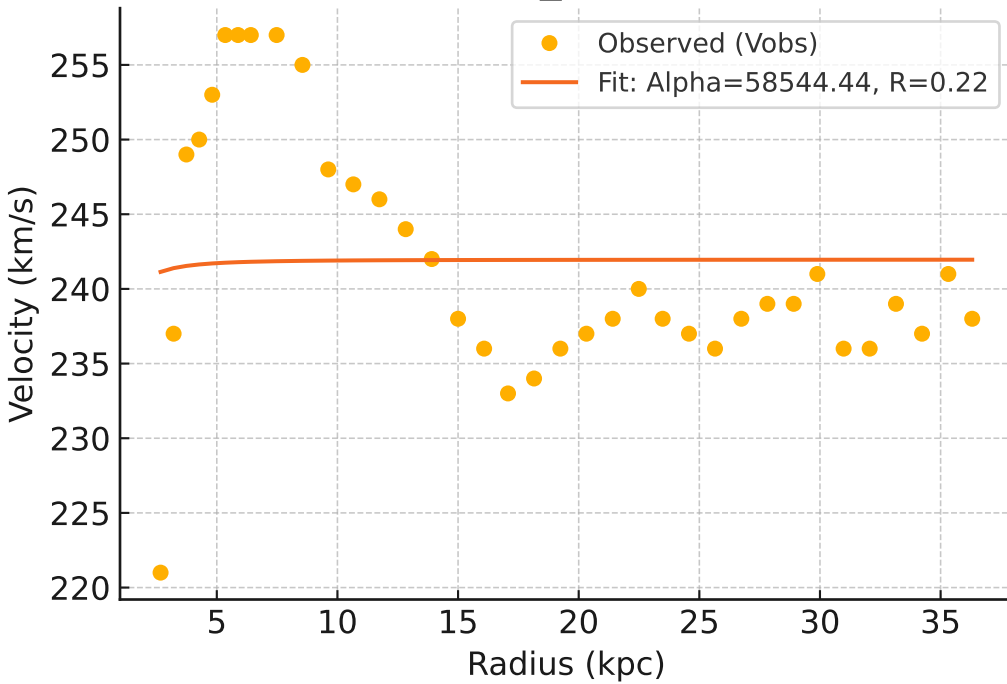
Galaxy: NGC6789_rotmod ($R^2=0.990$)



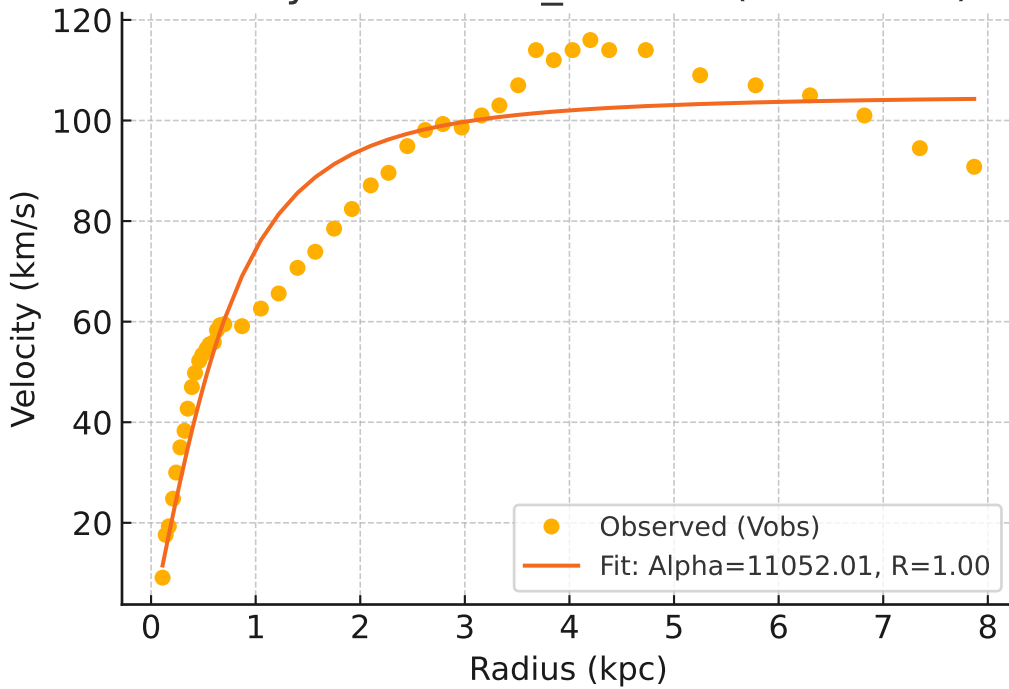
Galaxy: NGC6946_rotmod ($R^2=0.028$)



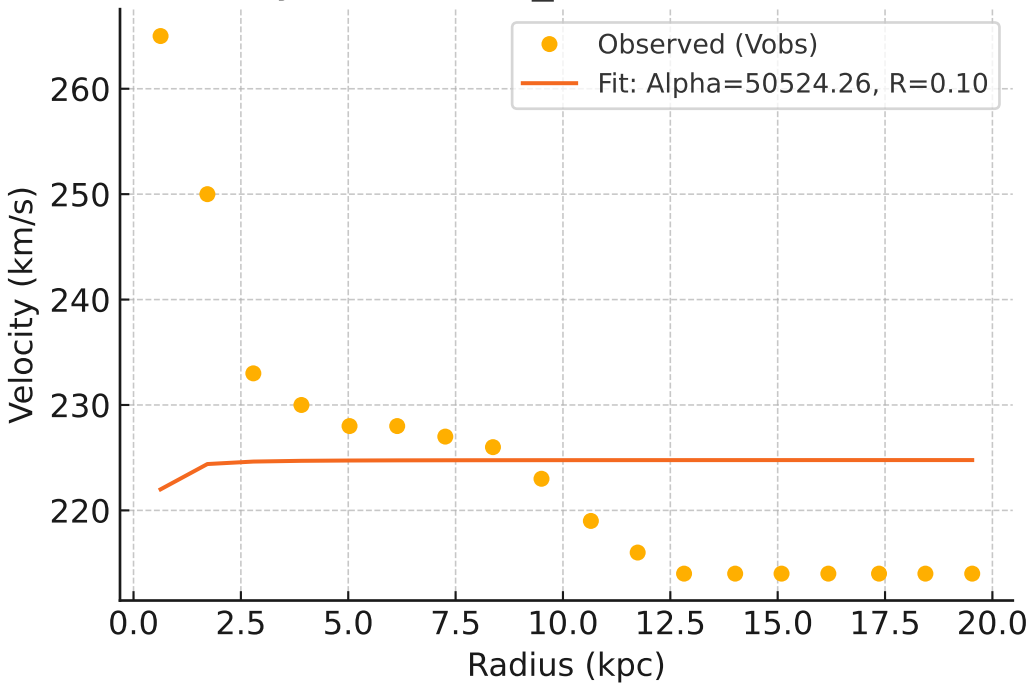
Galaxy: NGC7331_rotmod ($R^2=0.001$)



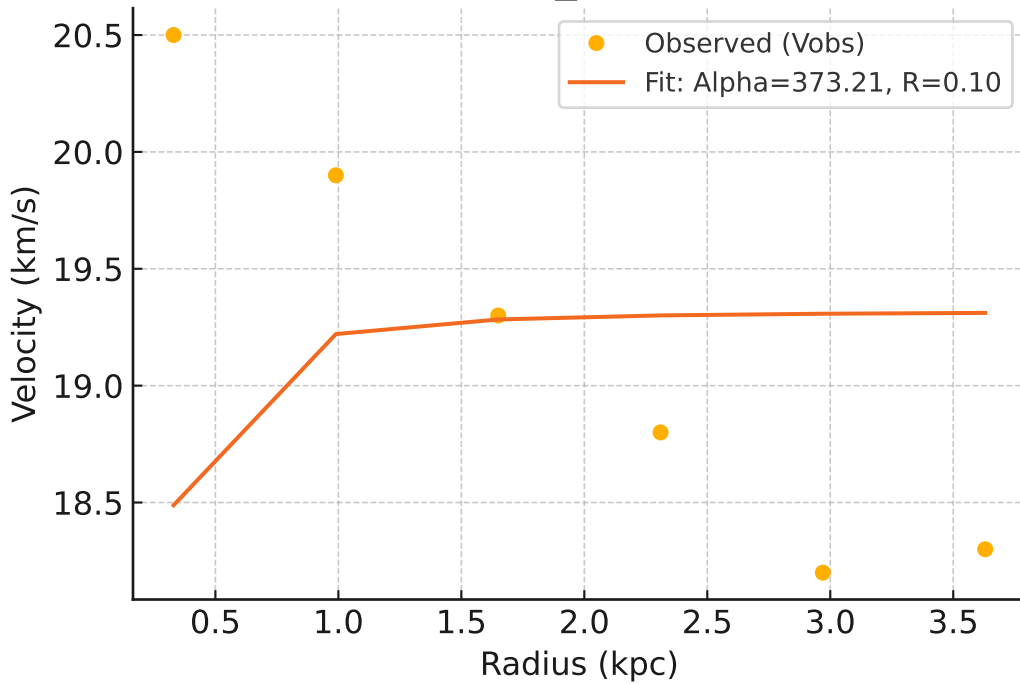
Galaxy: NGC7793_rotmod ($R^2=0.927$)



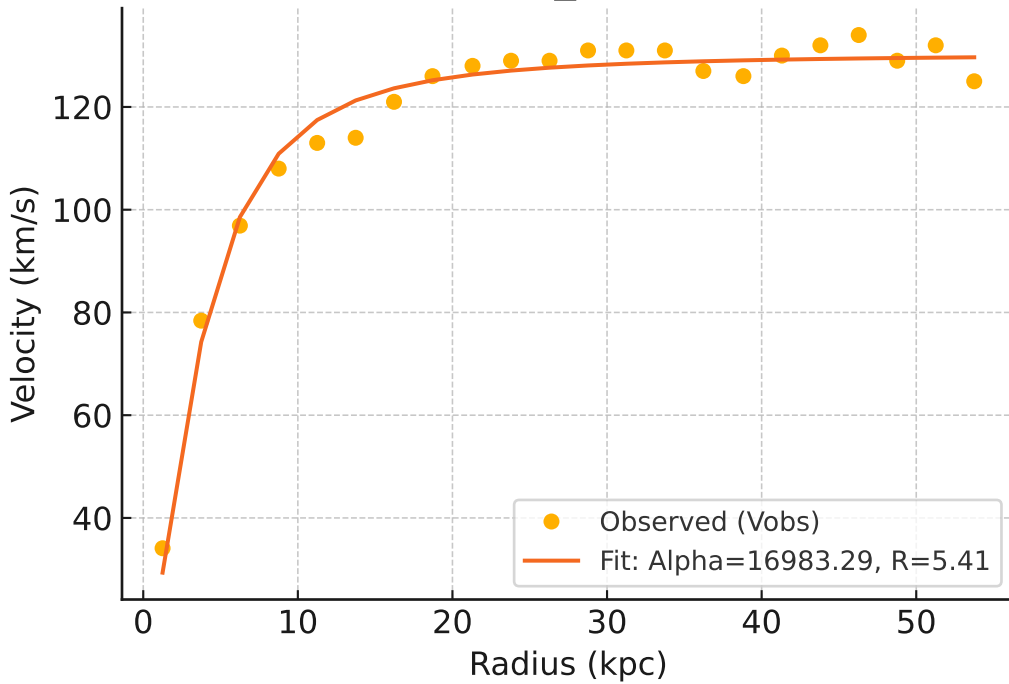
Galaxy: NGC7814_rotmod ($R^2=-0.077$)



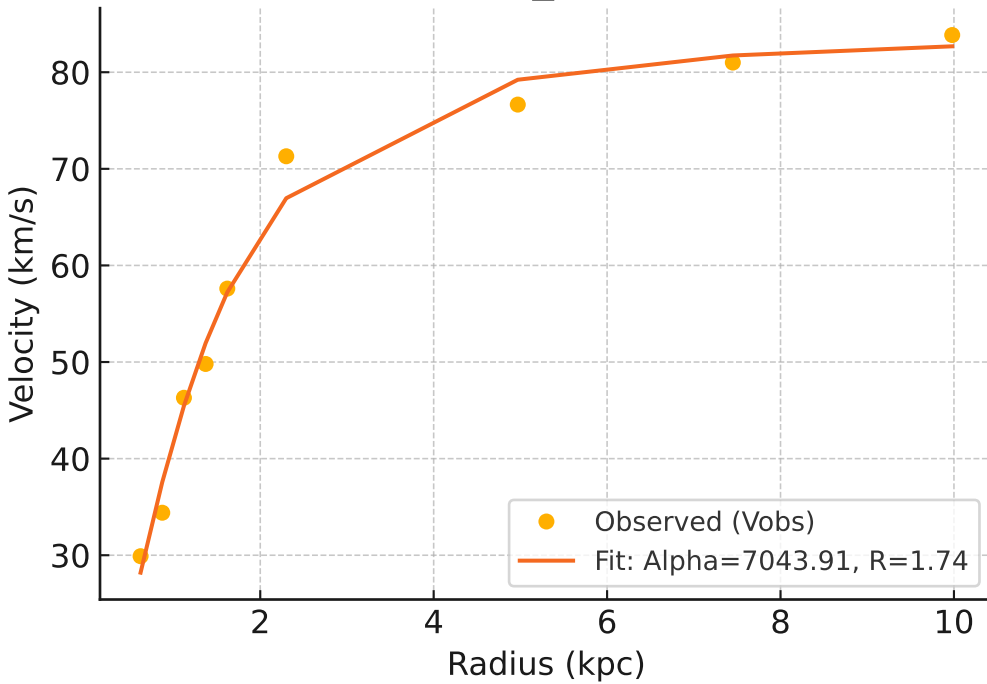
Galaxy: PGC51017_rotmod ($R^2=-0.687$)



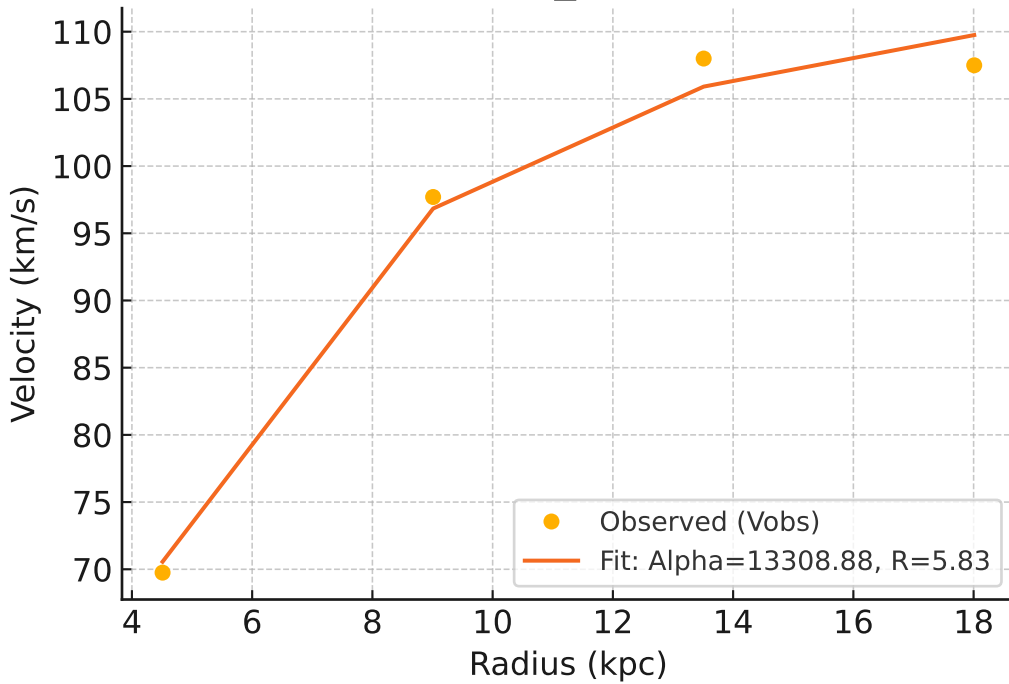
Galaxy: UGC00128_rotmod ($R^2=0.980$)



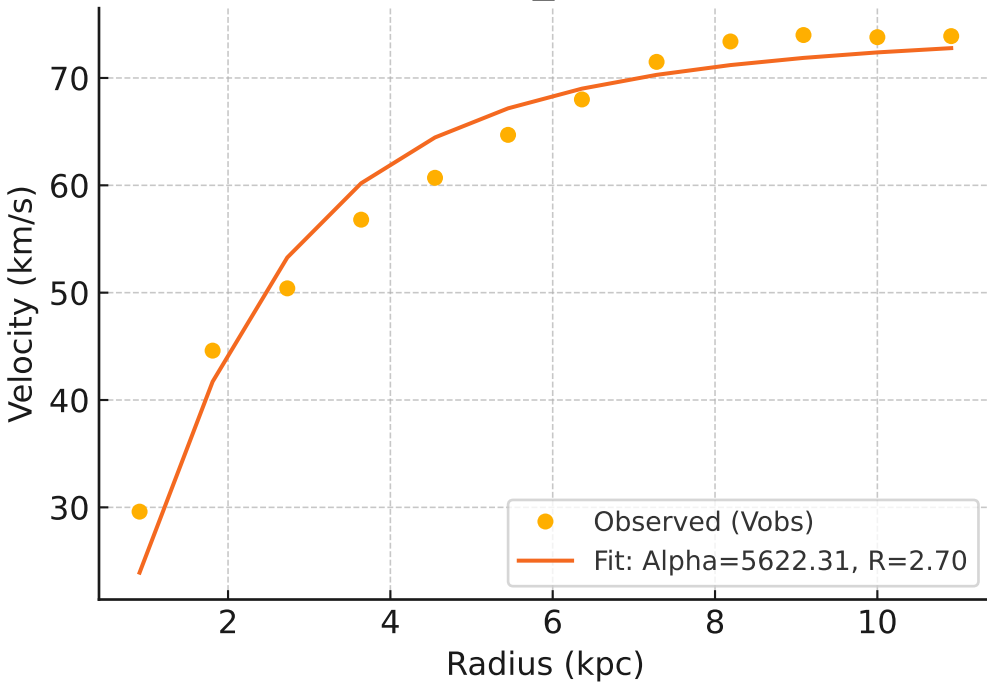
Galaxy: UGC00191_rotmod ($R^2=0.986$)



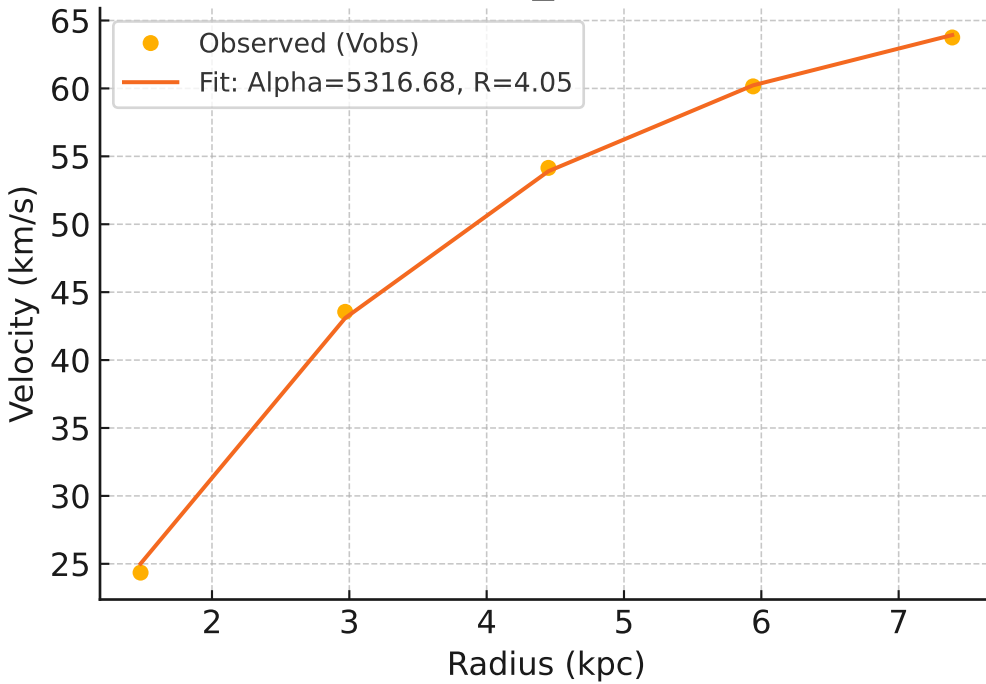
Galaxy: UGC00634_rotmod ($R^2=0.989$)



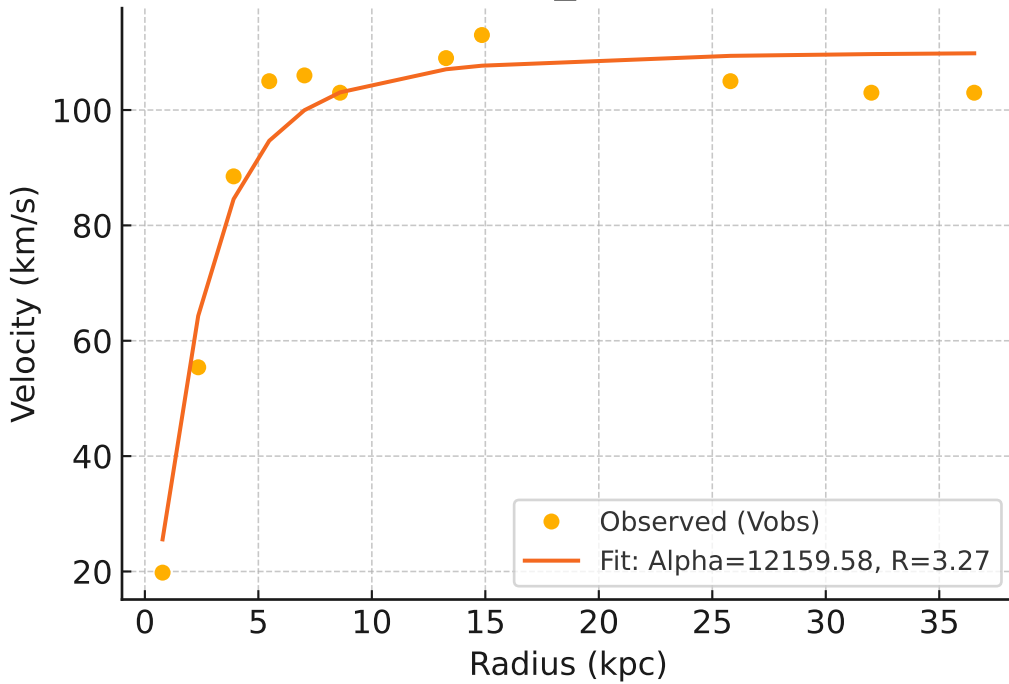
Galaxy: UGC00731_rotmod ($R^2=0.957$)



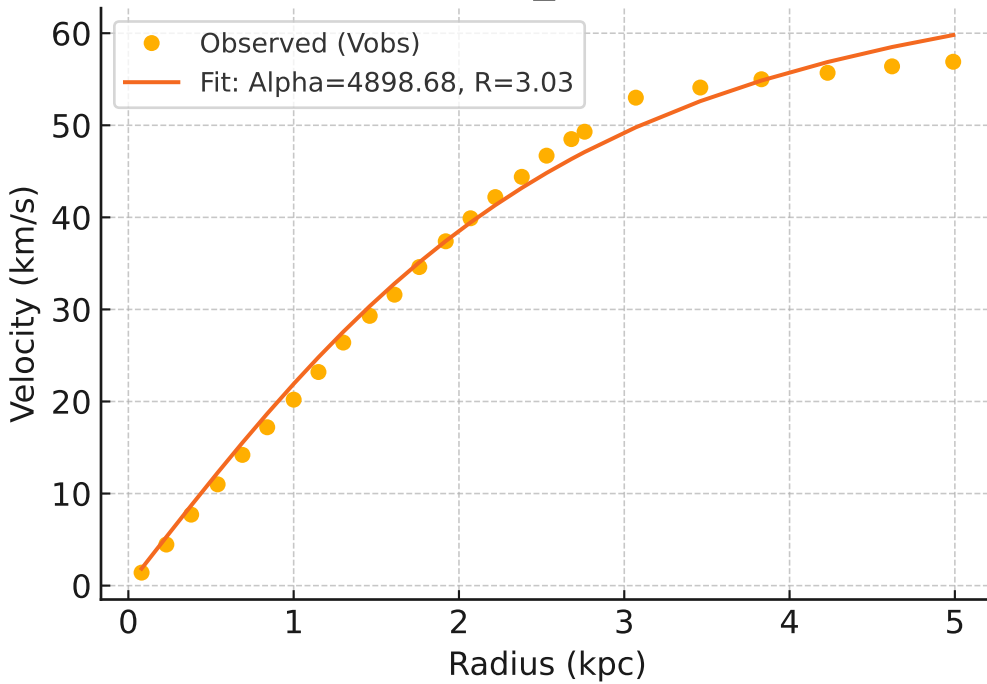
Galaxy: UGC00891_rotmod ($R^2=0.999$)



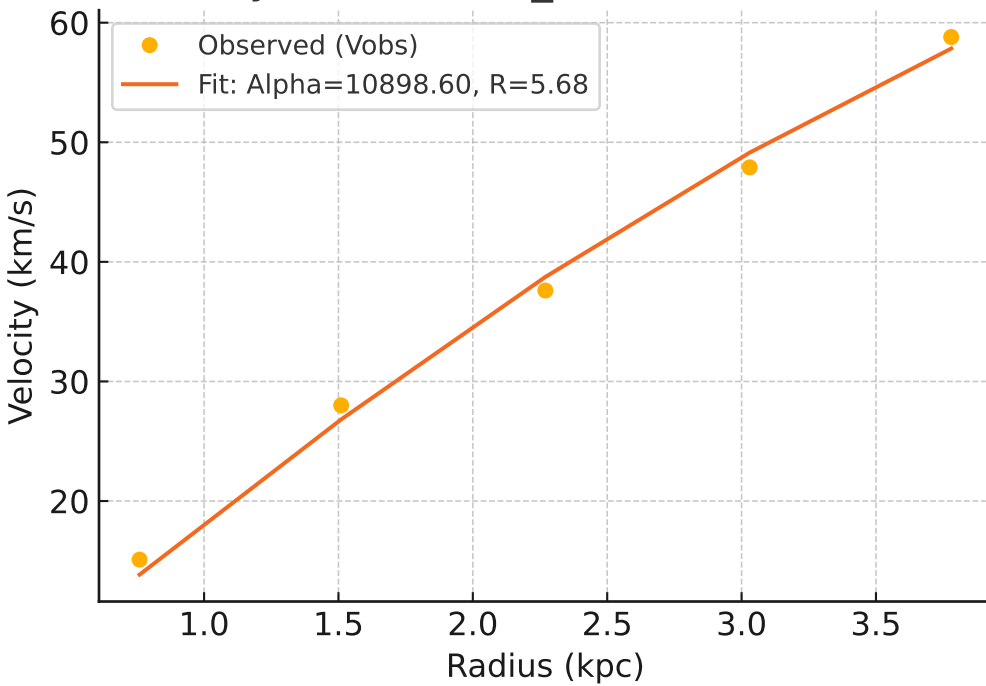
Galaxy: UGC01230_rotmod ($R^2=0.949$)



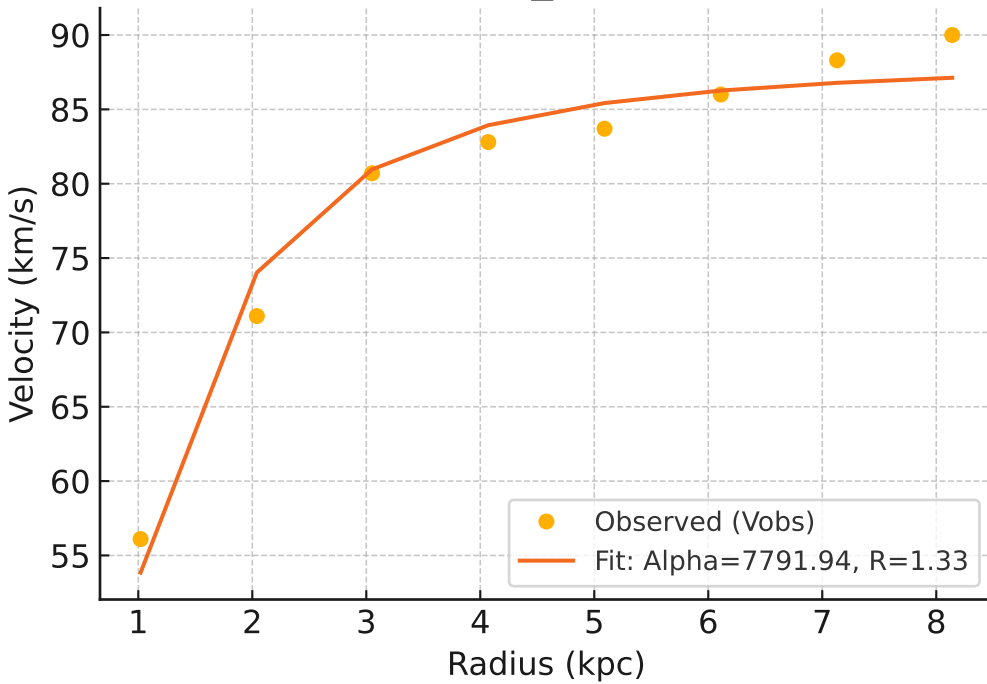
Galaxy: UGC01281_rotmod ($R^2=0.992$)



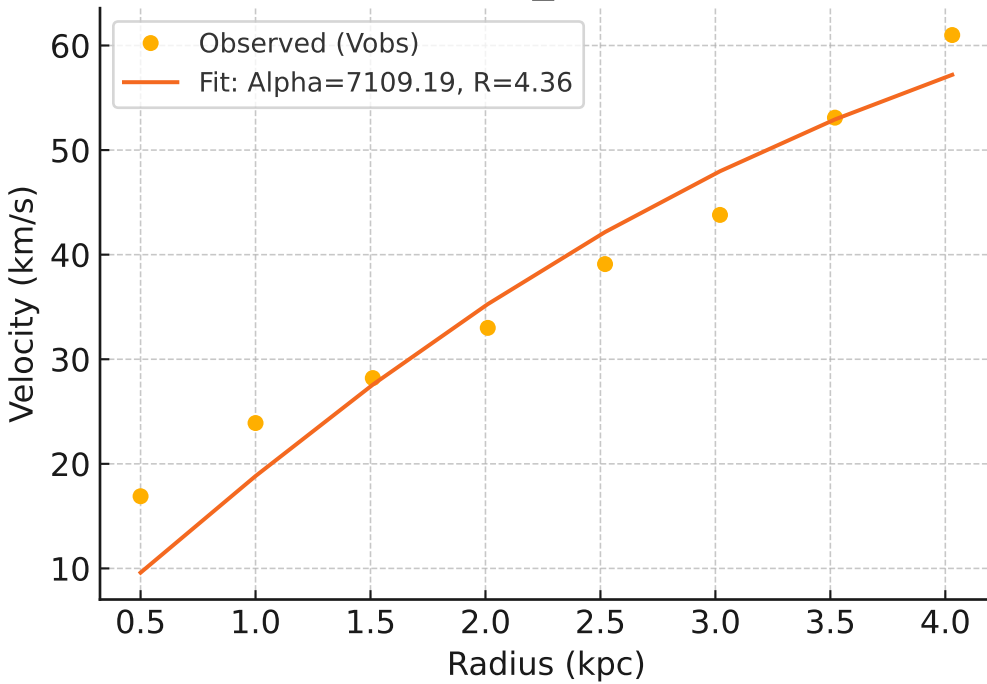
Galaxy: UGC02023_rotmod ($R^2=0.994$)



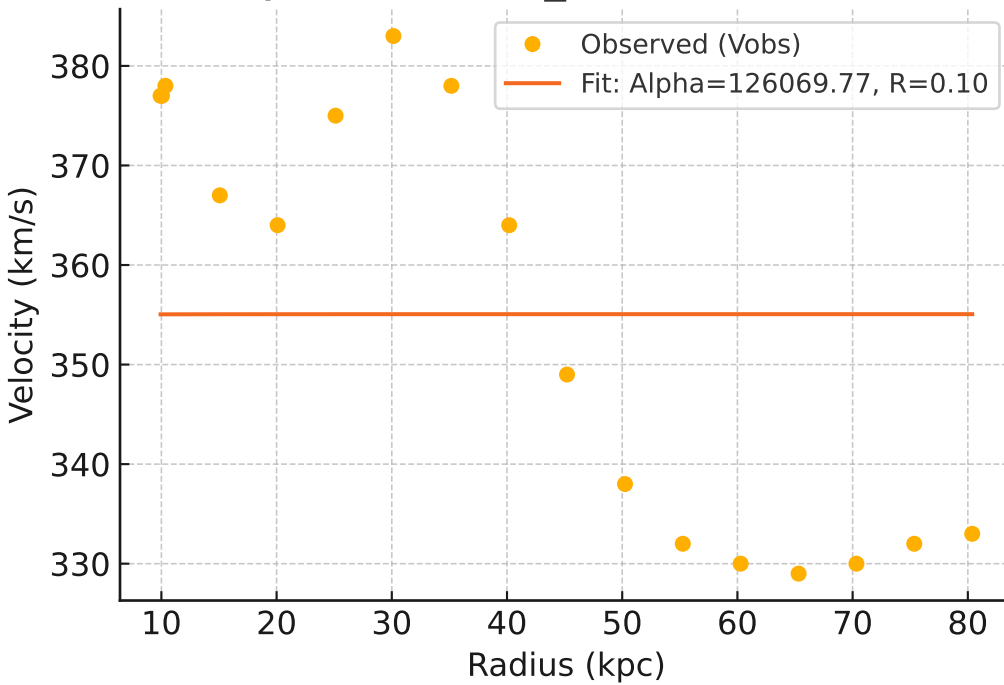
Galaxy: UGC02259_rotmod ($R^2=0.967$)



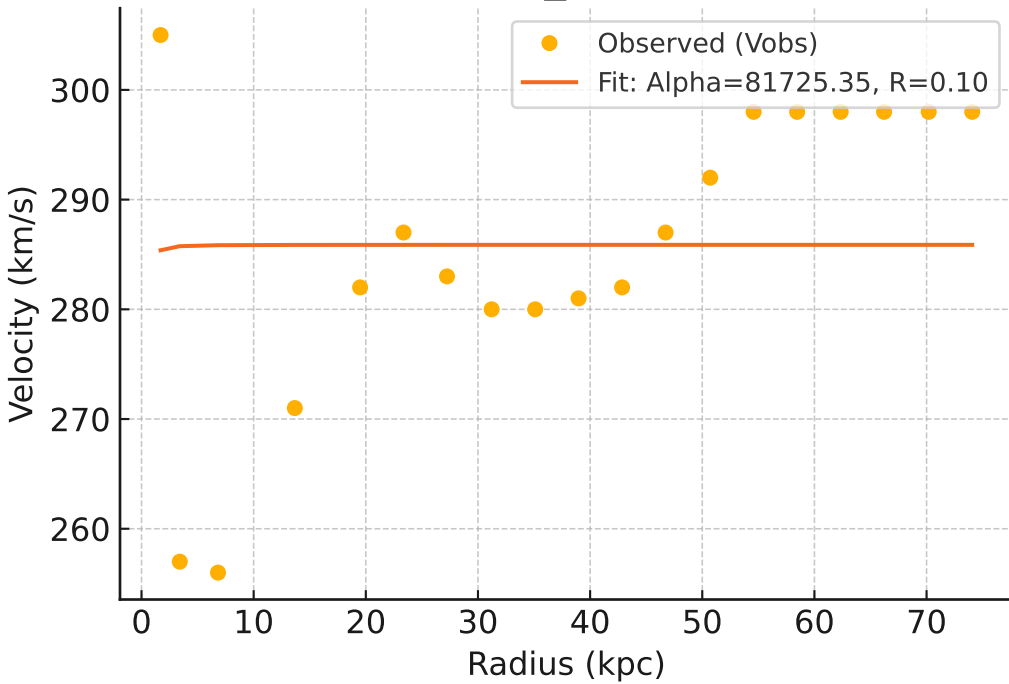
Galaxy: UGC02455_rotmod ($R^2=0.919$)



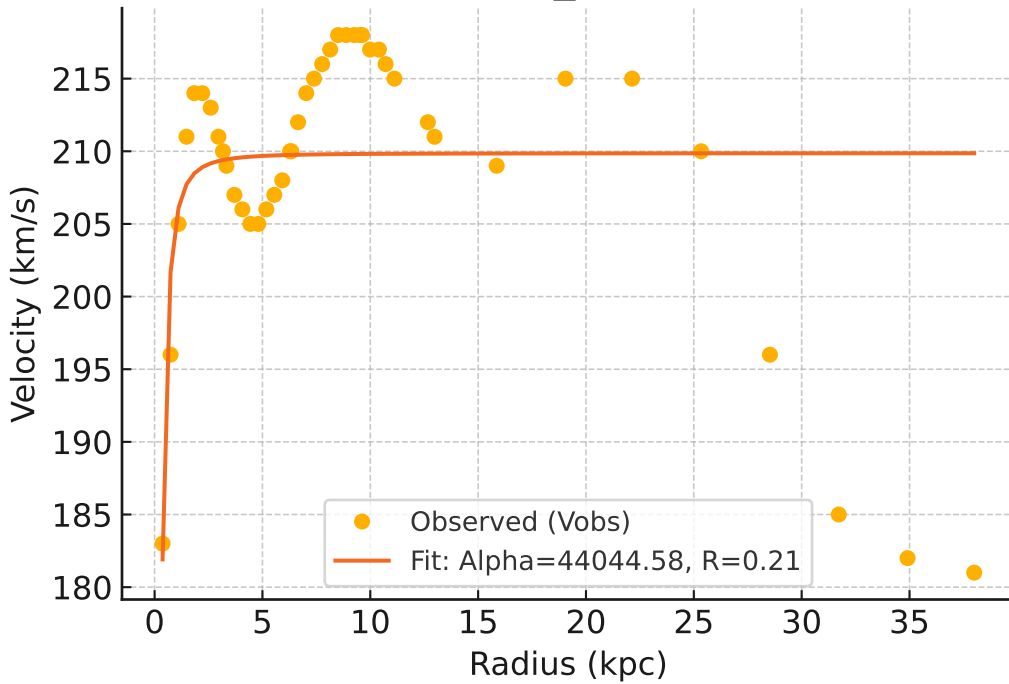
Galaxy: UGC02487_rotmod ($R^2=-0.000$)



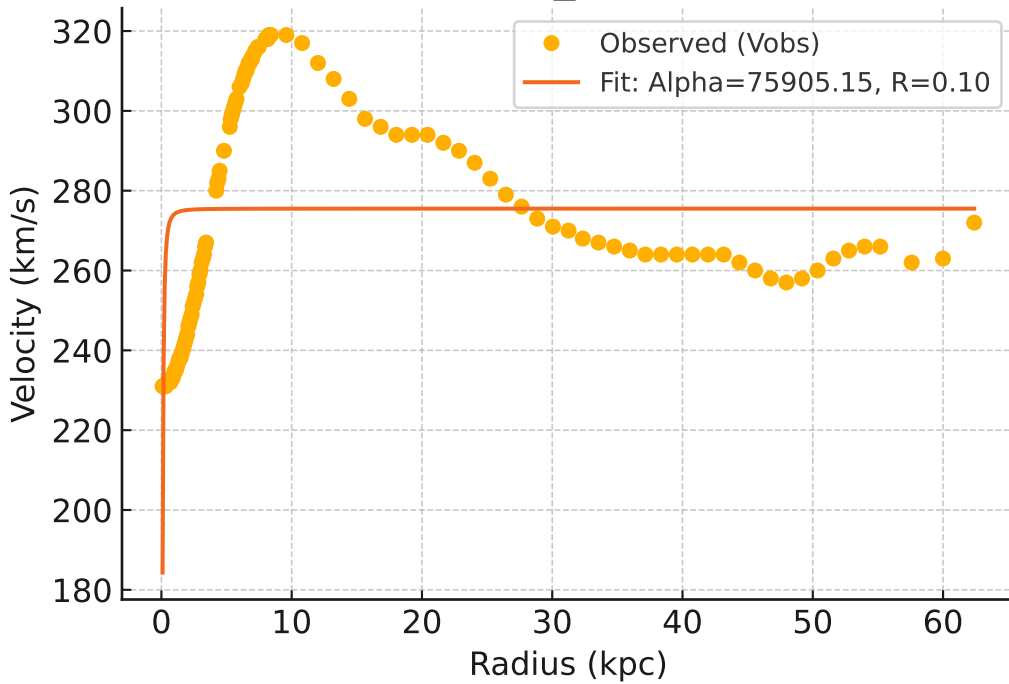
Galaxy: UGC02885_rotmod ($R^2=-0.003$)



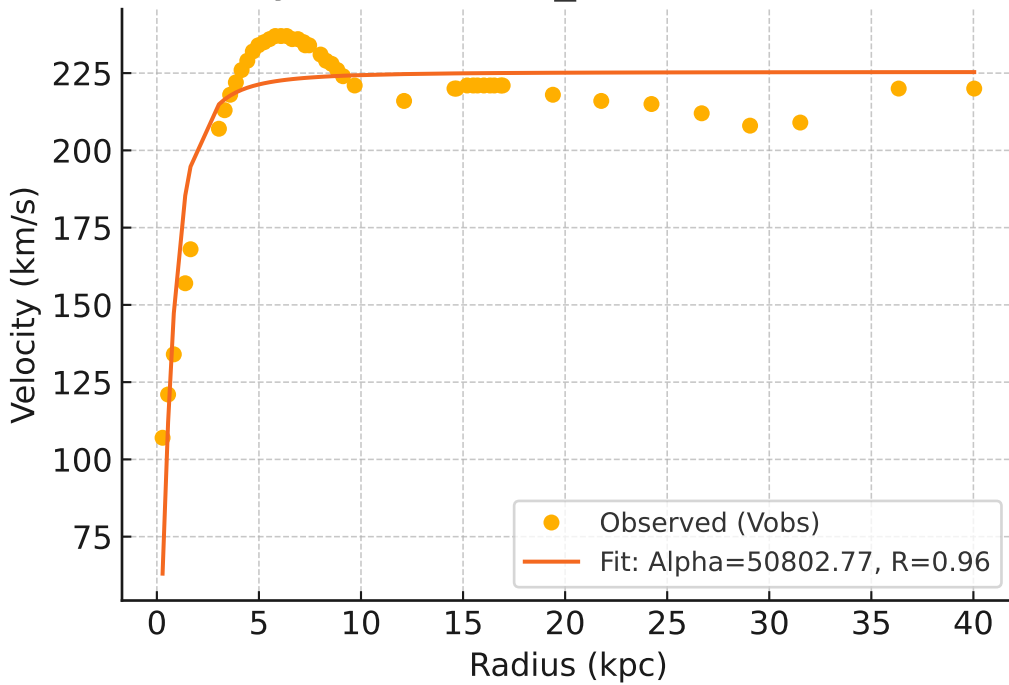
Galaxy: UGC02916_rotmod ($R^2=0.195$)



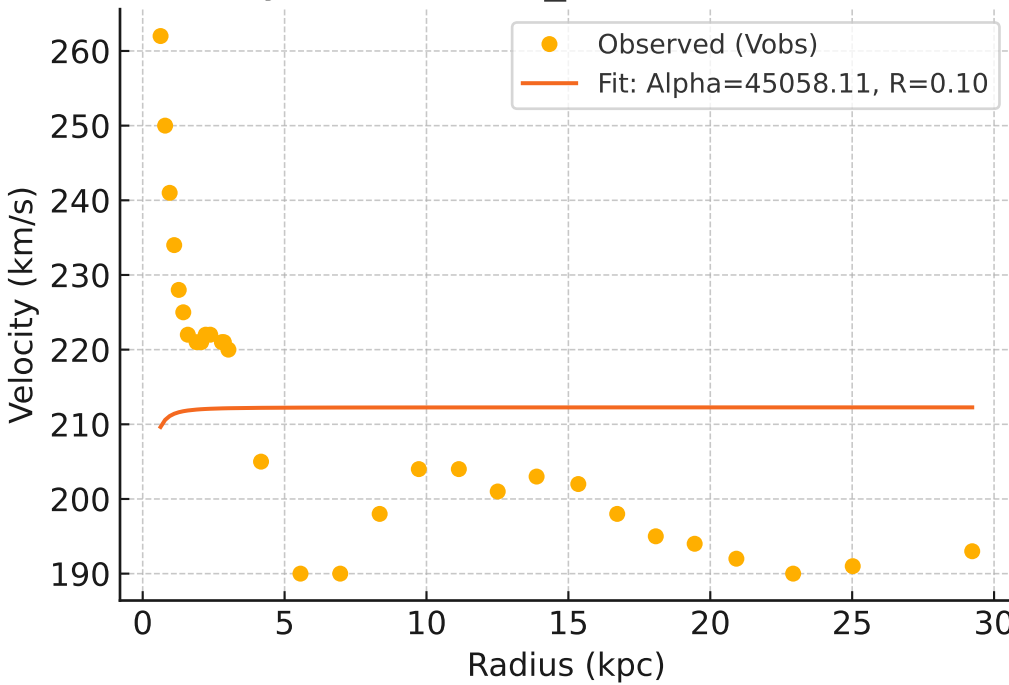
Galaxy: UGC02953_rotmod ($R^2=0.068$)



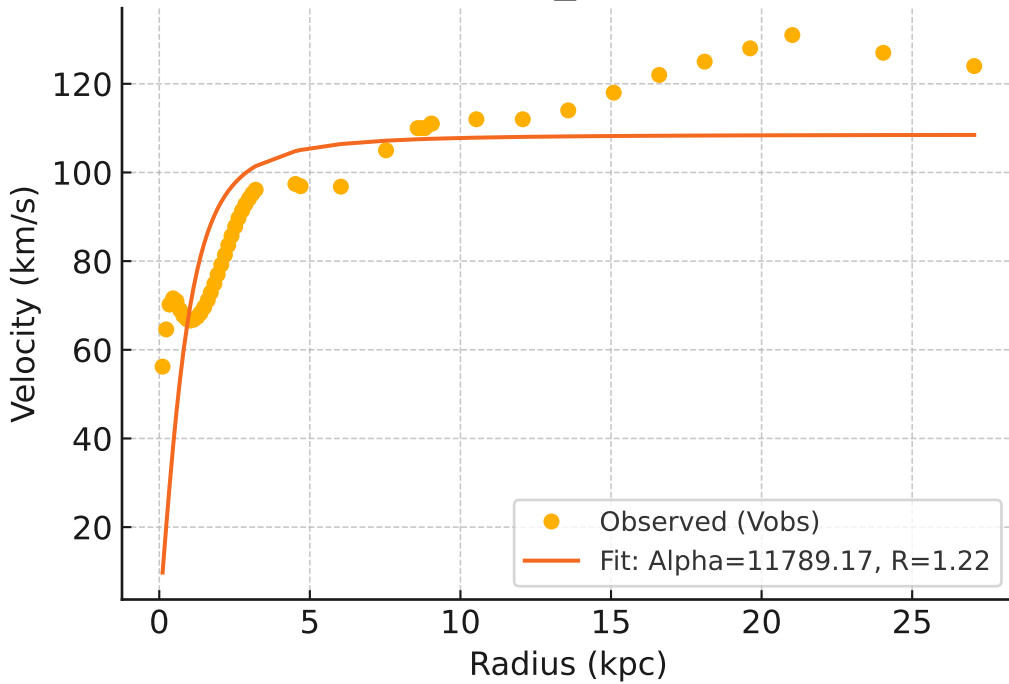
Galaxy: UGC03205_rotmod ($R^2=0.815$)



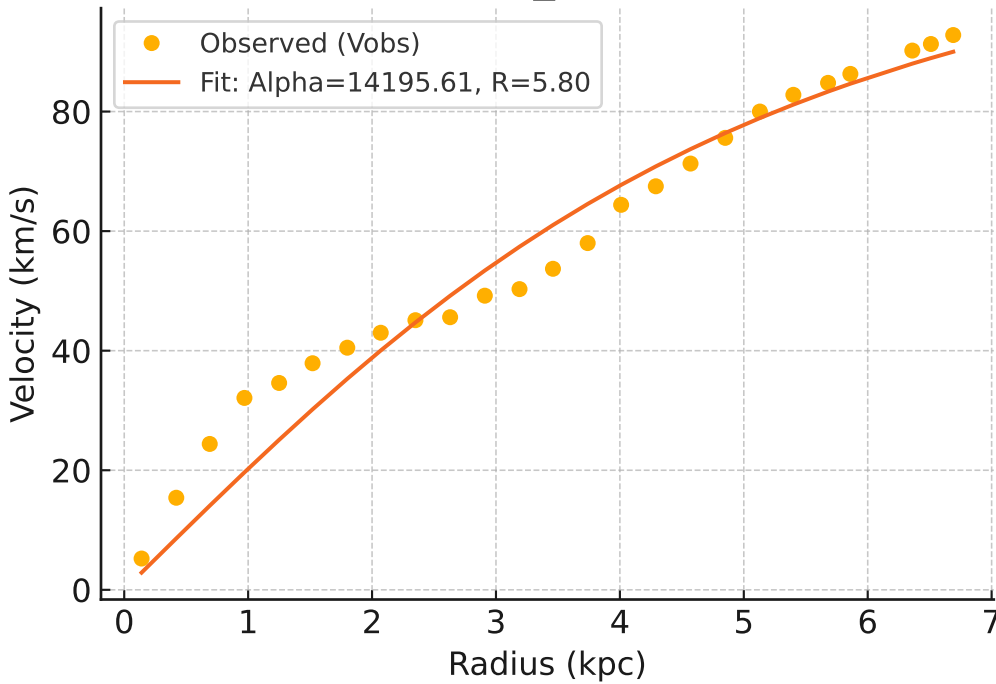
Galaxy: UGC03546_rotmod ($R^2=-0.054$)



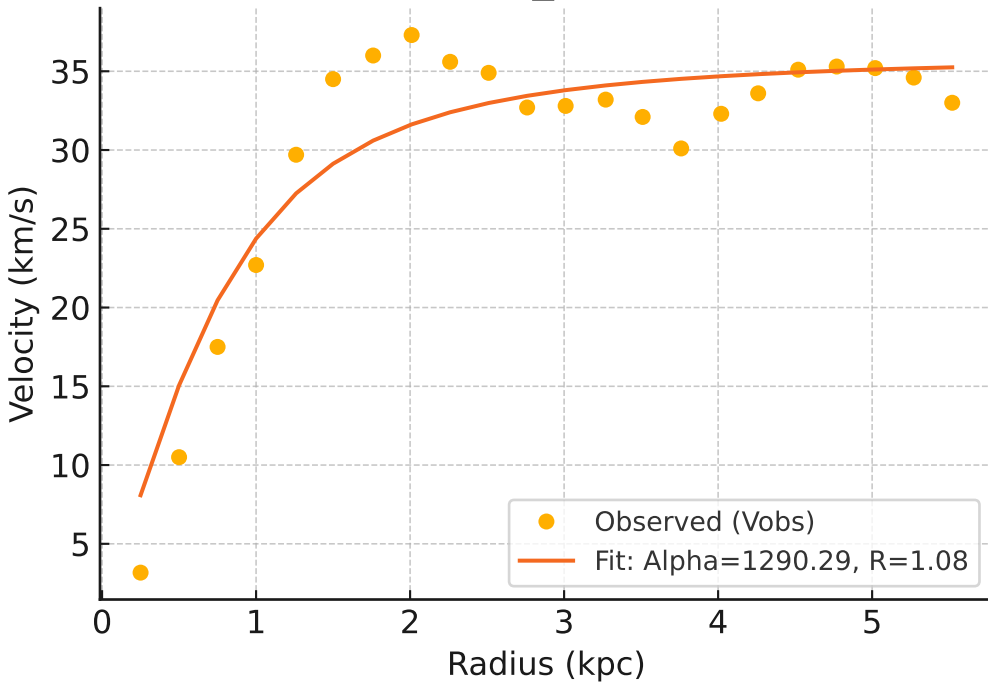
Galaxy: UGC03580_rotmod ($R^2=0.385$)



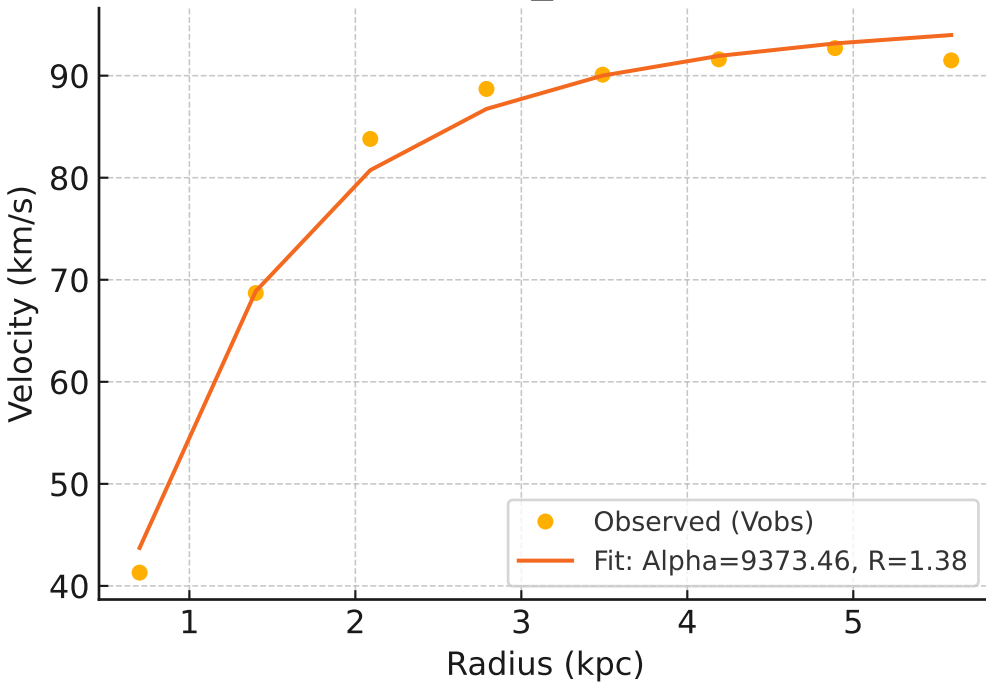
Galaxy: UGC04278_rotmod ($R^2=0.951$)



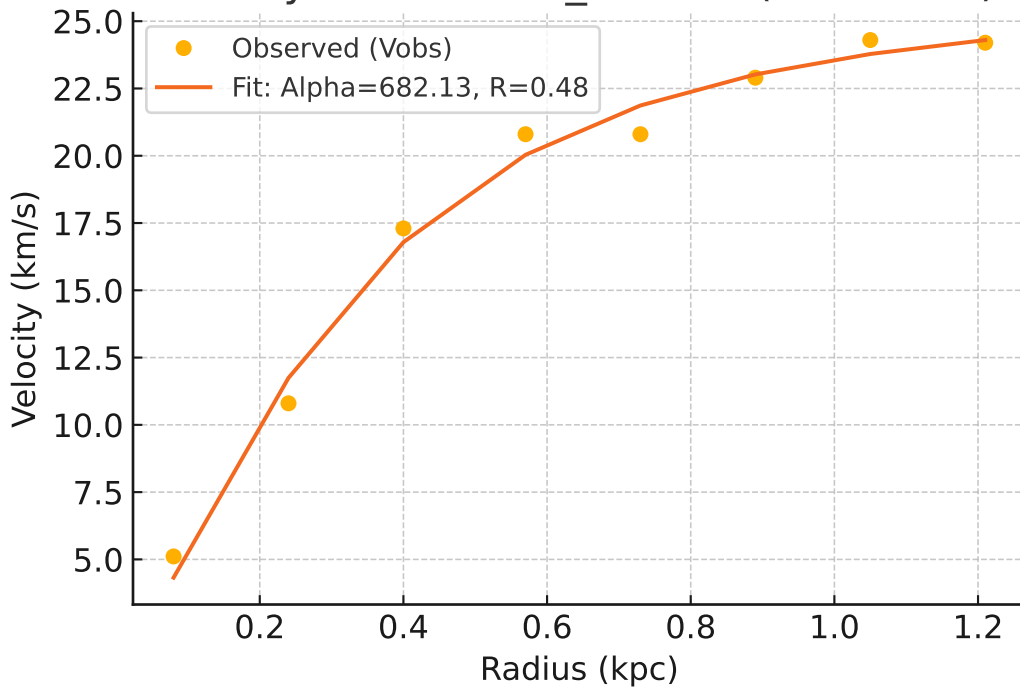
Galaxy: UGC04305_rotmod ($R^2=0.874$)



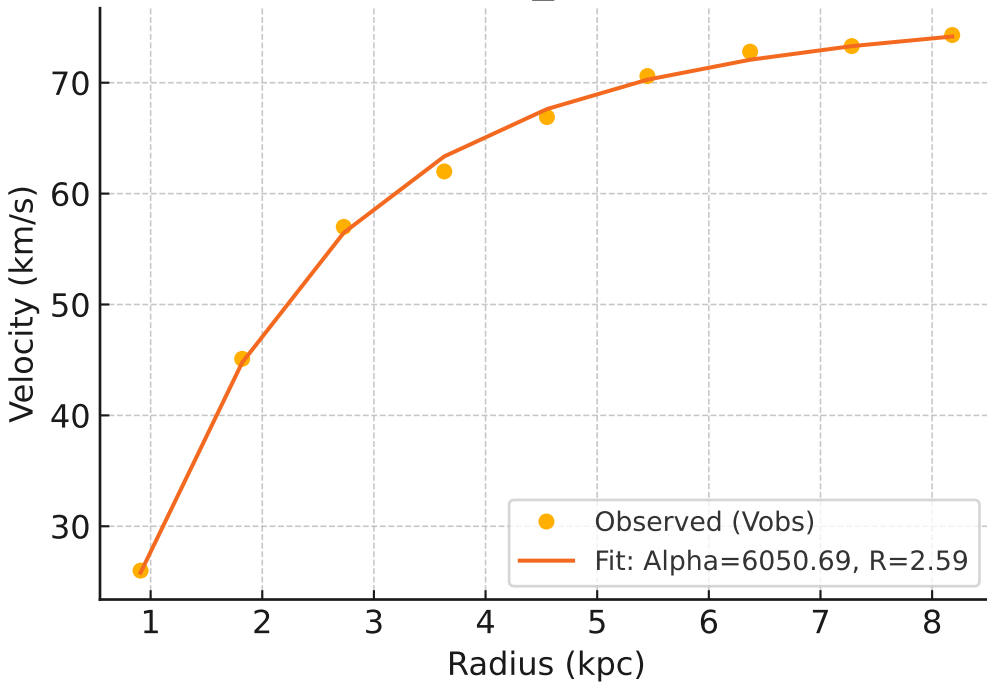
Galaxy: UGC04325_rotmod ($R^2=0.989$)



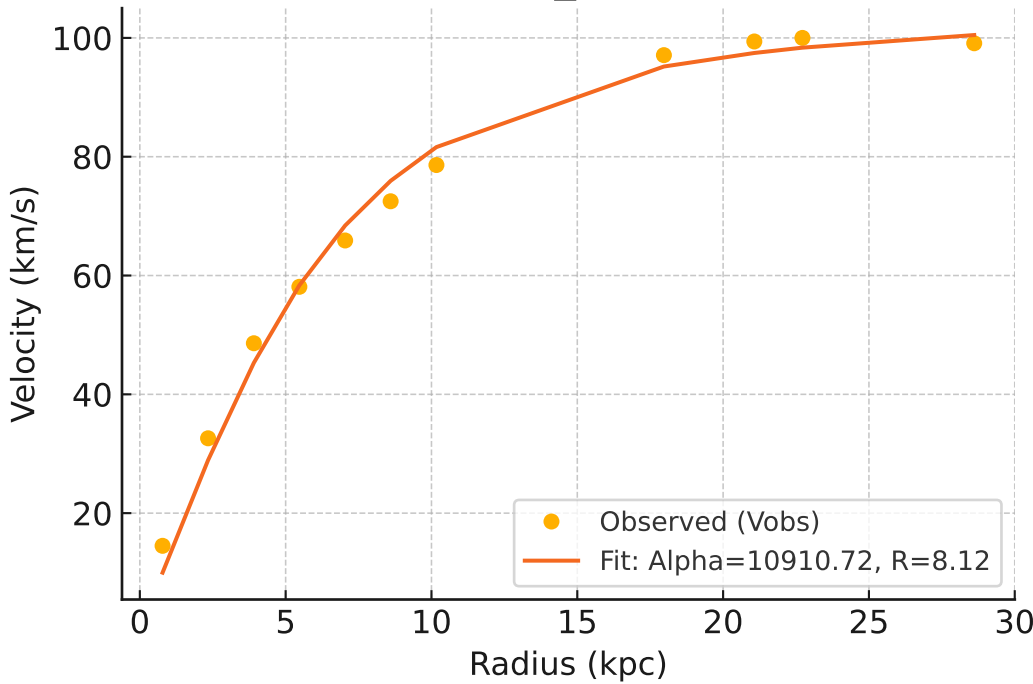
Galaxy: UGC04483_rotmod ($R^2=0.989$)



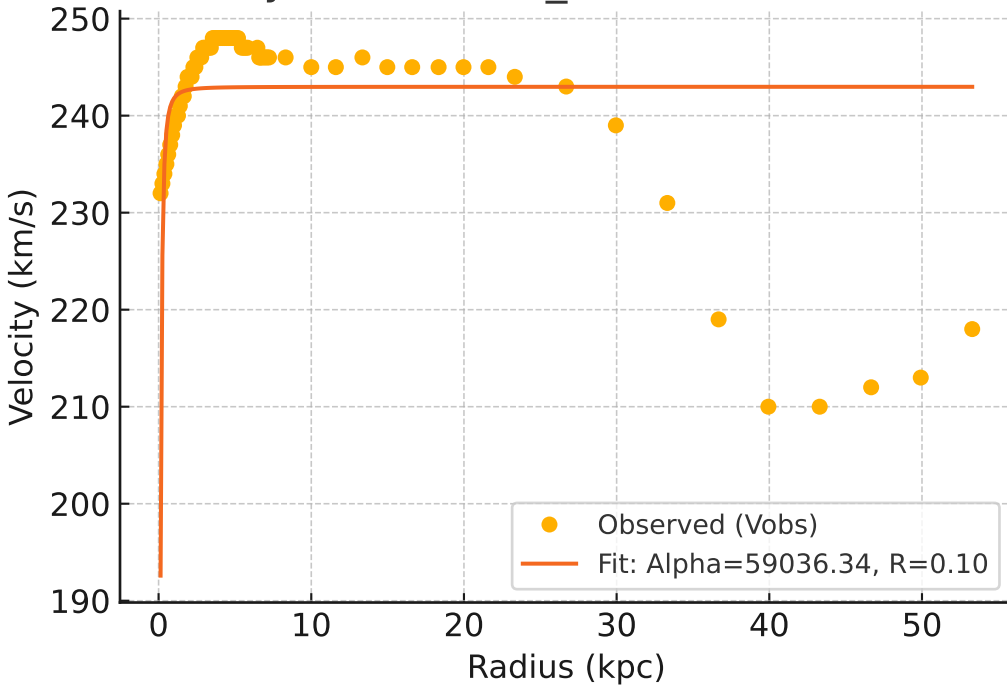
Galaxy: UGC04499_rotmod ($R^2=0.998$)



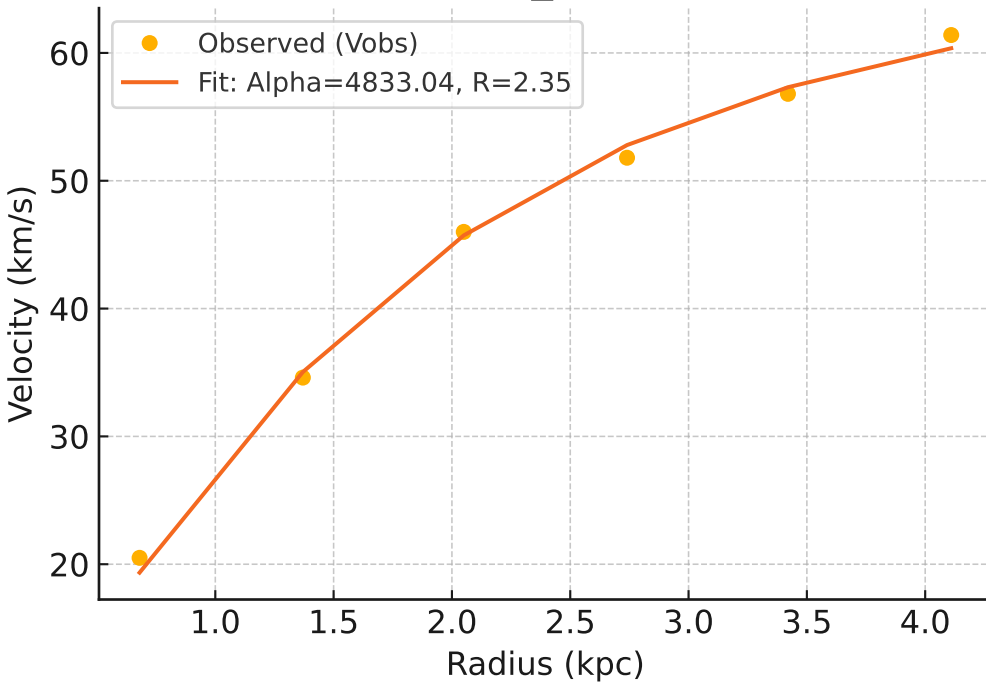
Galaxy: UGC05005_rotmod ($R^2=0.990$)



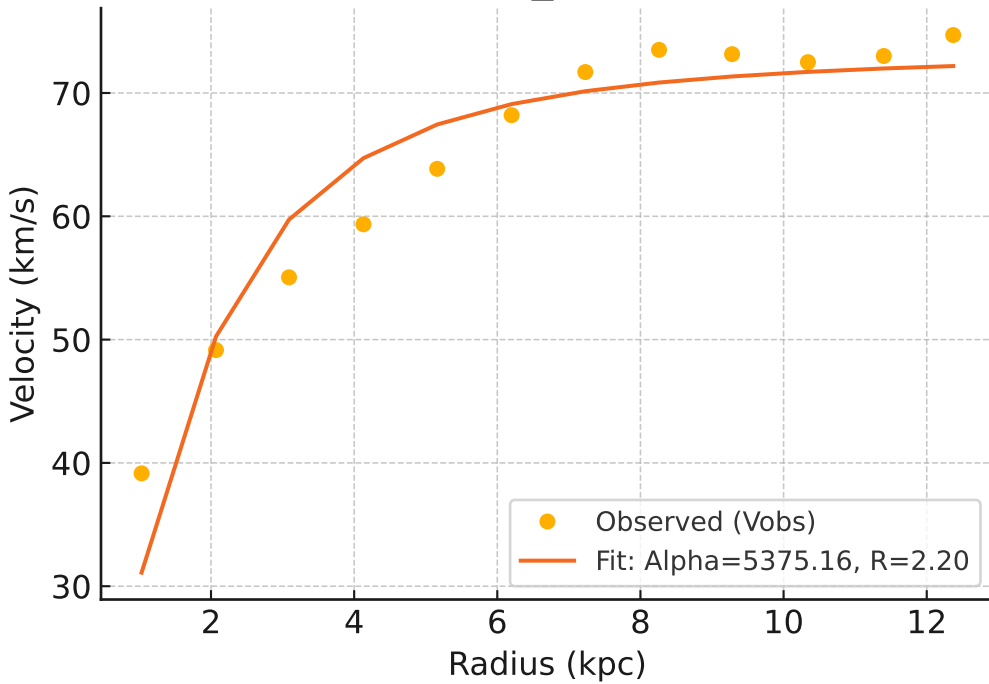
Galaxy: UGC05253_rotmod ($R^2=-0.200$)



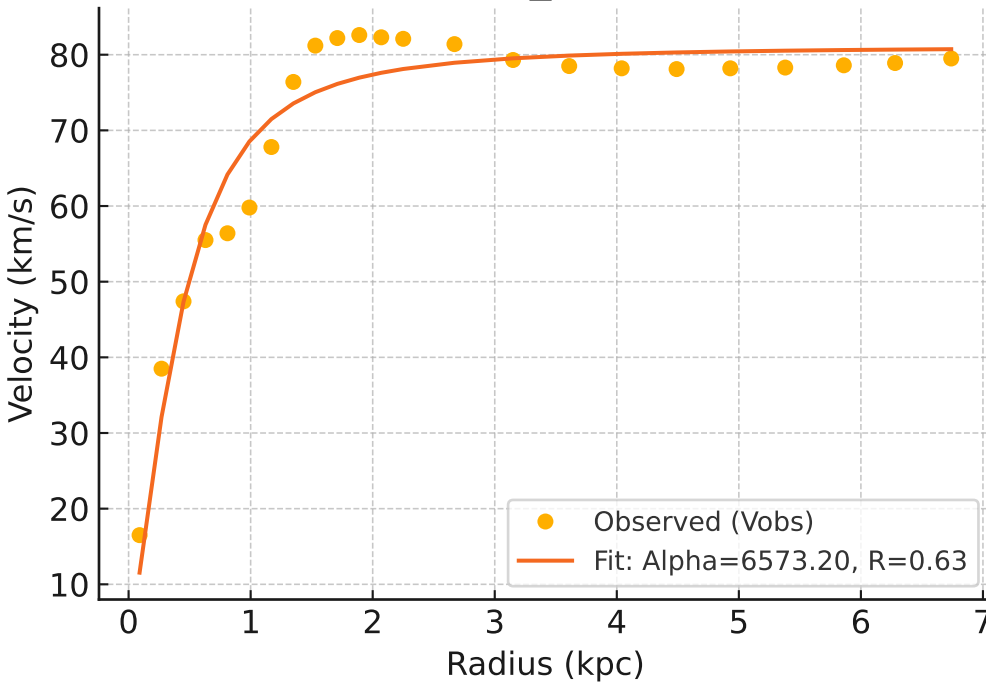
Galaxy: UGC05414_rotmod ($R^2=0.997$)



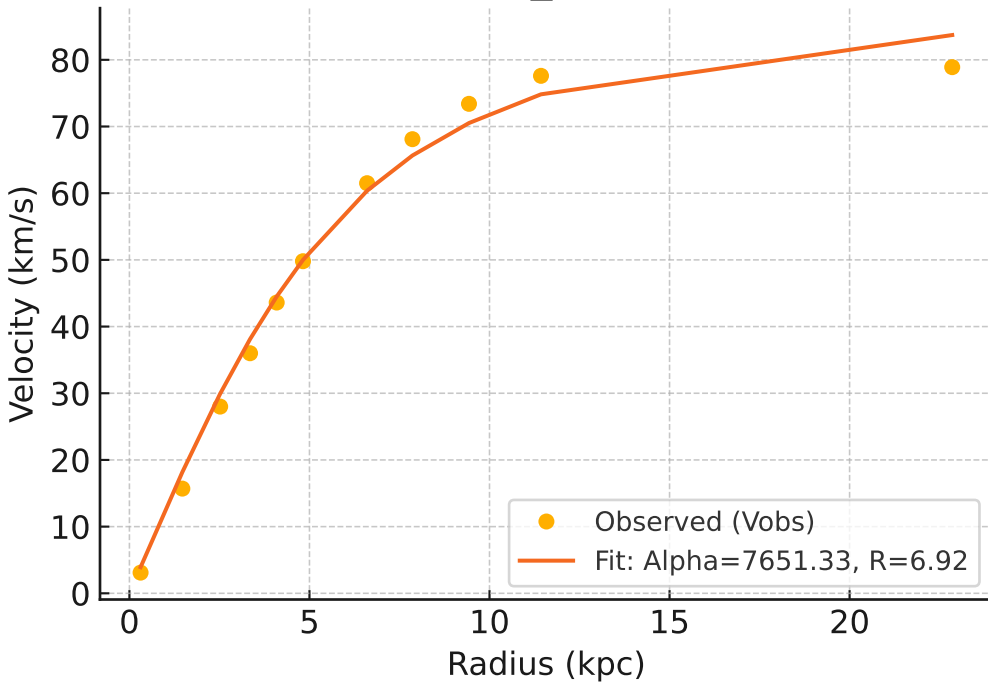
Galaxy: UGC05716_rotmod ($R^2=0.896$)



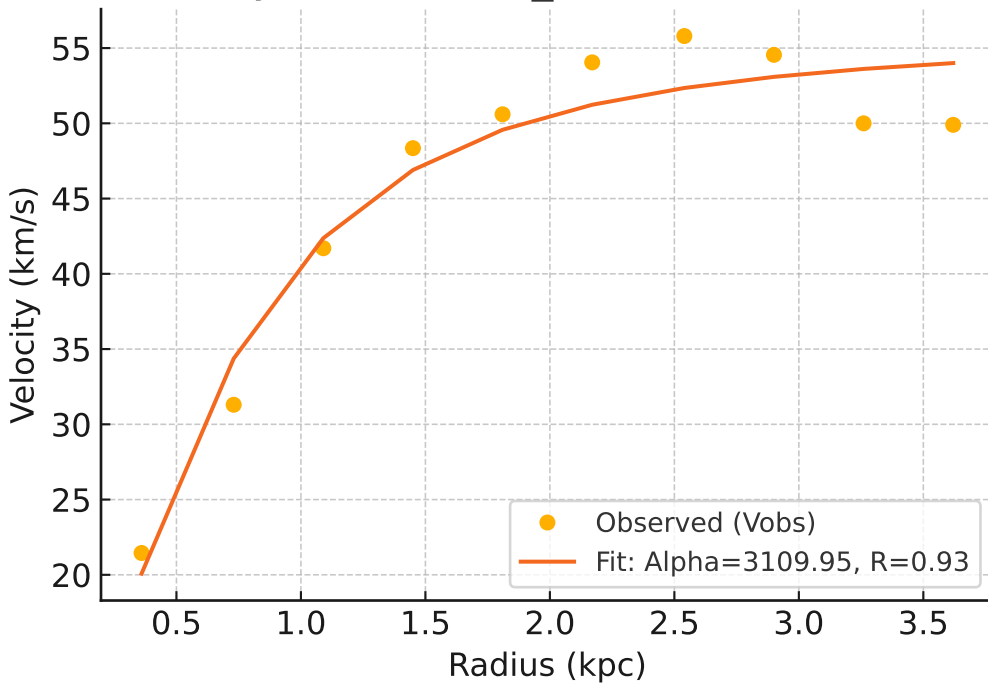
Galaxy: UGC05721_rotmod ($R^2=0.937$)



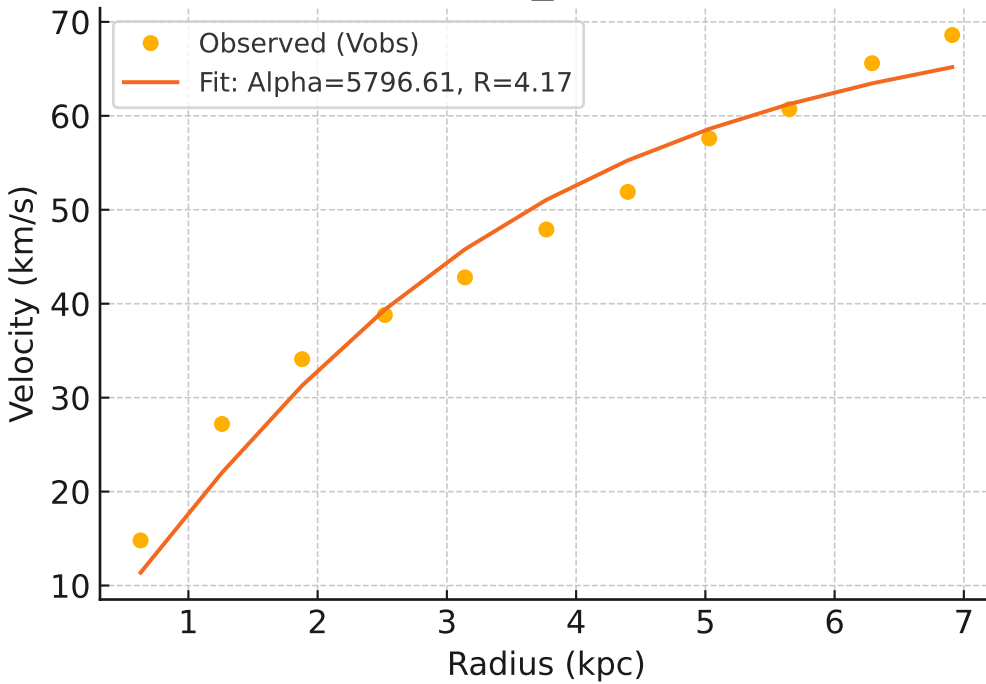
Galaxy: UGC05750_rotmod ($R^2=0.991$)



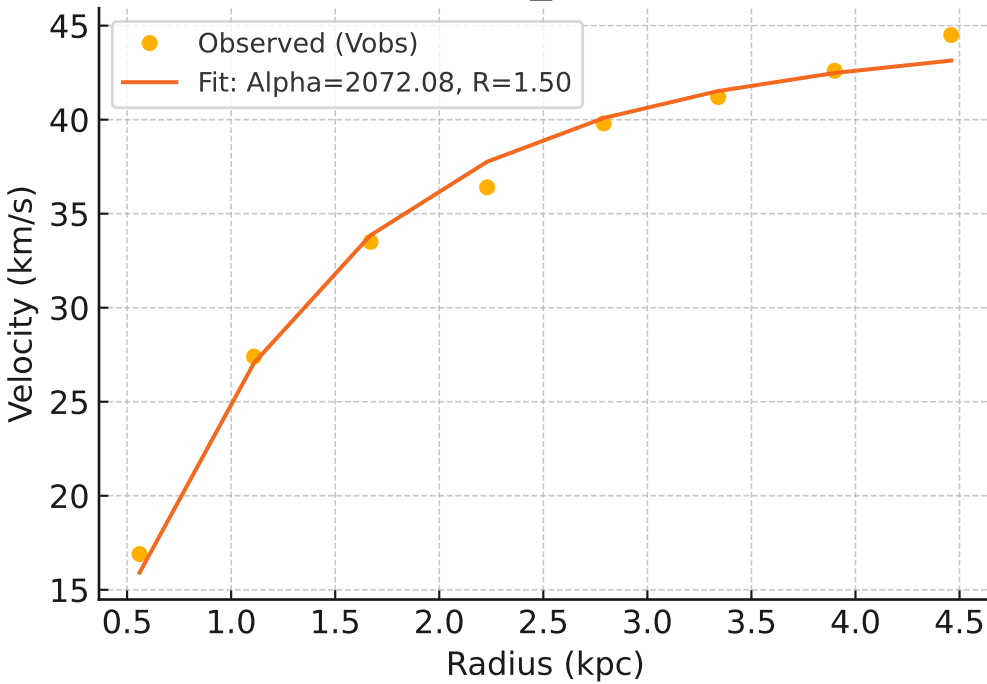
Galaxy: UGC05764_rotmod ($R^2=0.941$)



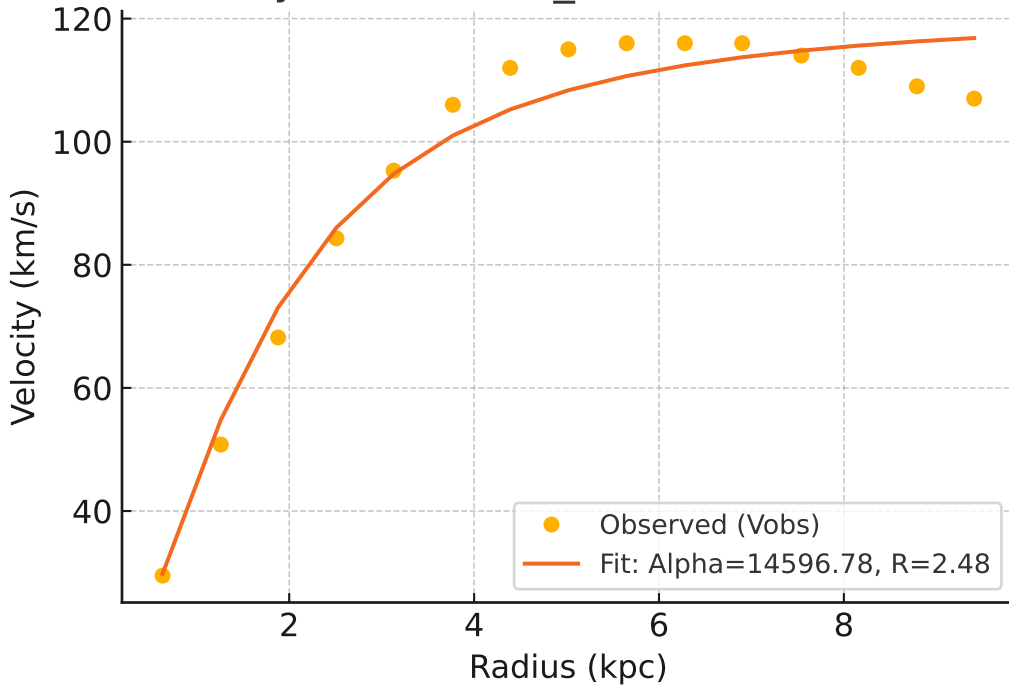
Galaxy: UGC05829_rotmod ($R^2=0.966$)



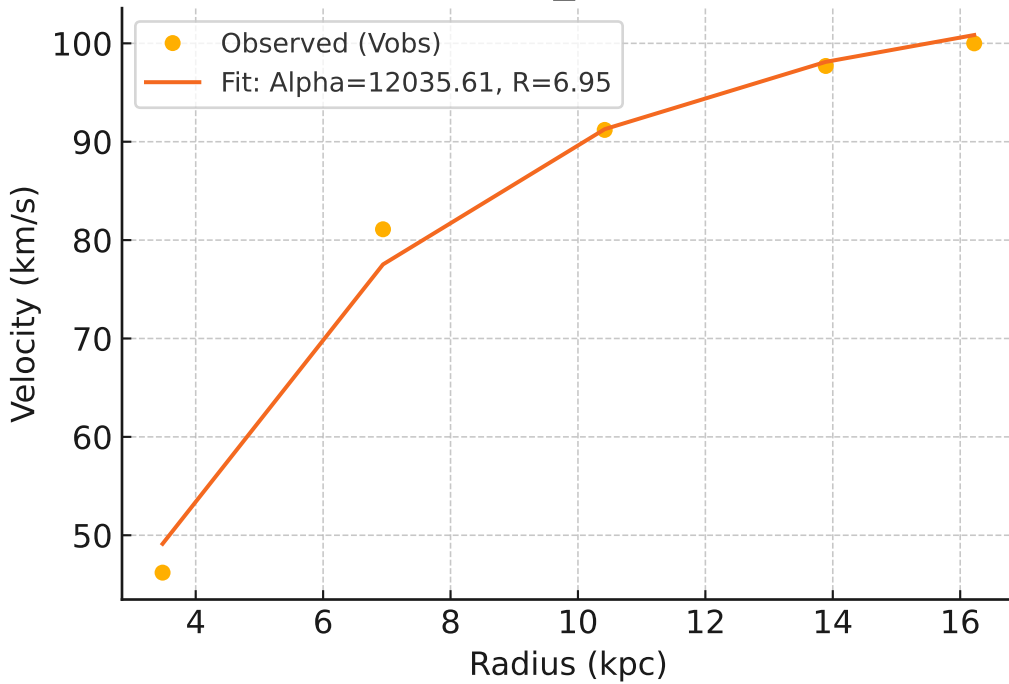
Galaxy: UGC05918_rotmod ($R^2=0.991$)



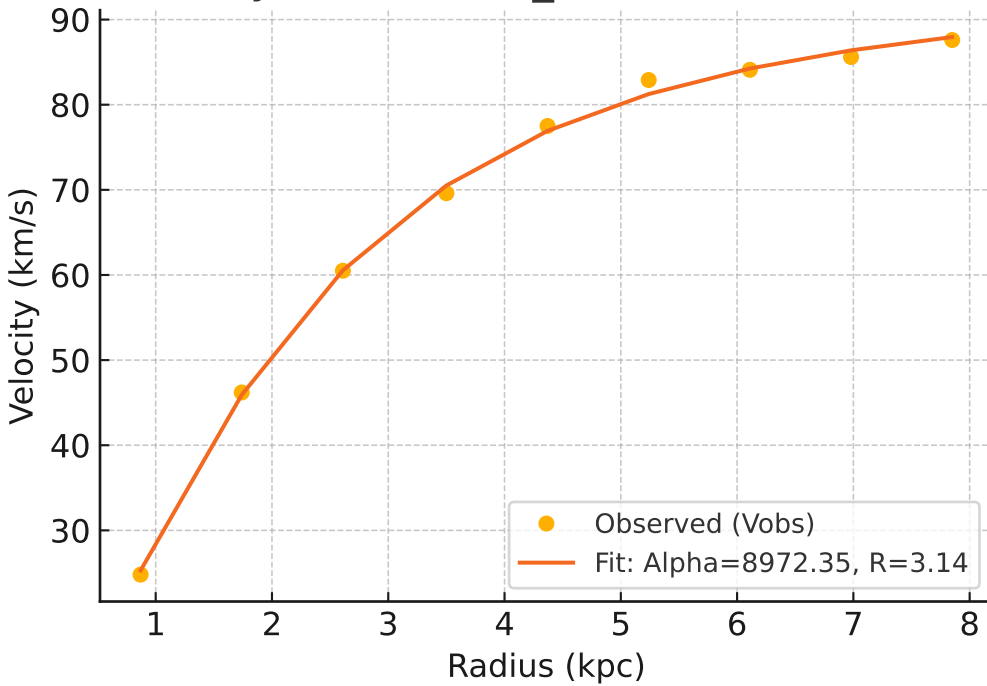
Galaxy: UGC05986_rotmod ($R^2=0.964$)



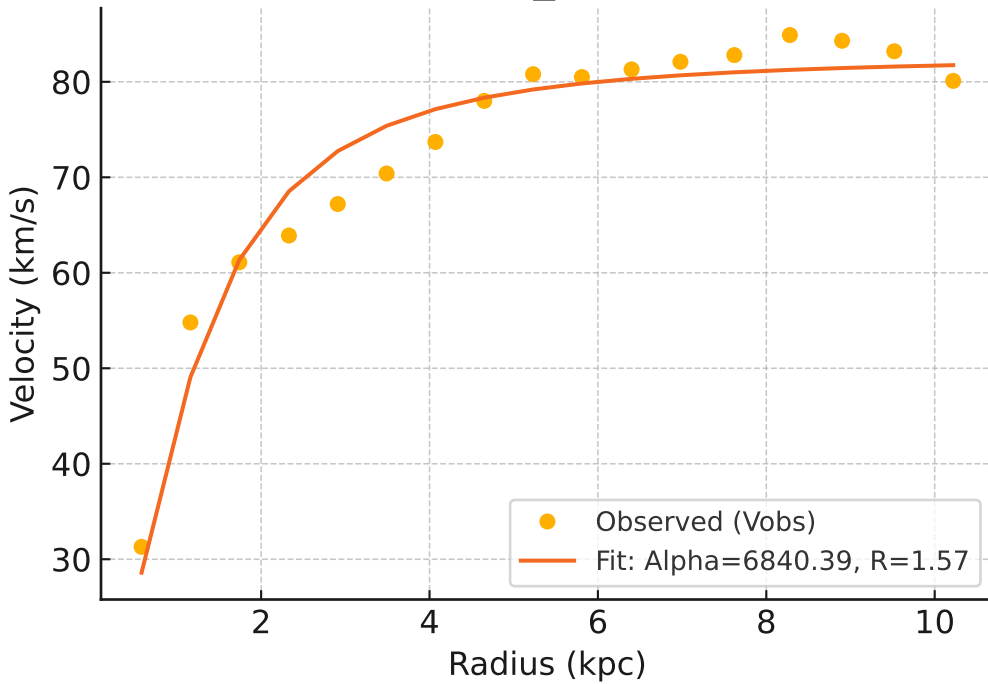
Galaxy: UGC05999_rotmod ($R^2=0.988$)



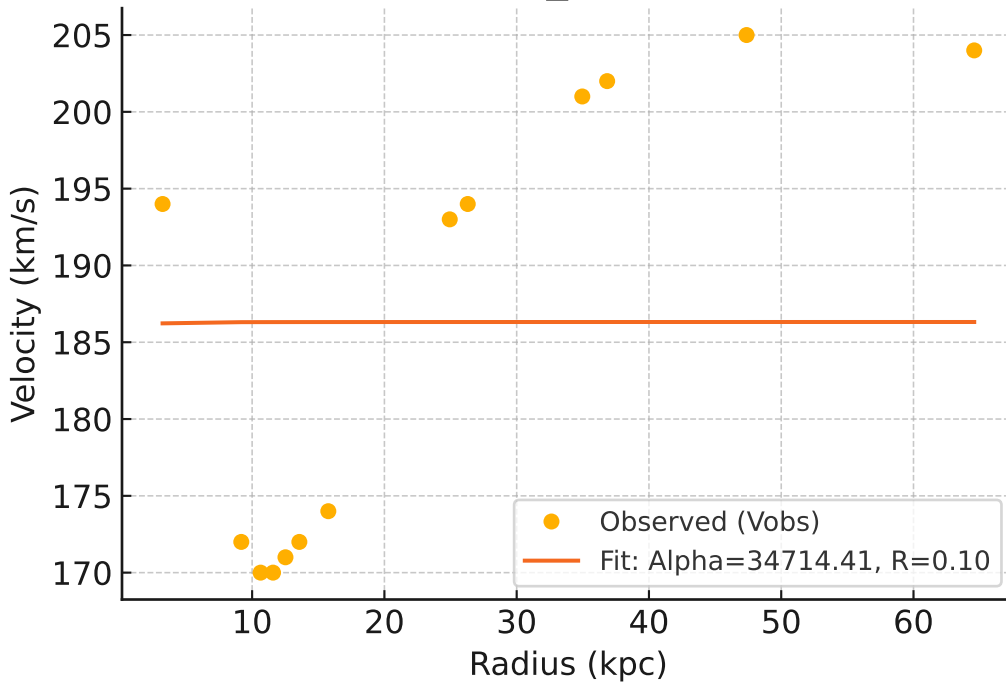
Galaxy: UGC06399_rotmod ($R^2=0.999$)



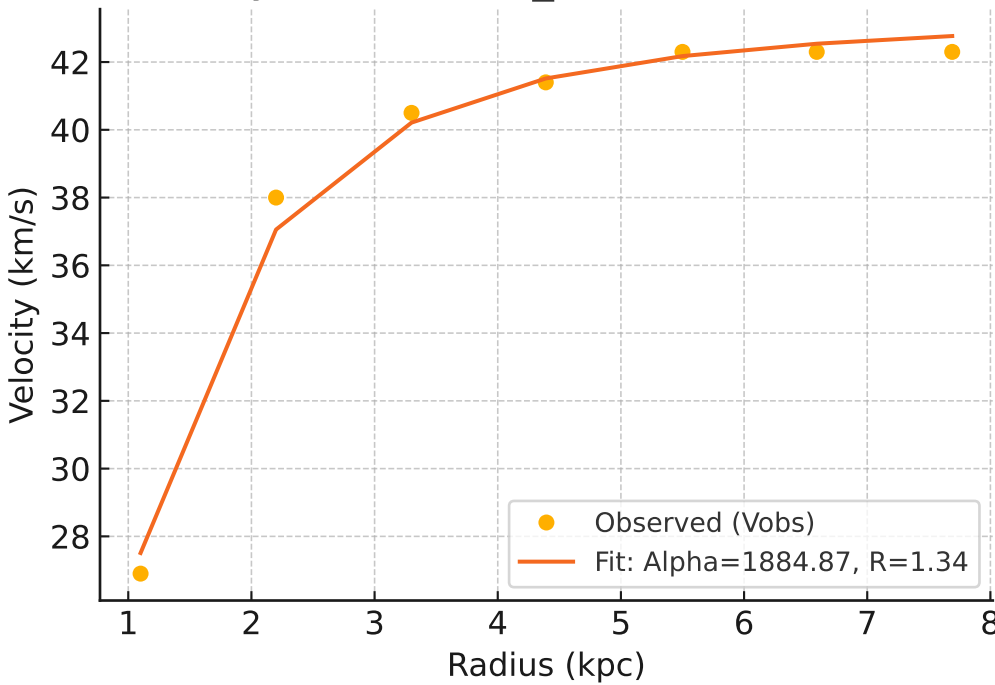
Galaxy: UGC06446_rotmod ($R^2=0.947$)



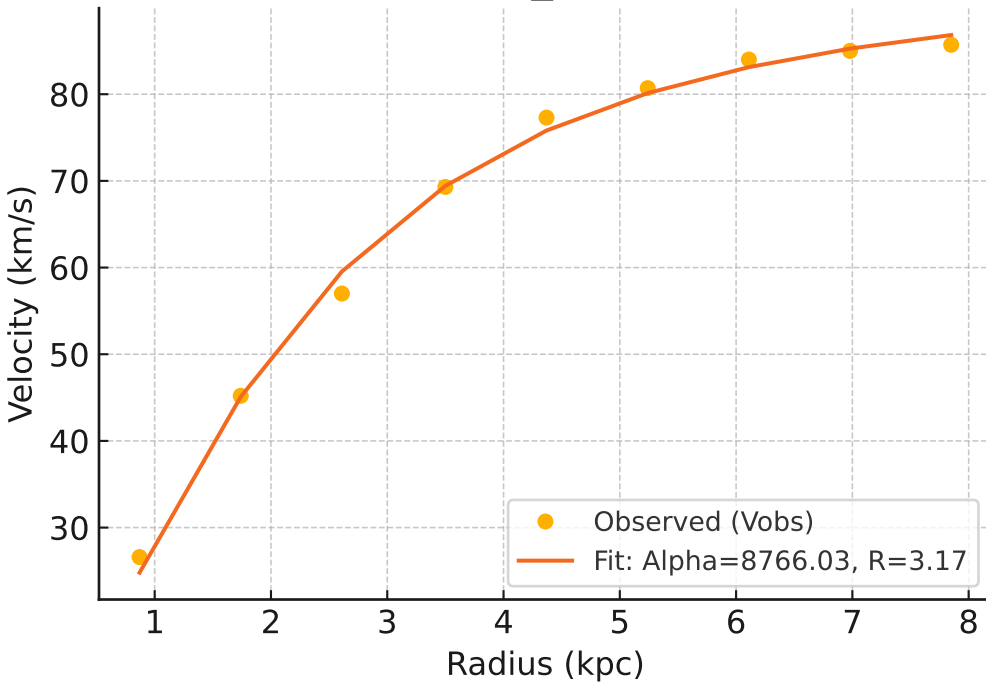
Galaxy: UGC06614_rotmod ($R^2=-0.000$)



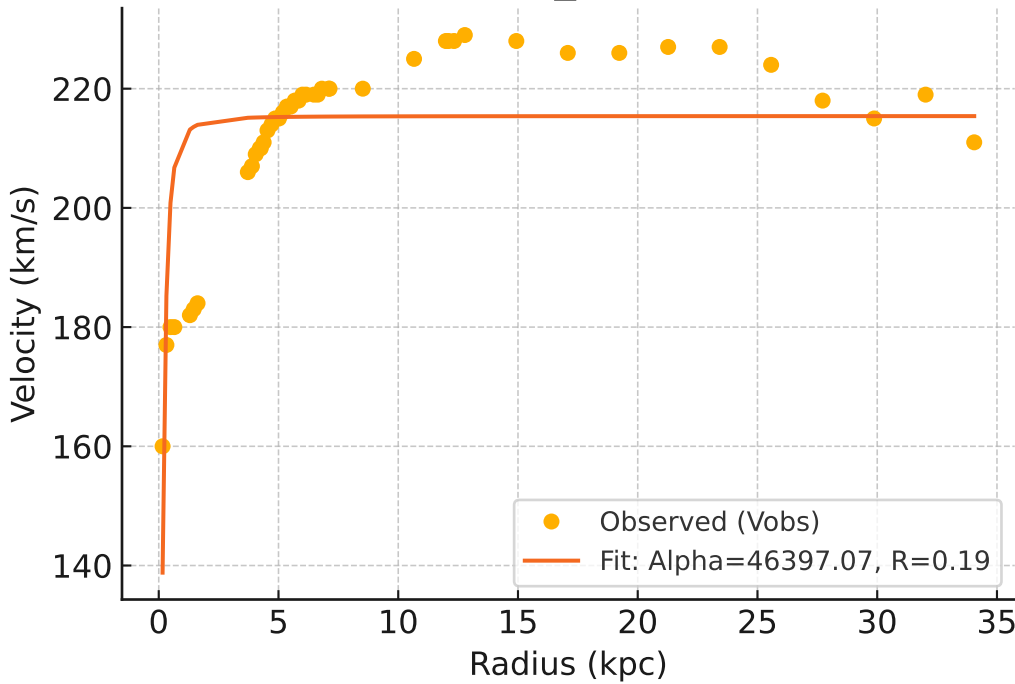
Galaxy: UGC06628_rotmod ($R^2=0.991$)



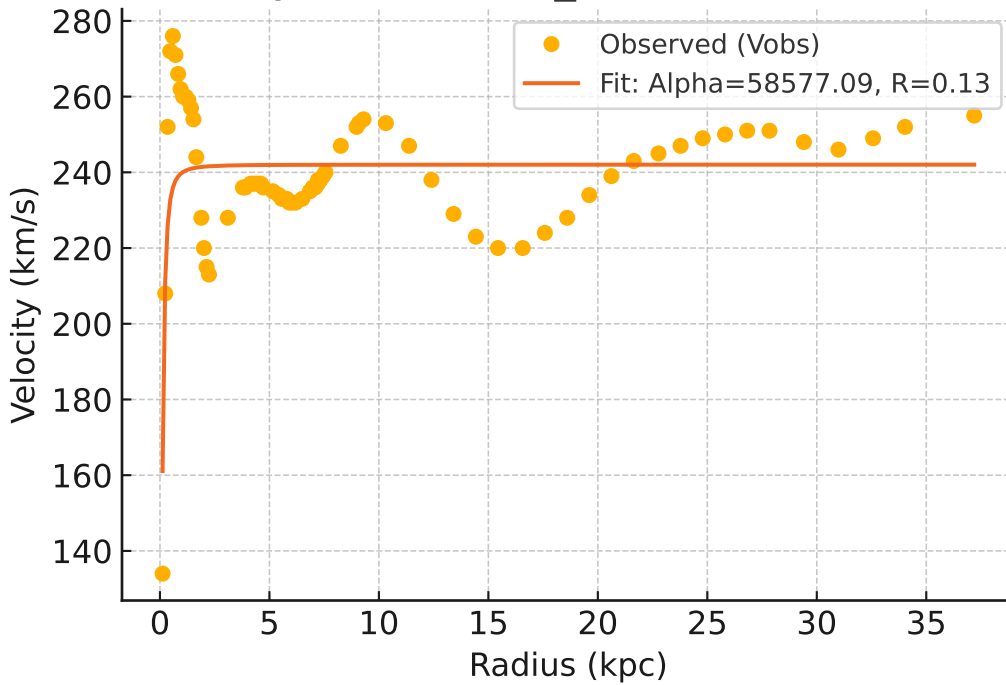
Galaxy: UGC06667_rotmod ($R^2=0.996$)



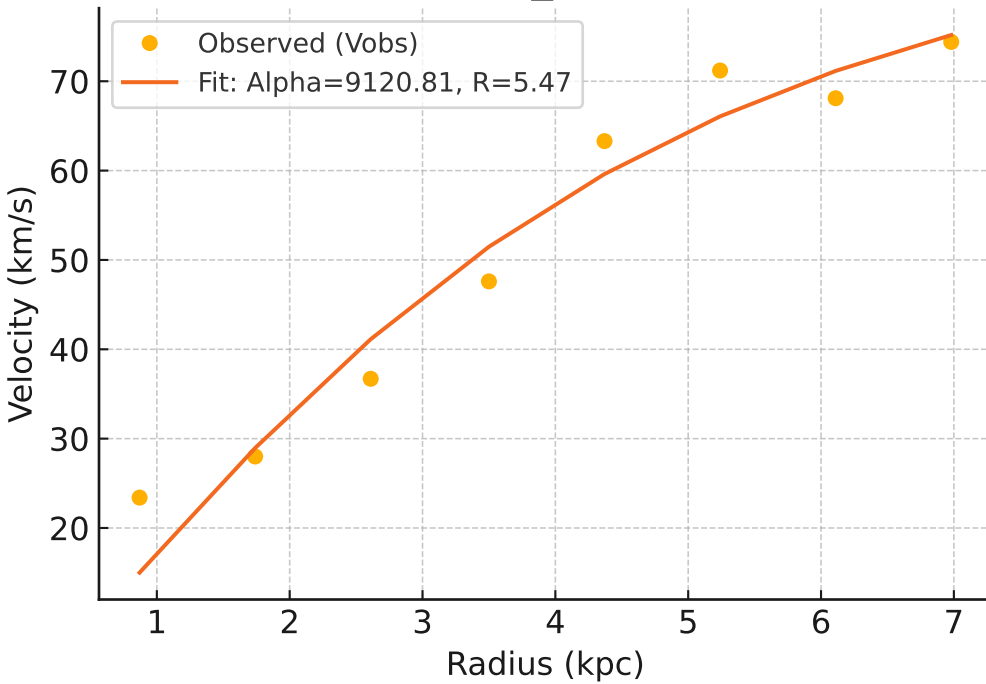
Galaxy: UGC06786_rotmod ($R^2=0.453$)



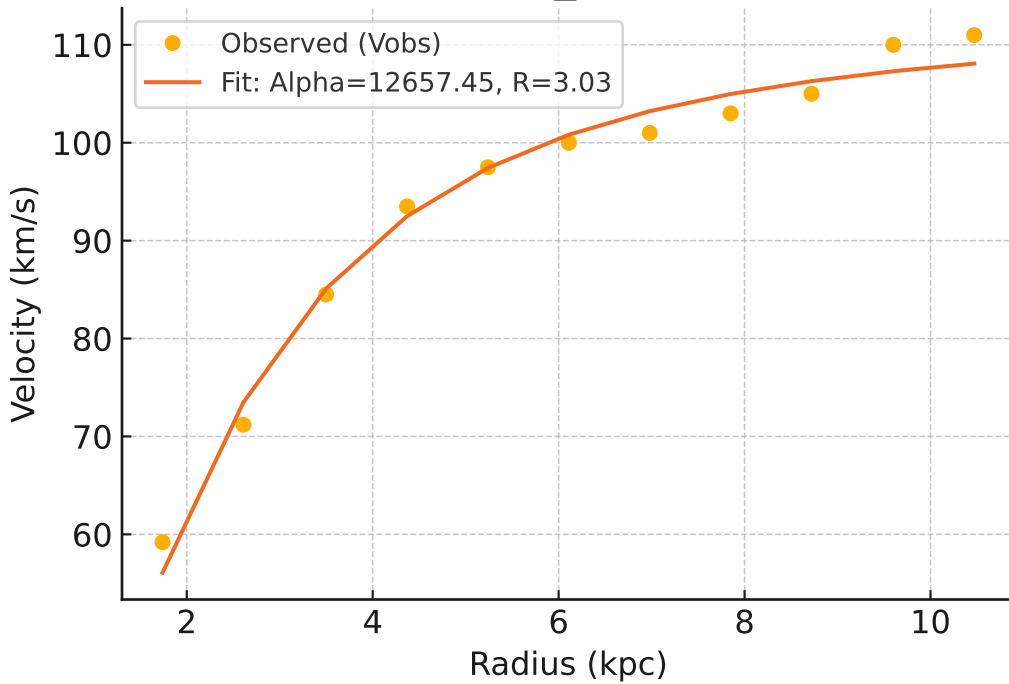
Galaxy: UGC06787_rotmod ($R^2=0.380$)



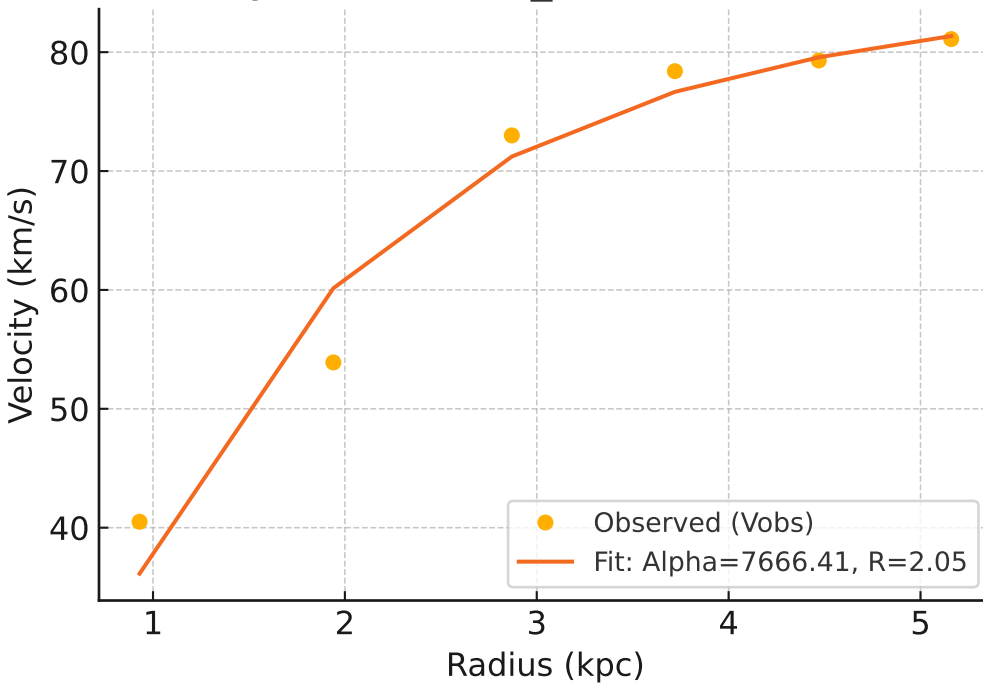
Galaxy: UGC06818_rotmod ($R^2=0.946$)



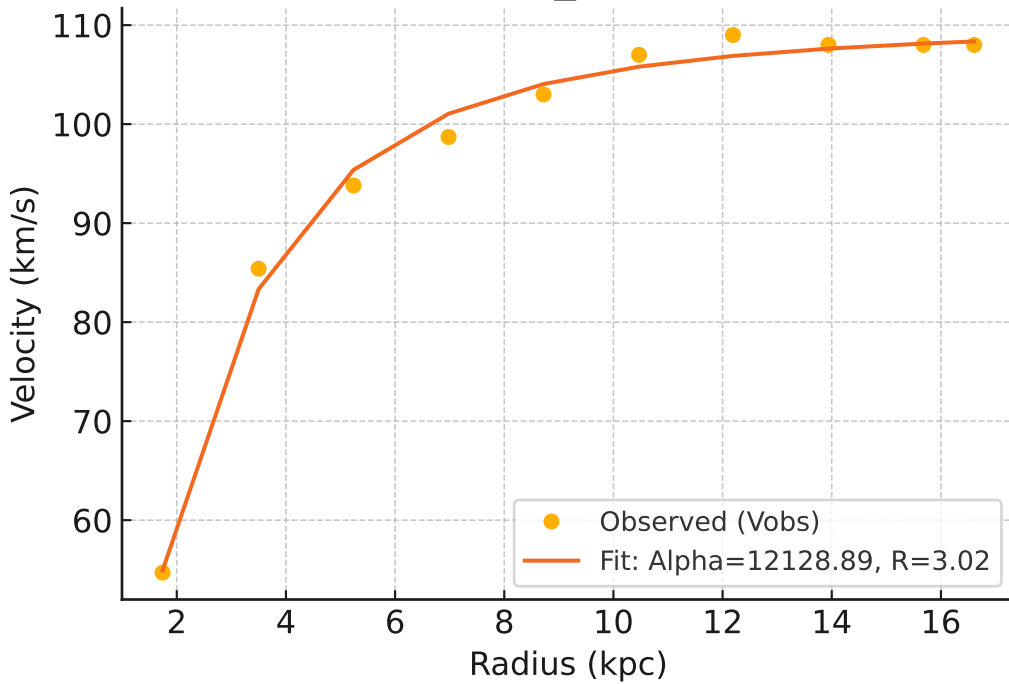
Galaxy: UGC06917_rotmod ($R^2=0.984$)



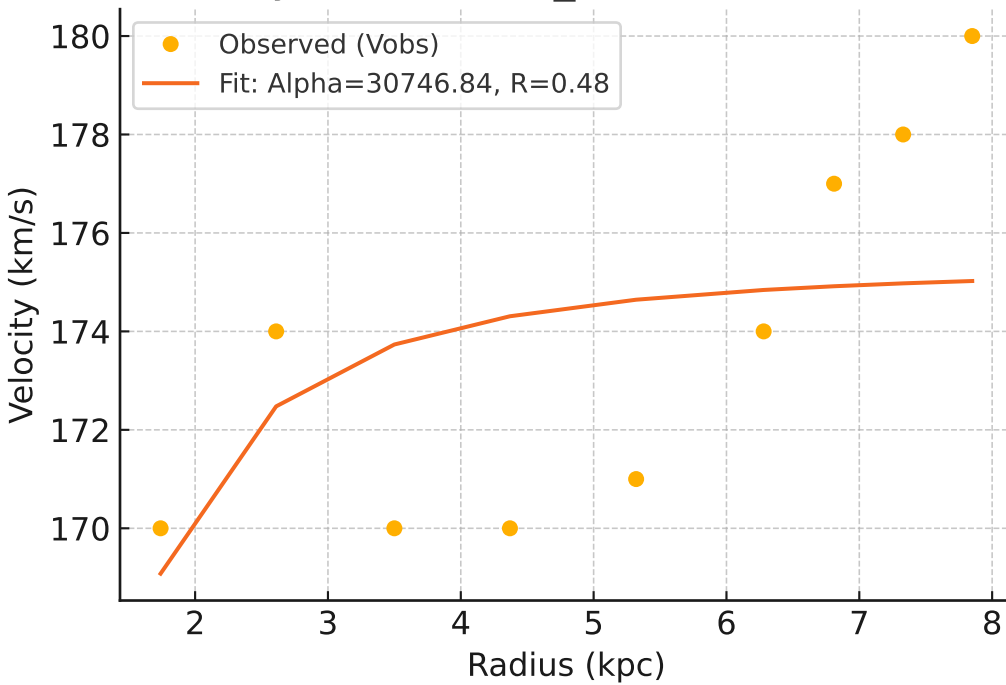
Galaxy: UGC06923_rotmod ($R^2=0.954$)



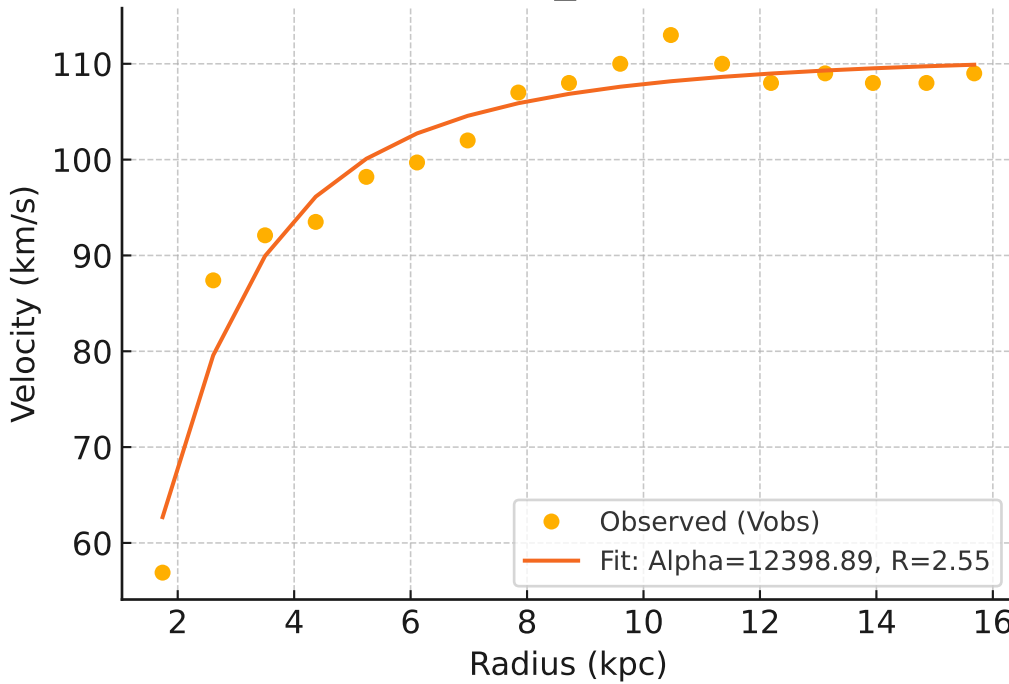
Galaxy: UGC06930_rotmod ($R^2=0.992$)



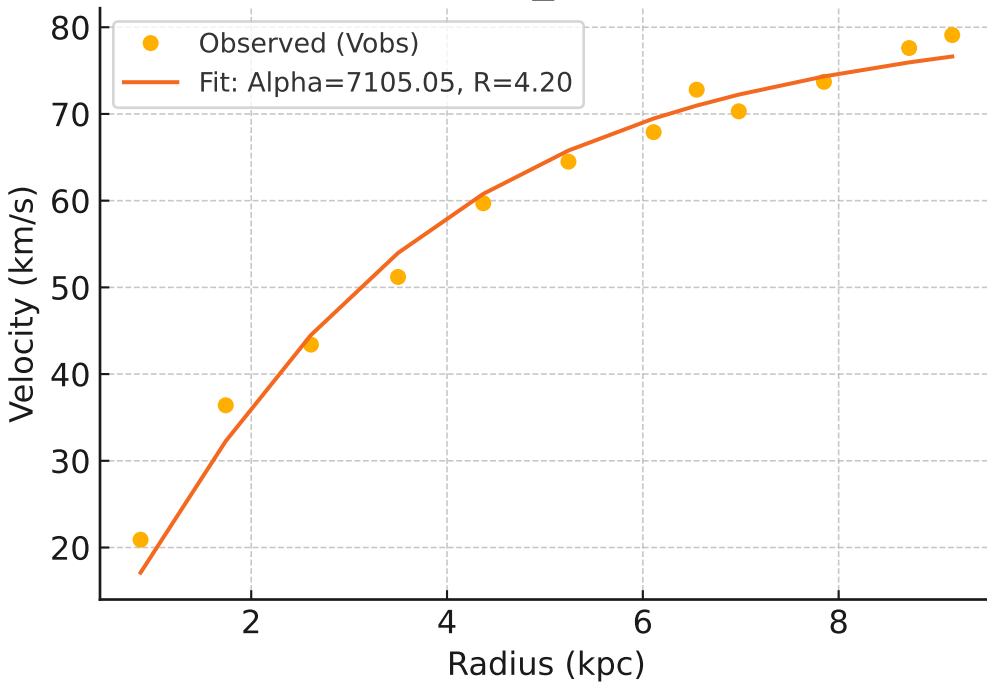
Galaxy: UGC06973_rotmod ($R^2=0.252$)



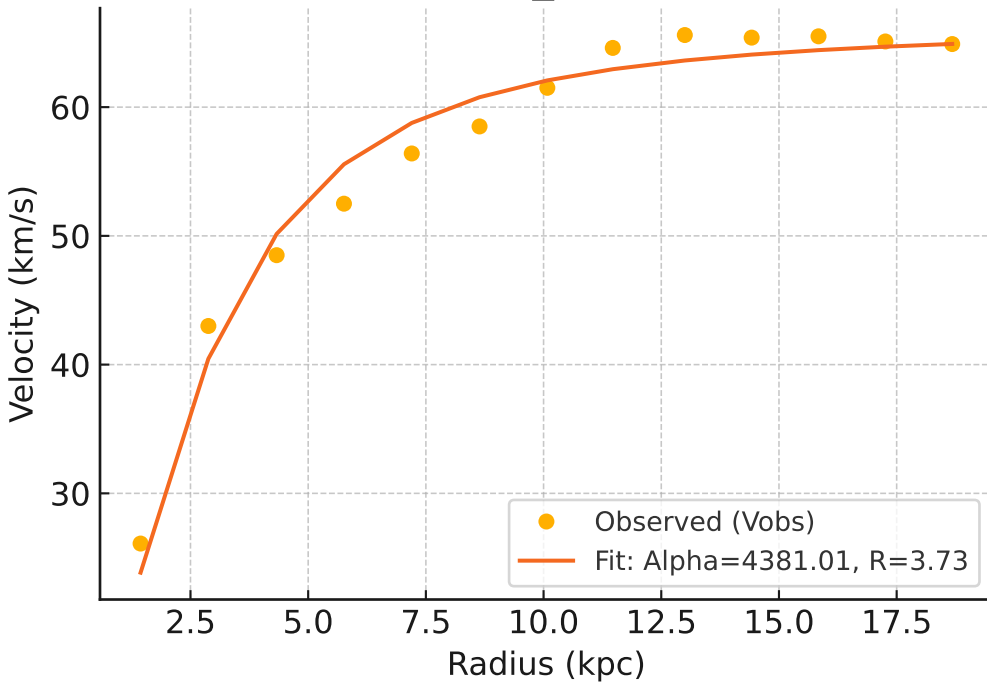
Galaxy: UGC06983_rotmod ($R^2=0.943$)



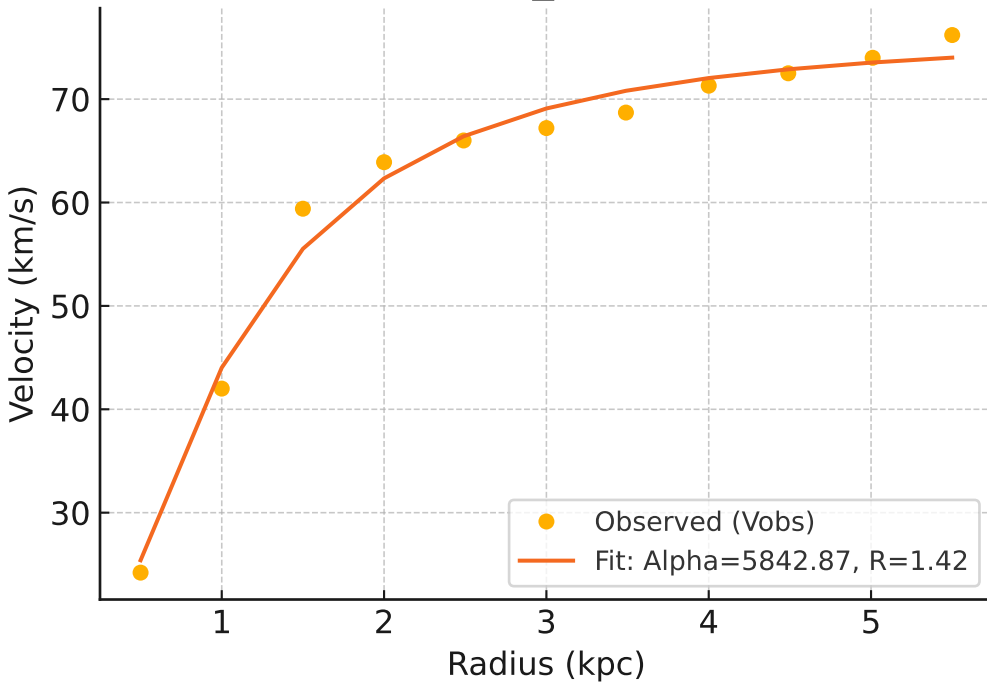
Galaxy: UGC07089_rotmod ($R^2=0.983$)



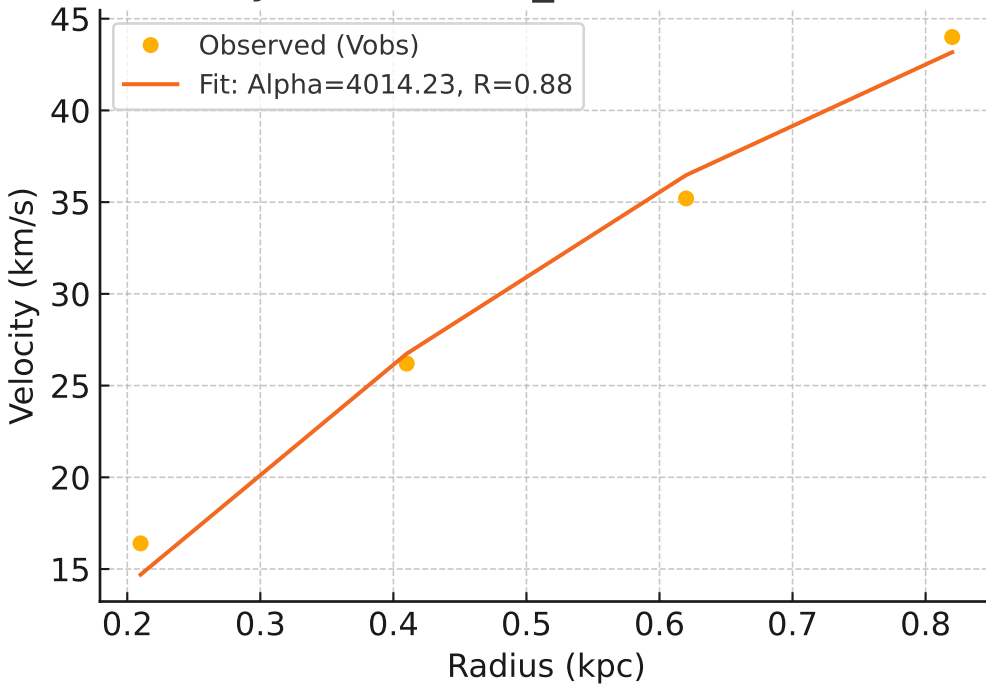
Galaxy: UGC07125_rotmod ($R^2=0.973$)



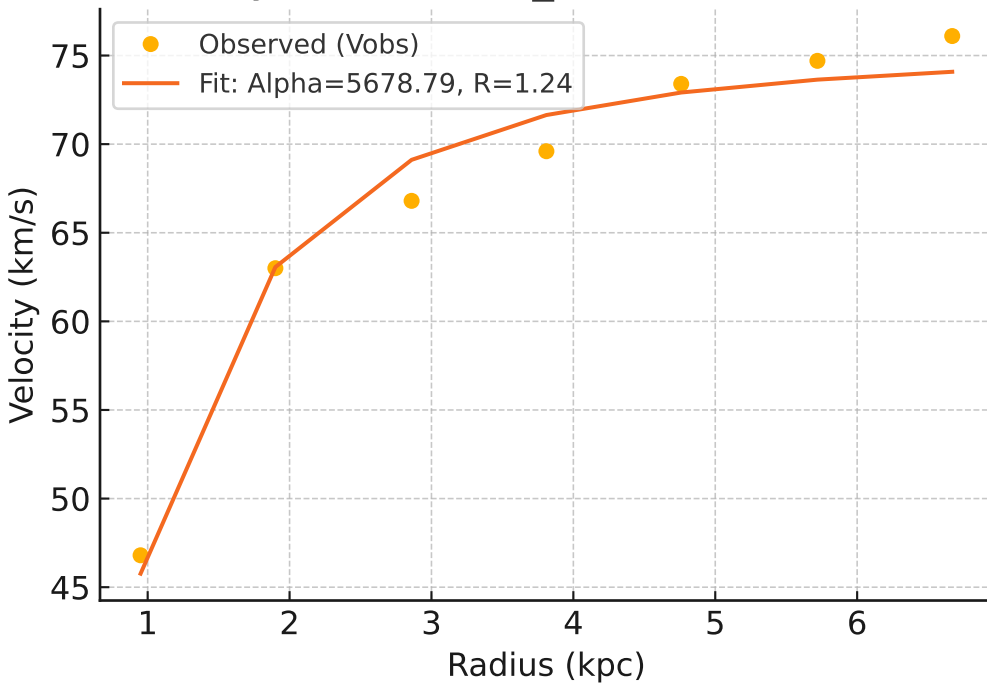
Galaxy: UGC07151_rotmod ($R^2=0.985$)



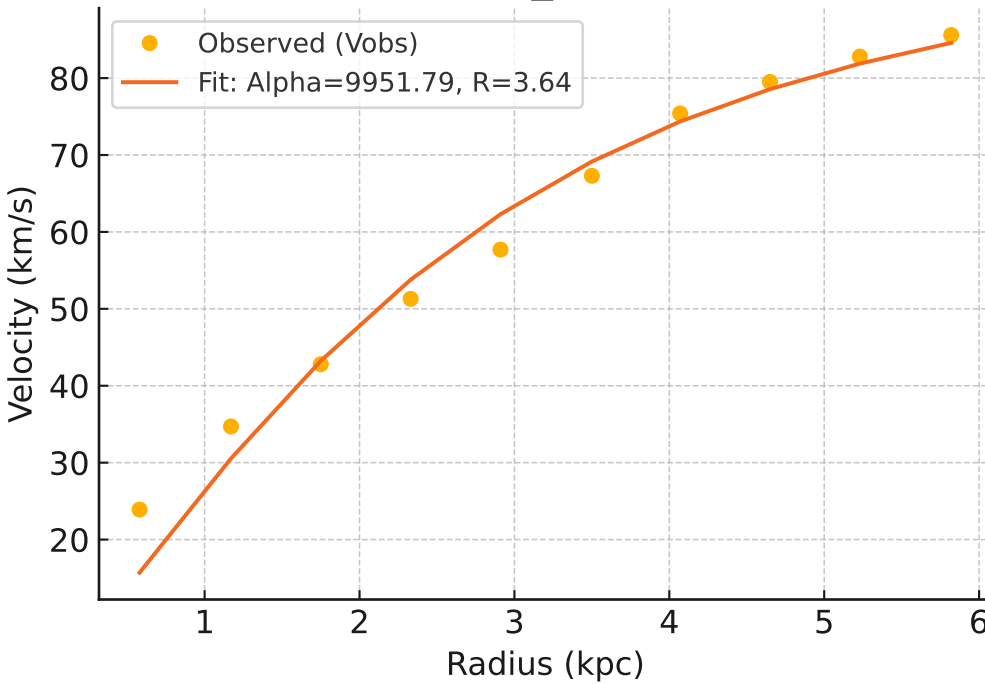
Galaxy: UGC07232_rotmod ($R^2=0.987$)



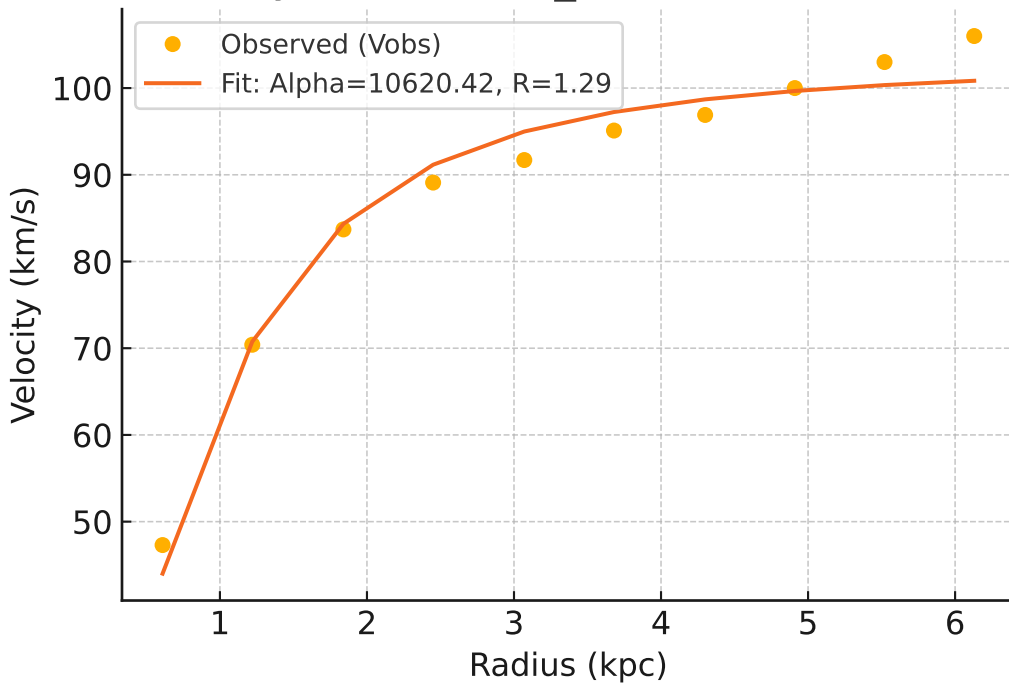
Galaxy: UGC07261_rotmod ($R^2=0.974$)



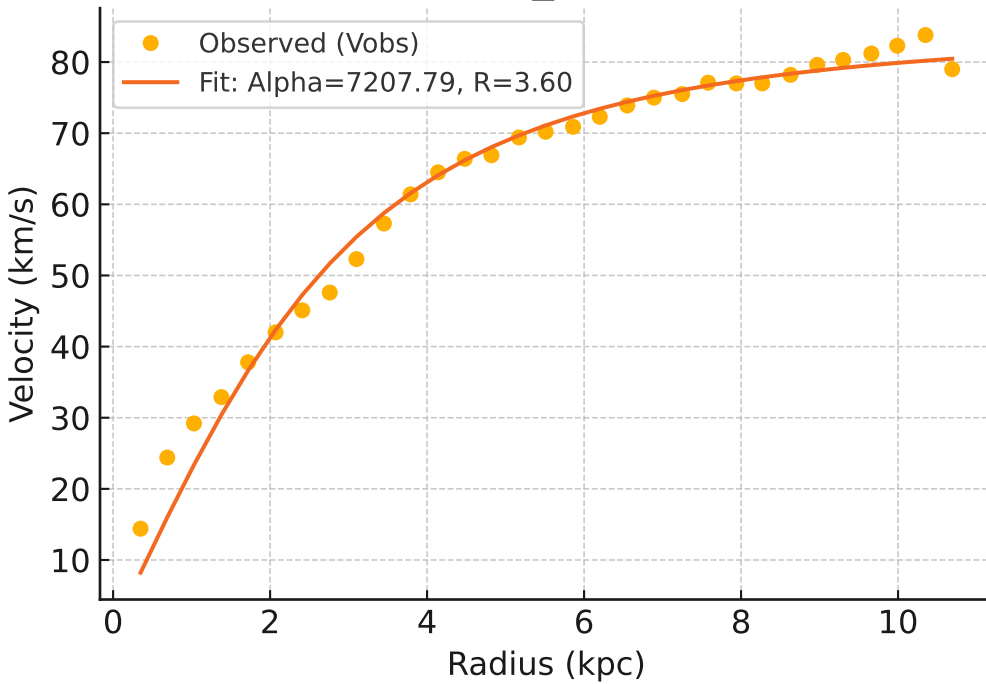
Galaxy: UGC07323_rotmod ($R^2=0.971$)



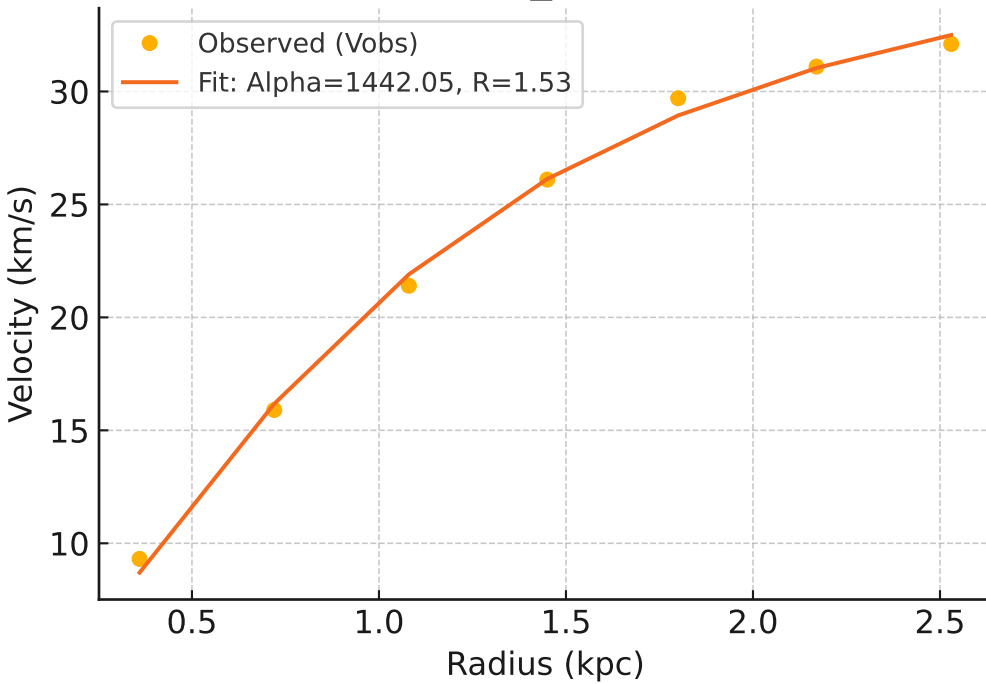
Galaxy: UGC07399_rotmod ($R^2=0.976$)



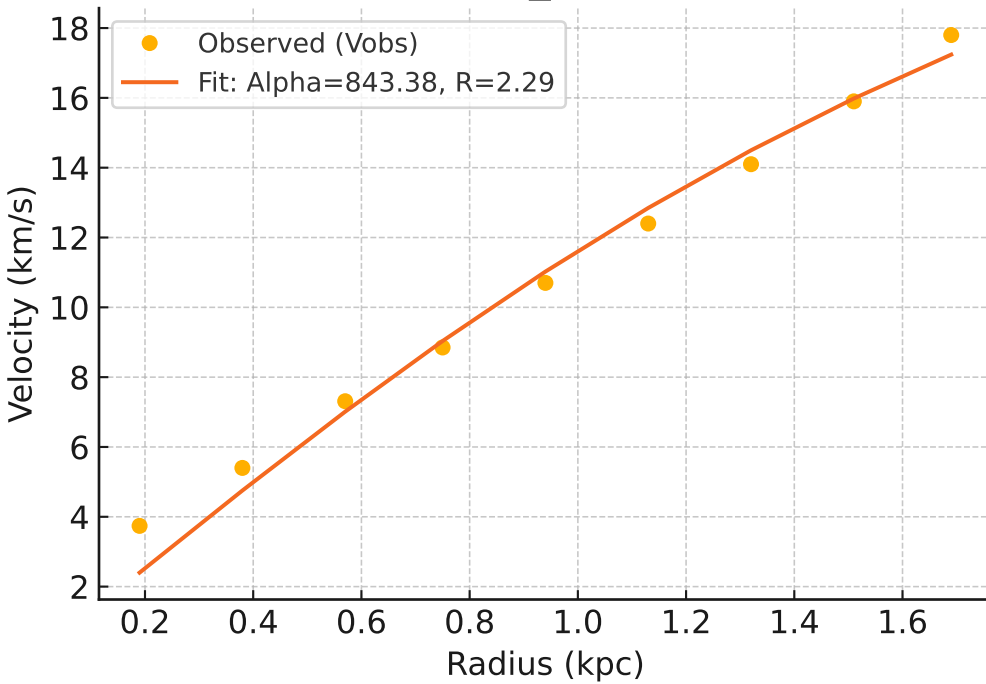
Galaxy: UGC07524_rotmod ($R^2=0.981$)



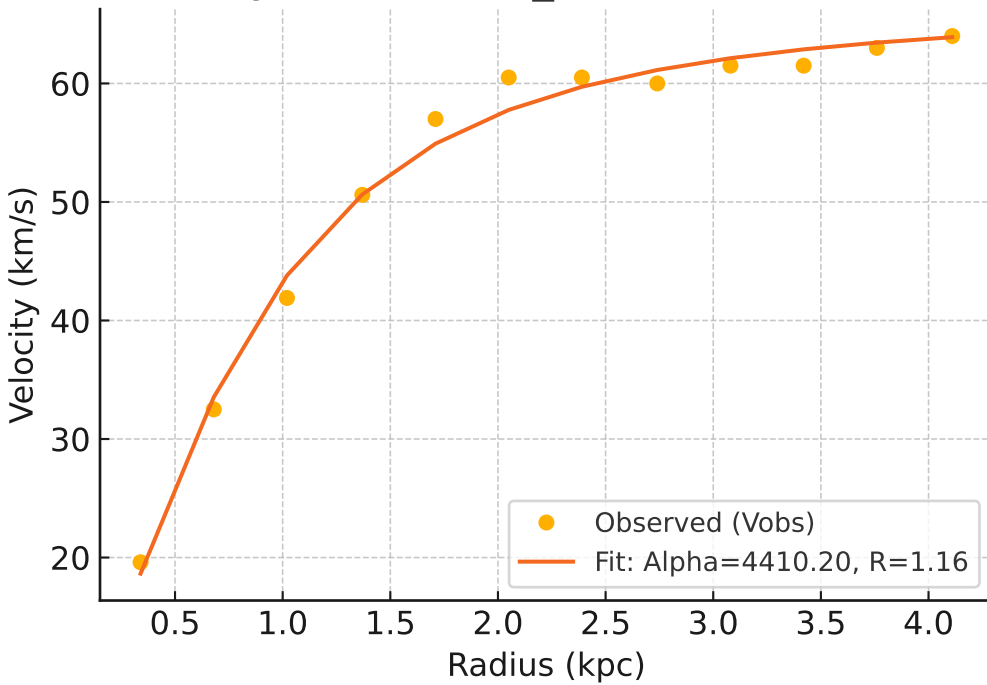
Galaxy: UGC07559_rotmod ($R^2=0.997$)



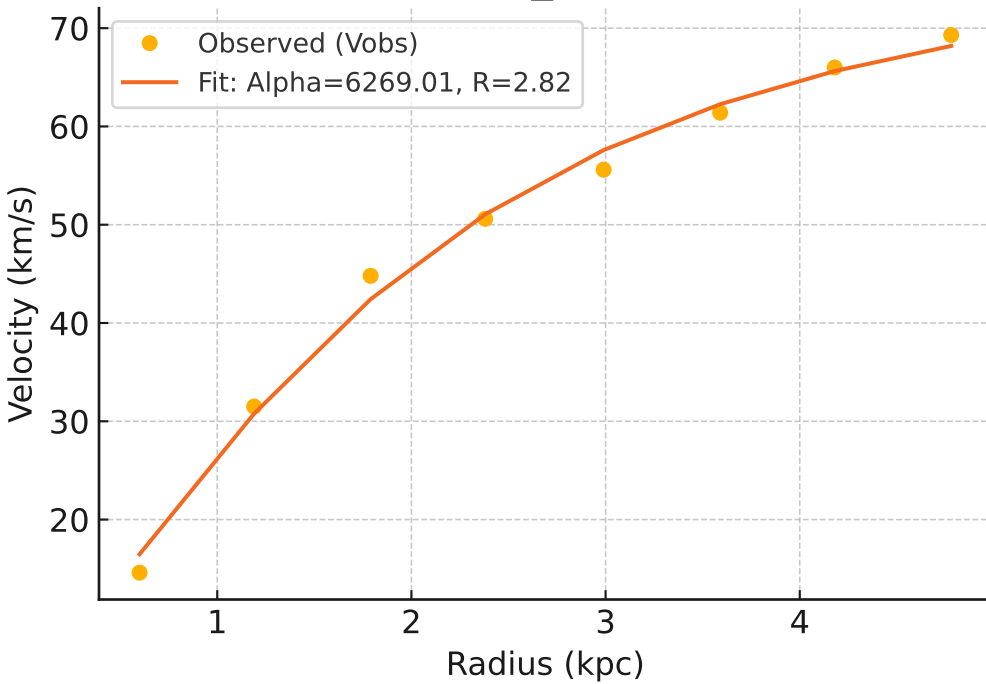
Galaxy: UGC07577_rotmod ($R^2=0.983$)



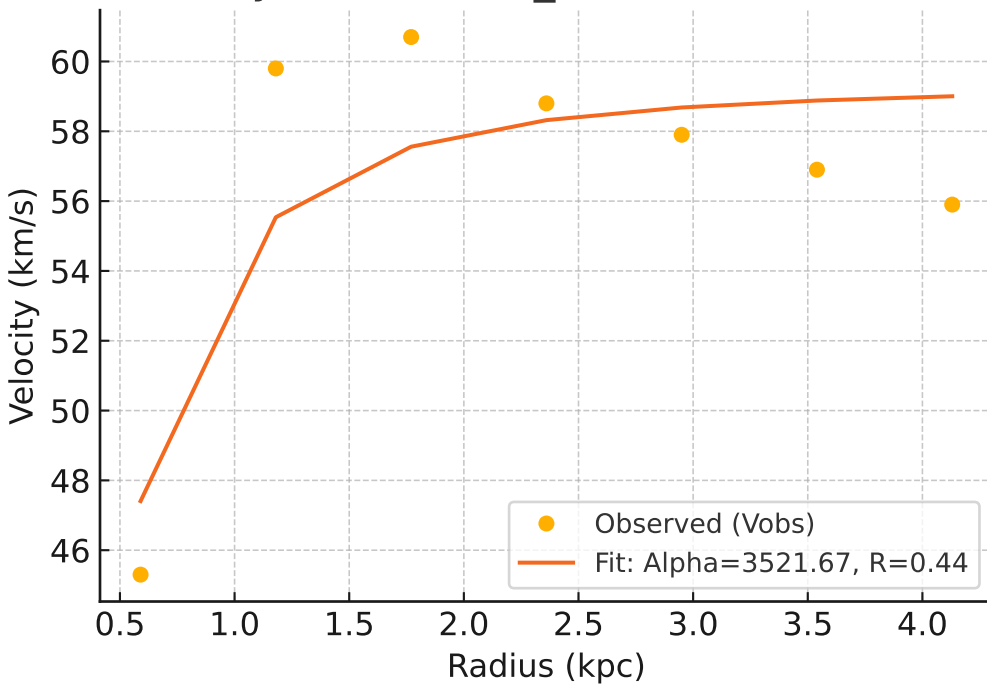
Galaxy: UGC07603_rotmod ($R^2=0.990$)



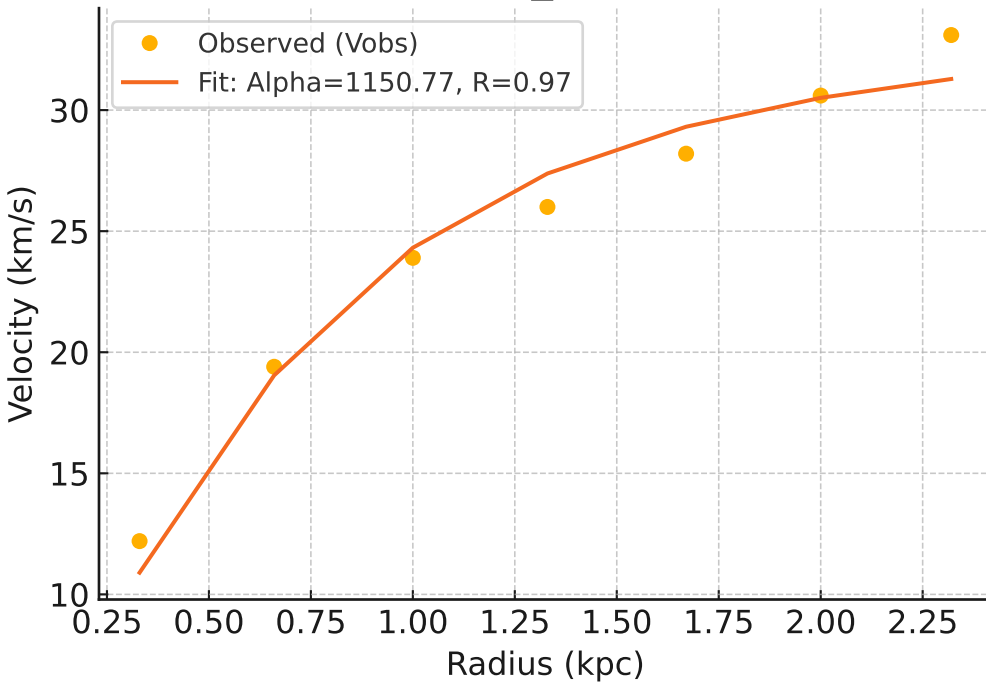
Galaxy: UGC07608_rotmod ($R^2=0.993$)



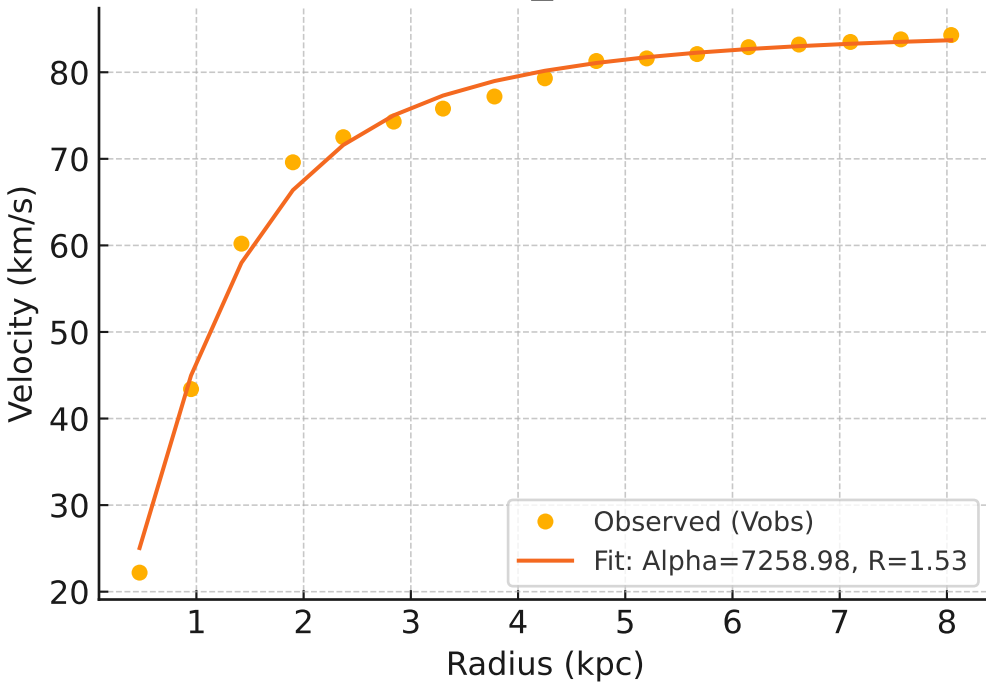
Galaxy: UGC07690_rotmod ($R^2=0.710$)



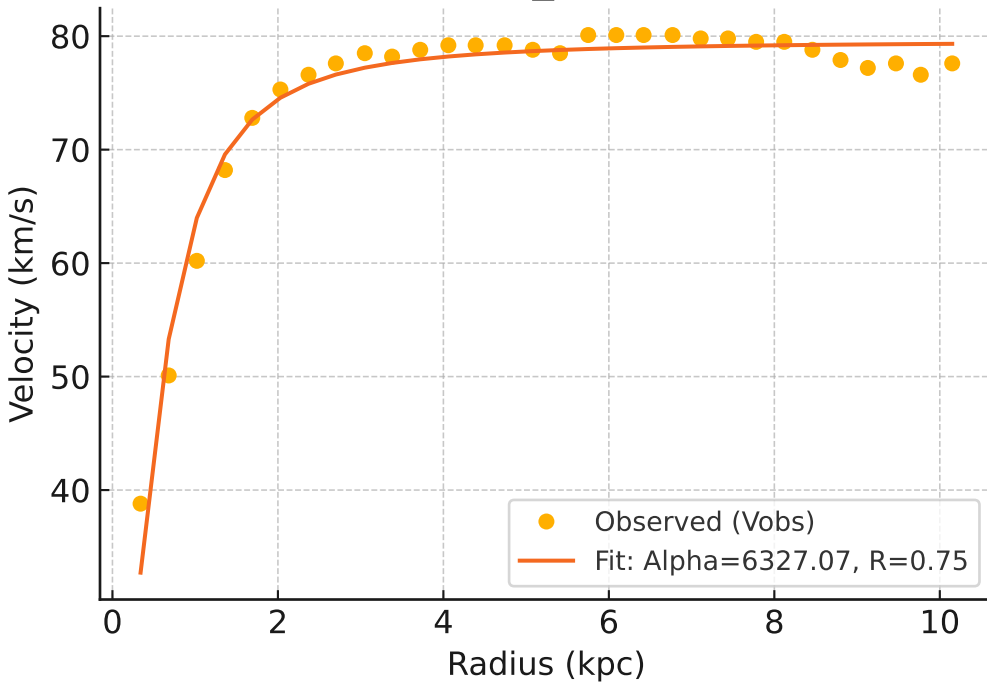
Galaxy: UGC07866_rotmod ($R^2=0.972$)



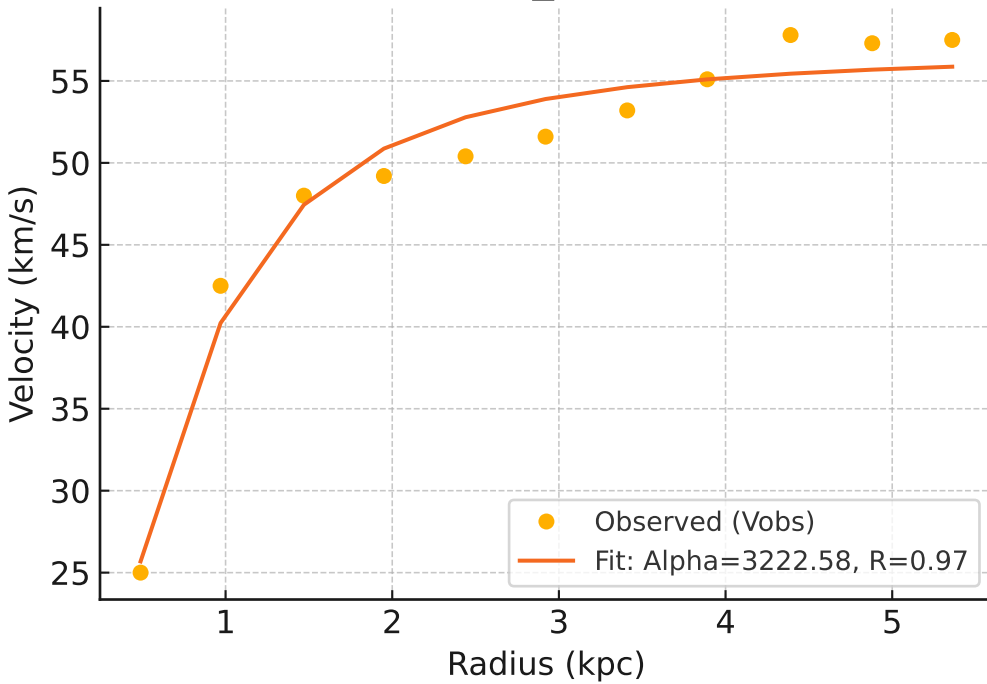
Galaxy: UGC08286_rotmod ($R^2=0.992$)



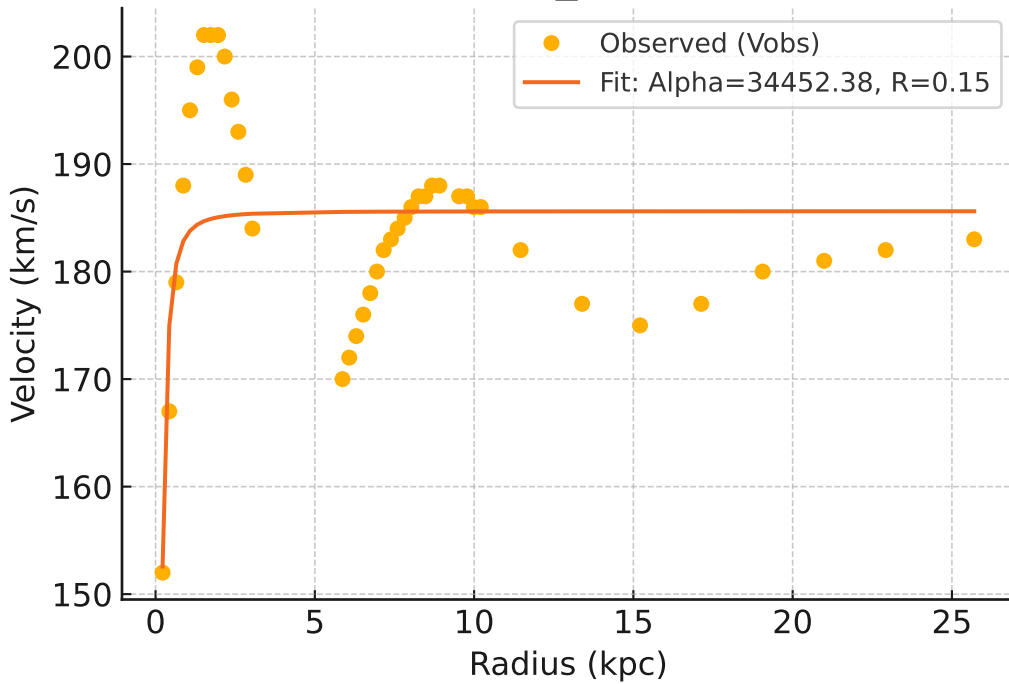
Galaxy: UGC08490_rotmod ($R^2=0.962$)



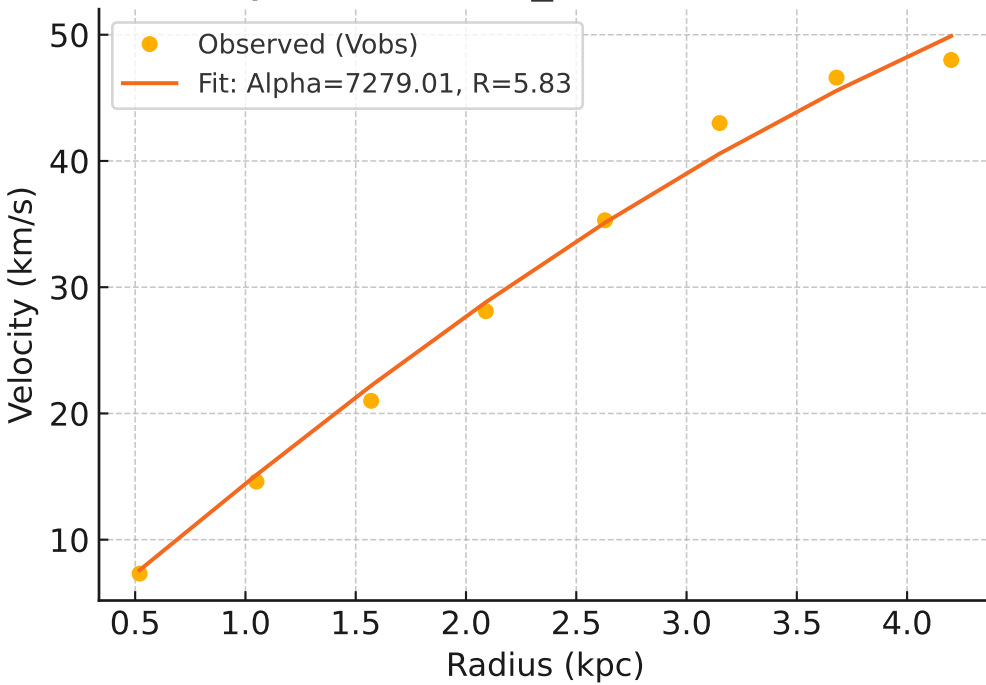
Galaxy: UGC08550_rotmod ($R^2=0.964$)



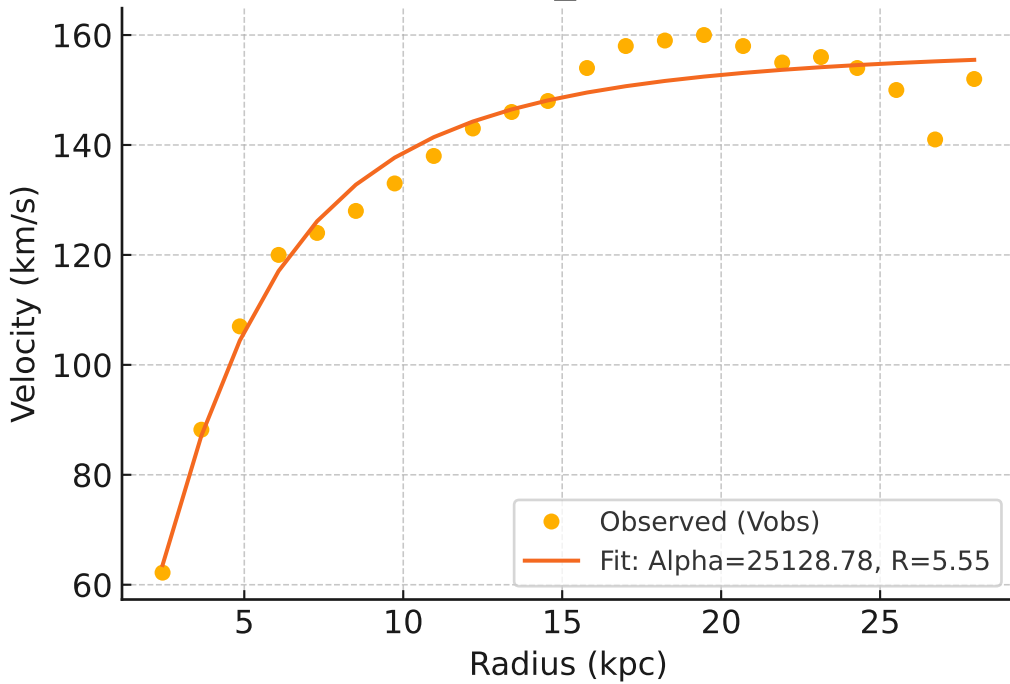
Galaxy: UGC08699_rotmod ($R^2=0.293$)



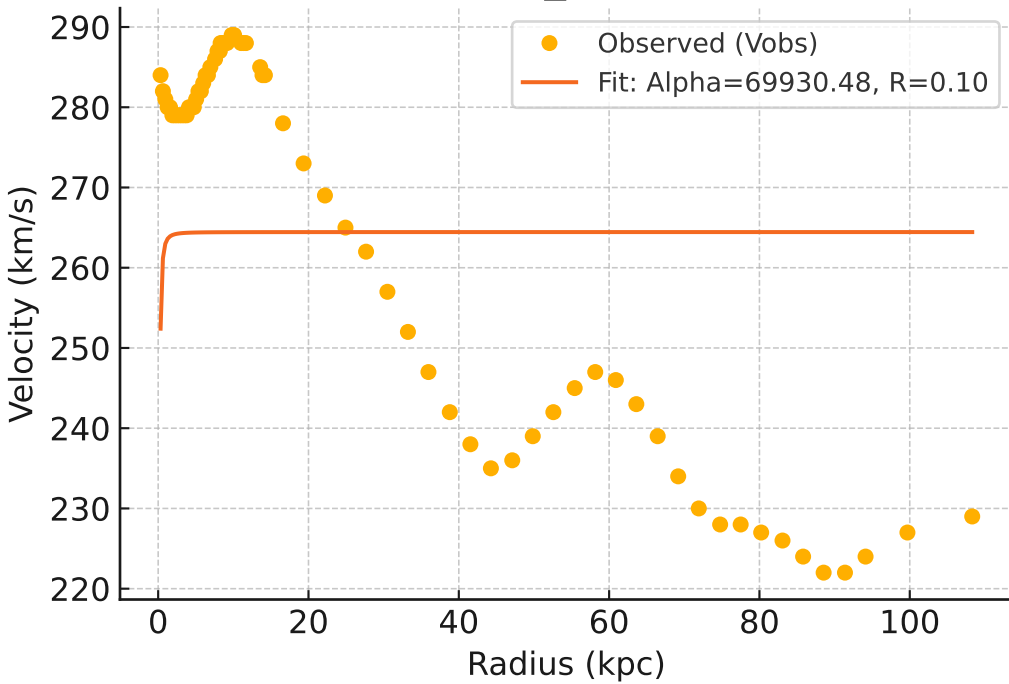
Galaxy: UGC08837_rotmod ($R^2=0.992$)



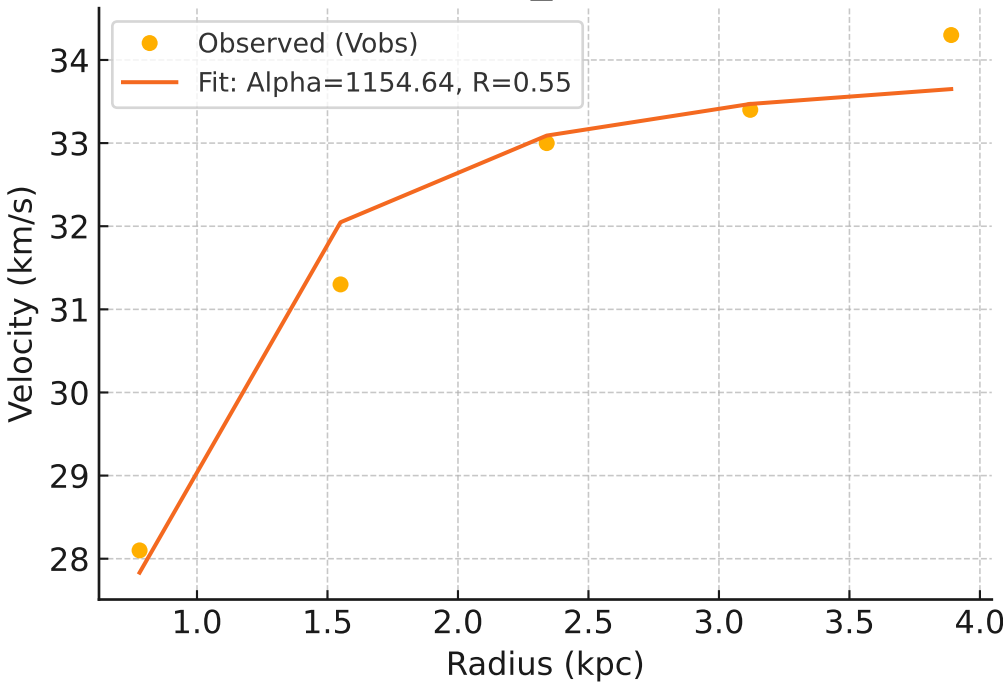
Galaxy: UGC09037_rotmod ($R^2=0.960$)



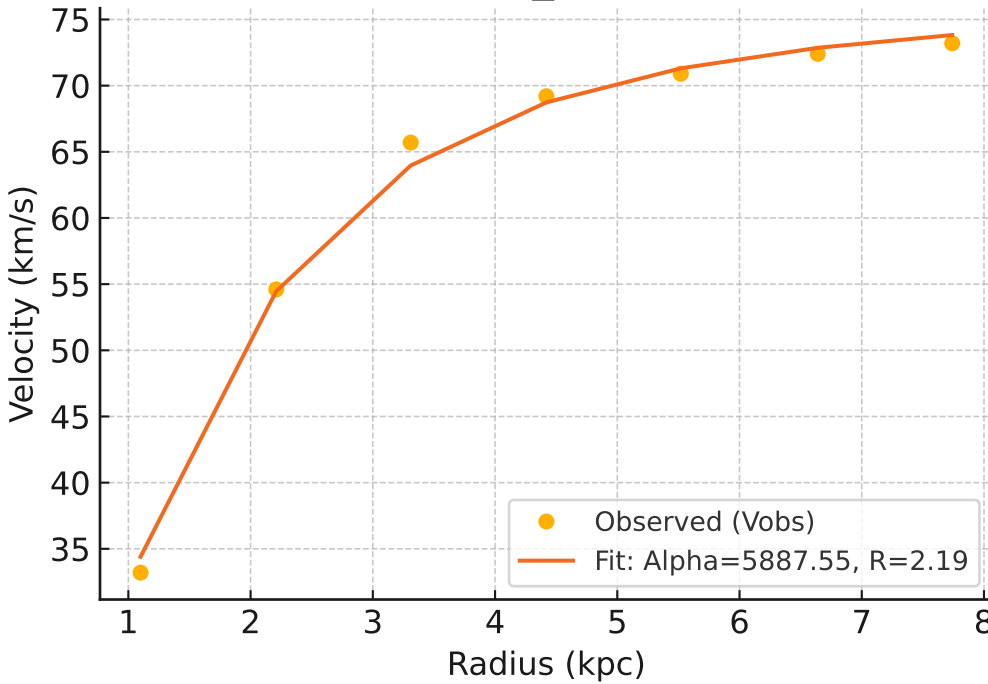
Galaxy: UGC09133_rotmod ($R^2=-0.024$)



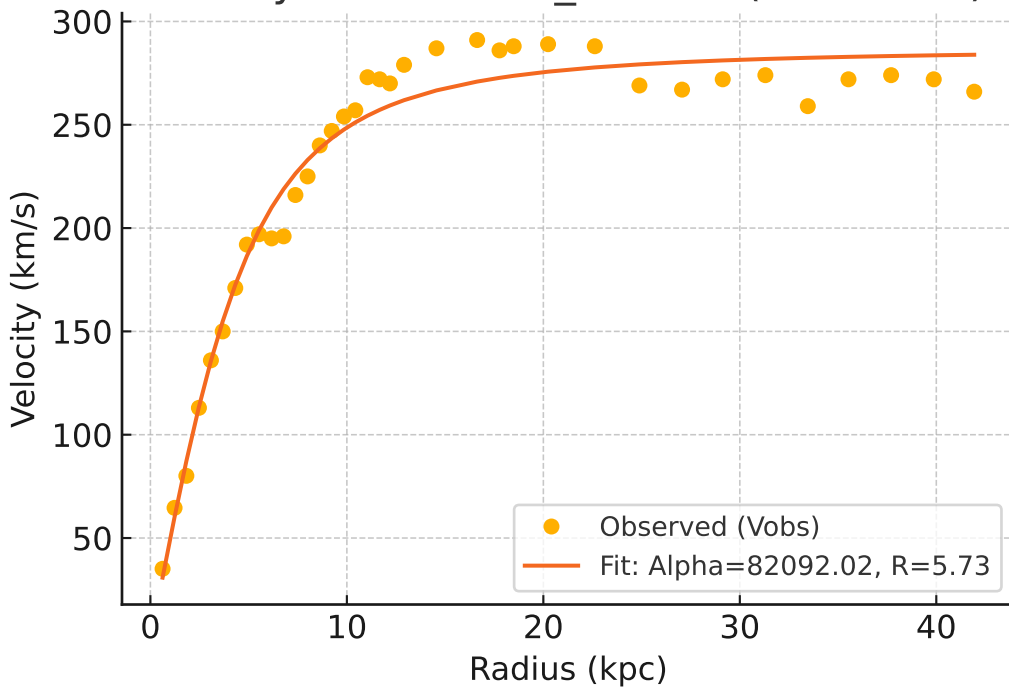
Galaxy: UGC09992_rotmod ($R^2=0.955$)



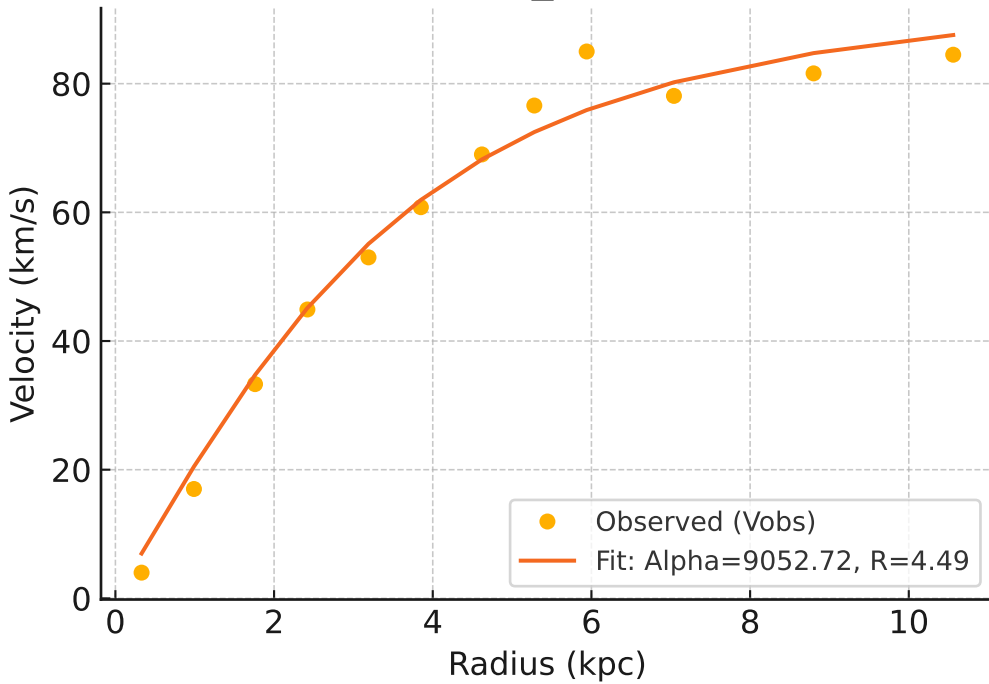
Galaxy: UGC10310_rotmod ($R^2=0.996$)



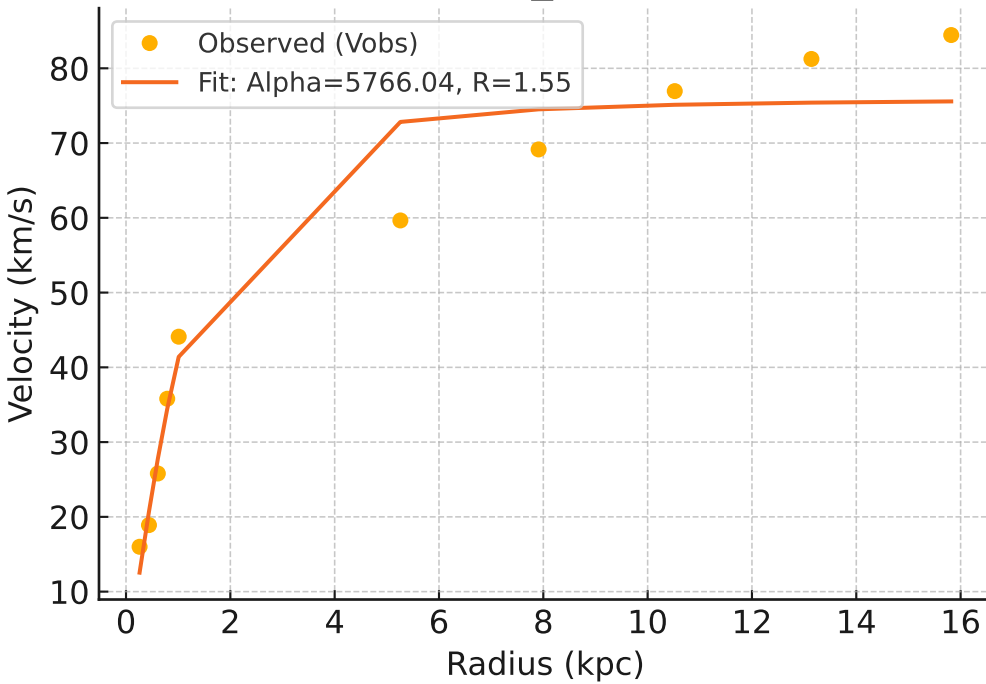
Galaxy: UGC11455_rotmod ($R^2=0.969$)



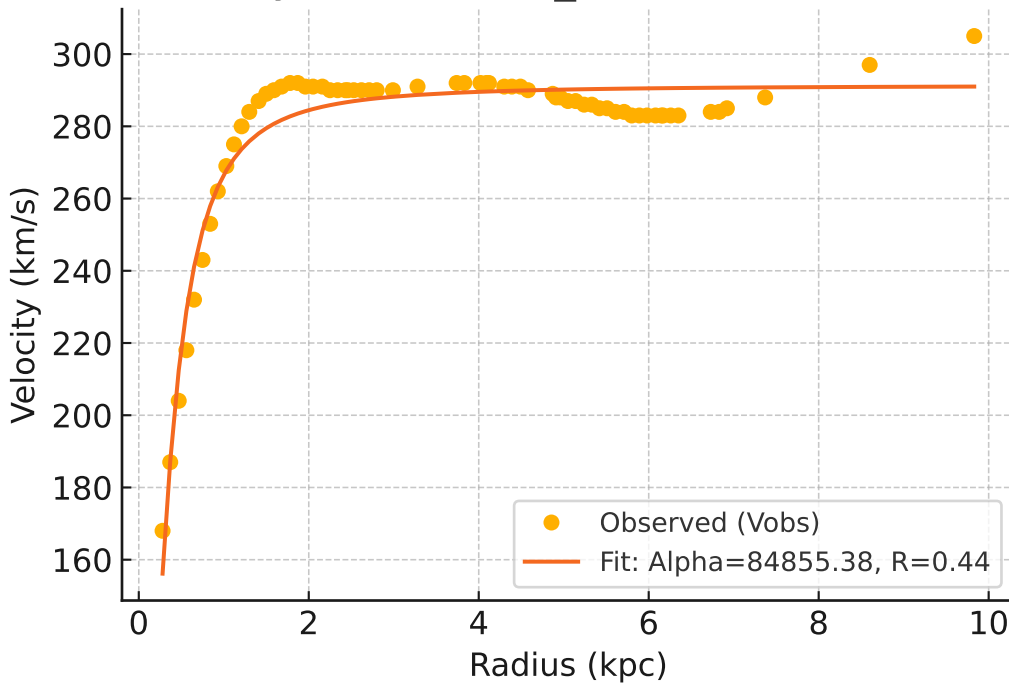
Galaxy: UGC11557_rotmod ($R^2=0.981$)



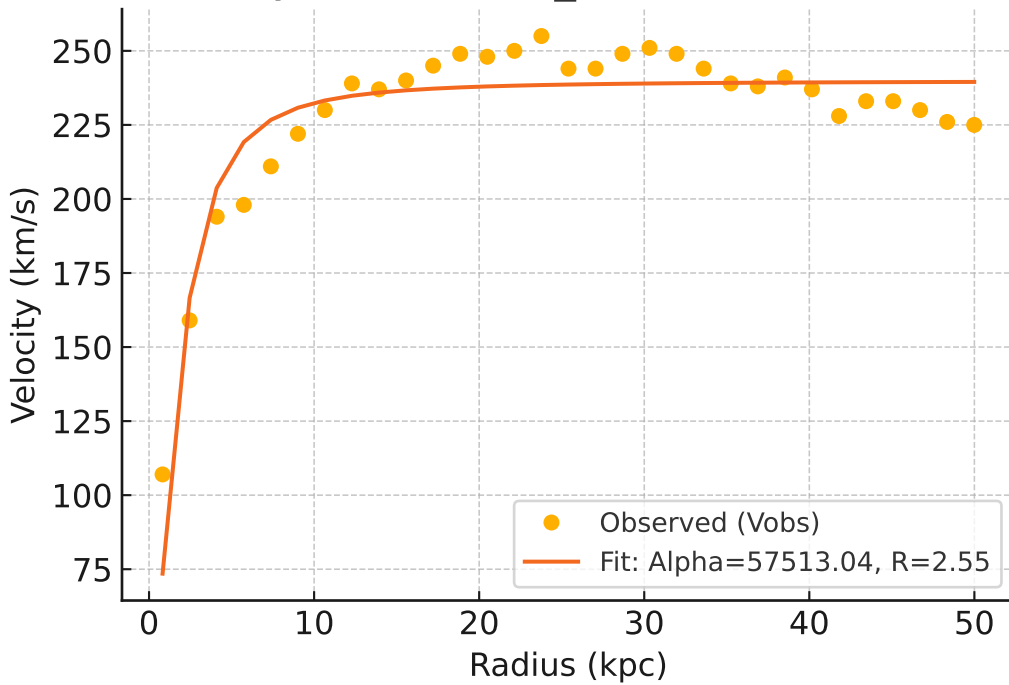
Galaxy: UGC11820_rotmod ($R^2=0.945$)



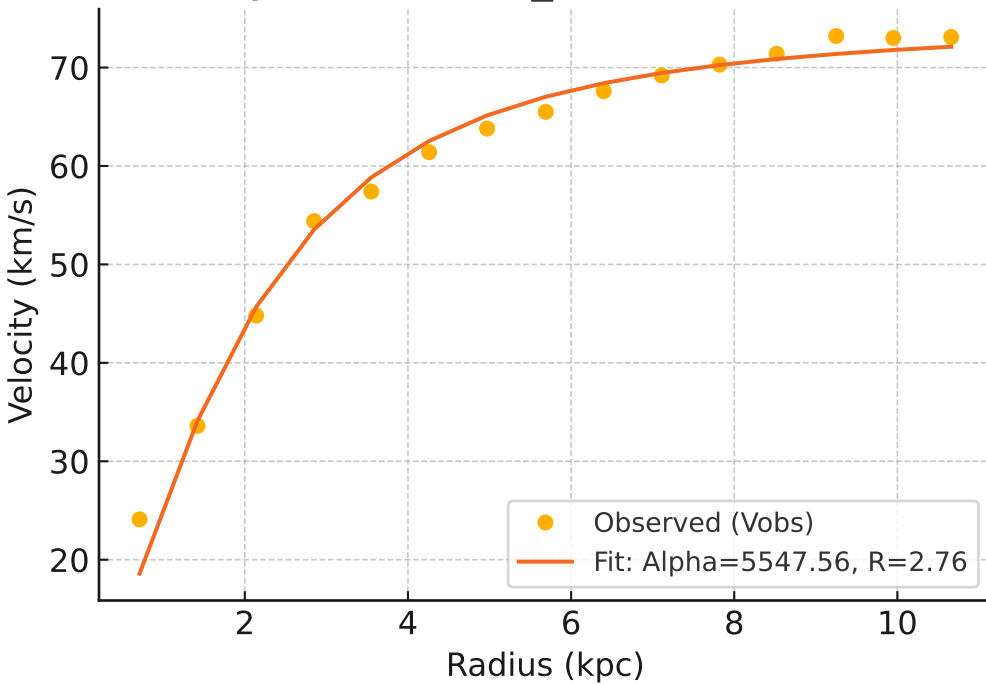
Galaxy: UGC11914_rotmod ($R^2=0.941$)



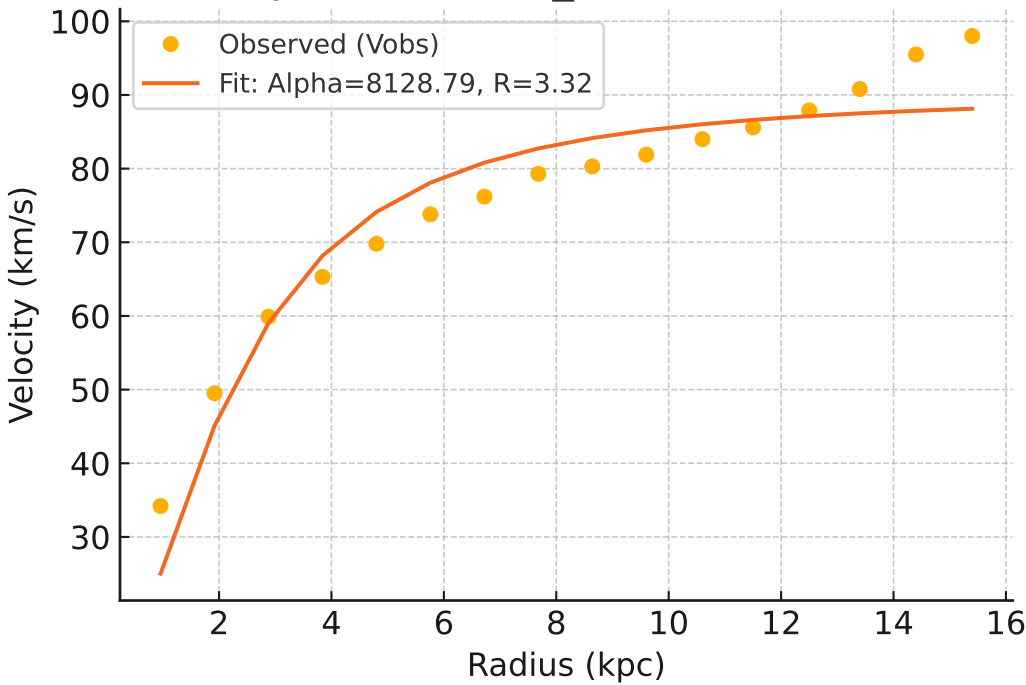
Galaxy: UGC12506_rotmod ($R^2=0.856$)



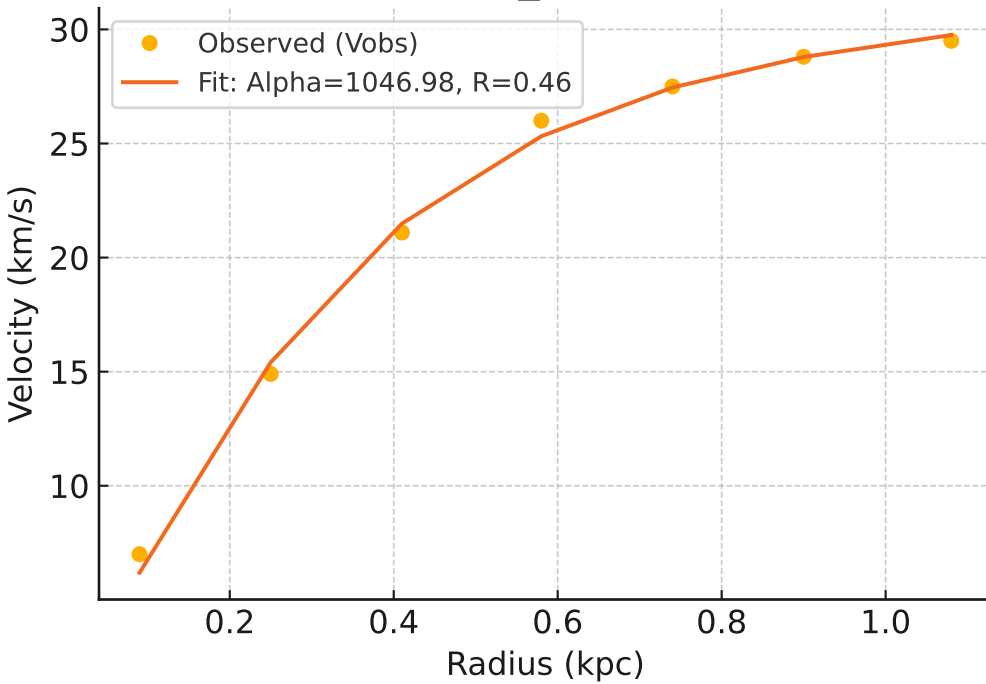
Galaxy: UGC12632_rotmod ($R^2=0.985$)



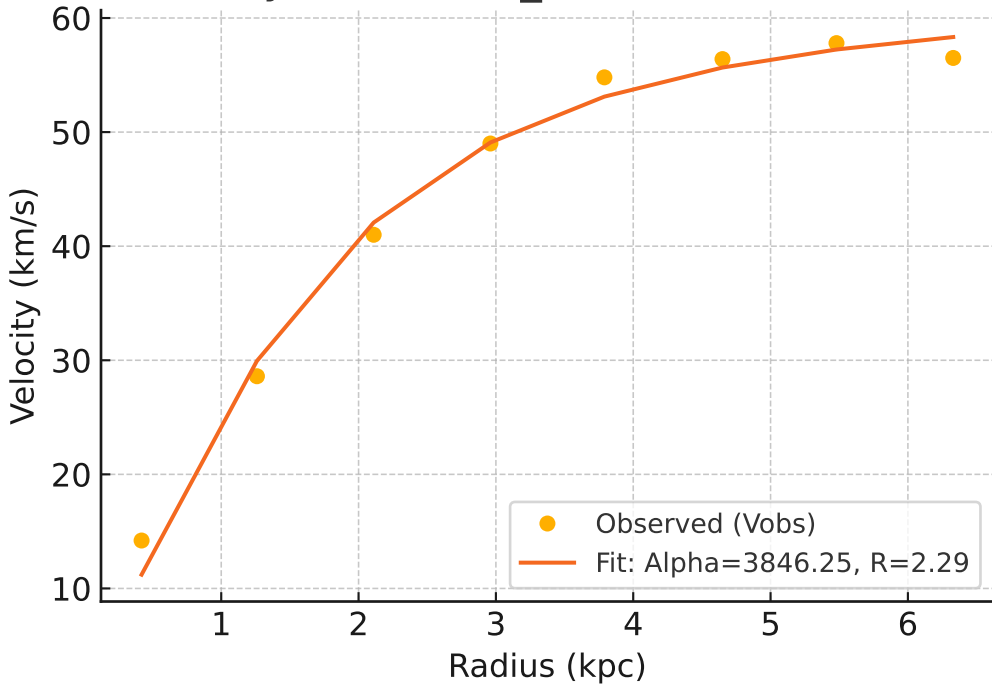
Galaxy: UGC12732_rotmod ($R^2=0.912$)



Galaxy: UGCA281_rotmod ($R^2=0.996$)



Galaxy: UGCA442_rotmod ($R^2=0.989$)



Galaxy: UGCA444_rotmod ($R^2=0.977$)

